Vol. 104 No. 1 January 1, 1979 ISSN 0003-2670

ANALYTICA CHIMICA ACTA

International journal devoted to all branches of analytical chemistry

ELSEVIER SCIENTIFIC PUBLISHING COMPANY

ANALYTICA CHIMICA ACTA

International journal devoted to all branches of analytical chemistry
Revue internationale consacrée à tous les domaines de la chimie analytique
Internationale Zeitschrift für alle Gebiete der analytischen Chemie

PUBLICATION SCHEDULE FOR 1979 (incorporating the section on Computer Techniques and Optimization).

	J	F	M	A	M	J	J	A	S	O	N	D
Analytica Chimica Acta	104/1	104/2	105	106/1	106/2	107	108	109/1	109/2	110/1	110/2	111
Section on Computer Techniques and Optimization			112/1			112/2			112/3			112/4

Scope. *Analytica Chimica Acta* publishes original papers, short communications, and reviews dealing with every aspect of modern chemical analysis, both fundamental and applied. The section on *Computer Techniques and Optimization* is devoted to new developments in chemical analysis by the application of computer techniques and by interdisciplinary approaches, including statistics, systems theory and operation research. The section deals with the following topics: Computerized acquisition, processing and evaluation of data. Computerized methods for the interpretation of analytical data including chemometrics, cluster analysis, and pattern recognition. Storage and retrieval systems. Optimization procedures and their application. Automated analysis for industrial processes and quality control. Organizational problems.

Submission of Papers. Manuscripts (three copies) should be submitted to:
for *Analytica Chimica Acta:* Dr. A. M. G. Macdonald, Department of Chemistry, The University, P.O. Box 363; Birmingham B15 2TT, England;
for the section on *Computer Techniques and Optimization:* Dr. J. T. Clerc, Universität Bern, Pharmazeutisches Institut, Sahlistrasse 10, CH-3012 Bern, Switzerland.

Information for Authors. Papers in English, French and German are published. There are no page charges. Manuscripts should conform in layout and style to the papers published in this Volume. Authors should consult Vol. 102, p. 253 for detailed information. Reprints of this information are available from the Editors or from: Elsevier Editorial Services Ltd., Mayfield House, 256 Banbury Road, Oxford OX2 7DE (Great Britain).

Reprints. Fifty reprints will be supplied free of charge. Additional reprints (minimum 100) can be ordered. An order form containing price quotations will be sent to the authors together with the proofs of their article.

Advertisements. Advertisement rates are available from the publisher.

Subscriptions. Subscriptions should be sent to: Elsevier Scientific Publishing Company, P.O. Box 211, 1000 AE Amsterdam, The Netherlands. The section on *Computer Techniques and Optimization* can be subscribed to separately.

Publication. *Analytica Chimica Acta* (including the section on *Computer Techniques and Optimization*) appears in 9 volumes in 1979. The subscription for 1979 (Vols. 104–112) is Dfl. 1179.00 plus Dfl. 135.00 (postage) (Total approx. U.S. $536.32). The subscription for the *Computer Techniques and Optimization* section only (Vol. 112) is Dfl. 131.00 plus Dfl. 15.00 (postage) (Total approx. U.S. $64.89). Journals are sent automatically by air mail to the U.S.A. and Canada at no extra cost and to Japan, Australia and New Zealand for a small additional postal charge. All earlier volumes (Vols. 1–95) except Vols. 23 and 28 are available at Dfl. 144.00 (U.S. $64.00), plus Dfl. 10.00 (U.S. $4.44) postage and handling, per volume.

Claims for issues not received should be made within three months of publication of the issue, otherwise they cannot be honoured free of charge.

Customers in the U.S.A. and Canada who wish to obtain additional bibliographic information on this and other Elsevier journals should contact Elsevier/North Holland Inc., Journal Information Center, 52, Vanderbilt Avenue, New York, NY 10017. Tel: (212) 867-9040.

ANALYTICA CHIMICA ACTA
VOL. 104 (1979)

ANALYTICA CHIMICA ACTA

International journal devoted to all branches of analytical chemistry

ELSEVIER SCIENTIFIC PUBLISHING COMPANY

Anal. Chim. Acta, Vol. 104 (1979)

Analytica Chimica Acta, 104 (1979) 1—9

DETERMINATION OF CORRECTION CONSTANTS IN X-RAY FLUORESCENCE SPECTROMETRY BY A MULTIVARIATE LEAST-SQUARES METHOD

B. W. BUDESINSKY

Phelps Dodge Corporation, Morenci, Arizona 85540 (U.S.A.)

(Received 15th April 1978)

SUMMARY

The multivariate least-squares method in combination with the Doolittle—Crout method is used for calculation of Lachance—Traill and Rasberry—Heinrich correction coefficients from experimental data. Inter-element, structural and particle size effects are thus taken into the account. The approach has been tested on the following systems: iron—nickel—chromium, copper—iron—sulfur (reverberatory matte), copper—iron—sulfur—silica—calcium oxide—aluminium oxide (copper concentrate) and copper—ferrous oxide—silica—calcium oxide—aluminum oxide (reverberatory slag). The average relative deviation does not exceed 1.04% for the Rasberry—Heinrich method and 2.17% for the Lachance—Traill method.

Shiraiwa and Fujino [1] and Criss and Birks [2] have used the theoretical relationship between fluorescence intensity and concentration of elements for estimation of the elements. The method works quite well, its only significant disadvantage being that it requires a large computer. Lachance and Traill [3], Rasberry and Heinrich [4] and Claisse and Quintin [5] have developed empirical or semi-empirical relationships between x-ray intensity and concentration. Those methods give reasonable results for alloys and for liquid or solid solutions. Their main advantage is relatively simple mathematics so that a minicomputer or even a desk calculator can be used for the calculation of results. Recently [6—8], a combination of both types of methods has been used. The theoretical relationship between intensity and concentration is used to calculate the correction constants of the empirical and semi-empirical methods. That relatively extensive calculation has to be done only once for given conditions (type of the x-ray tube and geometry of the x-ray spectrometer), so that the remaining practical calculation is again very simple.

For efficient analysis, powder specimens are most convenient. Unfortunately, the particle size and structural effects can then affect the quality of the analysis. Criss [9] described an interesting study of particle size effect, and suggested a method of eliminating a large part of the effect. However, the structural effect cannot be eliminated that way [10], because a knowledge of the spatial distribution of all atoms in the specimen would be required to estimate the theoretical correction constant.

The difficulties with powder specimens raise the question of whether a statistical method of determining the correction constants from standard specimens of a particular type, with respect to particle size and structure, would not be the optimal solution. That approach would eliminate the need for knowledge of the spectrometer geometry, of the calculation of mixed absorption coefficients for chemical compounds, and of the spectral distribution of the primary spectrum from the tube. Moreover, there would be no need for lengthy calculations, and, last but not least, the effects of particle size and structure would be eliminated. It is noteworthy that a correct statistical approach based on the multivariate least-squares method has not yet been employed for the determination of correction constants. Such an approach is described below.

EXPERIMENTAL

Apparatus

The instrument used was a Norelco Corporation (Mount Vernon, N.Y.) universal x-ray vacuum spectrometer with a chromium target tube.

The specimens were ground by means of a Wigl-bug (Crescent Dental Co., Chicago, Ill.) with a tungsten carbide capsule of 6-ml effective volume.

Materials

The copper concentrates, reverberatory mattes and slags were the usual daily samples. They were analyzed by conventional wet chemical methods: potentiometry with cerium(IV) for iron, electrolytic gravimetry for copper, barium sulfate gravimetry for sulfur, titration with permanganate via the oxalate for calcium, silicon dioxide gravimetry for silica, and gravimetry as aluminum phosphate for aluminum [11]. All chemicals used were Baker-Analyzed reagents.

Measurements

Plastic cups of 26-mm diameter and 7-ml effective volume with a 1-mm hole in the bottom (for measurements in vacuum) were used. About 2 g of specimen (300 mesh) was placed into each cup, covered with Spex-Film (Spex Industries, Inc., Metuchen, N.J.), inserted into the metallic holder, tapped gently on a bakelite plate and inserted into the spectrometer. The parameters of measurement for the individual elements are listed in Table 1.

THEORETICAL

Semi-empirical equations

The relationship between the relative intensity R_A of a particular element (or compound) A and the concentrations c_A, c_B, ... c_Z of other elements (or compounds) is given, according to Lachance and Traill [3], by the equation

$$c_A/R_A = 1 + \sum_B^Z A_X c_X \tag{1}$$

or, according to Rasberry and Heinrich [4], by the equation

$$c_A/R_A = 1 + \sum_B^Z A_X c_X + [1/(1 + c_A)] \sum_B^Z \bar{A}_X c_X \tag{2}$$

where A_X and $\bar{A}_X$ are the corresponding correction constants for the elements (or compounds) B, C, ...Z for the determination of A. An important condition must be met, at least approximately, for both eqns. (1) and (2):

$$\sum_A^Z c_X = 1 \tag{3}$$

provided that the concentration of the individual elements (or compounds) is expressed as a weight fraction of the total weight of the specimen.

If the terms

$$y_i = (c_A/R_A - 1)_i \tag{4}$$

$$x_{ij} = (c_X)_i \tag{5}$$

are introduced for the Lachance—Traill method, or

$$x_{ij} = [c_X/(1 + c_A)]_i \tag{6}$$

for the Rasberry—Heinrich method, where i designates the specimen and j the element (= A, B, C, ...Z), then for both eqn. (1) and eqn. (2),

$$y_i = \sum_1^J k_j x_{ij} \tag{7}$$

where $k_j = A_X$ and x_{ij} is given by eqn. (5) or $k_j = \bar{A}_X$ and x_{ij} is given by eqn. (6).

Multivariate least-squares method

If I specimens of the given type are analyzed, the squared total deviation is then

$$Q = \sum_1^I w_i (y_i - \sum_1^J k_j x_{ij})^2 \tag{8}$$

where w_i is the statistical weight of the specimen i analysis. If the value of w_i is considered a constant (see below), the minimum deviation requires that

$$\delta Q/\delta k_r = -2w_i \sum_1^I (y_i - \sum_1^J k_j x_{ij})\, x_{ir} = 0 \tag{9}$$

TABLE 1

Instrument settings for individual elements

Parameter	Element[a]					
	Fe	Cu	Ca	S	Si	Al
Pulse-height analyzer base-line (V)	8.0	9.0	6.0	12.0	11.0	9.0
Pulse-height analyzer window (V)	25.0	46.0	21.0	16.0	13.0	12.0
Measurement time (s)	20	10	10	20	50	50
Spectrometer angle, 2θ (°)	57.55	45.05	14.95	45.87	79.21	115.09
Crystal	LiF	LiF	PET[b]	PET	PET	PET
Path medium	air	air v	vac[c]	vac	vac	vac
Detector[d]	S	S	P	P	P	P
Detector voltage (kV)	0.8	0.8	1.5	1.5	1.5	1.5

[a]X-ray tube voltage, 45 kV; current, 18 mA; linear amplifier attenuation 5; and coarse collimation were used throughout. [b]Pentaerythritol. [c]Pressure 0.2 mm Hg (10% methane and 90% argon). [d]S is the scintillation detector and P the proportional detector. All the measured intensities were corrected for the counting dead-time.

Thus after rearrangement:

$$\sum_1^I x_{ir} \left(\sum_1^J k_j x_{ij}\right) = \sum_1^I y_i x_{ir} \tag{10}$$

or

$$\begin{aligned}
k_1 \sum_1^I x_{i1}x_{i1} + k_2 \sum_1^I x_{i1}x_{i2} + \cdots + k_J \sum_1^I x_{i1}x_{iJ} &= \sum_1^I y_i x_{i1} \\
k_1 \sum_1^I x_{i2}x_{i1} + k_2 \sum_1^I x_{i2}x_{i2} + \cdots + k_J \sum_1^I x_{i2}x_{iJ} &= \sum_1^I y_i x_{i2} \qquad (11) \\
k_1 \sum_1^I x_{iJ}x_{i1} + k_2 \sum_1^I x_{iJ}x_{i2} + \cdots + k_J \sum_1^I x_{iJ}x_{iJ} &= \sum_1^I y_i x_{iJ}
\end{aligned}$$

where the coefficients $\Sigma_1^I x_{ir}x_{ij}$ on the left-hand side represent a symmetric matrix. Methods for the solution of eqn. (11) are either direct (Gauss [12], Crout [13], Doolittle [14], Margenau and Murphy [15]) or indirect, i.e. by iteration (Gauss and Seidel [16], Jacobi [17], Hestenes and Stiefel [18], Southwell [19]). The latter methods are more accurate (the use of a computer or calculator is assumed); however, the convergence of the iteration still remains a problem in some cases. For that reason, the direct methods, of which the Doolittle method and the very similar Crout method modified for symmetric matrixes are the most economical, are preferred here. Final refinement of results can always be made by means of an iteration.

The method used is described in detail by Ralston [14].

Statistical weight

The effect of statistical weight was examined for the Lachance—Traill method on a theoretical model of three elements. The results obtained (Table 2) show that the statistical weight increases with increased change in concentration of individual elements, Δc_x, and increased relative intensity, R_A, so that

$$w_i = K_A(\Delta c_A, \Delta c_B, \ldots R_A)_i \qquad (12)$$

where K_A is the proportionality constant.

To eliminate the effect of statistical weight in practice, it is therefore advisable to use standards with a concentration distribution similar to those of normal samples.

Calculation of x-ray analyses

The values of the correction constants A_X and $\bar{A}_X$ for various specimens were determined by the method described above. They are collected in Table 3. The corresponding experimental values of the relative intensities are shown in Table 4.

The calculations of practical determinations were done by means of the iterative method described earlier [7], which is a modification of the Gauss—Seidel method [16]. The results obtained are presented in Table 5.

CONCLUSIONS

The multivariate least-squares method proposed for the estimation of correction constants improves the precision and accuracy of determinations compared with the original methods where the correction constants were estimated either graphically or by direct solution of the corresponding system of simultaneous linear equations. If J is the number of elements to be

TABLE 2

The effect of concentration distribution and relative intensity values on statistical weight for a theoretical model[a]

Δc_A		0.0			0.2			0.4			0.6	
Δc_B	R_A	$\bar{A}_B$	A_C	R_A	$\bar{A}_B$	A_C	R_A	$\bar{A}_B$	A_C	R_A	$\bar{A}_B$	A_C
0.0[b]	0.0392	—	—	0.1395	0.5091	2.0024	0.2857	0.5085	2.0023	0.5185	0.5028	2.0016
0.2[b]	0.0488	0.5070	2.0021	0.1818	0.5014	2.0015	0.4000	0.5009	2.0014	0.8235	0.4999	2.0013
0.4[b]	0.0645	0.5003	2.0013	0.2609	0.5008	2.0014	0.6667	0.5001	2.0013	—	—	—
0.6[b]	0.0952	0.4998	2.0013	0.4615	0.4999	2.0013	—	—	—	—	—	—
0.8[b]	0.1818	0.4999	2.0013	—	—	—	—	—	—	—	—	—
0.0[c]	0.0488	—	—	0.1818	0.4929	1.9951	0.4000	0.4986	1.9979	0.8235	0.4999	1.9986
0.3[c]	0.0769	0.4982	1.9977	0.3333	0.4996	1.9984	—	—	—	—	—	—
0.6[c]	0.1818	0.4999	1.9986	—	—	—	—	—	—	—	—	—

[a]Theoretical values of the Lachance—Traill equation: $\bar{A}_B = -0.5000$, $A_C = 2.0000$.
$\Delta c_A = c'_A - c_A$, $\Delta c_B = c'_B - c_B$, $c_A + c_B + c_C = c'_A + c'_B + c'_C = 1$.
[b]$c_A = c_B = 0.1$.
[c]$c_A = 0.1$, $c_B = 0.3$.

TABLE 3

Correction constants

(a) Iron—nickel—chromium alloy

A	A_{Fe}	A_{Ni}	A_{Cr}
Fe	—	−0.4776	2.1815
Ni	1.6052	—	1.4949
Cr	−0.3288	−0.1663	—

	A_{Fe}	$\bar{A}_{Fe}$	A_{Ni}	$\bar{A}_{Ni}$	A_{Cr}	$\bar{A}_{Cr}$
Fe[a]	—	—	−0.4085	−0.2814	0.9977	2.0224
Ni[a]	2.4678	−1.2095	—	—	−0.3460	2.8065
Cr[a]	−0.1887	−0.1808	2.0448	−2.6284	—	—
Fe[b]	—	—	—	−0.4813	2.0829	—
Ni[b]	1.6052	—	—	—	1.4949	—
Cr[b]	—	−0.4011	—	−0.1971	—	—

(b) Reverberatory matte

A	A_{Fe}	A_{Cu}	A_S
Fe	—	−0.6087	−0.1644
Cu	−0.6365	—	1.5919
S	3.2203	1.2082	—

	A_{Fe}	$\bar{A}_{Fe}$	A_{Cu}	$\bar{A}_{Cu}$	A_S	$\bar{A}_S$
Fe[a]	—	—	0.7288	−2.5483	−6.2463	9.1196
Cu[a]	13.5574	−19.6067	—	—	−16.5287	25.0302
S[a]	−10.2538	18.0423	−10.1404	13.5166	—	—
Fe[b]	—	—	—	−0.5720	—	−0.5258
Cu[b]	—	−0.6541	—	—	1.4015	—
S[b]	3.2206	—	1.2082	—	—	—

(c) Copper concentrate

A	A_{Fe}	A_{Cu}	A_{CaO}	A_S	A_{SiO_2}	$A_{Al_2O_3}$
Fe	—	−0.5754	0.7390	0.3114	−1.5883	−7.3113
Cu	2.7804	—	−3.9160	−2.4717	−1.8794	15.2729
CaO	−17.6763	26.8692	—	−11.8752	130.7534	−52.2711
S	2.7280	1.0485	8.9835	—	4.9016	−7.3894
SiO_2	−10.5836	7.4547	15.4435	5.5086	—	−30.6359
Al_2O_3	1.5648	12.7304	73.5286	−8.9888	−2.1003	—

(d) Reverberatory slag

A	A_{FeO}	A_{Cu}	A_{CaO}	A_{SiO_2}	$A_{Al_2O_3}$
FeO	—	−7.6996	−0.5968	−0.7291	0.3356
Cu	−0.4005	—	−1.0570	−1.6360	1.4044
CaO	17.9882	−288.0844	—	−34.3467	95.8665

TABLE 3 (continued)

A	A_{FeO}	A_{Cu}	A_{CaO}	A_{SiO_2}	$A_{Al_2O_3}$
SiO_2	1.5903	−4.4715	3.2959	—	−0.6790
Al_2O_3	0.7916	58.8968	10.6338	−0.6682	—

[a]Modified Rasberry–Heinrich method [7].
[b]Original Rasberry–Heinrich method.

TABLE 4

Relative intensities R_A

(a) Iron–nickel–chromium alloy [4]

Specimen No.	R_{Fe}	R_{Ni}	R_{Cr}
1a	0.4511	0.0203	0.3258
2a	0.4971	0.0416	0.2651
3a	0.3529	0.0821	0.3311
4a	0.4343	0.0898	0.2582
5a	0.5298	0.0343	0.2536
6a	0.1460	0.4367	0.2072
7a	0.0125	0.5630	0.2263

(b) Reverberatory matte

Specimen No.	R_{Fe}	R_{Cu}	R_S
1b	0.4717	0.2710	0.1093
2b	0.4394	0.3042	0.1059
3b	0.4210	0.3131	0.1126
4b	0.4295	0.3062	0.1042
5b	0.4395	0.3094	0.1052

(c) Copper concentrate

Specimen No.	R_{Fe}	R_{Cu}	R_{Ca}	R_S	R_{Si}	R_{Al}
1c	0.3792	0.2387	0.0015	0.1453	0.0349	0.0080
2c	0.3694	0.2395	0.0011	0.1463	0.0282	0.0074
3c	0.3760	0.2353	0.0021	0.1440	0.0457	0.0074
4c	0.3789	0.2505	0.0009	0.1520	0.0251	0.0066
5c	0.3894	0.2542	0.0010	0.1555	0.0245	0.0073
6c	0.3817	0.2364	0.0015	0.1615	0.0402	0.0106
7c	0.3684	0.2357	0.0017	0.1531	0.0357	0.0083
8c	0.3838	0.2427	0.0013	0.1592	0.0347	0.0091

(d) Reverberatory slag

Specimen No.	R_{Fe}	R_{Cu}	R_{Ca}	R_{Si}	R_{Al}
1d	0.7501	0.0204	0.0112	0.1846	0.0274
2d	0.7316	0.0192	0.0148	0.1895	0.0320
3d	0.7126	0.0180	0.0183	0.1951	0.0298
4d	0.6626	0.0168	0.0334	0.2028	0.0322
5d	0.6761	0.0224	0.0198	0.2155	0.0371
6d	0.6772	0.0217	0.0208	0.2297	0.0414

TABLE 5

Comparison of wet chemical and x-ray methods[a]

(a) Iron—nickel—chromium alloy

Specimen No.	% Fe				% Ni				% Cr			
	Wet	LT	RH_o	RH_m	Wet	LT	RH_o	RH_m	Wet	LT	RH_o	RH
1a	68.38	68.59	68.15	68.61	4.98	5.02	5.02	5.05	25.25	24.96	25.21	25.
2a	69.45	69.07	68.96	68.66	9.96	10.02	10.01	9.90	19.88	20.05	19.96	19.
3a	52.80	52.51	52.81	53.46	19.27	18.37	18.44	19.06	26.96	26.38	26.62	27.
4a	59.19	58.23	58.77	58.05	20.02	20.06	20.12	20.17	19.88	20.01	19.89	19.
5a	71.59	72.74	72.49	72.10	8.29	8.41	8.38	8.22	18.79	18.94	18.80	18.
6a	15.01	15.54	15.85	15.01	64.29	65.92	66.07	65.16	16.88	17.39	17.30	16.
7a	1.40	1.35	1.32	1.39	72.60	74.13	74.13	72.78	20.30	19.74	19.77	20.
AD (±)	—	0.510	0.424	0.501	—	0.617	0.631	0.230	—	0.341	0.204	0.

(b) Reverberatory matte

Specimen No.	% Fe				% Cu				% S			
	Wet	LT	RH_o	RH_m	Wet	LT	RH_o	RH_m	Wet	LT	RH_o	RH
1b	35.60	35.55	35.53	35.43	32.83	32.96	32.91	32.87	27.64	27.79	27.78	27.
2b	32.00	32.17	32.32	31.89	37.17	36.92	36.95	37.06	26.42	26.28	26.34	26.
3b	30.60	30.20	30.22	30.46	38.62	39.01	38.93	38.64	27.02	27.52	27.51	27.
4b	31.40	31.47	31.63	31.20	37.23	36.98	37.02	37.24	26.16	25.63	25.69	25.
5b	31.80	32.03	32.23	31.64	37.52	37.50	37.56	37.64	26.09	26.13	26.21	26.
AD (±)	—	0.184	0.286	0.156	—	0.208	0.172	0.060	—	0.272	0.260	0.

(c) Copper concentrate

Specimen No.	% Fe		% Cu		% CaO		% S		% SiO_2		% Al_2O_3	
	Wet	LT	Wet	LT	Wet	LT	Wet	LT	Wet	LT	Wet	LT
1c	27.51	27.27	27.50	27.56	0.78	0.79	31.90	31.93	4.77	4.98	2.08	2.
2c	27.44	27.55	27.71	27.97	0.50	0.47	31.67	31.48	4.03	4.02	1.83	1.
3c	27.90	27.82	24.85	24.76	1.35	1.29	33.44	33.32	6.45	6.35	1.71	1.
4c	29.55	29.43	28.50	28.49	0.33	0.31	33.53	33.41	3.68	3.63	1.39	1.
5c	29.50	29.61	29.67	29.30	0.37	0.34	34.40	34.19	3.55	3.61	1.69	1.
6c	28.63	28.48	25.38	25.11	0.82	0.69	36.05	36.02	5.32	5.49	1.88	1.
7c	28.11	27.96	25.42	25.48	0.74	0.76	33.75	33.90	5.01	4.98	1.70	1.
8c	29.19	29.06	26.55	26.42	0.59	0.54	35.41	35.42	4.87	4.83	1.82	1.
AD (±)	—	0.136	—	0.156	—	0.044	—	0.108	—	0.084	—	0.

(d) Reverberatory slag

Specimen No.	% FeO		% Cu		% CaO		% SiO_2		% Al_2O_3	
	Wet	LT	Wet	LT	Wet	LT	Wet	LT	Wet	LT
1d	53.39	53.37	0.56	0.55	2.04	1.99	34.30	34.29	4.82	4.74
2d	51.46	51.44	0.49	0.50	3.38	3.32	35.11	35.35	5.75	5.83
3d	50.56	50.37	0.43	0.47	2.40	2.41	35.80	35.61	5.08	5.04
4d	46.06	46.45	0.43	0.45	3.41	3.23	36.52	36.25	5.66	5.57
5d	46.68	46.89	0.43	0.61	1.50	1.44	37.03	27.16	6.17	6.08
6d	46.24	46.62	9.54	0.55	0.89	0.87	39.40	39.11	6.30	6.31
AD (±)	—	0.202	—	0.018	—	0.063	—	0.188	—	0.060

[a]LT is the Lachance—Traill method; RH_o and RH_m refer to the original and modified Rasberry—Heinrich methods, respectively. AD is the average deviation.

determined, then the minimum number of standards to be used is $J - 1$ for the Lachance—Traill method and the original Rasberry—Heinrich method (either $A_X \neq 0$, $\bar{A}_X = 0$, or $A_X \doteq 0$, $\bar{A}_X \neq 0$), and $2(J - 1)$ for the modified Rasberry—Heinrich method (A_X, $\bar{A}_X \neq 0$) [7] and the Claisse—Quintin method (where the cross-product terms are dropped) [5]. In agreement with previous findings, the modified Rasberry—Heinrich method [7] gives better results even in the multivariate least-squares modification than the original method (see Table 5). As Table 2 shows, the concentrations of some elements in standards can be zero; this depends on the distribution of elements in the given specimens.

Because of the different conditions and varying value of the statistical weight, the values of the correction constants are not the same as those determined by purely theoretical methods. This is particularly true for powder specimens and specimens containing some trace elements where the elimination of corresponding effects (see above) is already included in the value of the correction constant.

The least-squares modification of the Lachance—Traill and Rasberry—Heinrich methods described here is particularly appropriate for those who prefer to run some standards rather than indulge in lengthy theoretical calculations.

REFERENCES

1 T. Shiraiwa and N. Fujino, Japan. J. Appl. Phys., 5 (1966) 886.
2 J. W. Criss and L. S. Birks, Anal. Chem., 40 (1968) 1080.
3 G. R. Lachance and R. J. Traill, Can. J. Spectrosc., 11 (1966) 43.
4 S. D. Rasberry and K. F. J. Heinrich, Anal. Chem., 46 (1974) 81.
5 F. Claisse and M. Quintin, Can. J. Spectrosc., 12 (1967) 129.
6 R. Rousseau and F. Claisse, X-Ray Spectrom., 3 (1974) 129.
7 B. W. Budesinsky, X-Ray Spectrom., 4 (1975) 166.
8 A. R. Hawthorne and R. P. Gardner, Anal. Chem., 48 (1976) 2130.
9 J. W. Criss, Anal. Chem., 48 (1976) 179.
10 B. W. Budesinsky, Anal. Chim. Acta, 77 (1975) 87.
11 I. M. Kolthoff, E. B. Sandell, E. J. Meehan and S. Bruckenstein, Quantitative Chemical Analysis, Macmillan, London, 1969.
12 L. Fox, An Introduction to Numerical Linear Algebra, Oxford University Press, London, 1964.
13 P. D. Crout, Trans. AIEE, 60 (1941) 1235.
14 A. Ralston, A First Course in Numerical Analysis, McGraw-Hill, New York, 1965.
15 H. Margenau and G. M. Murphy, The Mathematics of Physics and Chemistry, Krieger, Huntington, N. Y., 1976, p. 498.
16 D. M. Young, Iterative Solution of Large Linear Systems, Academic Press, New York, 1971.
17 H. H. Goldstine, F. J. Murray and J. von Neumann, J. Assoc. Comp. Mach., 6 (1959) 59.
18 M. R. Hestenes and E. Stiefel, J. Res. Nat. Bur. Stand., 49 (1952) 409.
19 R. V. Southwell, Relaxation Methods in Engineering Science, Oxford University Press, Fair Lawn, N. J., 1940.

Analytica Chimica Acta, 104 (1979) 11—19

A STUDY OF INTERNAL STANDARDIZATION IN THE ANALYSIS OF FINE GOLD WITH THE GLOW-DISCHARGE SOURCE

P. PILLE, P. R. LOWE and A. M. GILLESPIE
Rand Refinery, Germiston (South Africa)
and L. R. P. BUTLER*
National Physical Research Laboratory, P.O. Box 395, Pretoria (South Africa)
(Received 14th February 1978)

SUMMARY

Methods of internal standardization in the glow-discharge spectrometric analysis of gold are discussed. The method recommended by Jäger, based on the amount of material sputtered from the sample, gives less precise results for the gold content than when results are calculated by a simple difference method. The Jäger method is also shown to give a false impression of sensitivity where this does not exist at high concentrations. Results obtained by difference with a direct-reading spectrometer and glow-discharge source compare well with fire-assay results.

The Grimm glow-discharge lamp has proved to be a valuable source for the emission spectrochemical analysis of metal samples [1]. The remarkable constancy of emission, relative lack of interelement effects and ease of operation have permitted its successful application to the analyses of gold [2, 3], silver [4], copper-base alloys [5], aluminium and magnesium alloys [6], steel [7, 8], etc. Exceptional demands regarding precision and accuracy are required in the analysis of precious metals, especially where the matrix is to be assayed. If spectrometric methods are therefore to be applied, careful steps must be taken to reduce errors to a minimum.

The discharge parameters in the glow-discharge source are more controllable than in other sources, such as sparks and arcs, but changes in absolute spectral line intensities may take place. These are generally the result of crystal structure changes in the sample, the presence of gas inclusions, slight changes in the geometry of the lamp due to metal build-up, etc. The most obvious way to prevent intensity changes from these causes is to apply internal standardization principles as far as possible.

The concept of internal standardization has been dealt with in many standard reference works [9]. The use of a non-dispersed beam from the source (direct or zero-order reflection from a grating or reflection from the front face of a prism) is used by many manufacturers as a reference, but this is not a true indication of the metallic spectral emission from the source.

With the glow-discharge source in particular, the directly reflected beam should not be used as a reference, because the carrier gas radiates strongly and this radiation constitutes more than 90% of the total. It is therefore not representative of the sample radiation.

There is seldom an element present in an alloy which occurs in constant quantities and it is impractical to add one. This paper considers the methods available for internal standardization in the analysis of gold. It shows that at higher purity levels, the most satisfactory results are obtained by integrating for a constant time with no internal standardization. The trace and minor elements are determined directly and the major element, gold, is determined by summing the concentrations of the impurity elements and subtracting from 100%. This method is in contrast to that recommended by Jäger [2, 3] which is discussed below in some detail.

INTERNAL STANDARD METHODS

Gerlach method

The normally accepted internal standard method requires that the intensity of the reference signal remain constant [9]. An improvement in the precision of results may be expected only if the statistical variation of this signal is appreciably better than the variation of the analytical element signal and that it changes proportionally to it, i.e. $I_a/I_s = (I_a \pm \Delta I_a)/(I_s \pm \Delta I_s)$, where I_a and I_s are the intensities of the analytical and internal standard lines, respectively, and ΔI_a and ΔI_s are variations in these intensities.

The method fails when a change in the intensity of the reference signal is caused by a change in concentration, or if any other factor causes the two signals to change independently.

Intensity ratio—concentration ratio method [10]

The intensity ratio—concentration ratio method may be used where the reference or internal standard signals change in such a way that there is a definite dependence on the concentration of the analysed element, e.g. as with higher alloys. Thus

$$I_1/I_2 = F_{1,2}\,(C_1/C_2)$$

where F is the function relating the intensities of the spectral lines to their concentrations, and $C_1 + C_2 = 100\%$. For multiple element systems

$$I_i/I_s = F_{is}\,(C_i/C_s)$$

where s is the major component and i is a minor component.

This method is generally used in alloy analyses where the elements vary over a wide range of concentrations. The precision of measurement depends on the precision of measurement of each component and is considered later in this paper.

Jäger method

Jäger [2, 3] used a method for the analysis of gold whereby he attempted to measure the degree of sputtering and relate this to the intensity. The method included the determination of the slope factor, the integrated sputtering and the normalized intensity.

The slope factor a was defined as $a_{El} = C_{El}/I_{El}$, where C is the concentration of an element and I is the intensity for that element. Integrated sputtering (S) (a preferred term to Jäger's "sputtering rate") is defined as

$$S = \sum_{j=1}^{n} a_j I_j \quad (1 \leqslant j \leqslant n)$$

where n represents all the elements in a sample and I is the measured intensity. The normalized intensity (J_{El}) is defined as $J_{El} = a_{El} I_{El}/S$. The prerequisites for this third definition are stringent and are not always realized, especially over wide concentration ranges. The slope factor a is required to remain constant for a particular spectral line for all standards and samples. This implies that the intensity should increase linearly over the concentration interval of interest, i.e. no self-absorption or other effects affecting linearity should be experienced.

Another prerequisite is that all elements measured constitute the composition of the samples and add up to 100%. In addition, the major element (in this case, gold) must show sensitivity, i.e. a change of intensity with concentration at the levels measured.

Although there have been claims that the glow-discharge source is free of any self-absorption [1], recent studies have shown this assumption to be untrue, especially in the case of resonance lines [11, 12]. Figure 1 shows

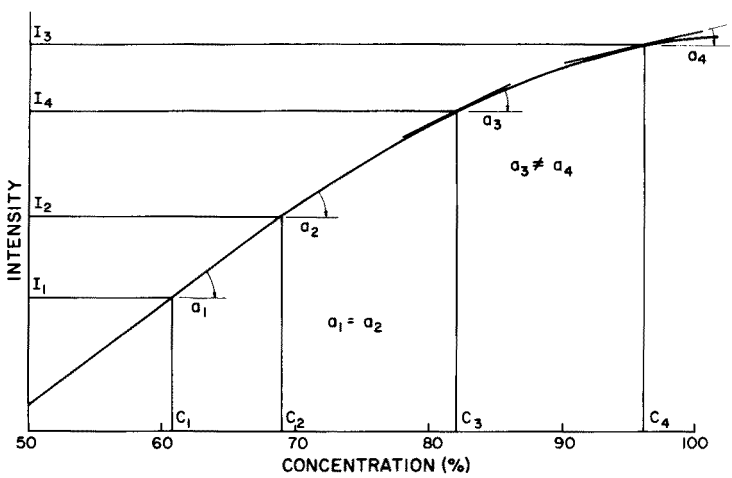

Fig. 1. Typical calibration curve obtained for an element at high concentrations with the glow-discharge source.

the relationship between intensity and concentration as measured for most spectral lines. There is a uniformly defined slope factor only in the linear portion C_1—C_2, but for C_3—C_4 there is no constant slope factor. Figure 2 shows the relationship of the slope factor a to concentration for the silver lines 381.1 nm which is a non-resonance line, and 338.3 nm which is a resonance line, determined in the region 2—14% silver. It can be seen that even the 381.1-nm line exhibits some change in the slope factor for an increase in concentration.

The Jäger definition requires that the raw intensity concentration graph is the same for all measured specimens. If for some reason (e.g. background) the graph does not pass through the origin, it will result in different slope factors which could lead to significant errors in the calculation, especially where samples fall outside the range covered by the standards.

Jäger calculated an average slope factor for a large number of standards over a range of concentrations. However, experience has shown that the slope factor may change continuously over a concentration range. This depends a good deal on the lamp discharge conditions and on the self-absorption properties of the spectral lines. Even under ideal conditions the phenomenon is evident at high concentrations. The compensation effects claimed for a difference in sputtering arising from different metallurgical histories, e.g. cast or rolled samples, may thus not hold.

In addition, the calibration function $J : C$ calculated by Jäger will always give a calculated slope of 1, even if an element does not show a true change of intensity with concentration change. This could lead one to believe that there is in fact a sensitivity change [3]. Thus the slope of the calibration curve is

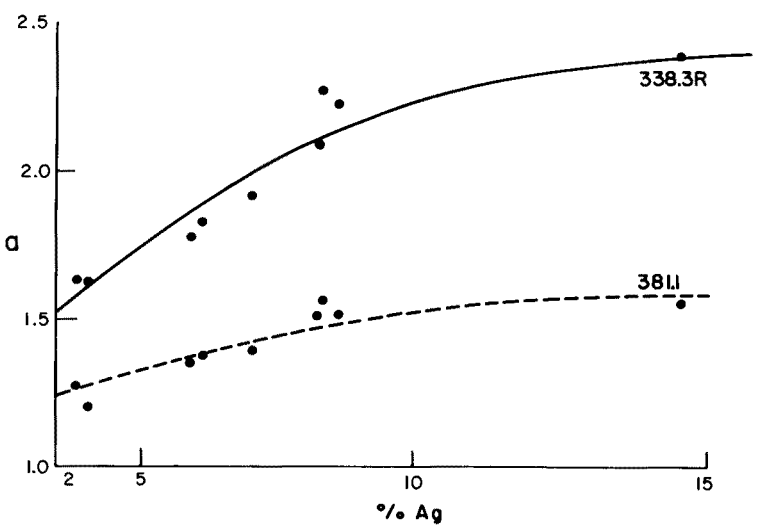

Fig. 2. Slope a factor obtained for two silver lines Ag 338.3 nm (R) and Ag 381.1 nm over the concentration range 4—15%. $a = C_{Ag}/I_{Ag}$.

$m = (J_2 - J_1)/(C_2 - C_1)$, but $J_i = a_i I_i/S$, hence

$m = (aI_2 - aI_1)/S\ (C_2 - C_1)$;

but

$$S = \sum_{i=1}^{n} a_i I_i = \sum_{i=1}^{n} C_i = 1\ (\equiv 100\%), \text{ hence}$$

$m = (aI_2 - aI_1)/1\ (C_2 - C_1)$

However, by definition, $a = C/I$, hence $aI_2 = C_2$ and $aI_1 = C_1$, and therefore $m = 1$.

In contrast, the raw intensity—concentration graph may not reveal the existence of sensitivity dI/dC over a specific concentration range.

The intensity ratio—concentration ratio method and the Jäger method in fact reduce to virtually the same functions. It has been clearly stated [10] that the ratio method must be applied very carefully and this must therefore apply to the Jäger method too. In fact, the methods may be applied only where the lines of all elements measured show a change of intensity with concentration and where background correction has been introduced.

EXPERIMENTAL

A large number of analyses was carried out to determine the most precise method for fine gold analysis. The gold alloys investigated were of bullion grade, i.e. +99.5% gold. The main impurities are silver, copper, lead, zinc and iron, with traces of platinum group metals and other metals.

Refined fine gold standards (chemically analysed and assayed) were exposed on a 1.5-m Ebert direct-reading spectrometer (Messrs R. S. V. Präzisionsmessgeräte, 8031 Hechendorf Pils., West Germany) fitted with a glow-discharge lamp. Lamp parameters selected were: gas pressure 500 Pa argon, voltage 1.2 kV, and current 100 mA. Raw intensity data were acquired by means of a SATI computer integrating for a constant time exposure period with a predetermined burn-in period. Table 1 shows the a factors obtained from the calibration samples.

TABLE 1

Slope factor a for elements in gold ca. 99.5% purity

	Au 312.2 nm	Ag 338.3 nm	Cu 324.7 nm	Pb 405.8 nm	Fe 302.0 nm	Zn 213.9 nm
Slope for raw I vs. C:	0	0.690	0.107	0.900	1.698	0.098

RESULTS AND DISCUSSION

The relationships between raw intensity and concentration were tested experimentally for several different spectral lines with a large number of pre-analysed standards. In Fig. 3 the intensities obtained are shown against the concentrations for the resonance gold line 242.8 nm and the non-resonance line 406.5 nm. It can be seen that even for the non-resonance line there is a distinct flattening off of the spread of results, indicated by the shaded area, above a concentration of 96%.

A *t*-test was run on the raw intensity for the highest and lowest refined gold production samples to investigate statistically if a significant change in intensity for gold took place across the analytical range selected. The results are summarized in Table 2. It may be seen that there is little or no difference in the measured intensities between the two series of measurements.

According to the method of Jäger, normalized data do however show a relationship between J_{Au} and C_{Au}. This casts doubt on the claim that gold can be determined "directly" at the 99.50% concentration level. It is suggested rather that Jäger normalization is due to the change in the impurities rather than in the matrix line intensities.

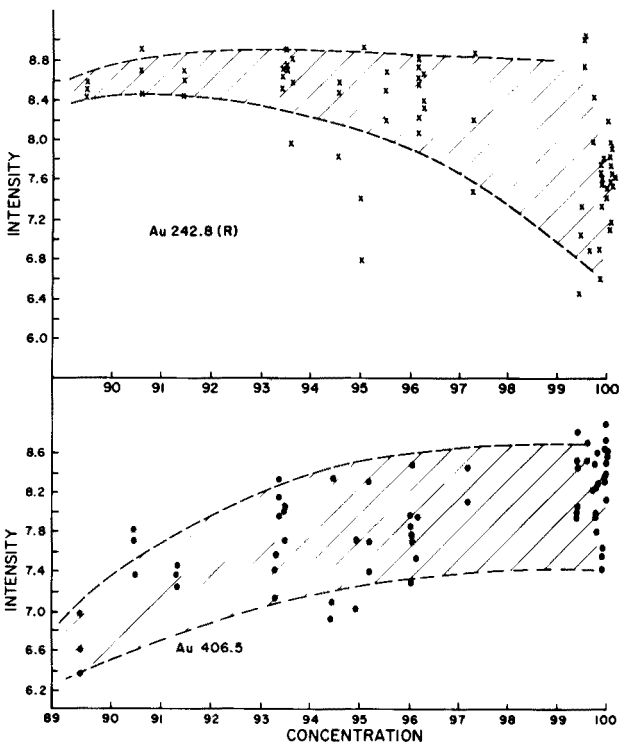

Fig. 3. Calibration graphs for the gold lines Au 242.8 nm and Au 406.5 nm based on raw intensity.

TABLE 2

Comparison of t-test for gold in two different samples

Sample (Au conc.)	99.78%	99.47%
Number of determinations (n)	10	10
Average intensity I	0.37841	0.37561
Variance S^2	11.818×10^{-5} (S_1^2)	3.907×10^{-5} (S_2^2)

F-test : $F = S_1^2/S_2^2 = 3.025$ (3.18 for 95% confidence)

$\therefore$ Variances may be pooled

$$S_w^2 = \frac{(n_1 - 1)\ S_1^2 + (n_2 - 1)\ S_2^2}{n_1 + n_2 - 2} = 8.736 \times 10^{-5}$$

Std. error of difference $S_w^2 = S^2 \cdot \frac{2}{10} = 4.18 \times 10^{-3}$

t-test: $[(I_1 - I_2)/S_w^2] \times [n_1\, n_2/(n + n_2)] = [(I_1 - I_2)/S_w^2] \times \frac{n}{2}$ (if $n_1 = n_2$)

= 0.6699 (1.812 for 90% confidence)

The contribution of various terms to the integrated sputtering of fine gold should be considered in order to understand how the relationship of J_{Au} and C_{Au} comes about:

$$S = \sum_{i=1}^{6} a_i I_i = a_{Au}.I_{Au} + a_{Ag}.I_{Ag} + a_{Cu}.I_{Cu} + a_{Pb}.I_{Pb} + a_{Fe}.I_{Fe} + a_{Zn}.I_{Zn}$$

The concentrations of the elements, zinc, iron and lead, are very low, their a factors are very small, and they may therefore be ignored. Thus:

$$S = a_{Au}.I_{Au} + a_{Ag}.I_{Ag} + a_{Cu}.I_{Cu}$$

If I_{Au} is a random intensity which shows no relation to C_{Au},

$$S = a_{Au}.I_{Au} + a_{Ag}.I_{Ag} + a_{Cu}.I_{Cu} = a_{Au}.I_{Au} + \sum (C_{El})$$

where $a_{Au}.I_{Au}$ is a response which varies between fixed values, i.e. it is noise.

According to the definition of normalized intensity, $J_{El} = a_{El}I_{El}/S$,

$$J_{Au} = a_{Au}.I_{Au}/[a_{Au}.I_{Au} + \sum (a_{El}.I_{El})]$$

This term can be expanded to

$$J_{Au} = 1 - \sum (a_{El}.I_{El}) + \sum (a_{El}.I_{El})^2 - \sum (a_{El}.I_{El})^3 \cdots\cdots$$

whenever $\sum (a_{El}.I_{El})$ is small in relation to $a_{Au}.I_{Au}$.

It can now be seen that the normalized intensity (J_{Au}) of gold is a function of the intensity of silver and copper, but not of gold itself. Thus a gold calibration which owes its existence to silver and copper has been artificially created. Mathematically, a calibration has been achieved although no physical measurement is at hand, i.e. in essence gold is measured by difference. Since the Jäger approach involved several assumptions which do not hold, the use of raw intensities to determine silver and copper is more appropriate. Subtraction of these major impurities from the total metal content (i.e. effectively 100.000%) yields the most reliable figure by difference.

Gold by difference

If two elements (1 and 2) present in the gold are measured with a precision S, then the total variance can be expressed as

$$S^2 \text{ total} = (n_1 S_1^2 + n_2 S_2^2)/(n_1 + n_2 - 2)$$

where n is the number of measurements. The main impurities in fine gold are silver and copper. These may be determined with a precision of ca. 1.2% relative. Since the sum of these impurities never exceeds 0.5% the precision on the gold should be of the order of 99.5 ± 0.006%. This precision is considered acceptable as the fire-assay method gives a value of 99.5 ± 0.005%.

Comparison of various internal standardization methods

Figure 4 shows the calibration graphs for silver by the three methods: (a) raw intensity, (b) Jäger method, and (c) the usual intensity ratio (Gerlach) method, with gold as internal standard. It can be seen that the scatter of points around the raw intensity concentration graph is less than for the other two cases. It can then be deduced that the use of gold for internal standardization causes less precise values to be obtained for silver and other impurity elements because of the variation in its intensity.

Table 3 shows values obtained for gold by difference, by the Jäger method, and by accurate fire assay.

Conclusions

The results of the investigation show that the use of the integrated sputtering factor as a means for internal standardization does not improve results when fine gold is analysed. The success of the Jäger method depends markedly on the assumptions that linearity for intensity vs. concentration

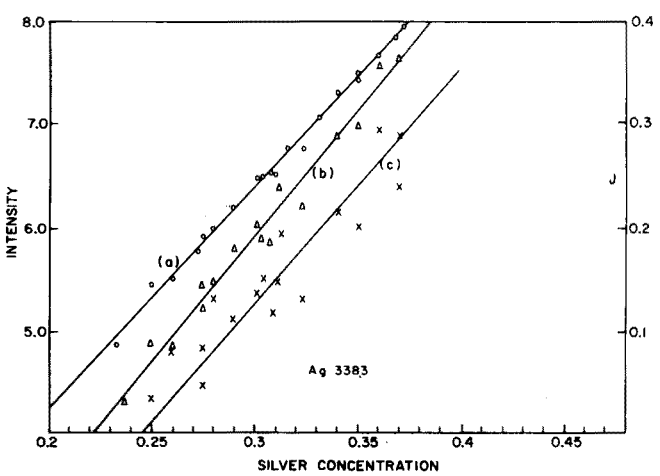

Fig. 4. Comparison between calibration graphs for silver at 338.3 nm based on (a) raw intensity (o), (b) Jäger method, $a_{Ag}I_{Ag}/S$ (Δ), and (c) Gerlach method, I_{Ag}/I_{Au} (242.8 nm) (×).

TABLE 3

Comparison of gold values obtained by various methods

Reference fire assay standard	Au by (J_{Au})	Au by difference (Gerlach)	Au by difference (Raw I of Cu and Ag)
99.50	99.517	99.513	99.508
99.65	99.628	99.633	99.647
99.67	99.657	99.668	99.673
99.70	99.686	99.692	99.712
99.72	99.734	99.730	99.718
99.64	99.647	99.642	99.640
99.68	99.661	99.675	99.677
99.70	99.728	99.725	99.695
99.63	99.628	99.625	99.633
99.62	99.643	99.639	99.624
99.65	99.640	99.641	99.658
99.75	99.766	99.767	99.748
99.54	99.517	99.531	99.550

data exists for all elements and that the concentrations of all elements measured add up to 100%. These conditions do not hold for pure metals.

In addition, it has been shown that the use of the matrix element as a reference when it does not exhibit sensitivity, adversely affects the precision of results. This is true for gold as well as for other elements.

If the impurity elements are each determined accurately and their sum subtracted from 100%, the difference gives a more accurate figure than does the Jäger method of normalization. These findings hold only for fine gold, where the assumptions made to qualify the Jäger method do not apply.

The Jäger method, which is almost identical to the intensity ratio—concentration ratio method, is valid in cases where sensitivity exists and where background does not play a role.

Valuable suggestions by Dr Phil Gerrard of Johnson Matthey are gratefully acknowledged.

REFERENCES

1 W. Grimm, Spectrochim. Acta, Part B, 23 (1968) 443.
2 H. Jäger, Anal. Chim. Acta, 58 (1972) 57.
3 H. Jäger, Anal. Chim. Acta, 60 (1972) 303.
4 N. P. Ferreira, Analyst, 103 (1978) 607.
5 R. A. Kruger, C. J. Liebenberg, R. G. Böhmer and L. R. P. Butler, Analyst, 102 (1977) 949.
6 K. Laqua, Pure Appl. Chem., 49 (1977) 1595.
7 H. W. Radmacher, Spectrochim. Acta, Part B, 30 (1975) 353.
8 A. Butterworth, British Steel Technical Report/552/1/75c. (1975).
9 W. Gerlach, Z. Anorg. Chem., 142 (1925) 383.
10 American Society for Testing Materials, Methods for Emission Spectrochemical Analysis, 6th edn., E158 (1971) 127.
11 C. D. West and H. G. C. Human, Spectrochim. Acta, Part B, 31 (1976) 81.
12 R. A. Kruger, D.Sc. thesis, University of Pretoria, S.A. (1976).

Analytica Chimica Acta, 104 (1979) 21—28

EXTRACTION BASED ON THE FLOW-INJECTION PRINCIPLE
Part 2. Determination of Codeine as the Picrate Ion-pair in Acetylsalicylic acid Tablets

BO KARLBERG*, PER-ARNE JOHANSSON and SIDSEL THELANDER
Astra Pharmaceuticals AB, Analytical Control, S-151 85 Södertälje (Sweden)
(Received 10th July 1978)

SUMMARY

Codeine in aqueous samples is extracted as its picrate ion pair into chloroform in a continuous flow system. The sample is introduced into an aqueous picrate stream buffered at pH 6.5; its dispersion gives controlled mixing before the aqueous stream is segmented by a chloroform stream. A specially constructed fitting is included to produce segments, typically 5—10 mm long, which pass into a Teflon coil (2 m long; inner diameter, 0.8 mm). At the outlet of the coil, the phases are separated and a fraction of the chloroform phase is passed through a spectrophotometric flow cell. The sample volume is in the range 25—40 μl, the sampling rate about 60/h, and the relative standard deviation of the order of 1%.

In a previous paper [1] an extraction system was described allowing rapid extractions in a continuous stream of two phases. The sample, typically 25 μl, was introduced into the aqueous phase just before segmentation with the organic phase took place. The extraction process was very simple: caffeine in the aqueous phase was extracted into the chloroform phase, and after separation of the two phases, the absorbance of the chloroform phase was measured in a flow-through spectrophotometric cell. A sampling frequency of about 100/h was readily accomplished.

A logical extension of the work was the adaptation of the system to more complicated extraction procedures. A very common application at this laboratory was selected, namely the determination of codeine in acetylsalicylic acid tablets. The USP method [2] for codeine (in codeine phosphate tablets) comprises rather tedious operations, such as intermittent shaking for 2 h, filtering, evaporation to dryness, etc., and so the picrate ion-pair method [3—7] was adopted. In this method picrate is added to the test solution, the codeine picrate ion pair is extracted into an organic phase, e.g. chloroform, and the absorbance is measured.

THEORY

The extraction of the codeine cation, HB^+, into chloroform as an ion pair with the picrate ion, P^-,

$HB^+_{aq} + P^-_{aq} \rightleftharpoons HBP_{org}$

is governed by the extraction constant

$$K_{ex(HBP)} = [HBP]_{org}/[HB^+]\,[P^-] \quad (1)$$

(The square brackets denote molar concentrations.) Obviously, the extraction yield of HBP will be influenced by the pH of the aqueous phase, as illustrated by the reactions

$HB^+_{aq} + H_2O \rightleftharpoons B_{org} + H_3O^+$ and $HP_{org} + H_2O \rightleftharpoons P^-_{aq} + H_3O^+$

which may be expressed in equilibrium constants by

$$a_{H^+}\,[B]_{org}/[HB^+] = K'_{HB}\,K_{D(B)} \quad (2)$$

and

$$a_{H^+}[P^-]/[HP]_{org} = K'_{HP}/K_{D(HP)} \quad (3)$$

respectively. In eqns. (2) and (3), a_{H^+} denotes the hydrogen ion activity, K' the apparent acid dissociation constant and K_D the distribution constant.

The special application discussed here involves the determination of codeine in the presence of acetylsalicylic acid, HA, which is distributed, like HP, into chloroform, (cf. eqn. 3). Dimerization of HA in the organic phase may occur [8], but at low concentrations ($\leqslant 10^{-3}$ M) this process is negligible. The equilibrium constants for the reactions discussed are given in Table 1. Based on these constants, a logarithmic diagram was constructed (cf. [9]) for the actual concentrations in the extraction coil of the system (see Fig. 1). Figure 1 shows that the aqueous phase should be kept below pH 7 to obtain $\geqslant$ 90% of the codeine in the HBP form; if the pH is too low, however, HP will be extracted into the organic phase, and will cause increased background absorbance.

At pH 6.5, the recommended pH for the picrate solution, a suitable compromise is reached; the amounts of picric acid and acetylsalicylic acid extracted into the organic phase are low, while the percentage of the codeine present as the ion pair with picrate is sufficiently high.

TABLE 1

Acid dissociation constants, distribution constants and extraction constants with chloroform as the organic phase

Compound	$\log K'/K_D$	$-\log K'_{HB} \times K_{D(B)}$	$\log K_{ex(HBP)}$
Acetylsalicylic acid (HA)	3.70[a]	—	—
Codeine (B)	—	5.81[a]	3.63[c]
Picric acid (HP)	1.80[b]	—	—

[a]From ref. 8. [b]From ref. 5. [c]Determined as described by Gustavii and Schill [4].

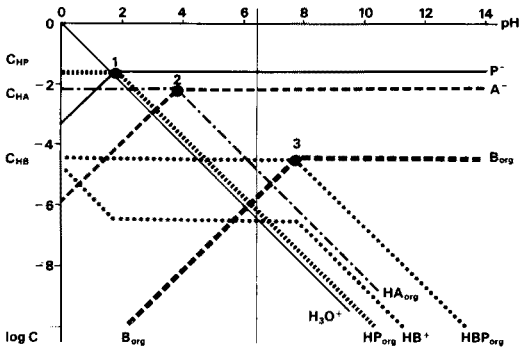

Fig. 1. Logarithmic diagram for the system acetylsalicylic acid, codeine and picric acid in chloroform—water. System points: (1) pH = log ($K_{D(HP)}/K'_{HP}$); (2) pH = log ($K_{D(HA)}/K_{HA}$); (3) pH = log $K_{ex(HBP)}$ —log ($K_{D(B)} \times K_{HB}$) + log C_{HP}.
log C_{HP} = —1.60; log C_{HA} = —2.15; log C_B = —4.45.

EXPERIMENTAL

Reagents

The codeine phosphate standard substance was of pharmacopeia quality; all other chemicals were of analytical-grade quality. The picric acid (Merck) was used without drying or recrystallization.

The compositions of sample and standard solutions given here refer to routine measurements of codeine in acetylsalicylic acid tablets. For the aqueous stream, picric acid dissolved in phosphate buffer pH 6.5, is neutralized with an equivalent amount of sodium hydroxide and diluted with buffer to a final concentration of 0.025 M of the picrate. The total concentration of phosphate should be about 0.065 M. This solution must be degassed before use. For the codeine standard solutions, sodium lauryl sulphate is added to give a final concentration of 0.040 mg ml^{-1}, the concentration range of codeine being $2—5 \times 10^{-4}$ M. Phosphate buffer pH 6.5 is added, the total phosphate concentration being about 0.065 M.

For the sample solutions, the tablets are homogenized, and an amount corresponding to a final concentration of $2.5—4.5 \times 10^{-4}$ M codeine is dissolved in 0.065 M phosphate buffer pH 6.5.

Apparatus

The equipment used has been described previously [1]: a five-channel peristaltic pump, a rotary valve with a volume of 25 or 39 μl, specially constructed fittings for merging and separation of the phases, a spectrophotometer with a 40-μl flow cell, and a recorder. In addition, a chromatographic valve (Rheodyne 7120, Berkley, USA) was used; this allowed easy variation of the injected volumes.

Figure 2 shows the manifold used for routine analysis of codeine. The mixing coil was of Teflon (i.d. 0.8 mm). The absorbance was measured at 355 nm. Base-line drift was observed in the initial stages of this work; the

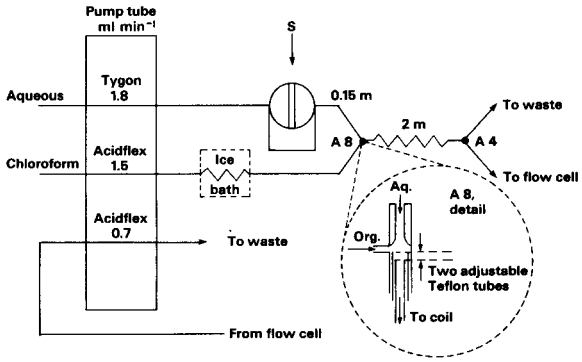

Fig. 2. Manifold for routine determination of codeine. S denotes the filling port of the rotary valve (25 μl).

drift was traced to very small droplets of aqueous phase sticking to the walls of the cuvette. This was prevented by a special procedure on starting up the system; the chloroform phase was introduced first, and air was pumped instead of the aqueous phase. Before the pumping of the aqueous phase started, the overall flow rate was decreased. When the volume proportion between the two phases had attained "steady state" in the separating device, the flow rates were successively increased up to the final values. If contamination of the flow cell by water occurred accidentally, air was introduced instead of the aqueous phase and ethanol instead of the chloroform phase. The system was rinsed in this way for a few minutes and then starting up could proceed as recommended above. It is important to keep the Teflon fibers in the separator free of water.

The system was closed down as follows: the aqueous stream was replaced by air and after a couple of minutes the chloroform phase was replaced first by ethanol and finally by air.

The segment size in the extraction coil was varied by adjusting the positions of the Teflon tubes in fitting A8 (Fig. 2). A segment length of at least 5 mm was used in routine measurements.

RESULTS AND DISCUSSION

Routine analysis

The maximum practical sampling frequency with the manifold shown in Fig. 2 is about 60/h. The calibration graph is perfectly linear within the concentration range 0.5—9.0 $\times$ 10^{-4} M in the solution introduced and intersects the origin. Introduction of pure water via the rotary valve did not yield any positive or negative peak. Over 1000 codeine analyses have so far been performed with this design of the extraction system, with excellent reliability. The procedure adopted entailed calibration with three standard solutions, one run on each, three samples run in duplicate, the three standard solutions again, three samples, and so on. Typical results are shown in Fig. 3. The injected

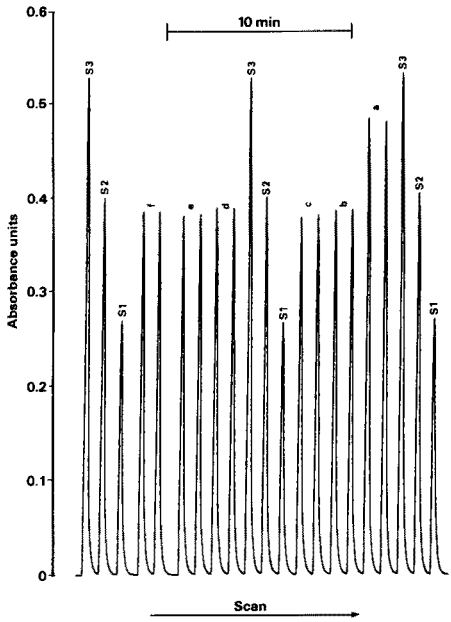

Fig. 3. Typical results of codeine samples run in duplicate. Standard solutions: S1, 2.62×10^{-4} M; S2, 3.50×10^{-4} M; S3, 5.25×10^{-4} M.

volume was 25 μl. The coefficient of variation of the standards was about 1.5% during continuous analysis for 2 h. It is obvious from Fig. 3 that the repeatability for a single sample was much better when a time range of the order of 5—15 min was considered. Thus, 15 repetitive injections of one sample gave a relative standard deviation of 0.4% of the resulting peak heights. The duplicate runs of the samples must merely be regarded as a precautionary measure, and probably it is unnecessary to introduce standard solutions so frequently. However, the procedure adopted was shown to reduce the relative standard deviation to less than 1%.

Influence of sodium lauryl sulphate

Sodium lauryl sulphate is a common constituent of acetylsalicylic acid tablets and its presence influenced the extraction efficiency, probably because of the formation of ion pairs between codeine and lauryl sulphate [10]: $HB^+_{aq} + L^-_{aq} \rightleftharpoons HBL_{org}$, where L^-_{aq} denotes the lauryl sulphate ion in the aqueous phase. This ion-pair formation would lead to a decrease in the amount of codeine picrate, and so cause lower peaks; the species HBL does not contribute to the absorbance measured at 355 nm.

Figure 4 shows the effect of sodium lauryl sulphate, as well as the effect of segment size. With no lauryl sulphate present (line a), the segment size is of no concern; curve (b) was obtained with a sodium lauryl sulphate concentration corresponding to that specified for the acetylsalicylic acid tablets, and curve (c) with twice this concentration. It is quite obvious from Fig. 4

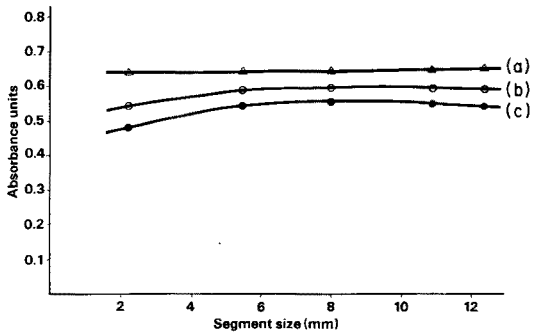

Fig. 4. Influence of segment size at different concentrations (mg ml^{-1}) of sodium lauryl sulphate. (a) 0, (b) 0.040, (c) 0.080 mg ml^{-1}. Codeine concentration, 5.25×10^{-4} M. Sample volume, 39 μl.

that lauryl sulphate, under the conditions specified, interferes significantly. However, the variation in the lauryl sulphate assay from tablet to tablet is known to be slight, much less than the variation in codeine if the two constituents are compared on a relative basis. Thus, an assay of lauryl sulphate corresponding to 102% of the label value would give a codeine value 0.1% too high, based on the results in Fig. 4. This calculation assumes that the segments exceed a length of 5 mm. For smaller segments the effect of lauryl sulphate becomes larger. This phenomenon is not predictable from the reaction given above, and so some other effect must be involved. Probably, the amount of lauryl sulphate present at the interfaces between the organic and aqueous phases increases when this area becomes larger, i.e., when the segment length decreases. A larger proportion of the codeine will then form an ion pair with the lauryl sulphate at the interface and will pass to some extent into the waste stream from the separator.

Dispersion

Controlled dispersion is one of the cornerstones in flow injection analysis (f.i.a.) [11]. The dispersion in the extraction system occurs mainly at the actual injection and during the movement of the aqueous stream from the injection site to the segmentation fitting. There is also some dispersion in the organic stream, from the separator up to the flow cell. The overall dispersion, D, in the extraction system may be defined similarly to the definition of Růžička and Hansen [11] for single-phase f.i.a.: $D = C_0/C_{cell}$, where C_0 is the concentration of the injected sample and C_{cell} is the concentration of the very small fraction of the stream flowing through the cell and corresponding to the peak maximum. However, in two-phase f.i.a., D must be regarded as an apparent dispersion, because C_{cell} also depends on the extraction process in the coil. For instance, if the pH or the picrate concentration of the aqueous stream changes, the value of C_{cell} will also change even if the flow rates, the volume of the sample injected, etc., are kept constant. Hence, the concept of dispersion must be carefully used in this connection.

Within the extraction coil, two different modes of transfer of species from

one segment to the adjacent segment of the same phase may be distinguished. First, the extraction process may be very rapid so that the species originally present in a segment at a high concentration move across the interposed segment of the other phase into the next segment of the same phase. Secondly, and far more probably, the washing in the extraction coil may be incomplete which would mean that the transfer of the species occurs via the walls of the coil. Lengthening of the coil would, if both types of transfer are assumed to take place, increase the dispersion. However, no changes of the peak maxima were observed when the coil length was increased from 1 m to 6 m.

The apparent dispersion of the system, according to Fig. 2, lies at about 10. It is reasonable to assume that most of the dispersion occurs in the aqueous phase up to the segmentation site; this value was therefore used in calculating the actual concentrations in the extraction coil when constructing the logarithmic diagram shown in Fig. 1.

Obviously, an increase in the volume of the injected sample will decrease the dispersion. However, the picrate ion concentration will drop correspondingly, so that the ion-pair formation with codeine will be suppressed. As quantitative formation requires an excess of picrate, a substantial loss of sensitivity will result. This effect is shown in Fig. 5. The samples were introduced via a chromatographic valve furnished with a sample tube of variable length. In all other respects, the system was the same as has already been described. Some rapid scans of the peaks are also illustrated in Fig. 5. These peaks are not symmetrical: for sample volumes below 300 μl, a single peak appeared, but for larger volumes an indication of double peak behaviour could be observed. A double peak would be expected if the dispersion process were ideal in the system, for the valley between the peaks would then have been caused by the deficit of picrate ions in the centre of the sample plug owing to incomplete mixing with the surrounding reagent stream. The variation of the sample volume has been exaggerated in Fig. 5 merely to stress the importance of having picrate in excess during the extraction. For the concentrations used in this study, a sample volume of maximum 70—80 μl can be recommended; above this volume the deviation from linear behaviour becomes manifest.

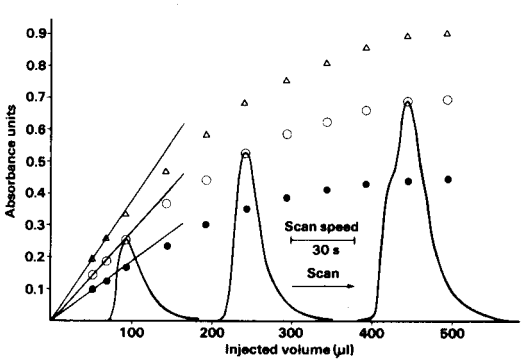

Fig. 5. Absorbance of peak maximum as a function of the injected volume. Codeine concentrations: (△) 1.1×10^{-4} M; (○) 8.0×10^{-5} M; (●) 5.3×10^{-5} M.

Determination of equilibrium constants

In the theoretical part, it was assumed that equilibrium was attained in the extraction coil, and thus that eqns. (1—3) are valid. This assumption seems to be justified since a $K_{ex(HBP)}$ value of $10^{3.53}$, which is in good agreement with the value $10^{3.63}$ determined by batch extraction (Table 1), was obtained by use of the flow-injection system in Fig. 2. Similar investigations for other compounds, e.g. brompheniramine, tetraethylammonium ion and phenol, were also in good agreement with literature data, confirming that equilibrium was also attained in these cases. Further details concerning the determination of K_{ex} and K_D values (cf. eqns. 1—3) by the flow-injection technique will be given in subsequent papers.

Conclusions

Mechanization of analytical methods based on ion-pair extraction is possible by using the continuous flow system originally developed for "simple" extractions. The dispersion occurring before mixing of the two phases is used as an analytical tool and must therefore be controlled carefully. During the relatively short residence time (about 20 s) of the sample in the extraction coil, equilibrium seems to be attained. This may be used as a new and convenient way of determining extraction and distribution constants.

Compared with the conventional batch extraction procedures, this system offers considerably better economy regarding reagent consumption and the time required for an analysis without any loss of precision. Furthermore, exposure to organic solvent vapours can be appreciably decreased because the extraction is carried out in a closed system.

REFERENCES

1 B. Karlberg and S. Thelander, Anal. Chim. Acta, 98 (1978) 1.
2 U.S. Pharmacopeia XIX, 1975, p. 102.
3 A. H. J. Cross, D. McLaren and S. G. E. Stevens, J. Pharm. Pharmacol., 11 (1959) 103T.
4 K. Gustavii and G. Schill, Acta Pharm. Suec., 3 (1966) 241.
5 K. Gustavii, Acta Pharm. Suec., 4 (1967) 233.
6 G. L. Starobinets and E. M. Rakhman'ko, Vestsi Akad. Navuk Belarus. SSR, Ser. Khim. Navuk, (1971) 45; Chem. Abstr., 76 (1972) 104480.
7 S. Hugosson, L. Nyberg and L. Nilsson, Acta Pharm. Suec., 9 (1972) 249.
8 P.-A. Johansson and K. Gustavii, Acta Pharm. Suec., 13 (1976) 407.
9 P.-A. Johansson and K. Gustavii, Acta Pharm. Suec., 14 (1977) 1.
10 S. O. Jansson, R. Modin and G. Schill, Talanta, 21 (1974) 905.
11 J. Růžička and E. H. Hansen, Anal. Chim. Acta, 99 (1978) 37.

Analytica Chimica Acta, 104 (1979) 29—45

SIMULTANEOUS DETERMINATION OF NOREPINEPHRINE, DOPAMINE, AND SEROTONIN IN BRAIN TISSUE BY HIGH-PRESSURE LIQUID CHROMATOGRAPHY WITH ELECTROCHEMICAL DETECTION

SULEIMAN SASA[‡] and C. LeROY BLANK*

Department of Chemistry, University of Oklahoma, 620 Parrington Oval, Norman, OK 73019 (U.S.A.)

(Received 16th June 1978)

SUMMARY

High-pressure liquid chromatography with electrochemical detection (l.c.e.c.) is utilized in a procedure for the simultaneous determination of three of the most important neurotransmitters in nervous tissue samples. The high degree of selectivity and sensitivity (subpicomole limits for each component) makes this technique directly applicable to extremely small samples. After optimal conditions had been established, the procedure was employed in the determination of all three components in whole mouse brains, seven separate mouse brain parts, and diurnal variations of whole mouse brains. The technique outlined does not require sample splitting, tissue pooling, component derivatization, or coupled enzymatic reactions to achieve the desired results. Twenty individual samples may be accommodated per day.

A great deal of information has now been accumulated suggesting important roles for both the catecholaminergic and serotonergic transmitter systems in the central nervous systems of mammals. These systems employ the catecholamines [1], norepinephrine (NE), dopamine (DA) and serotonin (5-hydroxytryptamine or 5-HT), as chemical neurotransmitters.

A growing body of data has implicated one or more of these transmitters in the affective disorders [2—4]. This has been especially evident in the now routine treatment of Parkinsonian patients with L-Dopa, the biosynthetic precursor to dopamine [5]. Involvement of these transmitters has also been mentioned in connection with schizophrenia [6, 7], self-stimulation [8], depressive suicides [9], eating and over-responsiveness to both internal and external stimulae [10], sleep disturbances, heightened sexuality, irritability, aggression, and general behavioral changes [7]. But each of these studies has tended to focus upon alterations in only one of the transmitter systems and the resultant effect upon the measured activity. This approach has recently given way to the seemingly more resonable assessment of two or more of

---

[‡]Present Address: Department of Chemistry, College of Arts and Sciences, Yarmouk University, Irbid (Jordan).

these systems in the expectation of significant interactions among the various monoamines [11—13]. The anatomical complexity of the central nervous system as well as the diversity of associated behavioral responses warrants such an approach. Additionally, it has become obvious that a better understanding of the underlying neurochemical correlates of behavior demands the analysis of very precise, and often quite small areas of the brain. The selective effects on regional concentrations of brain biogenic amines as a result of drug [14—16] and other treatments [17, 18] has been well established.

Our attention has been focused on the development of precise, sensitive, and selective procedures for the simultaneous determination of as many of these biogenic amines as possible in very small samples. The present report covers such a procedure for three of the most frequently studied neurotransmitters: NE, DA and 5-HT.

The presently available analytical techniques for the determination of NE, DA and/or 5-HT in tissue samples [19—34] generally involve three basic steps: homogenization with precipitation of macromolecules and cellular debris followed by centrifugation; isolation and purification of the biogenic amines from the supernate; and following physical separations of the amines or the division of the sample into two or more distinct samples, the separate determination of each species. This third stage also incorporates chemical derivatization of the individual components to increase sensitivity. Radiochemical labelling by enzymatic processes [34—38] offers a slightly different procedure by interjecting an enzymatic derivatization of the desired species after the initial homogenization.

Deproteinization of samples is almost universally achieved by the addition of acid. Isolation and purification of the biogenic amines has generally employed column chromatography [20], liquid—liquid extractions [32] or alumina absorption [39], which is applicable only to the catecholamines.

Determination of the catecholamines and indoleamines has, in moderate to highly sensitive determinations, been accomplished with fluorescence, gas chromatography (with and without mass spectrometry), electrochemical detection coupled with liquid chromatography, and liquid scintillation counting of labelled species. Other methods are available for these transmitters, but their generally inadequate sensitivity precludes discussion of their application here. By far the most frequently employed technique is fluorescence. For the catecholamines, this includes oxidative rearrangement to the fluorophore by the trihydroxyindole technique [25]. For serotonin, such determinations have been achieved by native fluorescence in strong acid [26], prior derivatization with *o*-phthalaldehyde [23], or prior derivatization with ninhydrin [24]. The selectivity and sensitivity obtained by the fluorescence methodology is, unfortunately, not as high as one would desire. The lack of sensitivity may necessitate sample pooling of very small samples.

Gas chromatography (g.c.) with an electron capture detector is applicable to the determination of NE, DA, and 5-HT [27, 28], although this does not offer simultaneous determinations of all three, and the sensitivity is not high. G.c.—m.s., however, has a high degree of sensitivity for each of the desired trio [29, 40].

Radiochemical labelling and subsequent determination by scintillation counting also offer a high degree of sensitivity for the analysis of samples containing NE, DA, and 5-HT. Commercially available kits have appeared for the catecholamines, but the enzyme preparations required for serotonin [34] are not particularly stable.

High-pressure liquid chromatography with electrochemical detection (l.c.e.c.) offers a high degree of sensitivity and selectivity for the determination of biogenic amines. The introduction of this method to the field of neurochemical analysis [30, 41], initially concerned with the catecholamines, has been further extended and refined [42, 43], and l.c.e.c. has been used [31] to provide a technique for the concurrent determination of DA and 5-HT but not for the simultaneous determination of NE, DA, and 5-HT. Because of the critical importance of data on all of these species to many neurological studies, it was decided to try to apply l.c.e.c. technology to their simultaneous determinations.

EXPERIMENTAL

Apparatus

Tissue homogenizer. Brain tissue samples were homogenized with an ultrasonic cell disrupter (Model W200P, Ultrasonics, Inc.) equipped with a long probe tip, especially useful for small volume work, and operated at medium power output and a 50% duty cycle to minimize heating. The component most likely to be altered [44] by such methodology, i.e. serotonin, is unaffected under these conditions [31].

Centrifuge. A Sorvall RC-2B refrigerated (4°C), high-speed centrifuge equipped with an SM-24 or SS-34 rotor was employed for centrifugal separations. Polypropylene tubes and lids that just fit these rotor heads were conveniently utilized for both the solvent extractions and subsequent centrifugal operations. This minimized unnecessary transfer steps.

Shaker. Extractions were performed at 15°C and 280 cycles/min with an Eberbach shaker immersed in an air bath. The extraction tubes were placed on their sides with the long axes parallel to the direction of shaking.

Liquid chromatograph. The high-performance liquid chromatograph with electrochemical detection has been previously described [30, 31, 41—43]. The essential differences in the present system are: a 250 × 3-mm column of Zipax SCX strong cation-exchange resin in series with a 500 × 2-mm column of Vydac SCX strong cation-exchange resin; the eluting solvent was a citrate—acetate buffer; the flow rate was ca. 0.6 ml min^{-1}; the carbon paste electrode potential was set at +0.60 V vs. SCE. The columns and eluting solvent enabled simultaneous determinations of all three biogenic amines, as well as an internal standard, to be made.

Animals

Adult male mice, typically 6—12 weeks old, of the ARS-HA/ICR (albino) strain (Sprague-Dawley, Madison, WI) were used. They weighed ca. 25 g at the time of sacrifice. They were maintained on a 12-h light/12-h dark cycle

(lights on at 7.00 a.m.) and were allowed food and water ad libitum The mice were not employed in the experiments until they had become accustomed to these conditions (one week or more after arrival). As fluctuations in brain biogenic amine levels occur [7], the animals were sacrificed at a fixed time (10.00—10.30 a.m.) each day except in the study of diurnal variations.

Reagents

Citrate—acetate buffer. This solution, used in the procedure for standards and after dilution as the eluting solvent for the l.c.e.c. system, was prepared by dissolving 8.2 g of anhydrous sodium acetate, 2.1 ml of glacial acetic acid, 4.8 g of sodium hydroxide, and 10.5 g of citric acid monohydrate in 1 l of water. The final solution had pH 5.1. Before use in the l.c.e.c., this buffer was diluted (3 parts buffer to 2 parts water) and filtered through a 0.45-μm Millipore filter to prolong pump life. (This dilution ratio may have to be altered for a particular set of columns to obtain proper chromatographic separation.) The diluted form was used only as an eluant for chromatography.

Extraction solvents. Reagent-grade n-butanol (Mallinkrodt) and heptane (Baker Analyzed) were employed; products of comparable purity from other suppliers created large solvent fronts but a purification procedure [32] gives a product suitable for the procedure regardless of the supplier.

Biogenic amines and internal standard. Norepinephrine (NE) hydrochloride, dopamine (DA) hydrochloride, 3,4-dihydro-xybenzylamine hydrobromide (DHBA, the internal standard) and, serotonin (5-HT) creatinine sulfate of the highest possible purity were obtained from commercial sources. All concentrations of the biogenic amines are expressed as the free base.

Stock standard solution. A solution containing NE (about 40 μg ml^{-1}), DA (90 μg ml^{-1}), and 5-HT (75 μg ml^{-1}) was prepared by dissolving appropriate amounts of their salts, accurately weighed, in 100.0 ml of 0.01 M HCl, previously deaerated with oxygen-free nitrogen [30] for 15 min. The final solution was stable for up to one month when stored in the refrigerator at 4°C, but a fresh solution was prepared each week. The concentrations in this mixture are appropriate to whole mouse brain determinations. Specific modifications for brain parts are mentioned later; alterations for other tissues or fluids should be made such that the stock standard contains concentrations ca. 100 times (expressed ng ml^{-1}) that of the desired sample (expressed as ng g^{-1} or ng ml^{-1}).

Working standard solution. On the day of analysis, 1.00 ml of the stock standard solution was diluted to 100.0 ml with deaerated 0.01 M HCl. For whole mouse brain this yielded a solution containing NE (400 ng ml^{-1}), DA (900 ng ml^{-1}), and 5-HT (750 ng ml^{-1}).

Internal standard solution. For whole mouse brain determinations, a solution containing 1×10^{-5} M DHBA was prepared by dissolving an appropriate amount of its salt in deaerated 0.01 M HCl; the stability was adequate when stored at 4°C in a refrigerator for up to one month. Because of the internal standard, an accurate knowledge of the concentration of this solution is not required, but, the same volume of the same solution of DHBA must be

employed for both the standards and samples in a single determination to obtain the desired precision.

Ascorbic acid. A solution of ascorbic acid (11 mg ml^{-1}) was prepared in deaerated 0.01 M HCl 2 h before use. Modifications in this concentration for brain parts are noted later.

EDTA. A solution of 0.1 M EDTA was prepared by dissolving 3.72 g of the anhydrous disodium salt and 1.00 g of NaOH in ca. 90 ml of water. After dissolution, 2.15 ml of 12 M HCl was added to neutralize the NaOH and the mixture was diluted to 100 ml with water.

HCl solutions. 0.01 M and 0.025 M solutions were prepared in water. The former was used in the preparation of various solutions and as the aqueous media for the final extraction; the latter was used only for tissue homogenization.

The water was either deionized or doubly distilled. Other compounds, including those examined for possible interferences, were obtained commercially in the highest possible purity.

Procedure

Whole mouse brains. The mice were sacrificed by cervical dislocation. The brains were removed as rapidly as possible, transferred to one of the small centrifuge tubes, frozen in liquid nitrogen, and stored on solid CO_2. Only brain tissue in front of the most posterior portion of the cerebellum was employed. Each sample was weighed to the nearest mg. For standards, a 500-μl aliquot of the working standard and 10 μl of the ascorbic acid solution replaced the brain tissue. The following solutions were then added to the tube: 750 μl of 0.025 M HCl (750 μl of the citrate—acetate buffer for standards); 100 μl of 1×10^{-5} M DHBA; and 100 μl of 0.1 M EDTA.

The mixture was subjected to ultrasonic homogenization, resulting in a homogenate pH of ca. 5.1, and saturated with salt by addition of 3—4 g of NaCl. Butanol (12.0 ml) was added, the tube capped, and the sample shaken for 60 min (20 min for standards) at 15°C. The mixture was centrifuged at 7900 G for 10 min at 4°C to separate the water and butanol layers completely. Carryover of any of the aqueous phase to the following steps causes great disturbances (large solvent front) in the final chromatography. For this reason, great care was required in the subsequent transfer of 10.0 ml of the butanol (top) layer to one of the large centrifuge tubes. Ths second centrifuge tube already contained 17.0 ml of heptane and 200 μl of 0.01 M HCl. This mixture was shaken for 5 min at 15°C and then centrifuged for 5 min at 8000 G at 4°C. However, this second centrifugation appeared to be unnecessary and could be replaced by allowing the layers to separate naturally for about 10 min. The aqueous layer was then transferred (Pasteur pipet) to a small vial and frozen on dry ice. When ready for analysis, the sample was liquefied by holding in the hand and a 10-μl aliquot was injected into the l.c.e.c. Injection volumes larger than 10 μl could be employed if necessary for sensitivity, but volumes of 50 μl produced noticeable losses in resolution. At times between the operations noted above, the samples were stored on ice.

Brain parts. Each of the seven individual mouse brain parts was analyzed in the same way as the whole brains. Sacrifice was followed by dissection, freezing, etc. Some of the parameters given for whole brain, however, required modification to make them more appropriate to the parts. In order to maintain reasonable consistency with the whole brain analyses, the following conditions were met as closely as possible: the ratio of aqueous to butanol volumes in the initial extraction was kept at ca. 1:10; the ratio of butanol to heptane in the second extraction was ca. 1:1.75; the volume of 0.01 M HCl used in the final extraction was 200 μl, as smaller volumes are difficult to manipulate; the volume of working standards (in μl) was similar to the tissue weight (mg); the shaking times for the first and second extractions were 60 min and 5 min, respectively (20 min and 5 min for standards); the concentrations of the internal standard and the working standards were modified to approximate more closely the results obtained from those samples or, for the internal standard, to be similar to the endogenous biogenic amine values; the critical volumes of solutions, i.e. of the internal and working standards, were selected to be sufficient ($\geqslant$50 μl) to give a high degree of precision.

A summary of the differences between the determinations involving whole brain and individual mouse brain parts is given in Tables 1—3. Typical weights for these samples are: whole brain, 450 mg; cerebellum, medulla-pons, hippocampus, midbrain, and diencephalon; 25—50 mg; striatum, 25 mg; cortex, 200 mg.

Recovery studies

The percentage recovery in the presence and absence of brain tissue was examined for NE, DHBA, DA, and 5-HT, simultaneously. These studies involved three different groups of samples.

A brain homogenate was prepared ultrasonically from ten mouse brains in a mixture of 1.00 ml of 0.1 M EDTA, 7.50 ml of 0.025 M HCl and 1.00 ml of 0.01 M HCl (to replace the usual DHBA). A 1.00-ml aliquot of the homogenate was transferred to each of ten separate centrifuge tubes. To five of

TABLE 1

Solutions added prior to homogenization for determinations involving brain parts

Brain part	0.1 M EDTA (μl)	DHBA		0.025 M HCl (samples) or buffer (standards) (μl)
		(μM)	(μl)	
Cerebellum, Hippocampus, Medulla-pons, Midbrain	10	1	50	100
Diencephalon	10	1	50	150
Striatum	10	4	100	150
Cortex	50	4	100	350
(Whole Brain)	100	10	100	750

TABLE 2

Composition of working standards and ascorbic acid solutions for determinations involving brain parts[a]

Brain part	Working standards				Ascorbic acid	
		Concentrations (ng ml^{-1})				
	(μl)	NE	DA	5-HT	(mg ml^{-1})	(μl)
Cerebellum, Hippocampus, Medulla-pons, Midbrain, Diencephalon	50	400	800	700	2	5
Striatum	50	300	1600	700	2	5
Cortex	200	400	800	700	11	5
(Whole Brain)	500	400	900	750	11	10

[a]Solutions prepared with deaerated 0.01 M HCl.

TABLE 3

Volumes of butanol and heptane employed in determinations involving brain parts[a]

Brain part	Butanol (ml)		Heptane (ml)
	For Initial Extraction	For Final Extraction	For Final Extraction
Cerebellum, Hippocampus, Medulla-pons, Midbrain, Diencephalon	2.2	1.5	2.5
Striatum	3.2	2.5	4.2
Cortex	7.0	5.0	9.0
(Whole Brain)	12.0	10.0	17.0

[a]The final extraction was into 200 μl of 0.01 M HCl. Also, for all parts, 1 g of NaCl was employed for salt saturation instead of the 3—4 g used for whole brains.

these tubes was added a 50-μl aliquot of 0.01 M HCl containing 2.1×10^{-6} M NE, 2.4×10^{-6} M DHBA, 3.7×10^{-6} M DA, and 3.2×10^{-6} M 5-HT. These tubes are referred to as group A. To the remaining five tubes (group B) a 50-μl aliquot of 0.01 M HCl was added to equalize the volume. Additional centrifuge tubes (standards), constituting group C, were prepared with each containing 100 μl of 0.1 M EDTA, 10 μl of ascorbic acid solution, 900 μl of the citrate—acetate buffer, and 50 μl of the same standard solution as above containing NE, DHBA, DA, and 5-HT.

Each sample was then subjected to ultrasonic treatment for approximately 20 s, whether or not it contained brain tissue, resulting in a "homogenate"

of pH 5.1. Some samples from group C were then removed from the procedure and injected into the l.c.e.c. to establish peak heights for standards prior to extraction.

After the addition of 1 g of NaCl, exactly 10.5 ml of butanol was added to each of the tubes, and extraction was done by shaking at 15°C for 60 min (20 min for samples without brain tissue). Centrifugation of the resultant mixture at 4°C and 7900 G was followed by removal of a 9.6-ml aliquot of the butanol layer. The removed butanol was added to a second, larger centrifuge tube containing 17.0 ml of heptane and 200 μl of 0.01 M HCl This tube was capped, shaken for 5 min, and centrifuged at 121 G and 4°C for 5 min. The final aqueous layer was then transferred to a small vial and frozen on solid CO_2 to await injection into the l.c.e.c. When ready for such an injection, the sample was thawed and a 10—20-μl aliquot was injected as before.

Samples which were carried through the extraction procedure and contained only standards (group C) were compared to the unextracted results from the same group to obtain percentage recoveries in the absence of tissue; recoveries in the presence of tissue were determined by subtracting the peak heights of the samples that contained only brains (group B) from those containing both brains and the standards (group A) and comparing to the unextracted results for each component.

Calculations

The concentrations of each of the biogenic amines in brain tissue are established from the chromatographic peak heights for each component which are easier to assess than peak areas in routine manual analyses. The methodology is similar to that described earlier [30], but is repeated here because of an error in that report.

For a typical determination, assume that a sample (462 mg) has yielded peak heights of 17.0, 14.6, 20.2, and 6.8 cm for NE, DHBA, DA, and 5-HT, respectively. Likewise, assume that a standard (employing a 500-μl aliquot of a solution containing NE (412 ng ml^{-1}), DA (926 ng ml^{-1}) and 5-HT (733 ng ml^{-} has yielded peak height values of 16.4, 13.8, 19.4, and 8.4 cm for NE, DHBA, DA, and 5-HT, respectively. Then, the calculation is:

$$\text{NE (ng g}^{-1}) = (R_{\text{NE, sample}})\ (\text{ng NE in std.})/(R_{\text{NE, std.}})\ (\text{g tissue})$$

$$= \left[\left(\frac{17.0}{14.6}\right)(0.500\ \text{ml})\ (412\ \text{ng ml}^{-1})\right] \Big/ \left[\left(\frac{16.4}{13.8}\right)(0.462\ \text{g})\right] = 437\ \text{ng g}^{-1}$$

where R_{NE} = peak height, NE/peak height, DHBA. For DA and 5-HT, similar calculations yield values of DA = 986 ng g^{-1} and 5-HT = 783 ng g^{-1}.

The final result obtained for 5-HT by analogy to that given for NE must be multiplied by 1.29 to compensate for the poorer recovery of this component in the presence of brain tissue than in the absence of tissue (see below). Also, in a typical run, more than one standard is employed (usually three or four). Thus, the average values for $R_{\text{NE, std.}}$; $R_{\text{DA, std.}}$; and $R_{\text{5-HT, std.}}$ are established

from all the standards and these average results are used in the subsequent calculations for individual brain samples.

Uncertainties are expressed as the standard error of the mean (SEM). The significance of differences was examined by Student's *t*-test [45].

RESULTS AND DISCUSSION

Extraction procedure

A previous investigation of appropriate extraction parameters for DHBA, DA and 5-HT [31] was found to apply to the present conditions. Thus, only the additional parameters or potential trouble spots investigated will be discussed.

Pecentage recovery. The recovery of 5-HT was significantly different in the presence and absence of brain tissue [31]. So the values for all of the compounds of interest, including the previously unreported NE, were re-examined.

Table 4 shows that NE, DHBA, and DA provide results that are seemingly unaffected by the addition of tissue. However, 5-HT gives a significantly lower recovery in the presence of brain tissue, as was previously observed [31]. To compensate for this anomaly, the final 5-HT values must be multiplied by 1.29 [i.e., 29.4%/22.8%].

Stability of final aqueous solution. Frequently, only a part of a determination is required on a particular day, with the remainder completed later. Thus, the effect of storing the final aqueous extract on the peak height ratios R_{NE}, R_{DA} and $R_{5\text{-}HT}$ was investigated for both typical standards and whole brain samples. With the procedure described for whole brain determinations, the final aqueous solution was stored either on solid CO_2 or at room temperature. As shown in Tables 5 and 6, a decrease in these ratios is evident when both standards and samples are stored for only 1 h at room temperature, although the results are only significantly different for NE/DHBA in the standards ($P < 0.01$). The samples and standards stored on solid CO_2, however, did not exhibit significant alterations in these ratios for storage times up to 48 h. Similar results were obtained by examining the individual peaks instead of the ratios. Thus, the procedure can be done in two parts, with extraction and chromatography performed on succeeding days, when the samples are stored on solid CO_2.

TABLE 4

Recovery (%) in presence and absence of brain tissue[a]

	Compound			
	NE	DHBA	DA	5-HT
In presence of brain tissue	36.1 ± 0.6	36.0 ± 0.9	42.6 ± 1.1	22.8 ± 0.2
In absence of brain tissue	36.8 ± 0.4	35.8 ± 0.9	41.4 ± 1.0	29.4 ± 0.3

[a]All results represent eight separate determinations. Results expressed as mean ± SEM. Recoveries are significantly different only for 5-HT ($P < 0.001$).

TABLE 5

Stability of the final extract at 23°C in the presence of brain tissue

	Peak ratios[a]		
	NE/DHBA	DA/DHBA	5-HT/DHBA
Immediately after extraction	2.4 ± 0.2	2.3 ± 0.2	0.84 ± 0.02
1 h after extraction	2.3 ± 0.1	2.0 ± 0.1	0.82 ± 0.01
P-value	N.S.	N.S.	N.S.

[a]All values reported as mean ± SEM for six separate determinations.

TABLE 6

Stability of the final extract at ca 23°C in the absence of brain tissue[a]

	Peak ratios		
	NE/DHBA	DA/DHBA	5-HT/DHBA
Immediately after extraction	1.54 ± 0.02	1.38 ± 0.02	0.51 ± 0.02
1 h after extraction	1.44 ± 0.02	1.32 ± 0.03	0.50 ± 0.02
P-value	$P < 0.01$	N.S.	N.S.

[a]All values are reported as mean ± SEM for six separate determinations.

Whole mouse brain results

A typical l.c.e.c. chromatogram obtained for a determination on whole brain is presented in Fig. 1. The results obtained from some 48 separate

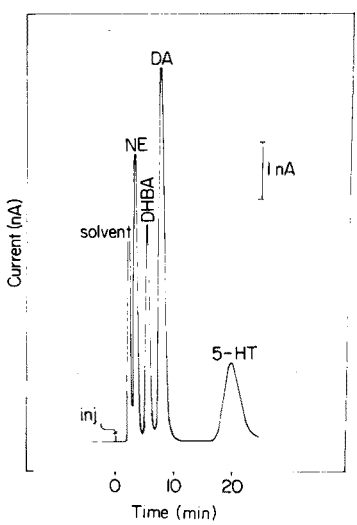

Fig. 1. Typical chromatogram for whole mouse brain from a 15-μl injection of final HCl solution containing 10.4 ng NE, 25.3 ng DA, and 15.0 ng 5-HT.

determinations yielded average (± SEM) values of: NE, 437 ± 7 ng g^{-1}; DA, 927 ± 11 ng g^{-1}; and 5-HT, 783 ± 9 ng g^{-1}. These are in good agreement with previously reported values for whole mouse brain [19, 31, 46–48].

Diurnal rhythms. Although many data exist for diurnal variations of NE, DA, and 5-HT in the rat brain, very few data have been established for mice [49]. It was decided to see if the time selected for sacrifice, i.e. 10.00–10.30 a.m., was indeed appropriate.

Groups of five mice were sacrificed at 4 h intervals beginning at 04.00 a.m. Additionally, groups of five mice were sacrificed 1 h before and 1 h after turning the lights on and turning the lights off. For all animals, the brains were removed as quickly as possible, weighed, stored on solid CO_2, and analyzed as a single group 32 h after the last group of five was collected. The results given in Table 7 show that there is a distinct diurnal rhythm for the three amines, with each exhibiting a clear maximum and fairly clear minimum some time during the 24-h period. NE displayed its greatest concentration at 24.00 h and its minimum at 12.00 h. Both DA and 5-HT exhibited a maximum at 04.00 h. DA seems to show a minimum value between 12.00 and 16.00 h but 5-HT shows a less well-defined minimum, somewhere between 08.00 and 20.00 h.

The ratio of the maximum to the minimum value for each species is: NE, 1.48; DA, 1.38; 5-HT, 1.25. The maximum value is significantly larger than the minimum ($P < 0.01$) in all three cases. This shows that diurnal variations should be considered in experiments including controls and/or experimental animals not sacrificed at the same time of day. For experiments desiring minimal diurnal interference, it appears that sacrificing between 08.00 and 16.00 h under the lighting and other conditions described, should yield minimal fluctuations.

TABLE 7

Norepinephrine, dopamine, and serotonin concentration in mouse brain at different times of day[a]

Time of sacrifice (h)	NE (ng g^{-1})	DA (ng g^{-1})	5-HT (ng g^{-1})
04.00	552 ± 16	1271 ± 83	910 ± 37
06.00	522 ± 13	1169 ± 69	821 ± 33
07.00	---------- Lights turned on ----------		
08.00	472 ± 16	974 ± 32	735 ± 15
12.00	414 ± 13	931 ± 20	793 ± 66
16.00	461 ± 12	919 ± 32	752 ± 26
18.00	515 ± 28	973 ± 97	785 ± 95
19.00	---------- Lights turned off ----------		
20.00	487 ± 52	953 ± 110	728 ± 77
24.00	613 ± 15	1058 ± 46	813 ± 36

[a]Each result represents the mean of 5 determinations ± SEM.

These results, of course, are highly dependent on the housing conditions employed. Since the animals were allowed food and water ad libitum, the results for 5-HT, especially, may be less than desirable. Brain 5-HT levels are easily altered [50] by changing the levels of blood tryptophan and other amino acids competing with tryptophan for uptake by the brain. Thus, the 5-HT fluctuations may reflect eating habits instead of endogenous variations. Similar arguments of tyrosine levels controlling NE and DA levels are not yet as convincing, but could also be a factor in the present results.

Determinations of brain parts

As with diurnal variations, many data exist concerning regional levels of NE, DA, and 5-HT in rat brain. But few data have been acquired for mouse brain parts. Until the appearance of g.c.—m.s. and radiolabelling techniques, this would have required pooling of samples to obtain reasonable sensitivity. Even with these new techniques, separate determinations must be made for NE, DA, and 5-HT (NE and DA, however, may be combined in the g.c.—m.s. methodology). Thus, to the best of our knowledge, this is the first such report for these seven parts of mouse brain. Typical chromatograms are presented for the analysis of striatum and cerebellum, respectively, in Figs. 2 and 3. These figures were selected because they are examples of the worst two situations.

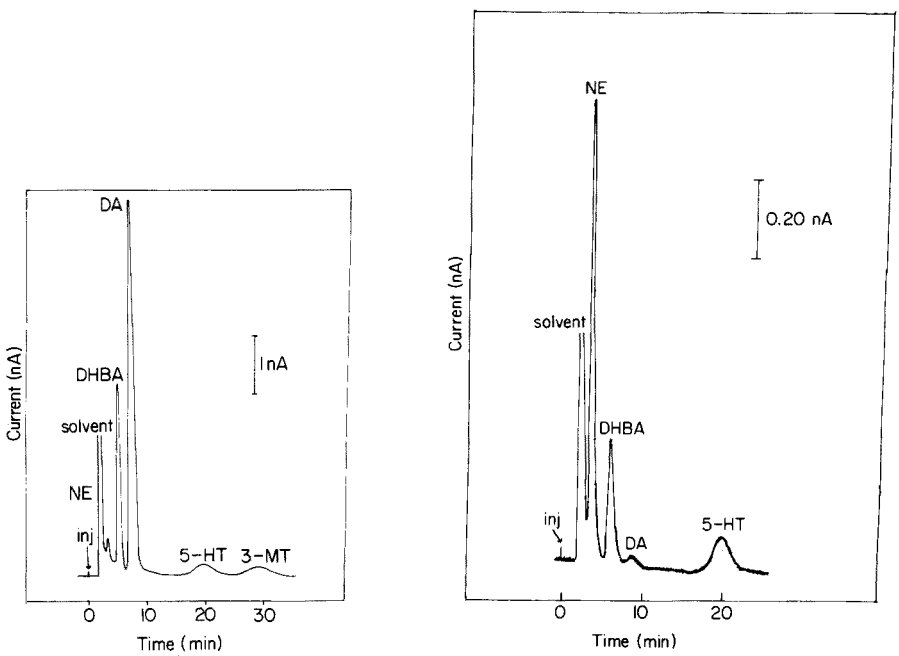

Fig. 2. Typical chromatogram for mouse brain striatum (10-μl injection containing 128 pg NE, 3.94 ng DA, and 391 pg 5-HT).

Fig. 3. Typical chromatogram for mouse brain cerebellum (15-μl injection containing 920 pg NE, 86 pg DA, and 259 pg 5-HT).

In striatum, DA concentrations are extremely large relative to the other two transmitters, but even here both NE and 5-HT are easily quantifiable. In cerebellum, DA values are exceedingly small in comparison to NE and 5-HT but all transmitters are obtainable from the chromatogram. 5-HT values (Table 8) are not small in any of the seven regions examined; the smallest value occurs in the cerebellum and a reasonable estimate of the sensitivity is seen in Fig. 3. Although comparable results are not available for mouse brains, these results agree fairly well with those obtained for rat brains [22, 23, 51—53].

An advantage of the technique is seen in the striatum analysis (Fig. 2). 3-Methoxytyramine (3-MT, also known as 3-*O*-methyldopamine) is clearly separated from all the other components of interest and easily measured in this particular brain part. Of course, quantification of 3-MT will require greater times for each injection and, thus, lengthen the total time of analysis. From the chromatograms obtained for these samples and including 3-MT in the standards, a value of 656 ± 47 ng g^{-1} (n = 6) was established for this component in striatum. 3-MT, however, only causes minor interference in the whole brain determinations (less than 2—3% errors) because of its relatively lower concentration in such samples. And, in brain parts other than striatum, 3-MT concentrations are so low that they are virtually invisible chromatographically. Nonetheless, 3-MT could be determined in almost all these cases by simply amplifying the detector response for that portion of the chromatogram corresponding to its elution.

Interferences

Any analytical technique devised to determine NE, DA, and 5-HT would not be useful unless the possible interferences are known not to disturb the final results. In this respect, l.c.e.c. offers a very high degree of selectivity through both the electrochemical detector and the chromatography. The carbon paste detector must be capable of oxidizing (or reducing, although reduction would produce easily discernible "negative" peaks) any potential

TABLE 8

Concentrations of NE, DA, and 5-HT in regions of mouse brain[a]

Brain region	Average weight (mg)	NE (ng g^{-1})	DA (ng g^{-1})	5-HT (ng g^{-1})
Cerebellum	57	296 ± 14	28 ± 4	103 ± 8
Medulla-pons	43	535 ± 40	59 ± 7	812 ± 54
Midbrain	36	616 ± 39	126 ± 9	1015 ± 49
Diencephelon	44	625 ± 41	200 ± 12	974 ± 76
Hippocampus	33	254 ± 46	84 ± 28	453 ± 93
Striatum	23	153 ± 13	4777 ± 380	579 ± 25
Cortex	198	256 ± 34	673 ± 67	630 ± 47

[a]All results represent mean values for 11 determinations ± SEM.

interferences at the selected voltage, i e. +0.60 V vs. SCE. This requirement alone eliminates the vast majority of tissue components from possible interfering roles. Likewise, any interfering component must be retained by the chromatographic column in a manner similar to the species determined or the internal standard. Any interference must also survive the homogenization, butanol extraction, and HCl extraction to yield a final concentration that is roughly greater than or equal to at least 1% of the component with which it is to interfere.

Considering all of these requirements for interference, the most likely suspects appear to be precursors and metabolites of the catecholamines and indoleamines. As shown in Table 9, the neutral and acidic metabolites, and the amino acid precursors, are not retained significantly under the chromatographic conditions used. The basic compounds, however, all appear clearly separated from the solvent front.The positions of most of these, however, would make their appearance in the technique easily detectable by a cursory examination of the usual chromatograms.The only real exception to this statement is epinephrine. Normally present in brain tissue in only exceedingly small quantities, it could present a problem in other samples. In such cases, a sample run without the internal standard, DHBA, would clearly show if

TABLE 9

Potential interferences examined[a]

Compound	Retention time t_R (min)	Peak width (min)
3,4-Dihydroxyphenethyl alcohol	2.4	1.2
3,4-Dihydroxyphenyl glycol	2.3	1.1
3,4-Dihydroxyphenylacetic acid	2.3	1.2
3,4-Dihydroxymandelic acid	2.3	1.2
3,4-Dihydroxyphenylalanine (DOPA)	2.3	1.2
L-3-*O*-Methyl-DOPA	2.3	1.1
5-Hydroxytryptophan	2.3	1.2
Norepinephrine	3.5	1.1
3,4-Dihydroxybenzylamine	5.5	2.0
Epinephrine	5.6	2.1
Normetanephrine	6.6	2.3
Dopamine	8.0	3.0
Epinine (*N*-methyldopamine)	15.0	5.0
Metanephrine	16.0	6.0
5-Hydroxytryptamine (serotonin)	20.0	5.0
5-Methoxytryptamine[b]	(21.0)	(33.0)
3-Methoxytyramine	27.0	6.0
Tryptamine[b]	(31.0)	(30.0)
4-Methoxy-3-hydroxyphenethylamine	41.0	13.0

[a]All compounds (except two[b]) investigated under the conditions described in the text.
[b]Chromatograms of these two compounds were obtainable at +0.94 V vs. SCE and not at the usual setting of +0.60 V.

there were any cause for concern. Also, in these as well as brain samples, the epinephrine could be determined along with NE, DA, and 5-HT by either (a) adopting another internal standard, like epinine, which elutes between DA and 5-HT, or (b) discarding the internal standard methodology altogether and utilizing a standard addition technique.

Comparison to other techniques

Of the two other techniques which offer sensitivity and selectivity of the same order as the l.c.e.c. method for NE, DA, and 5-HT, neither g.c.—m.s. nor radiochemical enzymatic labelling can provide values for all three components simultaneously. L.c.e.c. is the only method with sub-picomole sensitivity which can afford values for all three simultaneously. Both g.c.—m s. and the radiochemical methods (as well as all other reasonably sensitive techniques) for biogenic amines require derivatization of the components but l.c.e.c. does not and thus offers the distinct capability of greater precision. The sensitivity of l.c.e.c. is equal to or greater than that of g.c.—m.s. or radiochemical labelling for each of the species determined.

In terms of selectivity, g.c.—m.s. certainly has the most to offer through its multiple ion-monitoring capabilities. L.c.e.c. is rather more selective than the radiochemical techniques in routine applications. Both experience interferences from similar compounds, but without the addition of chromatographic separations these would not be identified in the radiochemical methods. For example, *N*-methyldopamine (epinine) could easily interfere in both the radiochemical and l.c.e.c. methods but it would appear virtually undetected in the former technique while it would be readily seen (and not interfere) in the chromatograms routinely obtained with l.c.e.c. An additional qualitative (selectivity) piece of information has gone practically unnoticed for l.c.e.c. determinations. As originally pointed out by Refshauge [54], and more recently by Shoup and Kissinger [55], successive injections of the sample solution can be made at different electrode potentials. A resultant plot of peak current vs. potential would yield a type of hydrodynamic voltammogram, with the half-wave potentials and peak shapes distinctive for a given compound at a given electrode in a given eluting solvent. This would provide investigators using l.c.e.c. with even greater selectivity than they now normally obtain. The high degree of selectivity available through utilization of l.c.e.c. for brain tissue, however, makes this added information generally superfluous and not worth the additional time required.

In terms of the time required for a typical analysis, g.c.—m.s. and radiochemistry appear to better the present technique if only one or, possibly, two of the components are desired. But, when all three are of concern, l.c.e.c. is quite comparable and, in fact, generally better. G.c.—m.s. requires minimal isolation/purification times and very minimal chromatographic times, but practical experience has shown g.c.—m.s. to be very demanding, especially for the most sensitive determinations. Indeed, proper maintenance for the very lowest levels would allow only ca. 15—20 samples to be run in a routine day.

At these lower sensitivity levels, the capabilities of l.c.e.c. do not differ from the higher levels where, by using the dual parallel apparatus [56], one can handle routinely ca. 15—20 samples per day. The extensive automation on radiochemical counting, should allow a much larger number of samples per day to be run, but even with highly labelled cofactors, the more sensitive radiochemical determinations can require longer individual counting times to attain the required precision. Automation of the chromatographic phase of the l.c.e.c. procedure, a distinct possibility with micro- or mini-computer technology, would make it very competitive with the radiochemical assays in this regard.

The time required for chromatographic elution of a single sample by l.c.e.c. is the most serious drawback of the present technique. Utilization of the dual parallel apparatus [56] and the possible utilization of automation can help minimize this problem, but a better solution will involve the column packing material and the eluting solvent. It appears that a shorter total elution time, possibly similar to that obtained by the conditions of Shoup and Kissinger [55], could be inserted directly into the present scheme to provide shorter analysis times. Alternatively, it may be possible to find a column and solvent that will allow, through greater resolution, elimination of the initial isolation/purification steps in the present procedure, similar to that employed by Plotsky et al. [57] for NE and DA determinations; both of these possibilities are under study.

The authors thank Mr. David Wassil for performing the mouse brain dissections, Drs. William B. Stavinoha and A. T. Modak for demonstrating the dissection technique, Mr. Rick Isernhagen for examination of some of the potential interferences, and Ms. Tammy Presley for help in running some of the analyses. This work was supported by Grant No. R 01 MH26866-03 from NIMH/DHEW/USPHS.

REFERENCES

1 T. Nagatsu, Biochemistry of Catecholamines, University Park Press, Baltimore, 1973.
2 D. Hawkins and L. Pauling, Orthomolecular Psychiatry, W. H. Freeman, San Franciso, 1973.
3 U. S. von Euler, Clin. Chem., 18 (1972) 1445.
4 A. Coppen, Brit. J. Psychiat., 113 (1967) 1237.
5 G. C. Cotzias, New Engl. J. Med., 278 (1968) 630.
6 W. E. Bunney, Jr., Psychopharmacol. Commun., 1 (1975) 599.
7 J. Barchas and E. Usdin (Eds.), Serotonin and Behavior, Academic, New York, 1973, pp. 487, 565, 567.
8 L. Stein and C. D. Wise, Science, 171 (1971) 1032.
9 D. M. Shaw, F. E. Camps and E. G. Eccleston, Brit J. Psychiat., 113 (1967) 1407.
10 S. T. Breisch, F. P. Zemilan, and B. G. Hoebel, Science, 192 (1976) 384.
11 P. L. Carlton, Psychol. Rev., 70 (1963) 19.
12 B. A. Campbell, L. D. Lytle and H. C. Fibiger, Science, 166 (1969) 635.
13 A. K. Swonger and R. H. Rech, J. Comp. Physiol., 81 (1972) 509.
14 J. H. Gordon and M. K. Shellenberger, Neuropharmacol.. 13 (1974) 129.

15 M. K. Shellenberger, Neuropharmacol., 10 (1971) 347.
16 M. K. Shellenberger, J. Pharmacol. Exp. Ther., 177 (1971) 481.
17 E. P. Miller, R. H. Cox, Jr., and R. P. Maickel, Science, 162 (1968) 463.
18 R. C. Hanig and M. H. Aprison, Life Sci., 10 (1971) 279.
19 A. S. Welch and B. L. Welch, Anal. Biochem., 30 (1969) 161.
20 K. M. Taylor and R. Laverty, J. Neurochem., 16 (1969) 1367.
21 G. B. Ansell and M. F. Beeson, Anal. Biochem., 23 (1968) 169.
22 M. K. Schellenberger and J. H. Gordon, Anal. Biochem., 39 (1971) 356.
23 R. P. Maickel, R. H. Cox, J. Saillant and F. P. Miller, Int. J. Neuropharmacol., 7 (1968) 725.
24 J. W. Vanable, Jr., Anal. Biochem., 6 (1963) 393.
25 U. S. von Euler, Pharmacol. Rev., 11 (1959) 262.
26 D. F. Bogdanski, A. Pletscher, B. B. Brodie and S. Udenfriend, J. Pharmacol. Exp. Ther., 117 (1956) 82.
27 E. L. Arnold and R. Ford, Anal. Chem., 45 (1973) 85.
28 I. L. Martin and G. B. Ansell, Biochem. Pharmacol., 22 (1973) 521.
29 S. H. Koslow, G. Racagni and E. Costa, Neuropharmacol., 13 (1974) 1123.
30 C. Refshauge, P. T. Kissinger, R. Dreiling, C. L. Blank, R. Freeman and R. N. Adams, Life Sci., 14 (1974) 311.
31 S. Sasa and C. L. Blank, Anal. Chem., 49 (1977) 354.
32 P. A. Shore and J. S. Olin, J. Pharmacol. Exp. Ther., 122 (1958) 295.
33 A. C. Cuello, R. Hiley and L. L. Iversen, J. Neurochem., 21 (1973) 1337.
34 J. M. Saavedra, B. Brownstein and J. Axelrod, J. Pharmacol. Exp. Ther., 186 (1973) 508.
35 K. Engelman, B. Portney and W. Lovenberg, Am. J. Med. Sci., 255 (1968) 259.
36 K. Engelman and B. Portney, Circ. Res., 26 (1970) 53.
37 J. T. Coyle and D. Henry, J. Neurochem., 21 (1973) 61.
38 M. Palkovits, M. Brownstein, J. M. Saavedra and J. Axelrod, Brain Res., 77 (1974) 137.
39 A. H. Antone and D. F. Sayre, J. Pharmacol. Exp. Ther., 138 (1960) 360.
40 E. Costa, S. H. Koslow and H. F. LeFevre, in L. L. Iversen, S. D. Iversen and S.H. Snyder (Eds.), Handbook of Psychopharmacology, Vol. 1, Plenum, New York, 1975.
41 P. J. Kissinger, C. Refsheuge, R. Dreiling and R. N. Adams, Anal. Lett., 6 (1973) 465.
42 R. Keller, A. Oke, I. Mefford and R. N. Adams, Life Sci., 19 (1976) 995.
43 P. T. Kissinger, R. M. Riggin, R. L. Alcorn and L. D. Rau, Biochem. Med., 13 (1975) 299.
44 R. E. Majors, Am. Lab., 7 (1975) 13.
45 J. H. Zar, Biostatistical Analysis, Prentice-Hall, Englewood Cliffs, N.J., 1974, p. 101.
46 R. M. Fleming, W. G. Clark, G. D. Fenster and J. B. Towne, Anal Chem., 37 (1965) 692.
47 S. T. Weintraub, W. B. Stavinoha, R. L. Pike, W. W. Morgan, A. T. Modak, S. H. Koslow and L. Blank, Life Sci., 17 (1975) 1423.
48 R. G. Wiegand and J. E. Perry, Biochem. Pharmacol., 7 (1961) 181.
49 P. Albrecht, W. B. Vischer, J. J. Bittner and F. Halberg, Proc. Soc. Exp. Biol. Med., 92 (1956) 702.
50 J. D. Fernstrom and R. J. Wurtman, Science, 173 (1971) 149.
51 R. F. Butterworth, F. Landreville, M. Guitard and A. B. Barbeau, Clin. Biochem., 8 (1975) 298.
52 L. E. Smith, J. D. Lane, P. A. Shea, W. J. McBride and M. H. Aprison, Anal. Biochem., 64 (1975) 149.
53 R. H. Cox, Jr. and J. L. Perhach, Jr., J. Neurochem., 20 (1973) 1777.
54 C. Refshauge, Ph.D. Thesis, Univ. Kansas, 1975.
55 R. E. Shoup and P. T. Kissinger, Clin. Chem., 23 (1977) 1268.
56 C. L. Blank, J. Chromatogr., 117 (1976) 35.
57 P. M. Plotsky, R. M. Wightman, W. Chey and R. N. Adams, Science, 197 (1977) 904.

Analytica Chimica Acta, 104 (1979) 47—53

RAPID ASSAY OF GALACTOSE IN BLOOD SERUM AND URINE BY AMPEROMETRIC MEASUREMENT OF ENZYME-CATALYZED OXYGEN CONSUMPTION

FRANK S. CHENG and GARY D. CHRISTIAN*

Department of Chemistry, University of Washington, Seattle, Washington 98195 (U.S.A.)

(Received 3rd July 1978)

SUMMARY

An enzymatic method for the direct, rapid determination of galactose in blood serum and urine is described. The method is based on amperometric measurement of the rate of oxygen depletion when galactose is oxidized by molecular oxygen in the presence of galactose oxidase. The method does not require incubation nor deproteinization. A single sample measurement requires less than 1 min.

The need for suitable methods for early detection of galactosemia and other disorders has prompted development of a variety of methods for determination of galactose in blood in recent years [1—4]. The classical redox methods are no longer recommended, because of interferences of other reducing sugars in biological samples. Enzymatic methods, based on either galactose oxidase [5, 6] or NAD-linked galactose dehydrogenase [7], have been employed for galactose measurements.

This paper describes a rapid approach for the measurement of galactose, based on the aerobic oxidation of galactose by molecular oxygen in the presence of galactose oxidase.

$$\text{D-galactose} + O_2 \xrightarrow{\text{galactose oxidase}} \text{D-galactohexodialdose} + H_2O_2$$

The maximum rate of oxygen depletion during the reaction is measured amperometrically with a membrane oxygen electrode and is directly proportional to the concentration of galactose in the sample. The procedure does not involve removal of protein from samples, and neither incubation nor extraction is necessary, which allows a direct and rapid determination in biological samples. Measurements require less than one minute.

EXPERIMENTAL

Apparatus

A Beckman Glucose Analyzer (Beckman Instruments, Inc.), in conjunction with a two-pen strip-chart recorder (Linear Instruments Corp., Irvine, CA

92714) was used to measure the rate of oxygen consumption. All the measurements were done in the U-mode of the analyzer to obtain the maximum sensitivity.

Helena Quickpettes (Helena Laboratories, Beaumont, Texas 77707) with pipetting ranges of 5—50 μl, 50—250 μl, and 250—1000 μl, respectively, were used to deliver samples and reagents.

Reagents

Buffers. The following reagents (Aldrich) were used, as received, to prepare buffer solutions: bicine [*N,N*-bis-(2-hydroxyethyl)glycine], tricine [*N*-(tris-(hydroxymethyl)methyl)glycine)] and glycylglycine. Hydrochloric acid and sodium hydroxide, both 1 M, were used to adjust the pH. Distilled, deionized water was used to prepare all solutions.

Enzymes. Galactose oxidase (galactose: O_2 oxidoreductase, E.C.1.1.3.9) as a lyophilized dry powder was obtained from Worthington Biochemical Corp., Freehold, N. J. The preparation contained about 65 absorption units per mg of dry protein, which corresponds to 35 I.U. mg^{-1}.

Galactose standard. Anhydrous D-(+)-galactose (2 g; Matheson, Coleman & Bell) was dissolved in 200 ml of water and allowed to stand at room temperature for 1 day before use, in order to assure complete mutarotational equilibrium. Each working day, this stock solution was diluted with water, serum or urine sample to obtain working standards containing 5—250 mg of galactose per 100 ml of solution.

Procedure

Place 0.700 ml of 0.10 M glycylglycine buffer solution, 1.0 mM in $K_3Fe(CN)_6$, 0.030 M in KI, and 0.4 mM in $(NH_4)_2MoO_4$ in the reaction cell of the analyzer. For 30—200 mg of galactose per 100 ml, pipet 30 μl of sample (serum or urine) or standard into the cell and let the oxygen in the solution come to equilibrium with atmospheric oxygen. This procedure is necessary because the temperature of the reagent is not the same as the instrument temperature (33°C). With <1 ml of solution in the reaction cup, it takes only a few s to reach oxygen equilibrium, which can be judged from the almost constant digital panel meter reading, with the selector switch in the "check" position.

Pipet 20 I.U. of galactose oxidase solution (in about 20 μl) into the cell to start the reaction, and record the rate of oxygen consumption vs. time. The peak (the maximum rate) is obtained about 30 s after the introduction of the enzyme, and is directly related to the galactose concentration.

The concentration range measured can be increased or the detection limit decreased by varying the sample size, the reagent volume or the amount of enzyme (see below).

RESULTS AND DISCUSSION

Effect of potassium hexacyanoferrate(III)

Hamilton et al. [8] and Libby [9] have demonstrated that hexacyanoferrate(III) ions can activate galactose oxidase-catalyzed oxidations under certain conditions: millimolar levels activate the reaction 2 to 3-fold, but micromolar levels cause up to about 60% inhibition. Dahodwala et al. [1] have also reported a similar activation of their covalently immobilized galactose oxidase.

Figure 1 shows the signals obtained in the absence and presence of activator in the present procedure. It is apparent that without the hexacyanoferrate(III), the galactose oxidation reaction is delayed and is slower. It takes 1 min to reach the maximum rate of oxygen consumption. However, when the reaction medium is 1 mM in $K_3Fe(CN)_6$, the maximum rate of oxygen depletion is obtained in about 30 s. In addition, the derivative signal (peak height) (Fig. 1) of the reaction in the presence of activator is twice that obtained in its absence. In both cases, however, the difference between the initial and final oxygen concentration (direct signals) is about the same, which, with only small oxygen diffusion from the atmosphere to the cell, corresponds very closely to the total amount of galactose present in the sample.

Figure 2 shows the effect of potassium hexacyanoferrate(III) concentration on the rate of oxygen depletion. The optimal concentration lies around 1 mM, which is in agreement with that observed by Hamilton et al. [8, 9].

Effect of pH

Since the discovery of galactose oxidase by Cooper et al. [5], the optimal pH for the enzyme has been reported by different investigators to range from 6.5 to 8.5 depending on reaction conditions [2, 5, 10—12]. In their extensive studies on galactose oxidase, Hamilton et al. [8, 9, 13] have found that the kinetic behavior of the enzyme is different in different buffers.

The effect of pH on the aerobic oxidation of galactose was studied in two buffers in the present procedure. Figure 3 shows the pH profile of the reaction

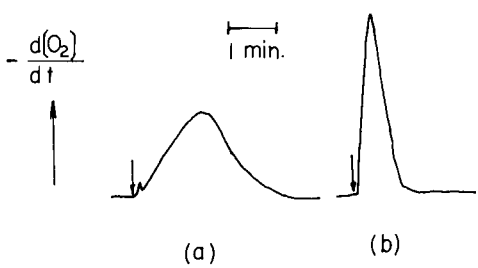

Fig. 1. Typical galactose oxidation responses obtained by adding 25 μl of galactose standard (180 mg/100 ml) to 0.7 ml of 0.1 M glycylglycine pH 7.8, containing 20 I.U. of galactose oxidase, and 0.03 M in iodide and 0.4 mM in Mo(VI). The small arrows indicate sample addition to start the reaction. (a) Absence, (b) presence of 1 mM $K_3Fe(CN)_6$ in the buffer solution.

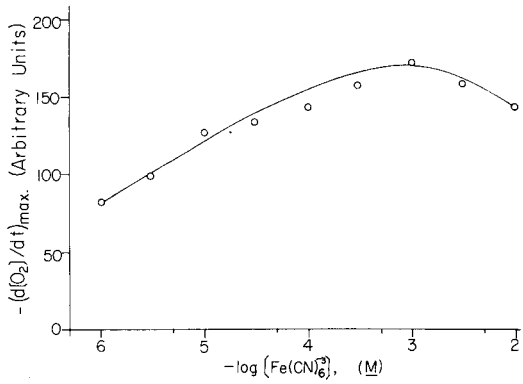

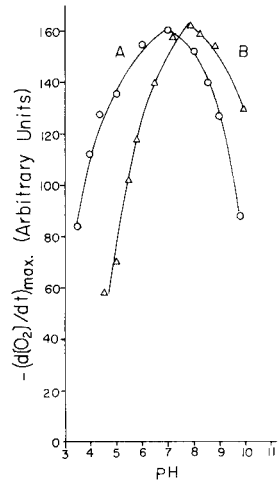

Fig. 2. Effect of hexacyanoferrate(III) concentration on the rate of oxygen depletion. Reaction conditions as in Fig. 1.

Fig. 3. Effect of pH (0.1 M buffer) on the rate of oxygen depletion. Reaction conditions as in Fig. 1(a) except for buffer type and 30 I.U. galactose oxidase. (A) Tricine; (B) Glycylglycine buffer.

in tricine and glycylglycine buffers. It is clear that, although the type of buffer does not change the maximum rate of reaction significantly, it causes a difference in the optimal pH of reaction, in agreement with previous investigators [8, 9, 13]. Under the present conditions, the optimal pH with tricine is 7.0 and with glycylglycine, about 8.0.

Effect of other additives

Hydrogen peroxide has been reported to inhibit and irreversibly inactivate galactose oxidase when it is allowed to reach high enough concentrations during the reaction [8]. In the present procedure, hydrogen peroxide is removed as it is produced by reaction with iodide ions, catalyzed by molybdate ions. By adding different amounts of iodide and molybdate to the reaction medium, it was found that the optimal concentrations for iodide and molybdate are 30 mM and 0.4 mM, respectively. These concentrations were used throughout the study.

Libby [9] has shown that the presence of 0.5 mM EDTA in galactose oxidase reactions not only activates, but also produces a shorter induction period, for the reaction. However, EDTA did not cause any activation in the present method whether or not 1 mM hexacyanoferrate(III) was added; this is in agreement with Taylor et al. [3].

Effect of enzyme activity

Figure 4 shows the effect of the amount of galactose oxidase in 0.1 M tricine buffer pH 7.0, on the maximum rate of reaction. The rate tends to level off slightly at high enzyme concentrations. In order to increase the signal, especially for low concentrations of galactose, it is preferable to use a large amount of enzyme. However, to minimize costs, the smallest possible quantity of enzyme should be used. Therefore, in most of the present measurements, 20 I.U. of enzyme were used.

Calibration data

Figure 5 shows some recorded derivative signals for aqueous galactose standards. The peak heights represent the maximum rate of oxygen depletion, and are directly proportional to galactose concentration in the sample. The magnitude of the signals can be read directly from the digital panel meter of the Glucose Analyzer with the mode selection switch on "U-mode". The derivative signals reach a plateau at the lower concentrations, which would suggest that the reaction proceeds at a constant rate for some time, rather than going through a peak maximum rate as expected. This is probably due to the back-diffusion of oxygen into the cell as a result of the relatively slow reaction at these concentrations after the initial rapid rate [14].

A linear plot of peak height vs. concentration of galactose is obtained from 30—200 mg/100 ml, when 30 μl of sample and 20 I.U. of enzyme are used. This, however, does not indicate the working range of the procedure, for the detection limits can be improved significantly by increased sample size and/or increased amount of enzyme. In contrast, with highly concentrated samples, the useful range of linearity can be extended considerably by increasing the

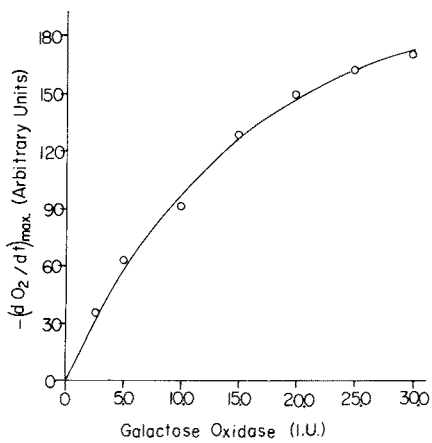

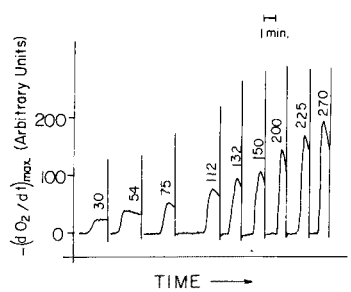

Fig. 4. Effect of amount of galactose oxidase on the initial rate (0.1 M tricine buffer pH 7.0).

Fig. 5. Recorded signals for 25 μl of aqueous galactose standards (0.1 M tricine buffer pH 7.0). Numbers on peaks represent galactose concentration (mg/100 ml).

amount of buffer to, e.g., 1 or 2 ml and decreasing the sample volume. The calibration procedure should be changed in the same manner. Although the galactose concentrations normally encountered range from several milligrams to about 400 mg per 100 ml [10], they can be easily covered by the procedures outlined above; no interference was observed in using larger amounts of samples.

Recovery study

In spite of extensive efforts, attempts to obtain serum, blood or urine samples from either clinical galactose tolerance tests or from patients with galactosemia were unsuccessful. In lieu of clinical samples, synthetic samples were prepared by adding known quantities of galactose to pooled serum, clinical control sera and urine samples.

Table 1 lists the relative recoveries of galactose from the three types of samples. The recovery ranges from 95 to 107%, with an average recovery of 101% and average deviation 3.47% (s.d. ± 4.11). There is no significant variation in recovery over the concentration range 50—200 mg/100 ml.

Selectivity and precision

Galactose oxidase has known catalytic activity for the oxidation of a number of substrates [6, 8, 9]. In order to study possible interferences, the relative reaction rate of several other substrates was measured. Table 2 lists the relative rates obtained under the present measuring procedure. Only lactose exhibits a measurable reaction in the presence of galactose oxidase, but is not normally present in blood or urine. The major reducing sugar in

TABLE 1

Recovery of galactose added to biological fluids by the recommended method

Sample	Galactose (mg/100 ml)		Recovery (%)
	Added	Found	
Pooled serum	0	0	
	50.0	52.0	104
	100	107	107
	150	144	96
	200	194	97
Beckman clinical chemistry control serum	0	0	
	50.0	48.0	96
	100	104	104
	150	155	103
	200	209	105
Normal adult urine	0	0	
	50.0	50.4	101
	100	95	95
	150	157	104
	200	204	102

TABLE 2

Relative reaction rates of galactose oxidase-catalyzed oxidation of various substrates (150 mg/100 ml) in the recommended method

Substrate[a]	Relative oxidation rate	
	Present procedure	Reported value [6]
D-Galactose	100	100
D-Glucose	0	0
Lactose	8	2
Maltose	0	—
Sucrose	0	—
Fructose	0	0
Galactose-1-phosphate	0	9

physiological samples, D-glucose, does not interfere with the proposed method at a concentration as high as 500 mg/100 ml.

The coefficient of variation was ± 4.88% for eight determinations of pooled serum containing 100 mg/100 ml galactose, when 25-μl samples were used.

REFERENCES

1 S. K. Dahodwala, M. K. Weibel and A. E. Humphrey, Biotech. Bioeng., 18 (1976) 1679.
2 C. D. McGlothlin and W. C. Purdy, Anal. Chim. Acta., 88 (1977) 33.
3 P. J. Taylor, E. Kmetec and J. M. Johnson, Anal. Chem., 49 (1977) 789.
4 G. A. Mason, G. K. Summer, H. H. Dutton and R. C. Schwaner, Jr., Clin. Chem., 23 (1977) 971.
5 J. A. D. Cooper, W. Smith, M. Bacila and H. Medina, J. Biol. Chem., 234 (1959) 445.
6 G. Avigad, D. Amaral, C. Asensio and B. L. Horecker, J. Biol. Chem., 237 (1962) 2736.
7 G. Kurz and K. Wallenfels, in H. U. Bergmeyer (Ed.), Methods of Enzymatic Analysis, Vol. 3, Academic Press, New York, 1974, p. 1279.
8 G. A. Hamilton, J. De Jersey and P. K. Adolf, in T. E. King, H. S. Mason and M. Morrison (Eds.), Oxidase and Related Redox Systems (Proceedings of the Second International Symposium), University Park Press, Baltimore, MD, 1973, p. 103.
9 R. D. Libby, Ph.D. Thesis, The Pennsylvania State University, 1974.
10 H. Roth, S. Segal and D. Bertoli, Anal. Biochem., 10 (1965) 32.
11 M. Hjelm and C. H. de Verdier, in H. U. Bergmeyer (Ed.), Methods of Enzymatic Analysis, 2nd ed., Vol. 3, Academic Press, New York, 1974, p. 1282.
12 C. D. Nordschow, Clin. Chim. Acta, 28 (1970) 89.
13 G. A. Hamilton, R. D. Libby and C. R. Hartzell, Biochem. Biophys. Res. Commun., 55 (1973) 333.
14 L. H. Thomas and G. D. Christian, Anal. Chim. Acta, 89 (1977) 83.

Analytica Chimica Acta, 104 (1979) 55—65

CYCLIC AND STRIPPING VOLTAMMETRY OF TIN IN THE PRESENCE OF LEAD IN PYROGALLOL MEDIUM AT HANGING AND FILM MERCURY ELECTRODES

STEFAN GLODOWSKI and ZENON KUBLIK*

Institute of Fundamental Problems of Chemistry, University of Warsaw, 02093 Warsaw, Pasteura 1 (Poland)

(Received 22nd June 1978)

SUMMARY

The influence of pyrogallol on the determination of traces of tin(IV) in the presence of lead was investigated by cyclic and stripping voltammetric technique at hanging drop and thin film mercury electrodes. The electroreduction of tin(IV) proceeds through an adsorption step; at more negative potentials, the adsorption process becomes limited and reduction ceases, particularly in stirred solutions. Such effects may decrease the sensitivity obtained for tin in anodic stripping voltammetry. Two methods are proposed for the determination of traces of tin(IV) in the presence of lead. In one, a silver-based mercury film electrode is used in a solution containing pyrogallol and oxalic acid; the peaks are thus separated by 90 mV, and the detection limit for tin, with a 10-fold amount of lead, is 2×10^{-8} mol l^{-1}. In the second less-sensitive method, a HMDE is used in a solution containing pyrogallol and perchloric acid; the separation of the stripping peaks for tin and lead is then poor but tin(IV) can be determined from the peak corresponding to oxidation of tin(II) to tin(IV).

The strong tendency of tin(IV) species to hydrolyse and polymerise as well as the overlap of the stripping peaks of tin and lead are serious obstacles to the determination of tin by anodic stripping at mercury electrodes. It seemed likely that selective complexation of tin(IV) would lead not only to decreased hydrolysis of tin(IV) but also to the separation of the tin and lead stripping peaks. The use of pyrogallol as a complexing agent appeared promising because it forms stable complexes with tin(IV) [1, 2] whereas it does not affect the electrochemical behaviour of lead [3, 4].

Information on the influence of pyrogallol on the behaviour of tin(IV) under stripping conditions is scarce and contradictory. DeMars [5] found that tin dissolves anodically from the hanging mercury drop electrode (HMDE) into pyrogallol medium in accordance with the Frankenthal and Shain equation [6]; Phillips [4] suggested that pyrogallol offers several advantages in overcoming the obstacles mentioned above. In contrast, Florence and Farrar [7] could not separate the anodic peaks of tin and lead in the presence of pyrogallol; moreover, in their experiments the height of the tin stripping peak was less than the theoretical value. According to Bard [2], the tin(IV)—pyrogallol

complex is reduced via an adsorption step, thus any changes in adsorption may affect the reduction of tin(IV). However, cyclic voltammetric curves for the tin(IV)—pyrogallol complex show adsorption effects only at high voltage scan rates or in the presence of surface-active agents [8].

The aim of the present work was to establish the best conditions for stripping determinations of traces of tin in the presence of lead in acidic pyrogallol medium.

EXPERIMENTAL

The voltammetric curves were recorded with a Radelkis OH-102 polarograph with a three-electrode arrangement, or with an arrangement consisting of a PAR Model 173 potentiostat equipped with a Model 176 current-to-voltage converter, a Chemipan Model GP-1 function generator and a Riken-Denshi F-2C XY recorder. A saturated calomel electrode was used as a reference electrode and all potentials given are referred to this electrode. The working electrodes were a hanging mercury drop electrode (HMDE) [9] and a silver-based mercury film electrode (MFE) with a prolonged lifetime [10] and with a geometric surface area of 0.03—0.042 cm^2. The thickness of the mercury film was calculated from the electrical charges consumed during mercury deposition or dissolution. These charges were measured with a PAR Model 173 potentiostat equipped with a Model 179 digital coulometer.

Standard tin(IV) solutions were prepared by dissolving tin metal in a hot hydrochloric—nitric acid mixture and boiling to remove oxides of nitrogen. The final stock solution was 2.15×10^{-2} M in tin(IV) and 2.6 M in hydrochloric acid. This solution was added directly to the supporting electrolyte containing pyrogallol; any further dilution needed was done with 2.5 M hydrochloric acid. Thus, some hydrochloric acid was always introduced into the test solutions along with the tin(IV). The remaining solutions were prepared with reagent-grade chemicals and twice-distilled water.

Before measurement, all solutions were deaerated with hydrogen produced electrolytically and purified by passing through acidic solutions of vanadium(II) sulphate over zinc amalgam. Most experiments were done at ambient room temperature (18—22°C). For quantitative work, a thermostatted circulating water bath was used to maintain the temperature at 20 ± 0.1°C.

Pyrogallol is susceptible to air oxidation [3, 11], and was therefore added as the solid to deaerated solution just before the addition of tin(IV) samples.

CYCLIC VOLTAMMETRY

Effect of pH and the composition of the supporting electrolyte

The best-defined polarographic waves of tin(IV) are obtained in a solution containing pyrogallol and 0.1 M perchloric acid [1]; tin(IV) forms a complex containing two molecules of pyrogallol whereas tin(II) is uncomplexed [2]. However, under these conditions the second reduction wave of tin(IV) and the reduction wave of lead(II) merge.

Variations in the composition of the supporting electrolyte were tested in attempts to find the best conditions for the separation of the anodic peaks of tin and lead. Figure 1 presents some of the cyclic curves obtained for tin(IV). In the absence of pyrogallol even at quite high concentrations of hydrochloric acid (curve 1), the reduction of tin(IV) to tin(II) is not diffusion-controlled. Instead of a cathodic peak only a small potential dependent current is observed. The peaks of the Sn(II)—Sn(Hg) are quite well defined, which means that the reduction of tin(II) to tin amalgam proceeds in a nearly reversible manner. However, under these conditions, the dissolution peaks of tin and lead cannot be separated either at the HMDE or the silver-based MFE.

A comparison of curves 1 and 2 shows clearly the advantages of the pyrogallol medium. Curve 2 shows two well-defined, practically reversible systems of peaks: c_1/a_1, corresponding to the Sn(IV)—Sn(II) couple and c_2/a_2 corresponding to the Sn(II)—Sn/Hg couple. The difference between the potentials of the dissolution peaks of tin and lead under these conditions does not exceed 35 mV, which is too low for adequate resolution of the peaks at either working electrode. However, under these conditions, peak a_1 is only slightly lower than peak a_2, and its peak potential does not coincide with the anodic peaks of other common metals. Peak a_1 may be used for tin(IV) determination by anodic stripping (see below).

With an increase in acidity, peaks c_1 and c_2 decrease, indicating that the extent of complexation of tin(IV) by pyrogallol is lower than at pH 1. Under these conditions, the second system of peaks shifts slightly towards more negative potentials but not enough to separate the dissolution peaks of tin and lead. With an increase of pH (curve 4), peak c_2 shifts to more negative potentials whereas the position of the dissolution peak of lead remains unchanged. This medium would be advantageous for the separation of the anodic peaks of tin and lead, but peaks c_2 and a_1 become sharper, which may mean that the intermediately formed tin(II) species are partly hydrolysed and adsorbed on the electrode surface. This harmful adsorption effect may be eliminated, without any change in pH, by the addition of a significant excess of formate buffer [4] but concentrated supporting electrolyte solutions are of poor utility for determinations of traces of metals by anodic stripping techniques.

In further experiments, instead of perchloric acid, other 0.1 M acids were used as supporting electrolytes while the concentrations of tin(IV) and pyrogallol were kept constant. The curves obtained in the presence of nitric acid or perchloric acid were the same. In the presence of sulphuric and hydrochloric acids, peaks c_1/a_1 shifted by about 25 mV towards more negative potentials without any change in the peak shape. In the presence of fluoride ion, even at only 0.01 mol l^{-1}, both peak systems vanished which is in accordance with the polarographic data given by Shaap et al. [12]. In the presence of formic acid (pH 1.7), acetic acid (pH 1.7) and salicylic acid (0.02 M, pH 1.8) the first system of peaks shifted slightly towards more negative potentials whereas peaks c_2 and a_1 became sharper. In malonic acid (pH 1.5) and chloroacetic acid (pH 1.4), the sharpening disappeared but peak c_1 was poorly defined.

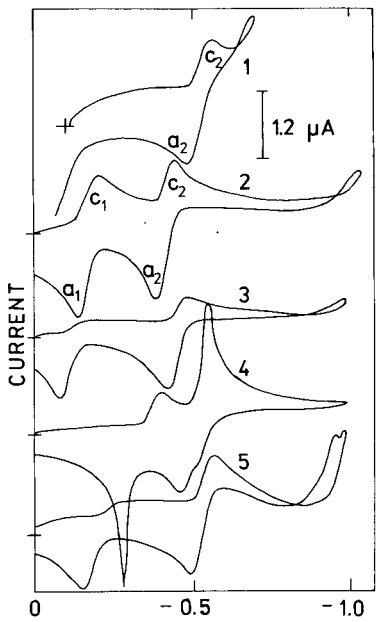

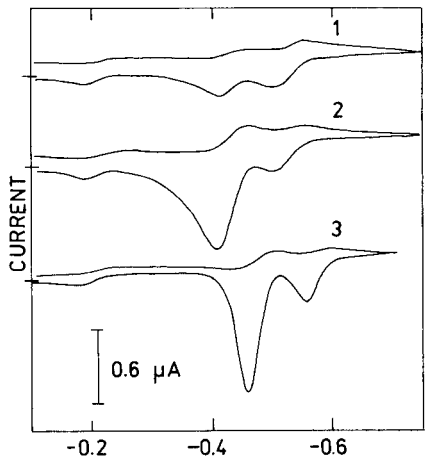

Fig. 1. Cyclic voltammetric curves at the HMDE for a voltage scan rate of 1.5 V min^{-1}. Solutions: (1) 1×10^{-4} mol l^{-1} Sn(IV) + 2 mol l^{-1} HCl; (2—5) 1×10^{-4} mol l^{-1} Sn(IV) + 0.01 mol l^{-1} pyrogallol containing (2) 0.1 mol l^{-1} $HClO_4$; (3) 0.7 mol l^{-1} $HClO_4$; (4) 0.2 mol l^{-1} formate buffer pH 3.7; (5) 0.1 mol l^{-1} $H_2C_2O_4$.

Fig. 2. Cyclic voltammetric curves obtained at (1, 2) HMDE with a surface area of 0.024 cm^2; (3) MFE with a surface area of 0.033 cm^2 and a mercury film thickness of 1.1 μm. The solutions contained 0.1 mol l^{-1} $H_2C_2O_4$ + 0.01 mol l^{-1} pyrogallol and 2×10^{-5} mol l^{-1} Sn(IV) with addition of (1) 1×10^{-5} mol l^{-1} Pb(II); (2, 3) 5×10^{-5} mol l^{-1} Pb(II). Voltage scan rate, 0.25 V min^{-1}.

None of these media appeared suitable for the simultaneous determination of tin and lead, but a medium containing pyrogallol and oxalic acid appeared promising.

The behaviour of tin(IV) in such a medium is shown in Fig. 1 (curve 5). The second system of peaks is shifted towards more negative potentials. Under these conditions, the position of the lead peak remains practically unchanged. This behaviour is in accordance with the data published by Geissler et al. [13], who eliminated the interference of tin on the lead peak by adding oxalic acid and methylene blue. However, even in the presence of pyrogallol, oxalic acid has a harmful effect on the first reduction step, which loses its diffusion-controlled shape.

The curves obtained for tin and lead in a solution containing pyrogallol

and oxalic acid are shown in Fig. 2. The E_p values for tin and lead under these conditions are separated by 90 mV and the height of the anodic tin peak is not affected even by a 5-fold amount of lead (curves 1 and 2). Curve 3 illustrates the potentialities of the silver-based MFE. In accordance with the theory of voltammetry at mercury film electrodes [14], the peaks of the Pb(II)–Pb/Hg and Sn(II)–Sn/Hg systems are displaced towards more negative potentials, but the difference between these peak potentials remains constant because in both cases the same number of electrons is consumed in the reduction of tin and lead. Separation of the two anodic peaks of the metals under these conditions is significantly better because of the decreased width of both peaks. The height of the anodic tin peak at the silver-based MFE may be quantitatively measured even in the presence of a 20-fold amount of lead.

Figure 3 illustrates the advantages and disadvantages of using a medium containing the concentrated formate buffer and pyrogallol. The difference

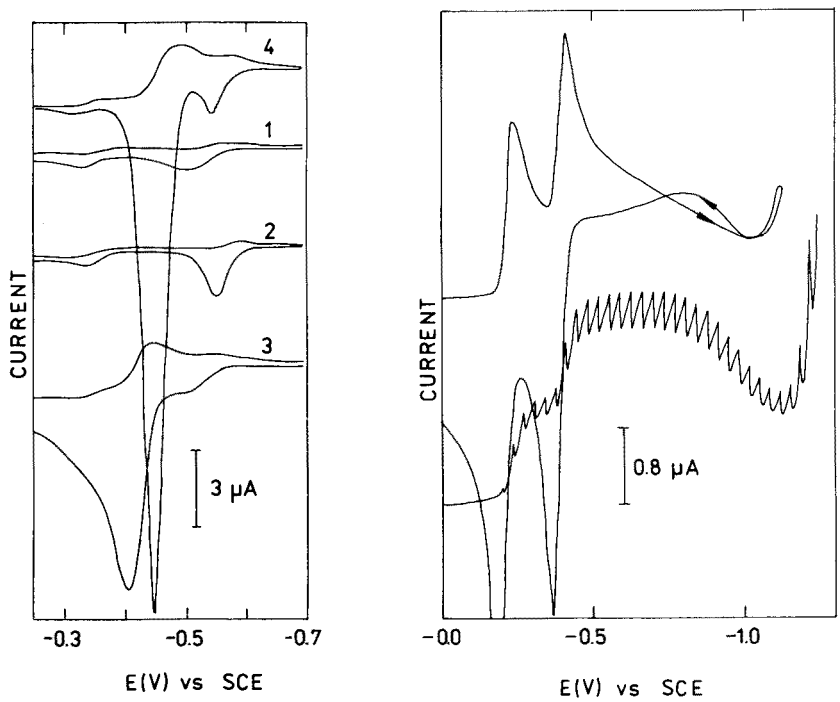

Fig. 3. Cyclic voltammetric curves obtained at (1, 3) HMDE with a surface area of 0.024 cm^2; (2, 4) MFE with a surface area of 0.03 cm^2 and a mercury film thickness of 1.5 μm. The solutions contained 2 mol l^{-1} formate buffer pH 3.7 + 0.01 mol l^{-1} pyrogallol with addition of (1, 2) 1×10^{-4} mol l^{-1} Sn(IV); (3, 4) 1×10^{-4} mol l^{-1} Sn(IV) + 5×10^{-4} mol l^{-1} Pb(II). Voltage scan rate, 0.25 V min^{-1}.

Fig. 4. Polarographic and voltammetric curves obtained for a solution containing 0.07 mol l^{-1} $HClO_4$ + 0.5 mol l^{-1} pyrogallol and 2×10^{-4} mol l^{-1} tin(IV). Voltage scan rate for voltammetric curve, 3 V min^{-1}.

between the E_p values for tin and lead is then close to 100 mV. Comparison of curves 1 and 3 obtained at the HMDE shows that the dissolution peak of tin in only slightly affected by a 5-fold amount of lead(II) in solution. However, the height of the tin dissolution peak is lower than that of the peak obtained for the same concentration of lead(II). Replacement of the HMDE by the MFE improves the shapes and separation of the two anodic peaks, again because the peaks become narrower. As is shown in curve 4, the ratio of $i_p(Sn)/i_p(Pb)$ becomes still smaller under these conditions. Clearly the tin deposition process suffers some interference in this medium, and these interferences are larger at the MFE than at the HMDE.

Investigation of the efficiency of tin deposition

The polarographic curve obtained for acidic solutions containing tin(IV) and pyrogallol (Fig. 4) is, in accordance with literature data [2], characterized by a minimum on the diffusion current plateau at quite negative potentials. The voltammetric reduction curves obtained in unstrirred solutions are usually characterized by a minimum or even minima appearing between the peak and the final rise of the current or between two peaks. It is therefore, not easy to appreciate whether the observed decay of the current corresponds to the "normal" minimum or is caused by interfering effects. Analysis of the cathodic portion of the voltammetric curve (Fig. 4) indicates that the current flowing after the second cathodic peak decreases more strongly than is usual for diffusion-controlled cases. However, the increase observed in the cathodic current during the anodic potential scan shows distinctly that the additional minimum also appears under voltammetric conditions. The minima of this type become less distinct on curves obtained for solutions containing less tin(IV) and pyrogallol, and more distinct when even a small amount of surface active agent is added to the solution.

In contrast to the results obtained in 0.1 M perchloric acid, the voltammetric curves obtained in the presence of oxalic acid exhibit a distinct minimum even at quite low concentrations of tin(IV) and pyrogallol. The shape of the minimum under these conditions is shown in Fig. 1 (curve 5).

This minimum on the voltammetric curves of tin(IV) in the presence of pyrogallol suggests that some inhibition might appear during the preelectrolysis step if the deposition process is held at sufficiently negative potentials. In order to elucidate this aspect, the current—time curves were recorded at various potentials in stirred and unstirred solutions containing pyrogallol and tin(IV). Figure 5 presents several typical curves at a deposition potential of —0.7 V as well as some results obtained for lead(II) and results for tin(IV) in the absence of pyrogallol.

The heights of the curves obtained in stirred solution for reduction of lead(II) in the presence of pyrogallol (curve 4) and for reduction of tin(IV) in the absence of pyrogallol (curve 5) are practically independent of the preelectrolysis time. In contrast, the curves obtained for tin(IV) in the presence of pyrogallol show a distinct diminution in the reduction current although the

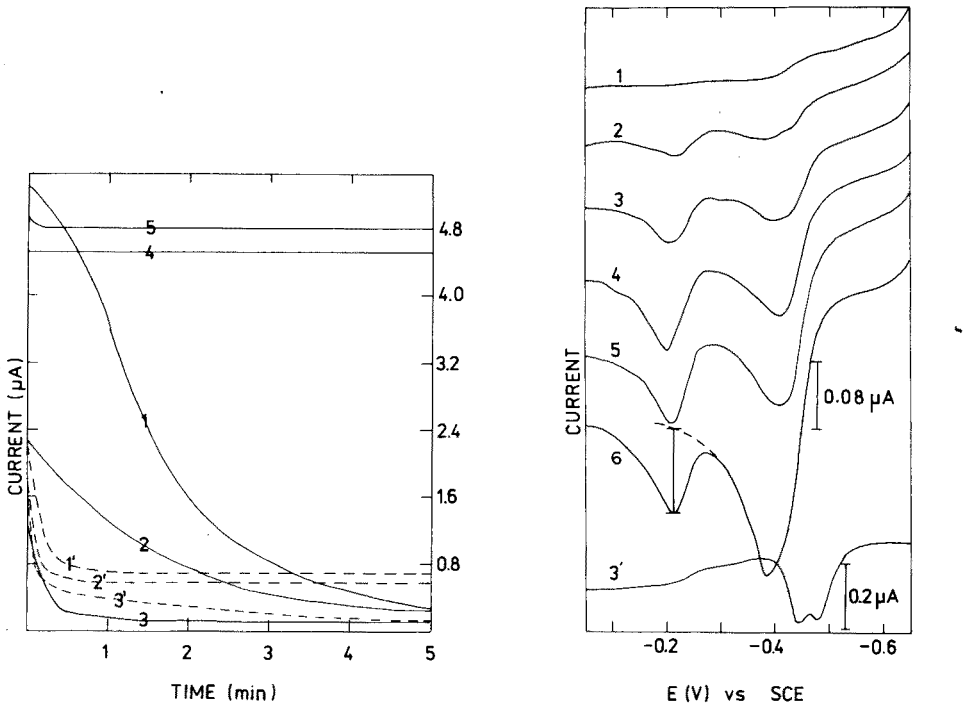

Fig. 5. Current—time curves obtained at the HMDE in stirred (1—5) and unstirred (1′—3′) solutions containing: (1, 1′) 0.1 mol l^{-1} $HClO_4$ + 0.1 mol l^{-1} pyrogallol + 2 × 10^{-4} mol l^{-1} Sn(IV); (2, 2′) 0.1 mol l^{-1} $H_2C_2O_4$ + 0.1 mol l^{-1} pyrogallol + 2 × 10^{-4} mol l^{-1} tin(IV); (3, 3′) 2 mol l^{-1} formate buffer pH 3.7 + 0.1 mol l^{-1} pyrogallol + 2 × 10^{-4} mol l^{-1} tin(IV); (4) 0.1 mol l^{-1} $HClO_4$ + 0.1 mol l^{-1} pyrogallol + 2 × 10^{-4} mol l^{-1} Pb(II); (5) 2 mol l^{-1} HCl + 2 × 10^{-4} mol l^{-1} tin(IV). Deposition potential —0.7 V. Residual currents subtracted.

Fig. 6. Stripping voltammetric curves obtained after deposition for 2 min at —0.65 V with stirring. (1—6) HMDE with a surface area of 0.024 cm^2; (3′) MFE with a surface area of 0.042 cm^2 and with a mercury film thickness of 1.1 μm. The solutions contained 0.1 mol l^{-1} $HClO_4$ + 0.1 mol l^{-1} pyrogallol with addition of (1) 5 × 10^{-6} mol l^{-1} Pb(II); (2) 5 × 10^{-6} mol l^{-1} Pb(II) + 2 × 10^{-7} mol l^{-1} Sn(IV); (3, 3′) 5 × 10^{-6} mol l^{-1} Pb(II) + 4 × 10^{-7} mol l^{-1} Sn(IV); (4) 5 × 10^{-6} mol l^{-1} Pb(II) + 8 × 10^{-7} mol l^{-1} Sn(IV); (5) 2.5 × 10^{-7} mol l^{-1} Pb(II) + 8 × 10^{-7} mol l^{-1} Sn(IV); (6) 8.5 × 10^{7} mol l^{-1} Pb(II) + 8 × 10^{-7} mol l^{-1} Sn(IV). Voltage scan rate, 1.5 V min^{-1}.

solution was stirred at the same speed as for curves 4 and 5. A larger decrease is observed when perchloric acid is replaced by oxalic acid, but the largest decrease appears when a concentrated solution of formate buffer is used. Comparison of the curves 1—1′, 2—2′ and 3—3′ shows that stirring exerts an unexpected influence. In stirred solutions, the current diminishes significantly as the electrolysis time increases; after several minutes or even seconds, it becomes smaller than that observed in the corresponding unstirred solution. It should be noted that in these experiments, the deposition potential was

about 0.2 V more negative than the potential of the second cathodic peak, i.e. the conditions were such that the minimum was not observed on the polarographic or voltammetric curves. The currents decreased more abruptly when the deposition was held at more negative potentials or when a surface-active agent was added. Attempts to perform similar experiments with much lower concentrations of tin(IV) were unsuccessful because the ratio of the tin(IV) reduction current to the residual current was then unfavourable.

The results presented show that the dependence of the height of the tin stripping peak on the deposition time cannot be linear, and that prolongation of the preelectrolysis step may sometimes give better results in unstirred solutions.

STRIPPING EXPERIMENTS

The shapes of the cyclic curves for tin suggest that there are possibilities of determining tin in the presence of lead by stripping voltammetry by means of the height of peak a_1. Figure 6 presents the stripping curves obtained for small concentrations of tin and lead. Even for trace concentrations of tin and lead, peak a_1 is quite well defined, whereas the dissolution peaks for lead and tin show significant overlapping on the curves obtained at the HMDE (curves 2—6) and at the silver-based MFE (curve 3′). The use of the MFE or of decreased scan rates is unfavourable because significant amounts of tin(II) can then diffuse away from the electrode surface before the oxidation potential of tin(II) is attained.

The curves presented in Fig. 6 were obtained in stirred solutions, and such conditions are much more favourable for the accumulation of lead than of tin (Fig. 5). When the preelectrolysis is done in unstirred solutions, the deposition of tin improves compared to that of lead, and tin(IV) can then be determined at higher concentration ratio of Pb(II) to Sn(IV). For instance, after a 10-min deposition time in unstirred solution, tin(IV) can be determined at the 10^{-7} M level in presence of a three-fold amount of lead(II). At higher concentration ratios of Pb(II) to Sn(IV), measuring of the peak height is significantly less accurate.

With increasing deposition times, the height of peak a_1 increases but this increase is not strictly proportional to the deposition time. As shown in Fig. 7, strict proportionality between the height of peak a_1 and the tin(IV) concentration in solution, either in the absence or presence of lead(II), is observed only when the height of peak a_1 is measured to the base line extended as shown in Fig. 6. The relative standard deviations calculated on the basis of five experiments for each concentration of tin(IV) marked in Fig. 7 varied from 2.8 to 6.3%.

Significantly better conditions for simultaneous tin(IV) and lead(II) determinations are found in media containing pyrogallol and oxalic acid. Figure 8 presents the stripping curves of tin and lead obtained at the silver-based MFE, which show that the peak separation is very good. Under such conditions, strict proportionality was obtained between the height of the stripping peak

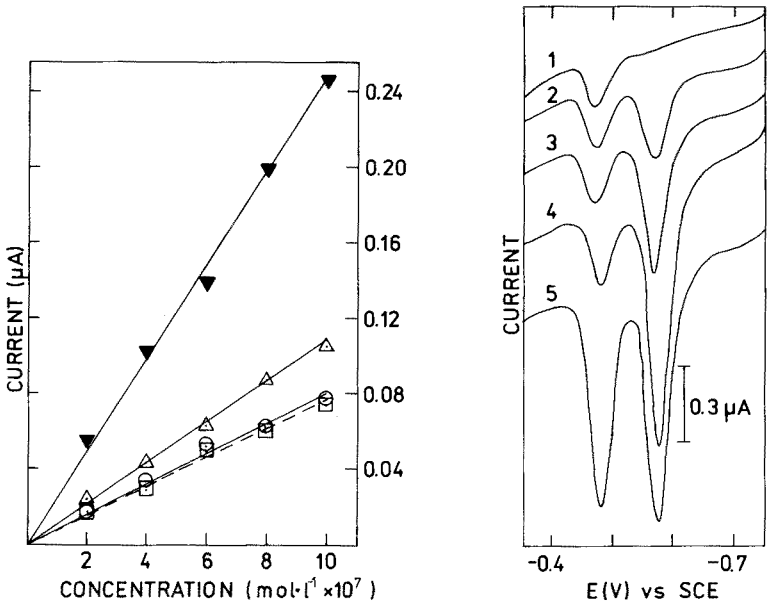

Fig. 7. The relationship between tin(IV) concentration and the anodic peak height at the HMDE after a 10-min deposition time at —0.65 V in unstirred solution containing 0.1 mol l^{-1} $HClO_4$ + 0.1 mol l^{-1} pyrogallol: (○) peak a_1 in the absence of Pb(II); (□) peak a_1 in the presence of equimolar concentrations of Pb(II); (▽) peak a_2 in the absence of Pb(II); (▼) peak a_2 in the presence of equimolar concentrations of Pb(II). Voltage scan rate, 1.5 V min^{-1}.

Fig. 8. Stripping voltammetric curves for increasing amounts of tin(IV) obtained after a 10-min deposition time at —0.75 V in unstirred solutions containing 0.1 mol l^{-1} $H_2C_2O_4$ + 0.1 mol l^{-1} pyrogallol + 3×10^{-8} mol l^{-1} Pb(II). Tin(IV) concentration: (1) 0; (2) 5×10^{-8} mol l^{-1}; (3) 1×10^{-7} mol l^{-1}; (4) 2×10^{-7} mol l^{-1}; (5) as (4) +1×10^{-7} mol l^{-1} Pb(II). The silver-based MFE had a surface area of 0.042 cm^2 and a mercury film thickness of 1.1 μm.

and the tin(IV) concentration in solution in the range 2×10^{-8}—3×10^{-7} M. The relative standard deviation calculated for these curves on the basis of 11 measurements was 9.5%.

Stirring of the solution during the deposition step exerted only a small influence on the height of the tin stripping peak but a significant effect on the lead stripping peak. This behaviour is in accordance with the data obtained in the study of the deposition process. Obviously, for tin(IV) determinations in the presence of lead, deposition in unstirred solutions is essential; in contrast, for lead(II) determinations in the presence of tin(IV), stirred solutions are preferable. Under such conditions, the detection limit for lead even with a 10-fold amount of tin(IV) is 1×10^{-8} mol l^{-1}.

The tin and lead dissolution peaks obtained in the same medium at the HMDE show practically the same difference in peak potentials as that observed at the silver-based MFE. However, because of severe tailing, simultaneous determinations of both metals at the HMDE are not really satisfactory.

As was shown in the cyclic experiments (Fig. 3), solutions containing pyrogallol and concentrated formate buffer appear to be promising for the separation of the dissolution peaks of tin and lead. However, for the determination of small concentrations of tin even in the absence of lead, this medium proved to be unsuitable. When 1×10^{-7} mol l^{-1} tin(IV) was added to this medium, the stripping peak of tin at the HMDE after a 3-min deposition time in stirred solution was almost invisible; even after a 10-min deposition time in unstirred solution, the tin(IV) peak was tiny though under these conditions the lead dissolution peak was quite high. Further increase of the preelectrolysis time in stirred solutions did not improve matters. After deposition from a solution containing 1×10^{-6} mol l^{-1} tin(IV), the tin stripping peak appeared, but its height was very much smaller than that of a lead stripping peak under similar conditions. The results obtained at the silver-based MFE in concentrated formate buffer containing pyrogallol were still worse.

DISCUSSION

The influence of weak adsorption of the substrate of the electrode reaction on the results obtained by anodic stripping voltammetry does not seem to have been discussed hitherto in the literature. The above study has shown that this influence may be harmful, particularly when the deposition potential is close to the desorption potential of the reactant. In such cases, an essential role is played by competition between adsorption of the electroactive reactant and other surface-active agents, which are usually present at very low levels even in very pure supporting electrolytes. During the preelectrolysis step, the amount of surface-active agent adsorbed on the electrode increases, hence adsorption of reactant must decrease. The sensitivity of stripping determinations in which adsorption of the reactant is a necessary preliminary to deposition, must therefore be less than the sensitivity of conventional stripping methods. Prolonged deposition times or faster stirring may not lead under these conditions to increased sensitivity.

The adsorption of reactant does not distort the height of the polarographic waves [2] for tin(IV) concentrations from 1.25 to 0.98×10^{-4} mol l^{-1}. However, the shape of peak a_1 (Fig. 1) shows some distortions which can be attributed to reactant adsorption [8]. The relationship between the height of the cathodic peak current and the tin(IV) concentration deviates from linearity at low tin(IV) concentrations and at high voltage scan rates. Moreover, at high scan rates, the ratio $i_p(c_1)/i_p(a_1)$ is significantly higher than 1. All these facts are in good agreement with the Wopschall and Shain theory [15] of weak adsorption of a reactant on the electrode surface.

According to Phillips [4], concentrated formate buffer containing pyrogallol should be a suitable medium for simultaneous determinations of traces of tin and lead at the 10^{-7}—10^{-8} M level. However, this conclusion was drawn on the basis of cyclic experiments done with moderate concentrations of tin(IV and lead(II), and is not confirmed by the present results; it was impossible to

determine 1×10^{-7} mol l^{-1} tin(IV) even in the absence of lead, and such high buffer concentrations must clearly cause difficulties through reactant adsorption.

The nature of the effect of oxalic acid on the reduction mechanism of tin(IV) is under study.

REFERENCES

1 S. L. Phillips and E. Morgan, Anal. Chem., 33 (1961) 1192.
2 A. J. Bard, Anal. Chem., 34 (1962) 266.
3 M. C. White and A. J. Bard, Anal. Chem., 38 (1966) 61.
4 S. L. Phillips, Anal. Chem., 39 (1967) 536.
5 R. D. DeMars, Anal. Chem., 34 (1962) 259.
6 R. P. Frankenthal and I. Shain, J. Am. Chem. Soc., 78 (1956) 2969.
7 T. M. Florence and Y. J. Farrar, J. Electroanal. Chem., 51 (1974) 191.
8 S. Glodowski and Z. Kublik, to be published.
9 W. Kemula and Z. Kublik, Anal. Chim. Acta, 18 (1958) 104.
10 Z. Stojek and Z. Kublik, J. Electroanal. Chem., 60 (1975) 349.
11 J. Doskocil, Collect. Czech. Chem. Commun., 15 (1950) 599.
12 W. B. Sharp, J. A. Davis and W. H. Nebergall, J. Am. Chem. Soc., 76 (1954) 5226.
13 M. Geissler, B. Schuftal and C. Kuhnard, Z. Chem., 15 (1975) 408.
14 W. T. de Vries and E. van Dalen, J. Electroanal. Chem., 14 (1967) 315.
15 R. H. Wopschall and I. Shain, Anal. Chem., 39 (1967) 1514.

Analytica Chimica Acta, 104 (1979) 67—74

DIRECT DETERMINATION OF TRACE METALS IN SOLID SAMPLES BY ATOMIC ABSORPTION SPECTROMETRY WITH ELECTROTHERMAL ATOMIZERS

Part 1. Investigations of Homogeneity for Lead and Antimony in Metallurgical Materials

ERIK LUNDBERG and WOLFGANG FRECH*

Department of Analytical Chemistry, University of Umeå, S-901 87 Umeå (Sweden)

(Received 23rd June 1978)

SUMMARY

A procedure for investigating the distribution of trace elements in metallurgical materials, illustrated for lead and antimony is described. The distribution is estimated by establishing the relative standard deviation for the trace metal content in five independent dissolutions of a certain sample weight, for different amounts of material (2—100 mg). The results obtained for lead in four materials (stainless steel, mild steel, ferromolybdenum and nickel-base alloy) and antimony in mild steel show that the metals are fairly evenly distributed in samples weighing as little as 2 mg. Graphite-furnace atomic absorption spectrometry was used for the determinations.

The direct determination of trace metals in solid samples by atomic absorption spectrometry (a.a.s.) with electrothermal atomizers offers potential advantages compared with methods involving a dissolution procedure. The dissolution step necessarily implies the addition of chemicals and dilution of the sample. By excluding this step, the risk of contamination is reduced and the high sensitivity of the technique can be fully utilized. In addition, the time needed for an analysis can be shortened, particularly for samples that are difficult to dissolve, e.g. geological materials. Nevertheless, the direct methods have certain limitations which restrict their fields of application. These include a narrow working range because of limited atomizer capacity, problems in finding adequate standardization procedures, and uneven distribution of trace elements in small samples. This last problem will be treated in this paper.

Commercial electrothermal atomizers cannot usually cope with more than a few mg of sample. However, not less than 0.1 mg of the sample can be manipulated conveniently, which means that the useful working range of the "solid sampling technique" is quite narrow. In order to increase the sample capacity, a number of home-made furnaces have been constructed [1—5]. With these furnaces up to 200 mg of sample can be atomized so that the working range is extended and sampling errors are reduced.

Relatively few papers concerned with the direct analysis of solids have apppeared in the literature. Reviews covering this field up to 1975 have been given by Langmyhr [6] and L'vov [1]. Only three papers dealing with metallurgical samples [7—9] seem to have been published since then. Table 1 summarizes some results which have been obtained by using the solid sampling technique for metallurgical materials. As can be seen, the detection limits are extremely low, especially for bismuth determined with the induction-heated furnace [7], but the overall relative standard deviation varies between 3 and 25% and is typically around 10%. It has often been suggested that this poor precision is caused by inhomogeneity in the steel samples. In order to investigate the potentialities of the solid sampling technique with regard to areas of application and attainable precision, it is essential to attain information about homogeneity.

This paper decribes a study of the distribution of lead and antimony in mild steel, and lead in high-alloy steel, nickel-base alloy and ferromolybdenum. In Part 2 [10], the solid sampling technique is applied to the determination of lead in metallurgical samples and factors affecting accuracy and precision are thoroughly investigated.

TABLE 1

Results obtained by the "solid sampling technique" for trace elements in metallurgical sample

Ref.	Elements	Sample weight (mg)	Sensitivity ($\mu g\ g^{-1}$)	Detection limit ($\mu g\ g^{-1}$)	R.s.d. (%)	Matrix	Furnace
18	Cd	1—12	0.08	—	3.6	Zinc	Induction
	Zn		12	—	4.2	Al—Si	
	Al		5	—	7.1	Mild steel	
	Sb		0.8	—	7.4	Mild steel	
	Sn		10	—	9.4	Steel	
7	Bi	1—12	—	0.004	3—10	Steel and cast iron	Induction
8	Pb	1 ± 0.5	—	0.02	9	Complex	Perkin-Elmer
	Bi		—	0.02	7	alloys	HGA 2100
	Se		—	0.2	17		
	Te		—	0.06	17		
	Tl		—	0.03	9		
	Sn		—	0.3	25		
8	Pb	1 ± 0.5	—	0.2	20	Complex	Varian-Techtro
	Bi		—	0.1	7	alloys	CRA 63
	Te		—	0.4	21		
	Tl		—	0.1	17		
	Sn		—	1.1	23		
9	Pb	2—5	—	0.1	16	Steel and	Instrumentatio
	Bi		—	0.03	12	nickel alloys	Laboratory 45
	Zn		—	1	10		
	Ag		—	0.01	10		
10	Pb	1—4	—	0.1	3—9	Steel and nickel alloys	Varian-Techtro CRA 90

EXPERIMENTAL

Instrumentation

A Perkin-Elmer atomic absorption spectrometer Model 372, provided with background correction and fitted with an HGA 74 furnace was used throughout. The HGA 74 was connected to a home-made power supply. Facilities for close temperature control of the graphite tube were installed. A fibre optic cable, directed towards the outer surface of the tube, was mounted on the furnace and the light emitted from the tube was monitored with a photodiode sensitive to infrared radiation. The principle for this optical feed-back control has been described earlier [11]. Temperature settings referring to the inner surface of the graphite tube were calibrated with a NiCr—Ni thermocouple (below 1000°C) and with an optical pyrometer (Keller Spezialtechnik Pyro Werk GmbH, Model PB06AF3) for higher temperatures. A Perkin-Elmer automatic sampler (Model AS-1) was used to dispense 20 μl of sample solutions. To the recorder output of the spectrometer a peak reader module was connected [12], providing simultaneous recording of the peak height and the peak area. The results given in this paper are based on the peak-height absorbance values, since better precision was obtained in this way. The peak reader was connected to a printer (Newport Laboratories Inc. Model 810) and a strip-chart recorder (Perkin-Elmer Model 56). The instrumental parameters are given in Table 2.

TABLE 2

Instrumental parameters

	Lead			Antimony		
	Time (s)	Temp. (°C)	Heating rate (°C s^{-1})	Time (s)	Temp. (°C)	Heating rate (°C s^{-1})
Drying	35	110	4	35	110	4
Ashing	50	660[a]	21	50	850[a]	21
Atomization	6	1600[a]	700	6	1900[a]	700
Outburning	3	Max	—	3	Max	—
Wavelength (nm)			283.3			217.6
Spectral bandwidth (nm)			0.7			0.2
Metal lamp			EDL[b]			HCL[c]
Background correction			Yes			No
Argon flow (ml min^{-1})						
internal			140[d]			140[d]
external			1000			1000
Hydrogen flow (ml min^{-1})						
internal			18			—

[a]Temperature-controlled heating [11]. [b]Electrodeless discharge lamp (Perkin-Elmer), operated at 10 W. [c]Hollow-cathode lamp (Varian-Techtron), operated at 18 mA. [d]Gas stop used.

Dissolution procedure for determination of lead

The sample (1 g) was dissolved in 25 ml of nitric acid and 50 ml of hydrochloric acid as described by Frech [13], and the solution was diluted to 500 g with water. For smaller sample weights, proportionally smaller volumes were used.

Dissolution procedure for determination of antimony

The samples were dissolved as described by Frech [14], and the solutions were diluted 2000 times with water (without addition of chromium).

Reagents and materials

Four metallurgical materials were used: British Chemical Standards BCS 330 (mild steel filings, certified as 0.003% for lead and 0.018% for antimony) and BCS 335 (austenitic stainless steel filings, certified as 0.0015% for lead), JK 16A (ferromolybdenum powder, certified as 0.0010% for lead; Institutet för Metallforskning, Sweden) and SANICRO 72 (nickel-base alloy chips, containing 0.0033% lead; provided by Sandvik AB, Sandviken, Sweden). The acids used were Merck Suprapur grade. Gases were of SR-grade purity.

All vessels were washed in 4M nitric acid. Solutions were stored in polyethylene bottles. The autosampler was loaded with Teflon cups only, in order to minimize contamination. Standard graphite tubes were used; each tube was replaced after 100 determinations.

RESULTS AND DISCUSSION

Optimization of analytical procedure

The relative standard deviations for lead given in Table 1 indicate that the uncertainty in the determinations caused by inhomogeneity is less than 10%. Therefore, to investigate the distribution of trace metals in metallurgical samples, it is essential to use an analytical method not only with high sensitivity, but also with a precision considerably better than 10%. Graphite-furnace a.a.s. fulfils these requirements. For the determination of lead in dissolved metallurgical samples a precision of approximately 5% is usually obtained [13]. An improved precision of 1.5% was achieved in the present work mainly by using an automatic sampler and by adding hydrogen to the internal gas flow. The advantages obtained with an autosampler have been described elsewhere [15]. Figure 1 shows the effect of adding hydrogen, as well as the influence of different ashing temperatures, on the lead signal. A dissolved austenitic steel, BCS 335, with a certified lead content of 15 $\mu g\ g^{-1}$ was used for these experiments. Comparison of the two diagrams in Fig. 1 shows that the useful ashing temperature range is considerably wider if hydrogen is added to the inner gas flow. Moreover, the precision was improved from 2.2% to 1.2% at the ashing temperature chosen, 660°C. The effect of hydrogen on the determination of lead in steels has been investigated earlier [16, 17]. It is interesting to note that at a given temperature, the non-specific absorbance (i.e. the

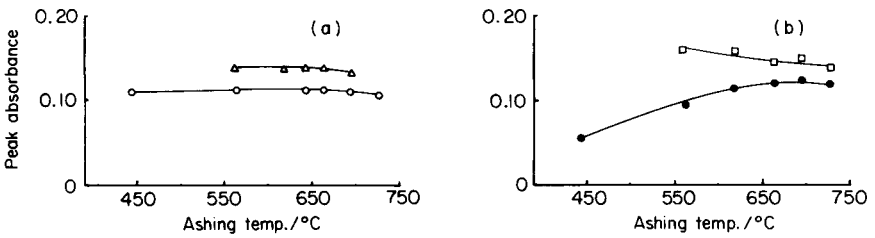

Fig. 1. Peak-height absorbance for lead in dissolved austenitic stainless steel as a function of the ashing temperature. Each symbol represents the mean of four determinations. (a) Hydrogen (18 ml min^{-1}) added to the internal gas flow; (b) no hydrogen added. (●,○) Corrected for non-specific absorbance; (△,□) total absorbance.

difference between the total and the corrected absorbances) increases as the specific absorbance decreases (Fig. 1b). This observation indicates a time overlap in the furnace between the volatilization of analyte atoms and interfering species (probably iron chlorides). The significance of the ashing time was also studied; the sample had to be ashed for at least 10 s at 660°C to eliminate interferences.

Distribution of lead and antimony in metallurgical samples

The homogeneity of the materials was studied by establishing the relative standard deviation (r.s.d.) for the lead contents in five independent dissolutions of a certain sample weight. Such r.s.d. values were calculated for different amounts of each material (2—100 mg). For practical purposes, 2 mg was the lowest weight that was analyzed by the dissolution procedure described. Table 3 shows some typical results obtained for lead and antimony, for particular sample weights, to give an idea of the reliability of the overall procedure. As can be seen, a master solution (prepared from 1 g of the material) was run between the independent dissolutions, to compensate for changes in sensitivity during the lifetime of the graphite tube; the Table shows the mean peak height values and the r.s.d. values for five determinations on each solution. As can be seen from the peak heights obtained for the master solution for lead (Table 3), the sensitivity decreased during the series of determinations. However, this decrease was not significant for all series. For lead and for antimony the Table gives a ratio of the response from a dissolution and the mean of the responses from its two adjacent master solutions. Five ratios for each sample weight investigated were thus obtained. The r.s.d. of each set of ratios was used to estimate the homogeneity of the material.

Table 4 shows the relative standard deviations of the ratios described for sample weights of 2—100 mg. It should be mentioned that 55 determinations were required to establish each of the values given in Table 4. Four types of metallurgical sample were investigated. BCS 335 was chosen as a representative for stainless steel, BCS 330 for mild steel, JK 16A for ferromolybdenum and SANICRO 72 for nickel-base alloys. As can be seen from Table 4, lead is

TABLE 3

Typical results for the determination of lead and antimony in metallurgical samples, illustrated for 50-mg dissolutions of BCS 335 for lead, and 25-mg dissolutions of BCS 330 for antimony.

Sample	Lead in BCS 335			Antimony in BCS 330		
	Peak height[a]	R.s.d. (%)	Ratio[b]	Peak height[a]	R.s.d. (%)	Ratio[b]
Master solution[c]	88	3.4	—	204	0.5	—
Dissolution No. 1	90	2.0	1.02	198	1.5	0.95
Master solution	88	1.2	—	211	1.5	—
Dissolution No. 2	88	1.2	1.02	205	2.1	0.98
Master solution	84	2.7	—	209	0.7	—
Dissolution No. 3	81	1.8	0.97	205	2.8	0.98
Master solution	83	0	—	210	1.4	—
Dissolution No. 4	83	1.0	1.01	198	0.9	0.94
Master solution	82	1.3	—	212	1.4	—
Dissolution No. 5	84	1.3	1.03	215	0.9	1.00
Master solution	81	2.1	—	217	1.5	—

[a]Mean of 5 determinations; values are given as 10^{-3} absorbance units. [b]Dissolution value divided by the mean of the adjacent master solution values. [c]Prepared from 1.000 g of the steel standard.

TABLE 4

Results reflecting the distribution of lead and antimony in metallurgical samples (The relative standard deviations of five ratios[a], such as those in Table 3, for different sample weights, are used as a measure of the homogeneity.)

Matrix	Austenitic stainless steel	Mild steel		Ferromolyb-denum	Nickel-base alloy
Sample	BCS 335	BCS 330		JK 16A	SANICRO 72
Element	Pb	Pb	Sb	Pb	Pb
Sample weight (mg)	R.s.d. (%)				
100	2.7	—	—	—	—
50	2.5	1.6	—	—	—
25	4.8	5.5	2.5	3.8	3.3
10	2.7	6.3	3.7	7.2	4.8
5	3.3	7.0	6.1	5.4	3.5
2	4.1	7.0	6.4	9.0	—

[a]See footnote 'b' in Table 3.

evenly distributed in the stainless steel and the nickel-base alloy for the sample weights studied. The low r.s.d. values for ratios obtained for 2 and 5 mg indicate that no serious errors are introduced by using small sample weights.

For that reason it seems probable that the higher values obtained for small sample weights of the mild steel and of ferromolybdenum are caused by inhomogeneity. Nevertheless, these errors are surprisingly small for all materials, considering that even completely homogeneous samples will produce an estimated r.s.d. of 3% for the ratios. With regard to these results, it should be observed that the number of particles which constitute a sample as well as the concentrations of the trace metals, are of importance for the distribution [6]. For that reason the results obtained for JK 16A are rather unfavourable with respect to homogeneity, because this standard was provided as a finely ground powder. In contrast, the BCS standards were provided as filings of varying shapes and weights and SANICRO 72 as evenly shaped chips (each ca. 5 mg).

During this investigation, it was felt that the sample shape might also be of importance for the distribution of the trace elements. In order to ascertain if this was the case, 25-mg portions of the stainless steel were collected, consisting of either (i) small filings, (ii) large filings, (iii) long and thin filings or (iv) compact filings. Table 5 shows the peak-height absorbances and the ratios obtained for the various sample shapes. The r.s.d. of the four ratios is 5.0%, a value of the same order of magnitude as those given in Table 4.

Conclusions

From the results reported, it is evident that inhomogeneity makes only a minor contribution to the relatively poor precisions that have been obtained so far with the solid sampling technique (Table 1). In addition, lead seems to be evenly distributed in filings of different shapes.

The authors thank Dr. Gillis Lundgren for valuable discussions, Mr. Ingemar Nilsson for carrying out most of the experiments, and Dr. Michael Sharp for linguistic revision of the manuscript.

TABLE 5

Distribution of lead in stainless steel filings (BCS 335) of different shapes (For each dissolution, 25 mg of filings with a particular shape were collected.)

Sample	Peak height[a]	Ratio[b]
Master solution[c]	104	—
Small filings	107	1.06
Master solution	97	—
Long and thin filings	105	1.08
Master solution	97	—
Compact filings	99	1.00
Master solution	102	—
Large filings	100	0.97
Master solution	104	—

[a,b,c]As Table 3.

REFERENCES

1 B. V. L'vov, Talanta, 23 (1976) 109.
2 J. B. Headridge and D. R. Smith, Talanta, 19 (1972) 833.
3 J. Talmi and G. H. Morrison, Anal. Chem., 44 (1972) 1455.
4 F. J. Langmyhr, Fresenius Z. Anal. Chem., 264 (1973) 122.
5 G. Lundgren and G. Johansson, Talanta, 21 (1974) 257.
6 F. J. Langmyhr, in E. Wänninen (Ed.), Analytical Chemistry, Essays in Memory of Anders Ringbom, Pergamon, Oxford, 1977, p. 461.
7 D. G. Andrews and J. B. Headridge, Analyst, 102 (1977) 436.
8 J. J. Marks, G. G. Welcher and R. J. Spellman, Appl. Spectrosc., 31 (1977) 9.
9 S. E. Bäckman, Lecture held at 6th Nordiska Konferensen i Spårelementanalys, Södertälje, Sweden, 1977.
10 E. Lundberg and W. Frech, Anal. Chim. Acta, 00 (1979) 000.
11 G. Lundgren, L. Lundmark and G. Johansson, Anal. Chem., 46 (1974) 1028.
12 E. Lundberg, Appl. Spectrosc., 32 (1978) 276.
13 W. Frech, Anal. Chim. Acta, 77 (1975) 43.
14 W. Frech, Talanta, 21 (1974) 565.
15 M. Stoeppler, M. Kampel and B. Welz, Fresenius Z. Anal. Chem., 282 (1976) 369.
16 W. Frech and A. Cedergren, Anal. Chim. Acta, 82 (1976) 83.
17 W. Frech and A. Cedergren, Anal. Chim. Acta, 83 (1976) 93.
18 J. B. Headridge, Lab. Pract., 23 (1974) 5.

Analytica Chimica Acta, 104 (1979) 75—84

DIRECT DETERMINATION OF TRACE METALS IN SOLID SAMPLES BY ATOMIC ABSORPTION SPECTROMETRY WITH ELECTROTHERMAL ATOMIZERS

Part 2. Determination of Lead in Steels and Nickel-base Alloys

ERIK LUNDBERG and WOLFGANG FRECH*

Department of Analytical Chemistry, University of Umeå, S-901 87 Umeå (Sweden)

(Received 23rd June 1978)

SUMMARY

The application of the solid sampling technique to the determination of lead in metallurgical samples is described. Comparison of non-isothermal and isothermal atomization, optimization of the atomization temperature, comparison of peak-height and peak-area measurements, and methods of extending the working range are reported. A method for the direct determination of lead in high- and low-alloy steels and in nickel-base alloys has been developed. The solid samples containing 0.2—60 μg Pb g^{-1}, are inserted into a Varian-Techtron CRA90 graphite cup held at constant temperature (1800°C). Concentrations are calculated from the integrated peak absorbances obtained for samples and arbitrary metallurgical standards. Good agreement with certified values was obtained for all materials investigated, with a typical relative standard deviation of 7%.

As was shown in Part 1 [1], lead can be determined in metallurgical samples weighing as little as 2—5 mg without introducing serious sampling errors. This means that a sample weight of about 2 mg should be sufficient to obtain high precision. There is every reason to believe, therefore, that the remarkably poor precision (e.g. 9—20% r.s.d. [2]) obtained for atomizers of limited sample capacity, e.g. the commercial Perkin-Elmer HGA74 and Varian-Techtron CRA63, cannot be attributed to the distribution of trace metals in the small samples used. Factors inherent in the atomization of the samples as well as the mode of measuring absorbance must be responsible for the poor results obtained with commercial atomizers. The aim of this work was to investigate the potential of the solid sampling technique with respect to both accuracy and precision. As an example, the direct determination of lead in metallurgical materials by means of the Varian-Techtron CRA90 graphite cup, was chosen. As will be shown here, better precision and accuracy were obtained by atomizing the sample under isothermal conditions and recording the peak area instead of the peak height, the advantage of which has been demonstrated by Lundberg [3]. For the determination of lead in a stainless steel wire with a Varian-Techtron CRA90 graphite cup operated in the "normal way" (i.e. samples are atomized during a rapid rise in temperature), Lundberg obtained

a precision of 5.4% for peak area values compared to 17% for peak height values. Although evaluation of the peak area resulted in good precision, the accuracy was not acceptable because standardization was done against pure aqueous solutions. As was discussed by L'vov [4], a prerequisite for obtaining accurate peak area values is to keep the mean residence time (τ_2) of free atoms in the absorbing volume constant. This means that the analyte atoms liberated from samples as well as standards have to be measured at the same temperature otherwise the atomic vapours will diffuse out of the light path at different rates, i.e. τ_2 will vary. When samples are atomized in the "normal way", the mean residence time of atoms is seldom constant and accuracy might, therefore, deteriorate seriously, because the analyte will be atomized as well as measured at different temperatures if the samples are of varying composition. The open nature of the CRA90 graphite cup permits sample introduction after the atomizer has reached constant temperature, and this facility is used in this paper to fulfil the main requirement for accurate peak area values.

EXPERIMENTAL

Instrumentation

A Varian-Techtron AA-6 atomic absorption spectrometer, provided with background correction and fitted with a carbon rod atomizer (CRA63) was used. To the CRA63 power supply was connected a CRA90 workhead. The power supply was modified to provide an "outburning" step immediately after the atomization step. Facilities for close temperature control of the graphite tube were installed [5]. Temperature settings referring to the outer surface of the carbon cup were calibrated with an optical pyrometer (Keller Spezialtechnik Pyro Werk GmbH, model PB06 AF3). To reduce gas consumption, a gas control unit was connected to the atomizer [6]. The signal damping of the AA-6 readout module was modified to obtain a faster response time of the electronics. The value of the DAMP A time constant was thus altered from the original 260 ms to 47 ms, as described earlier [7]. To the recorder output of the spectrometer a peak reader module was connected [3], providing simultaneous recording of the peak height and the peak area. For peak shape studies, a fast-response (250 ms) strip-chart recorder (Philips 8202) and a two-channel storage oscilloscope (Tektronix, model 564) were used.

Procedure

Single pieces of the materials (1—5 mg) were weighed on an electrobalance (Cahn, model 4100) and transferred with tweezers to small plastic vessels for storage before analysis. Some materials consisted of only larger pieces, weighing more than 5 mg (SANICRO 72, SSW, QRO 45). These were cut into smaller pieces and washed in 5 M nitric acid. The pieces were dropped into the standard cup (i.d. 2.9 mm) at ambient temperature (non-isothermal atomization) or into the larger cup (i.d. 4.5 mm) at constant final temperature (isothermal atomization). Welding glasses are necessary to protect the eyes from intense

light in the latter atomization mode. The instrumental parameters are given in Table 1.

Materials

The following metallurgical materials were used (from Sweden, except for the British Chemical Standards): BCS 273, BCS 330 (mild steels) and BCS 333—337 (austenitic stainless steels); standards JK 1C, JK 2C (mild steels) and JK 8C (austenitic stainless steel) supplied by Institutet för Metallforskning; materials Q 6850, Q 6856, Q 6893 (2% Mn, 20% Cr, 25% Ni, 4.5% Mo, 1.5% Cu) and WS 66 (1.6% Mn, 18% Cr, 13% Ni, 3% Mo) supplied by Hagfors steel factory; QRO 45 (tool steel; 0.4% V, 2.8% Cr, 2.6% Co, 2.6% Mo) supplied by Bofors steel factory; SF 50776 (tool steel; 1.4% V, 4.1% Cr, 17% W, 0.5% Mo) and SF 51820 (tool steel; 2.1% V, 4.0% Cr, 1.7% W, 8.5% Mo) supplied by Söderfors steel factory; SANICRO 72 (nickel-base alloy) supplied by Sandviken steel factory; and SSW (austenitic stainless steel wire) supplied by Fagersta steel factory.

The standard carbon cup (pyrolytically coated) as well as the larger carbon cup (uncoated) had to be replaced after 20—40 firings (both are available from Varian-Techtron).

TABLE 1

Instrumental parameters

	Time (s)	Temp. (°C)	Heating rate (°C s^{-1})
Drying[a]	25	110	10
Ashing	20[b]	560[c]	28
Atomization	7[d]; 3.5[e]	1800[c]	400[f]
Outburning	1[d]; 1.5[e]	2400	—
Wavelength (nm)		283.3	205.4
Spectral bandwidth (nm)		0.5	0.8
Lamp current (mA)		5	8
Hydrogen lamp[g] current (s.d.)		7	—
Noise on signal (absorbance)		±0.002[h]	±0.009
Integration time (s)		8[d]; 5[e]	
System time constant (ms)		100	
Argon flow (l min^{-1})		5	

[a]Omitted for solid samples. [b]Necessary for correct performance of the peak reader module [3]. [c]Temperature-controlled heating [5]. [d]Samples inserted at constant temperature. [e]Samples inserted at ambient temperature. [f]Mean value between 560 and 1800°C. The heating rate was faster at the beginning of the interval. [g]Normally not used. For initial checking of possible background absorption. [h]Noise was ±0.005 absorbance units when background corrector was on.

RESULTS AND DISCUSSION

Working range

The limited working range inherent in the solid sampling technique with the Varian CRA90 can be extended by using different amounts of the sample, using cups of different sizes, measuring the atom population at various heights above the bottom of the cup, and selecting alternative absorption lines. From a practical point of view, the sample weight can be varied only within the narrow range 1—5 mg when the standard cup is used. However, the concentration range of interest is approximately 0.1—100 μg Pb g^{-1} and this range cannot be covered by varying the sample weight five-fold. The possibility of using larger carbon cups is restricted by the design of the CRA90. Two types of cups are available from the supplier, a standard cup (i.d. 2.9 mm) and a cup with i.d. 4.5 mm. With the larger cup the sensitivity is reduced by a factor of two compared with the standard cup. The sensitivity can be further reduced by measuring the atoms above the cup instead of through the side apertures. At 3 mm above the upper edge of the cup the sensitivity was thirteen times lower than when measurements were made in the conventional manner. However, the main disadvantage of measuring above the cup is that the integrated signals for lead decrease with higher inert gas flows (see Table 2). Good control of the gas flow rate is therefore mandatory for high precision. In addition, the sensitivity is critically dependent on the exact position of the cup. To overcome the problem of readjusting the cup to a predetermined position, a masking plate with two additional holes for retaining it to the inert gas block of the CRA90 can be used. These holes are drilled at a defined distance beneath the original holes.

The possibility of using alternative absorption lines for a particular element is restricted by their number as well as their relative sensitivity. Table 3 shows the relative sensitivities for a number of lines for lead. With regard to the non-resonance lines, the sensitivity will depend on temperature according to the Boltzmann distribution. This dependence provides an additional way of extending the working range by using isothermal atomization at different

TABLE 2

Integrated absorbances ($A \times s$) for lead as a function of the inert gas flow rate

		Gas flow rate (l min^{-1})			
		4	6	8	10
Light path through side apertures[a]	Mean[b]	—	0.245	0.239	0.253
	R.s.d. (%)	—	8.8	8.6	8.2
	n	—	4	4	4
Light path 3 mm above the cup[c]	Mean[b]	0.164	0.132	0.128	0.116
	R.s.d. (%)	7.2	10.0	10.8	14.6
	n	7	8	8	8

[a]Stainless steel wire. [b]Normalized to 1 mg. [c]Stainless steel BCS 335.

TABLE 3

Relative sensitivities for alternative lead absorption lines

Wavelength (nm)	Relative sensitivity[a]	Wavelength (nm)	Relative sensitivity[a]
202.2[b]	46	283.3	2.5
205.4[b]	40	364.0	4700
217.0[b]	1	368.4	2700
261.4	1200		

[a]Measured relative to the 217.0-nm line with aqueous solutions in the carbon cup.
[b]Resonance lines.

temperatures [8]. This possibility is currently under investigation. Because of the intensities and sensitivities, the 283.3-nm line was chosen for samples with a lead content less than 7 ppm and the 205.4-nm line for higher contents. The intensity of the 205.4-nm line was too low to use the background corrector. However, the background signals at this line, checked by atomizing steel samples with low lead contents, were insignificant.

Non-isothermal atomization

In the normal procedure for the direct analysis of metallurgical solids, samples are placed in the carbon cup at ambient temperature. Atomization is accomplished by rapidly heating the cup, i.e. during non-isothermal conditions. For the transient signals obtained either the peak height or the peak area is usually evaluated. Figure 1 shows the results obtained for the determination of lead in pieces of a stainless steel wire (weighing 1 mg) for both recording modes at different temperatures. In general, poorer precision was obtained for the peak-height measurements (see below). The magnitude of the peak height increases considerably with the temperature, whereas the peak area is

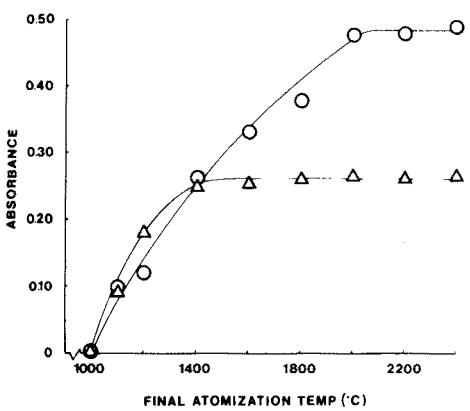

Fig. 1. Normalized peak-height (○) and peak-area (△) absorbance values for lead as a function of the final atomization temperature. Small pieces of the stainless steel wire (2.2 ppm Pb) were used.

approximately constant for temperatures above 1400°C. For lower temperatures lead is probably not completely vaporized during the atomization time used (3.5 s). The increase in peak-height values above 1400°C can be attributed to shorter atomization times at these temperatures. The atomization behaviour of volatile elements in solid samples differs from that of solutions. The latter are dried during the first heating step, and the residue is deposited on the graphite surface as a thin layer. The atomization time will then mainly be dependent on the heating rate of the furnace during the atomization interval [4]. Suggested mechanisms for the formation of free atoms involve either chemical reactions of the metal compounds or their thermal dissociation [9, 10]. In contrast, for solid metallurgical samples, the atomization time will depend on the diffusion rate of lead or its compounds through the sample. This rate is a function of the final temperature of the solid sample and is probably the reason for the higher peak height values seen for higher temperatures in Fig. 1. Corresponding experiments with solutions showed no increase in the peak height (or peak area) signal for lead above 1200°C. Thus, for solid samples, the peak area evaluation was used to improve precision as well as to reduce the influence of the temperature on sensitivity.

The potential of the non-isothermal atomization mode for the determination of lead in a variety of metallurgical samples was investigated. Table 4 shows the results obtained for three low-alloy steels, seven high-alloy steels of varying composition, three tool steels and one nickel-base alloy. During the lifetime of a graphite cup, the sensitivity generally decreased, probably because of the slag residue that is built up on its bottom. In order to account for this drift, samples and standards were run alternately and their normalized peak areas evaluated. The lead contents were then calculated separately for each run. Mean values of these determinations, as well as their relative standard

TABLE 4

Results obtained for the determination of lead in steels by use of non-isothermal atomization (Samples and standards were run alternately).

	Sample designation						
	BCS273[a]	BCS330[b]	BCS333[b]	BCS335[b]	BCS336[b]	BCS337[b]	SANICRO
Accepted value (ppm)	30	26	6	15	7	11	33
Mean value (ppm)	29	29	6.6	11	7.3	11	31
R.s.d. (%)	22	18	7	15	12	16	7.1
n	5	5	6	9	5	6	7
	Sample designation						
	JK2C[a]	JK8C[c]	Q6850[d]	Q6893[d]	QR045[c]	SF50776[c]	SF51820[c]
Accepted value (ppm)	4	2	5	38	4	2	6
Mean value (ppm)	3.9	1.8	5.3	38	3.1	2.2	6.2
R.s.d. (%)	9.2	20	9.2	9.1	2.5	3.1	8.8
n	5	7	7	7	7	7	5

Determined relative to [a]BCS 330; [b]BCS 334; [c]stainless steel wire (SSW); [d]Q 6856 (accepted value: 15 ppm).

deviations, are given in Table 4. As can be seen, the accuracy is fairly good for most of the materials, despite the variation in their composition. This indicates that interferences in general are of minor importance. One exception is the austenitic steel BCS 335, for which a significantly lower lead content than the certified value was obtained. The reason for this discrepancy is discussed below. The relative standard deviation varies between 2.5 and 22% and is typically 12%. This figure can be regarded as acceptable, at least for semi-quantitative determinations.

Isothermal atomization

One of the main requirements for obtaining comparable peak-area values for standards and samples is to keep the mean residence time of the analyte atoms equal. This can be accomplished by introducing the solid samples after the cup has reached a preselected constant temperature. In this way all absorbing atoms are liberated into a gas phase held at constant temperature. During non-isothermal atomization, the atoms enter a gas phase of rising temperature. The signal—time dependence for the two modes of atomization is illustrated in Fig. 2 for the low-alloy steel BCS 330. Although they are not seen in these Figures, double peaks from fractional atomization frequently occur, e.g. for nickel-base alloys. For non-isothermal atomization, even peak-area measurements will give erroneous results for standardization against an arbitrary steel standard, because of the variation in diffusion rate with temperature (Fig. 2). One of the advantages of isothermal atomization, therefore, is that the diffusion rate of atoms in the light path will be equal for samples and standards. Two additional benefits are worth mentioning: the first is that the heat transfer to the sample is no longer affected by irregularities in the slag residue on the bottom of the cup, which is probably the reason for the almost constant sensitivity obtained during its lifetime; the second is that removal of atoms through convection is unlikely to occur, which means that only diffusion processes have to be considered.

The influence of the temperature on the lead signal (isothermal atomization) was investigated for BCS 334 and BCS 335. The latter was chosen because the lead content obtained by using non-isothermal atomization was low. As can be

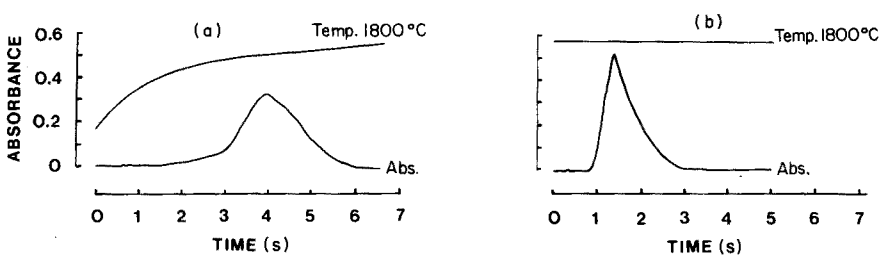

Fig. 2. Oscilloscopic traces showing the time dependence of the lead signal (BCS 330) and the temperature during (a) non-isothermal atomization and (b) isothermal atomization. The temperature was monitored by an infrared-sensitive photodiode.

TABLE 5

Determination of lead in BCS 335 by use of isothermal atomization

Temp (°C)	1400	1400	1800	1800
Designation	BCS334	BCS335	BCS334	BCS335
Mean peak height[a] (A)	0.115	0.086	0.171	0.184
R.s.d. (%)	12.3	23.4	11.8	17.3
n	8	9	10	11
Pb content found (ppm)[b]		8.2		11.8
Mean peak area[a] ($A \times s$)	0.079	0.092	0.068	0.086
R.s.d. (%)	4.0	10.7	8.0	10.4
n	8	9	10	11
Pb content found (ppm)[b]		12.8		13.9

[a]Normalized to 1 mg. [b]Relative to BCS 334 (11 ppm).

seen in Table 5, the normalized peak-area values decrease to a greater extent for BCS 334 than for BCS 335 from 1400°C to 1800°C (still more at 2000°C). This results in a higher calculated lead value for BCS 335 relative to BCS 334 at 1800°C. In general, the normalized peak areas decrease at higher temperatures because of higher diffusion rates. That this is not the case for BCS 335 indicates that larger amounts of lead are volatilized at 1800°C than at 1400°C. The peak-height values are included in Table 5 to stress that even for isothermal atomization their accuracy as well as their precision are inferior to those of peak-area values.

As was mentioned earlier, a sample weight range of 1—5 mg is feasible when the CRA90 is used. Table 6 shows peak areas and peak heights obtained for BCS 335 with different sample weights within this range. The normalized peak areas are unaffected by a five-fold increase in sample weight (relative standard deviation 6.8%), whereas the peak heights decrease significantly. This is one of the reasons for the poorer precision obtained with peak-height measurements.

To illustrate the usefulness of isothermal atomization, two low-alloy steels, six high-alloy steels, one nickel-base alloy and one tool steel were analyzed according to the parameters given in Table 1 (isothermal atomization). Table 7 shows the results obtained for these materials classified into 2 groups, <0.5—7 ppm and 7—60 ppm of lead. In each of these, the samples and the "standard" were run alternately in the order given in Table 7. The values reported were calculated from the mean of all normalized peak areas obtained for each material. This standardization procedure, with fewer calibration points compared with non-isothermal atomization, was possible because the drift in sensitivity was insignificant. The overall precision of the entire material is 7.1%. This value can be regarded as quite acceptable and is to be compared with the 5% generally obtained with a dissolution procedure [11]. With regard to accuracy, it should be observed that the determined lead content for BCS 335

TABLE 6

The effect of sample weight on peak heights and peak areas for sample BCS 335

Sample weight (mg)	1	2	3	4	5
Peak height (A)[a]	0.179	0.145	0.118	0.117	0.106
Peak area ($A \times s$)[a]	0.059	0.063	0.066	0.070	0.061

[a]Normalized to 1 mg; A = absorbance.

TABLE 7

Results for the determination of lead in metallurgical materials by use of isothermal atomization (Samples and standards were run alternately)

Designation	BCS330	BCS334[a]	BCS335[a]	Q6893[a]	SANICRO 72[a]	WS66[a]
Accepted value (ppm)	26	11	15	38	33	66
Mean value (ppm)	—	12	15	36	33	56[b]
R.s.d. (%)	4.2	8.3	4.2	9.2	2.6	8.0
n	7	7	7	7	7	6
Designation	JK1C[c]	JK2C	JK8C[c]	BCS336[c]	SF50776[c]	SSW[c]
Accepted value (ppm)	<0.5	4	2	7	2	2.2
Mean value (ppm)	0.2	—	1.9	6[b]	2.5	2.8
R.s.d. (%)	14.0	9.7	8.0	6.8	5.9	4.9
n	9	10	9	10	9	8

[a]Determined relative to BCS 330. [b]Not corrected for non-linear calibration curve. [c]Determined relative to JK 2C.

now agrees with the certified value. For WS66 and BCS 336, low values were obtained. These discrepancies are due to non-linearity of the calibration curves at high absorbance values.

Conclusions

As is evident from Tables 4 and 7, the isothermal atomization procedure gives better precision as well as accuracy and can therefore be recommended for metallurgical materials. However, this procedure is not in general applicable to samples that require an ashing step, e.g. most biological materials.

The authors thank Dr. Gillis Lundgren for valuable discussions, Mr. Ingemar Nilsson for performing most of the experimental work, and Dr. Michael Sharp for linguistic revision of the manuscript.

REFERENCES

1 E. Lundberg and W. Frech, Anal. Chim. Acta, 00 (1979) 000.
2 J. J. Marks, G. G. Welcher and R. J. Spellman, Appl. Spectrosc., 31 (1977) 9.
3 E. Lundberg, Appl. Spectrosc., 32 (1978) 276.
4 B. V. L'vov, Atomic Absorption Spectrochemical Analysis, Adam Hilger, London, 1970.
5 G. Lundgren and L. Lundmark, Anal. Chem., in press.

6 E.Lundberg and L. Lundmark, Chem. Instrum., submitted.
7 E. Lundberg, Chem. Instrum., 8 (1978) 197.
8 D. D. Siemer and R. W. Stone, Appl. Spectrosc., 29 (1975) 240.
9 W. C. Campbell and J. M. Ottaway, Talanta, 21 (1974) 837.
10 R. E. Sturgeon, C. L. Chakrabarti and C. H. Langford, Anal. Chem., 48 (1976) 1792.
11 W. Frech, Anal. Chim. Acta, 77 (1975) 43.

Analytica Chimica Acta, 104 (1979) 85—92

NON-DISPERSIVE ATOMIC FLUORESCENCE SPECTROMETRY WITH A CARBON FILAMENT ATOM RESERVOIR

M. HARGREAVES, A. F. KING**, J. D. NORRIS***, A. SANZ-MEDEL‡ and T. S. WEST*

Chemistry Department, Imperial College, London SW7 2AY (Gt. Britain)

(Received 5th June 1978)

SUMMARY

The non-dispersive atomic fluorescence spectrometric determination of Bi, Cd, Hg, Te, Tl and Zn on a carbon filament atom reservoir with electrodeless discharge lamp sources and reflecting microscope objective lenses is described. The non-dispersive system shows distinct advantages for an element such as tellurium whose principal fluorescence lines fall within the useful range of the solar-blind photomultiplier detector, and marginal advantages for mercury, cadmium and zinc where only one line is within the detector range. It is inferior for bismuth, thallium and lead where lines lie at the extremes of the useful detector range. The technique was applied successfully to the determination of cadmium (0.012%) in a copper-base alloy.

The advantages of non-dispersive atomic fluorescence spectrometry (a.f.s.) have been discussed by Larkins [1], and Vickers et al. [2]. Briefly these are: (a) greater energy throughput, i.e. no signal attenuation in the monochromator, hence observation of fluorescence over a large solid angle; (b) simultaneous collection of several fluorescence lines for many elements, within the range of the detector; and (c) simplicity of instrumentation.

Various non-dispersive and low-dispersive systems, replacing the conventional monochromator arrangement, have been reported for a.f.s. with flame cells. A low-dispersive system, with a narrow bandpass filter, was suggested by Jenkins [3] and later by West and Williams [4] and was reported by Warr for the determination of Hg [5] and Zn [6] in an air—acetylene flame, and subsequently by Elser and Winefordner [7]. Mitchell and Johansson had already incorporated interference filters in their multi-element a.f.s. spectrometer [8, 9]. A similar instrument was used by West et al. for the determination of six elements in soil extracts, aluminium alloys and sea-water samples [10—12]. Aldous [13] reported an ingenious determination of zinc, using a separated

Present Addresses:
**Chatfield Applied Research Laboratories, Croydon (Gt. Britain).
***British Carbonization Research Association, Chesterfield (Gt. Britain).
‡Department of Analytical Chemistry, Ciudad Universitaria, Madrid (Spain).
*Author for correspondence. Macaulay Institute for Soil Research, Craigiebuckler, Aberdeen (Gt. Britain).

air—hydrogen flame with an optical filter of 50% acetone in water.

The use of a completely non-dispersive a.f.s. system incorporating a solar-blind photomultiplier was reported by Larkins et al. [14] for the determination of iron and nickel in an air—actylene flame and by Vickers and Vaught [15] for the determinations of cadmium, zinc and mercury in an air—hydrogen flame. Larkins [1] gave detection limits for 24 elements in an argon- or nitrogen separated air—acetylene flame and described the use of a non-solar-blind photomultiplier with a glass absorption filter. Comparisons of nitrous oxide- and air-supported separated flames for seven elements were reported by Larkins and Willis [16]. Dispersive and non-dispersive systems for mercury and arsenic were compared by Vickers et al. [2]. The use of interference filters with solar-blind and non-solar-blind photomultipliers has also been described [16]. Norris and West have determined zinc in soil extracts and non-ferrous alloys in an argon-separated air—acetylene flame by non-dispersive a.f.s. [17].

The carbon filament atom reservoir (CFAR) which is much more easily utilized for a.f.s. measurements than resistively heated graphite tubes, was first used by West and Williams [18] for the determination of silver and magnesium by conventional a.f.s. Subsequently, the determination of eleven other elements (Au, Bi, Cd, Cu, Ga, Hg, Mn, Pb, Sb, Tl and Zn) by this method has been reported [19—27]. The low background emission reported with the CFAR when used in a dispersive system [21] recommends its application to non-dispersive a.f.s. where emission from the atom cell must be minimized. This paper reports the application of the CFAR in non-dispersive a.f.s. to the determination of six elements.

EXPERIMENTAL

Apparatus

Figure 1 shows a schematic diagram of the experimental arrangement used. The primary radiation source was an electrodeless discharge lamp, except for the determination of cadmium, when a high-intensity hollow-cathode lamp [28] powered by a Techtron AA4 lamp supply and booster unit was also used. Electrodeless discharge lamps were prepared as described elsewhere [29] and operated at 2450 ± 25 MHz in a 3/4 or 1/4-wave resonant cavity connected to a Microtron 200 microwave generator.

The CFAR was the standard design [20], with a 2.5-cm long, 2-mm diam. filament. It was arranged to subtend an angle of 45° to both the radiation source and the detector in order to minimize reflections from the filament end-caps. Argon was used throughout as the filament sheath gas.

The solar-blind photomultipliers employed were the EMI 9616B, Hamamatsu R431 (both 13-stage end-window) and Hamamatsu R166 (11-stage, side-window), run from a Brandenburg model 472R photomultiplier power supply. Signal amplification was either by a Telequipment type K amplifier with read-out on a Telequipment type D53S storage oscilloscope or by an operational amplifier based on the Philbrick type PF85AU amplifier [23] with readout on a Honeywell 1706 Visicorder oscillograph.

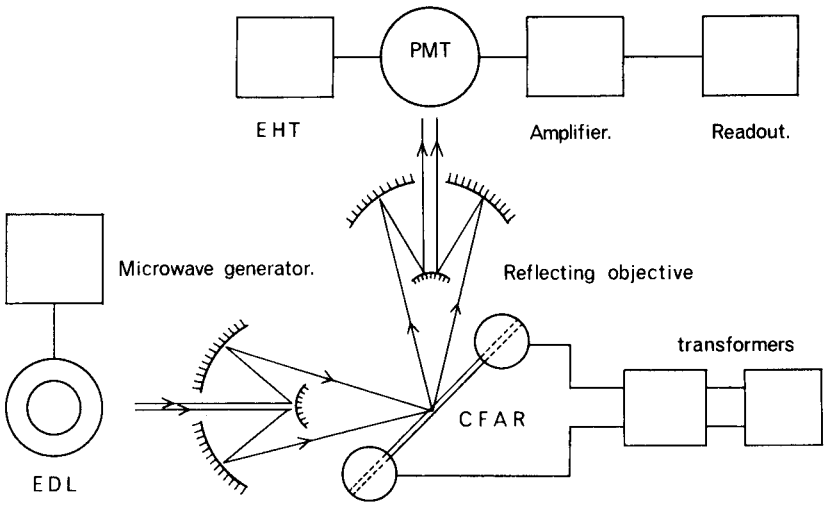

Fig. 1. Block diagram of non-dispersive atomic fluorescence equipment for use with a carbon filament atom reservoir.

In initial experiments on the determination of mercury, radiation from the discharge lamp was focused above the CFAR and the atomic fluorescence was focused onto the photomultiplier by means of silica lenses (35-mm diam., 70-mm focal length). In subsequent work, these were replaced by reflecting objectives (1-in. focal length; Beck Ltd.), which consist of two front-silvered mirrors and have the advantages over silica lenses of less light loss by absorption, and constant focal length for any wavelength in the u.v.-visible region. Optical filters, when used, were placed immediately in front of the photomultiplier. All components were rigidly mounted on optical bars.

Reagents

All reagents were of analytical grade; and water was glass-distilled and then de-ionized.

Procedures

The procedure followed in routine determinations has been described elsewhere [19]. Samples (1-μl) were dried and atomized at predetermined optimal voltages, with the lamp operating conditions, argon sheath gas flow-rate, EHT supply to the photomultiplier, signal amplification and height of observation above the filament being previously optimized.

Determination in a copper-base alloy. The copper-base alloy (0.2 g) was weighed into a 100-cm^3 beaker and dissolved in the minimum volume of (3 + 1) hydrochloric and nitric acids by warming, in the usual manner. When all the alloy had dissolved, the solution was diluted with water, transferred to a 100-cm^3 volumetric flask and diluted to volume with water. An aliquot (1 cm^3) of this

solution was transferred to a 100-cm^3 flask and diluted to volume with water; 1-μl samples were applied to the filament.

RESULTS AND DISCUSSION

Determination of mercury

The use of a silica lens to focus fluorescence radiation from just above the heated carbon filament onto the photomultiplier was found to be unsatisfactory because of the relatively large amount of background emission from the filament which tended to obscure the analytical signal. An optical filter (25-mm diam.; Baird Atomic Ltd. Type 14-08-7) was mounted in front of the EMI 9616B photomultiplier. This filter peaks at 250 ± 3 nm and gives greater than 50% of its peak transparency for a band of 7—10 nm. At the mercury 253.7-nm line the transparency was found to be 6%. With the filter in position, it was possible to separate the mercury fluorescence signal from the filament continuum. A detection limit of 4×10^{-11} g Hg (0.04 ppm for a 1-μl sample) was obtained. This is almost the same as that reported previously for a dispersive system with the CFAR [23]. A significant improvement in the detection limit would be expected owing to the removal of the monochromator, as was found with flame cells [1, 16], but this was nullified by the use of the filter.

The replacement of the lens by a reflecting objective gave a more closely defined field of view above the filament and a wider separation of fluorescence signal and filament emission. This made it possible to dispense with the filter and, with an R431 photomultiplier, a detection limit of 1×10^{-11} g Hg was obtained.

Determination of Cd, Zn, Tl, Te and Bi

These elements were determined with the completely non-dispersive system. Optimal operating conditions are listed in Table 1. The atomization voltage and height of observation were chosen to give the maximum signal strength

TABLE 1

Experimental conditions for non-dispersive a.f.s. with the CFAR and electrodeless discharge lamps
(The height of observation above the filament was 0.2 mm in all cases except for mercury for which 0.4 mm was used.)

Element	Lamp fill material	Incident microwave power (W)	Atomization voltage	Argon flow rate (dm^3 min^{-1})
Hg	Hg	20	6.0	3.75
Cd	$CdCl_2$ or Cd	40	6.0	3.50
Zn	Zn	50	7.2	3.75
Tl	$TlCl_3$	40	6.0	3.50
Te	I_2 and excess Te	35	6.0	3.50
Bi	I_2	25	5.4	3.50

compatible with separation of analytical signal and filament background emission. In general, the argon sheath flow rate was not critical within the range 3.0—4.0 dm^3 min^{-1} and for the elements so far considered a constant flow of 3.5 dm^3 min^{-1} gave acceptable results. A typical signal for 0.05 ppm of Cd is shown in Fig. 2(a). The cadmium fluorescence signal is completely separated from the filament emission as were the signals for the other elements in Table 2, except for the lead signal (Fig. 2b) which is not resolved from the filament emission.

Detection limits and calibration data are compared with those for a dispersive system with the CFAR in Table 2. Detection limits for Hg, Cd and Zn are only marginally superior to the best values reported for a dispersive system with the CFAR. The absence of any major improvement is because in each case the fluorescence emission was viewed at the main fluorescence wavelength only (Hg at 253.7 nm, Cd at 228.8 nm and Zn at 213.9 nm), the Cd 326.1-nm, Zn 307.6-nm and Hg 184.9-nm lines occurring at either extreme of the photomultiplier response range. The only advantage of a non-dispersive system in these cases is the observation of atomic fluorescence over a greater solid angle than in a conventional system. For thallium the non-dispersive detection limit is considerably worse because the main fluorescence line at 377.6 nm lies well outside the response range of the solar-blind photomultiplier, and only the minor lines at 258.0 nm, 276.8 nm and 238.0 nm are seen. Similarly with bismuth, the major fluorescence lines at 302.5 nm and 306.8 nm occur in the least sensitive portion of the photomultiplier response range.

Tellurium was selected as an ideal element for determination by non-dispersive a.f.s. Atomic fluorescence can be simultaneously monitored at 225.9 nm and 214.3 nm (resonance fluorescence) and at 253.0 nm, 238.3 nm, 238.6 nm and 277.0 nm (direct line fluorescence). The advantage of multiple collection of fluorescence lines is illustrated by the absolute detection limit of 1×10^{-12} g, which considerably improves on the previously reported absolute detection limit [30] of 0.05 ppm in an air—propane flame (10^{-7} g assuming a 2-cm^3 sample); tellurium has not been previously determined with the CFAR.

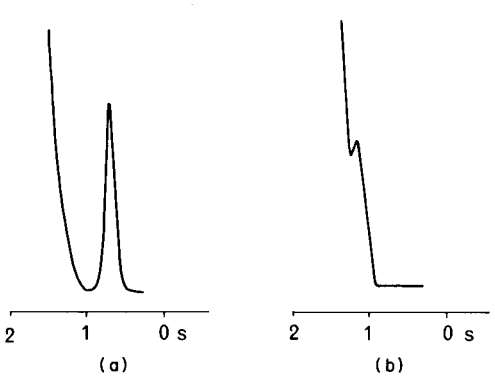

Fig. 2. (a) Typical fluorescence signal for 0.05 ppm Cd. (b) Typical fluorescence signal for 10 ppm Pb.

TABLE 2

Detection limits (DL) and linear analytical ranges of fluorescence on a carbon filament atom reservoir

Element	Non-dispersive a.f.s.		Low-dispersive a.f.s.[a]	Dispersive a.f.s.[b]		
	DL (g)	Upper conc. limit (g)	DL (g)	DL (g)	Upper conc. limit (g)	λ (nm)
Hg	1×10^{-11}	1×10^{-10}	2.5×10^{-9}	5×10^{-11}	1×10^{-8}	253.7
Cd[c]	1×10^{-14}	1×10^{-12}	—	1.5×10^{-13}	—	228.8
Cd[d]	7×10^{-12}	6×10^{-11}	4×10^{-13}	—	—	—
Zn	1×10^{-14}	6×10^{-11}	1.8×10^{-12}	2×10^{-14}	4×10^{-10}	213.9
Tl	1×10^{-9}	1×10^{-7}	—	5×10^{-11}	2×10^{-9}	377.6
Te	1×10^{-12}	3×10^{-10}	—	—	—	—
Bi	1×10^{-10}	5×10^{-8}	—	1×10^{-11}	1×10^{-8}	306.8

[a]With interference filters (lenses for Hg or reflectance objectives for Cd and Zn).
[b]With a monochromator and the CFAR.
[c]With a Cd electrodeless discharge lamp.
[d]With Cd high-intensity hollow-cathode lamp.

Analytical ranges are generally comparable to those obtained with a dispersive system with the CFAR.

When a filter (Baird Atomic Ltd. Type 31-24-0) with a transparency of 24% at 213.0 nm and 11% at 228.8 nm was used in the determination of Zn and Cd the detection limits, which are included in Table 2, were poorer than in the completely non-dispersive system.

Interference studies

Table 3 shows the effect of various interfering species on the atomic fluorescence of a 0.05 ppm solution of cadmium. Interference studies were carried out with 100-fold and 1000-fold amounts of interferent, but it seems likely that it is the absolute amount rather than the ratio of interfering species to analyte that determines the extent of the interference. Interferences are, in general, suppressive and are similar to results published for cadmium in a dispersive system with the CFAR [20].

Determination of cadmium in a copper-base alloy

To examine the application of the non-dispersive a.f.s.-CFAR system to the analysis of technical materials, cadmium was determined in a copper-base alloy The copper-base alloy was found to contain 0.012 ± 0.001% of cadmium, compared with 0.013% by independent analysis (Imperial Metal Industries Ltd

Determination of other elements

Arsenic and selenium are apparently ideal elements for determination by non-dispersive a.f.s., having several major fluorescence lines within the response of the solar-blind photomultiplier. Attempts to determine these were

TABLE 3

Interferences on 0.05 ppm Cd (5×10^{-11} g) in the non-dispersive CFAR technique

Element	Compound	% Interference		Element	Compound	% Interference	
		100-fold amount	1000-fold amount			100-fold amount	1000-fold amount
Hg	$HgCl_2$	0	−30	P	Na_2HPO_4	−65	−90
Zn	$ZnSO_4$	0	−30	Bi	$Bi(NO_3)_3$	−15	−40
Ni	$NiCl_2$	−10	−90	Sn	$SnCl_4$/HCl	−30	−60
Al	$Al_2(SO_4)_3$	−40	−100	Ti	$TiCl_4$/HCl	0	−30
Cu	$CuSO_4$	0	−10	Se	Se/HNO_3	−20	−20
Fe	$FeCl_3$	−10	−15	Au	$AuCl_3$	0	−20
As	As/HNO_3	−10	−45	V	NH_4VO_3	−20	−80

NaCl, KCl, $CaCl_2$, $MgSO_4$, $Pb(NO_3)_2$, $CoCl_2$, $MnSO_4$, $TlNO_3$, $AgNO_3$, $(NH_4)_2PdCl_4$, H_2PtCl_6 and $Cr_2(SO_4)_3$ gave no interference with 100- or 1000-fold amounts of the metal.

unsuccessful, only scatter signals being obtained, presumably because the elements leave the filament in molecular forms. Less volatile elements could not be determined with the present system, as the filament background obscured the fluorescence signal at the high temperatures necessary to atomize the samples. This is illustrated by a typical signal for 10 ppm Pb shown in Fig. 2(b). Improvements in the optical arrangement should minimize these problems of background interference.

Conclusion

The advantages of non-dispersive a.f.s. with the CFAR are similar to those with a flame cell. Superior detection limits were obtained for all of the six elements examined except for those with their main fluorescence wavelengths outside the response of the solar-blind photomultiplier. Interference effects were found to be no greater than for conventional a.f.s. with the CFAR. This technique appears to be applicable to the analysis of technical materials as illustrated by the determination of cadmium in a copper-base alloy.

We are grateful to the N.E.R.C. for the award of a grant to A. F. K. and to the Fundacion March (Spain) for the award of a grant to A. S. M.

REFERENCES

1 P. L. Larkins, Spectrochim. Acta, Part B, 26 (1971) 477.
2 T. J. Vickers, P. J. Slevin, V. I. Muscat and L. T. Farias, Anal. Chem., 44 (1972) 930.
3 D. R. Jenkins, Spectrochim. Acta, Part B, 23 (1967) 167.
4 T. S. West and X. K. Williams, Anal. Chem., 40 (1968) 335.
5 P. D. Warr, Talanta, 17 (1970) 543.
6 P. D. Warr, Talanta, 18 (1971) 234.
7 R. C. Elser and J. D. Winefordner, Appl. Spectrosc., 25 (1971) 345.

8 D. G. Mitchell and A. Johansson, Spectrochim. Acta, Part B, 25 (1970) 175.
9 D. G. Mitchell and A. Johansson, Spectrochim. Acta, Part B, 26 (1971) 677.
10 R. M. Dagnall, G. F. Kirkbright, T. S. West and R. Wood, Anal. Chem., 43 (1972) 1765.
11 R. M. Dagnall, G. F. Kirkbright, T. S. West and R. Wood, Analyst, 97 (1972) 245.
12 M. Jones, G. F. Kirkbright, L. Ranson and T. S. West, Anal. Chim. Acta, 63 (1973) 210.
13 K. M. Aldous, Pd.D thesis, Imperial College, 1970.
14 P. L. Larkins, R. M. Lowe, J. V. Sullivan and A. Walsh, Spectrochim. Acta, Part B, 24 (1969) 187.
15 T. J. Vickers and R. M. Vaught, Anal. Chem., 41 (1969) 1476.
16 P. L. Larkins and J. B. Willis, Spectrochim. Acta, Part B, 26 (1971) 491.
17 J. D. Norris and T. S. West, Anal. Chim. Acta, 71 (1974) 289.
18 T. S. West and X. K. Williams, Anal. Chim. Acta, 45 (1969) 27.
19 R. G. Anderson, I. S. Maines and T. S. West, Anal. Chim. Acta, 51 (1970) 355.
20 J. F. Alder and T. S. West, Anal. Chim. Acta, 51 (1970) 365.
21 J. Aggett and T. S. West, Anal. Chim. Acta, 55 (1971) 349.
22 J. Aggett and T. S. West, Anal. Chim. Acta, 57 (1971) 15.
23 D. Alger, R. G. Anderson, I. S. Maines and T. S. West, Anal. Chim. Acta, 57 (1971) 271.
24 L. Ebdon, G. F. Kirkbright and T. S. West, Talanta, 19 (1972) 1301.
25 M. D. Amos, P. A. Bennett, K. G. Brodie, P. W. Y. Lung and J. P. Matousek, Anal. Chem., 43 (1971) 211.
26 B. M. Patel, R. D. Reeves, R. F. Browner, C. J. Molnar and J. D. Winefordner, Appl. Spectrosc., 27 (1973) 171.
27 B. M. Patel and J. D. Winefordner, Anal. Chim. Acta, 64 (1973) 135.
28 J. V. Sullivan and A. Walsh, Spectrochim. Acta, 21 (1968) 721.
29 R. M. Dagnall and T. S. West, Appl. Opt., 7 (1968) 1287.
30 R. M. Dagnall, K. C. Thompson and T. S. West, Talanta, 14 (1967) 557.

Analytica Chimica Acta, 104 (1979) 93—98

AN ATOMIC ABSORPTION SPECTROMETRIC METHOD FOR THE DETERMINATION OF NON-IONIC SURFACTANTS

P. T. CRISP, J. M. ECKERT* and N. A. GIBSON

Department of Inorganic Chemistry, University of Sydney, Sydney, N.S.W. 2006 (Australia)

(Received 11th May 1978)

SUMMARY

A method is described for the determination of non-ionic surfactants in the concentration range 0.05—2 mg l^{-1}. Surfactant molecules are extracted into 1,2-dichlorobenzene as a neutral adduct with potassium tetrathiocyanatozincate(II) and the determination is completed by atomic absorption spectrometry. With a 150-ml water sample, the limit of detection is 0.03 mg l^{-1} (as Triton X-100). The method requires a single phase separation step, is applicable, without modification, to fresh, estuarine and sea-water samples and is relatively free from interference by anionic surfactants; the presence of up to 5 mg l^{-1} of anionic surfactant (as LAS) introduces an error of no more than 0.07 mg l^{-1} (as Triton X-100) in the apparent non-ionic surfactant concentration.

Non-ionic surfactants form neutral adducts with a variety of reagents such as ammonium tetrathiocyanatocobaltate, sodium picrate, barium molybdophosphate and calcium tungstophosphate. The solvent extraction of an adduct provides a convenient way of concentrating the surfactant and is the basis of several methods for the determination of non-ionic surfactants at low levels (below 10 mg l^{-1}).

In the widely used method of Greff et al. [1], non-ionic surfactant is extracted into benzene as an adduct with ammonium tetrathiocyanatocobaltate(II). The determination is completed spectrophotometrically at 320 nm. The method is simple, rapid, well-suited to the routine analysis of large numbers of samples, and applicable to surfactant concentrations in the range 0.1—20 mg l^{-1}. With this extraction system, it is necessary to saturate the water samples with sodium chloride, to improve extraction efficiency. A more serious disadvantage is interference by anionic surfactants.

Courtot-Coupez and Le Bihan [2] determined the optimum pH (7.4) for extraction of non-ionic surfactants with the $(NH_4)_2[Co(SCN)_4]$—benzene system. Cobalt in the extract is estimated by atomic absorption spectrometry (a.a.s.) after evaporation to dryness and dissolution of the residue in a suitable solvent (methyl isobutyl ketone). The method is applicable to surfactant concentrations in the range 0.02—0.5 mg l^{-1} and is not seriously affected by the presence of anionic surfactants.

In the method of Favretto and Tunis [3], a sodium picrate—surfactant adduct is extracted from a strongly alkaline sodium nitrate solution into 1,2-dichloroethane and the extract absorbance is measured at 378 nm. Anionic surfactants interfere at concentrations greater than 0.2 mg l^{-1}. Allowance for this effect may be made by the determination of anionic surfactants (as methylene blue-active substances) and reference to interference graphs.

In this paper, a new extractive method is reported for the determination of non-ionic surfactants, in which the surfactant is extracted into 1,2-dichlorobenzene as a neutral adduct with potassium tetrathiocyanatozincate(II). The adduct is colourless but zinc has high sensitivity by a.a.s. The determination is completed by flame a.a.s. for zinc in an acid back-extract. The performance of the method in the presence of anionic surfactants and with fresh and sea-water samples is assessed.

EXPERIMENTAL

Apparatus and reagents

A Varian-Techtron Model AA-6DA spectrometer was used.

Standard reference non-ionic surfactant solution. The reference non-ionic surfactant was Triton X-100 (Merck, gas chromatography grade; vacuum dried). Triton X-100 is polyethyleneglycol-mono-[*p*-(1,1,3,3-tetramethylbutyl)phenyl] ether, containing an average of approximately 10 ethoxy units; this was confirmed by n.m.r. in the sample used. A stock standard solution of Triton X-100 was prepared, containing 1500 mg l^{-1}, and diluted further as required.

Zinc—thiocyanate reagent. Dissolve 116 g of zinc sulphate heptahydrate, 312 g of potassium thiocyanate and 40 g of potassium acetate in hot water and dilute to 2 l with water. Extract the reagent with three 50-ml quantities of 1,2-dichlorobenzene before use.

1,2-Dichlorobenzene. Pass the commercial solvent through a 20-cm column of activated alumina before use and re-cycle used solvent by washing it with water, drying over anhydrous calcium chloride and passing through the alumina column.

Recommended procedure

Place a 150-ml water sample, containing not more than 2 mg of non-ionic surfactant per litre, in a 500-ml separating funnel, fitted with a Teflon stop-cock. If necessary, adjust the pH of the water sample to 6—8. Add 50.0 ml of zinc—thiocyanate reagent and 20.0 ml of 1,2-dichlorobenzene. Shake the funnel for 5 min and allow to stand until the phases separate. If a shaking table is available, the water sample is most conveniently extracted by shaking the mixture mechanically in a 500-ml flask, then pouring the mixture into a dry 250-ml separating funnel for phase separation. Run about 13 ml of the organic phase into a dry 15-ml graduated centrifuge tube, taking care that no droplets of the aqueous phase pass into the tube. Cover the top of the tube with a 5-cm square of aluminium foil and centrifuge at room temperature and 2500 r.p.m. for 30 min.

Pipette a 10.0-ml aliquot of the clarified extract into a 25-ml volumetric flask and add 10.0 ml of 0.1 M hydrochloric acid. Stopper the flask and shake it vigorously for 2 min. Allow the phases to separate and aspirate the aqueous (upper) layer directly from the flask into the a.a.s.; this can be done without removing the organic layer. Use the following a.a.s. working conditions: oxidizing air—acetylene flame, 5-mA lamp current, 213.9-nm wavelength and 0.2-nm spectral band pass.

Carry out a blank determination with 150 ml of distilled water. The blank absorbance should be small (0.000-0.001). Calculate the surfactant concentration in the sample (as mg Triton X-100 l^{-1}) by comparison with standards run simultaneously.

RESULTS AND DISCUSSION

The concentration of zinc in the zinc—thiocyanate reagent is 0.2 M and the mole ratio of zinc to thiocyanate is 1:8. The predominant zinc complex present is the tetrathiocyanatozincate(II) ion. The counter-ion is K^+ and acetate ions (0.2 M) are included to adjust the pH of the treated water samples to 6.5—7.0.

Since the working conditions of an atomic absorption spectrometer are optimized at the beginning of each run, standards must be measured with each batch of unknowns. Calibration graphs show slight curvature in the concentration range 0—2 mg l^{-1} and marked curvature beyond 2 mg l^{-1}. Water samples containing more than 2 mg of non-ionic surfactant per litre should be appropriately diluted.

The precision of the zinc—thiocyanate method was assessed by carrying out repeated determinations of standard Triton X-100 solutions. The results are shown in Table 1.

The limit of detection, taken to be the surfactant concentration which gave an absorbance equal to twice the standard deviation of a set of at least 10 readings at or near blank level, was found to be 0.03 mg l^{-1} (as Triton X-100).

Effect of polyethoxylate chain length

The effect of polyethoxylate chain length was examined by studying the response to the method of a range of n-nonylphenol ethoxylates containing up to 100 ethoxy units per molecule. The results are shown in Fig. 1. Response is greatest between 8 and approximately 40 ethoxy units.

Interferences

The effects of various ions on the recovery of Triton X-100 (1.00 mg l^{-1}) are shown in Table 2. Only sulphide, iron(III), aluminium(III) and chromium(III) ions interfere at concentrations likely to be found in contaminated waters. There is, however, no interference from sulphide at up to 100 mg l^{-1} if the water is treated with 1 ml of 30% hydrogen peroxide, shaken and allowed to stand for 10 min before addition of the zinc—thiocyanate reagent. Interference from up to 100 mg l^{-1} concentrations of iron(III), aluminium(III) or chromium(III)

TABLE 1

Precision of proposed method

Triton X-100 taken (mg l^{-1})	s^a (mg l^{-1})	s_r (%)
0.10	0.01	10
0.50	0.015	3
1.00	0.02	2
2.00	0.04	2

[a]9 determinations were carried out at each level.

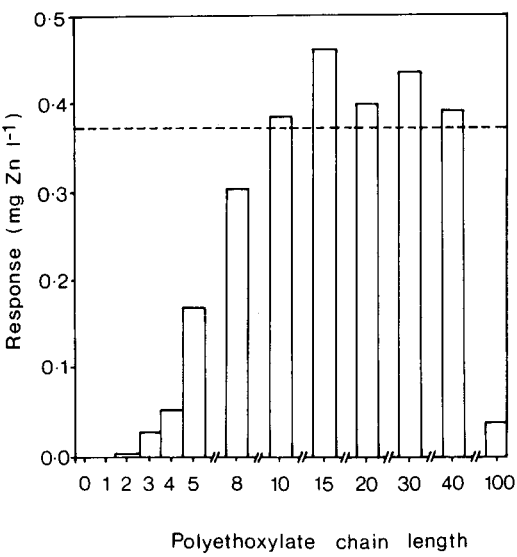

Fig. 1. Effect of polyethoxylate chain length. Response of 1.00 mg l^{-1} solutions of n-nonylphenol ethoxylates, containing 2—100 ethoxy units per molecule, is expressed as the concentration of zinc in the acid back-extract. The dashed line indicates the zinc concentration obtained from Triton X-100 (1.00 mg l^{-1}).

is suppressed by addition of 1 g of EDTA (disodium salt dihydrate) prior to the addition of the zinc—thiocyanate reagent; the EDTA is unnecessary, however, if the metals are present mainly as a suspension of the hydroxides.

The proposed method is well-suited to marine and estuarine analyses. Table 3 shows recovery data for different concentrations of Triton X-100 added to clean sea water.

The performance of the proposed method in the presence of anionic surfactants is of special importance, since most natural or waste-water samples which contain non-ionic surfactants also contain anionic surfactants. Recovery data for Triton X-100 from water and sea water containing the anionic

TABLE 2

Allowable concentrations of foreign ions[a]

Concentration	Ion
5 M	Cl^-, Na^+
0.5 M	NO_3^-, SO_4^{2-}
1000 mg l^{-1}	F^-, Br^-, I^-, NO_2^-, SCN^-, $CH_3CO_2^-$, K^+, Mg^{2+}
100 mg l^{-1}	$P_3O_{10}^{5-}$, NH_4^+, Ca^{2+}, Ni^{2+}, Co^{2+}, Mn^{2+}, Zn^{2+}
10 mg l^{-1}	Cu^{2+}
0.1 mg l^{-1}	S^{2-}, Fe^{3+}, Al^{3+}, Cr^{3+}

[a]95—105% recovery of Triton X-100 (1.00 mg l^{-1}) was obtained in the presence of the stated concentration.

TABLE 3

Recovery of Triton X-100 from sea water

Triton X-100 added (mg l^{-1})	Mean Triton X-100 found[a] (mg l^{-1})	s (mg l^{-1})	Recovery (%)
0	<0.03	0.01	—
0.10	0.14	0.02	140
0.50	0.49	0.02	98
1.00	1.02	0.04	102
2.00	2.05	0.03	103

[a]Mean of 9 determinations.

TABLE 4

Recovery of Triton X-100 from water and sea water in the presence of LAS

LAS present (mg l^{-1})	Triton X-100 added (mg l^{-1})	Mean Triton X-100 found[a] (mg l^{-1})	
		In water	In sea water
5	0	0.04	0.03
5	0.10	0.15	0.15
5	1.00	1.04	1.04
5	2.00	2.07	2.00
0.5	0	<0.03	<0.03
0.5	0.10	0.13	0.15
0.1	0	<0.03	<0.03
0.1	0.10	0.13	0.15

[a]Mean of duplicate determinations.

surfactants linear alkylbenzene sulphonates (LAS) are given in Table 4. The presence of up to 5 mg LAS l^{-1} increases the apparent concentration of non-ionic surfactant by a maximum of 0.07 mg l^{-1} (as Triton X-100).

Soaps, such as sodium stearate, do not interfere with the recovery of Triton X-100 (1.00 mg l^{-1}) when present at the same concentration (i.e., 1.00 mg l^{-1}). Cationic surfactants, however, form extractable ion-association compounds with the tetrathiocyanatozincate ion and interfere with the methc

The merits of the proposed method are (i) relative freedom from interferen by anionic surfactants — the presence of up to 5 mg LAS l^{-1} introduces an error of no more than 0.07 mg l^{-1} (as Triton X-100) in the apparent non-ionic surfactant concentration; and (ii) simplicity — a single phase separation step is required and the method is applicable, without modification, to fresh, estuarine and sea-water samples.

We acknowledge the support received by one of us (P. T. C.) from a Commonwealth Postgraduate Research Award. Our thanks are also due to I.C.I. Australia Ltd. for n-nonylphenol ethoxylate samples.

REFERENCES

1 R. A. Greff, E. A. Setzkorn and W. D. Leslie, J. Am. Oil Chem. Soc., 42 (1965) 180.
2 J. Courtot-Coupez and A. Le Bihan, Anal. Lett., 2 (1969) 567.
3 L. Favretto and F. Tunis, Analyst, 101 (1976) 198.

Analytica Chimica Acta, 104 (1979) 99—111

DIRECT DETERMINATION OF TRACES OF MOLYBDENUM IN SYNTHETIC SEA WATER BY ATOMIC ABSORPTION SPECTROMETRY WITH ELECTROTHERMAL ATOMIZATION AND SELECTIVE VOLATILIZATION OF THE SALT MATRIX

TAKETOSHI NAKAHARA* and CHUNI L. CHAKRABARTI

Metal Ions Group, Department of Chemistry, Carleton University, Ottawa, Ontario K1S 5B6 (Canada)

(Received 23rd June 1978)

SUMMARY

A simple and rapid method is described for the direct determination by graphite-furnace atomic absorption spectrometry (HGA-2100) of traces of molybdenum (0.1—4 ng) in synthetic sea water. It is shown that the salt matrix can be removed completely by selective volatilization at 1700—1850°C, but the original presence of NaCl, Na_2SO_4 and KCl causes a considerable decrease in molybdenum absorbance, and $MgCl_2$ and $CaCl_2$ a pronounced enhancement. The presence of $MgCl_2$ prevents the depressive effects. Samples of less than 50 μl can be analyzed directly without using a background corrector, with a precision of $< 10\%$.

Graphite-furnace atomic absorption spectrometry (a.a.s.) has been little used for direct determination of trace elements in sea water. This is attributed to the pronounced background absorption (i.e., non-specific absorption and scattering of incident radiation) which is due to the excessive amount of thermally stable, non-volatile salt matrix, in particular NaCl and Na_2SO_4, present in sea water [1—3], and to possible interferences of the matrix in the determination of trace elements [1, 4, 5]. The approach of correcting for molecular absorption by the use of a continuum source, e.g., a deuterium arc, does not work with sea water unless the bulk of the salt matrix is removed beforehand, as shown, for example, by Segar and Gonzalez [1].

In order to overcome this matrix problem, several procedures involving separation of the trace metals from the salt matrix before atomization have been reported. These include extraction of trace metals as chelates [6—19], retention of the matrix by a column of hydrated antimony pentoxide [20], separation of the analyte by a column of ion-exchange resin [21—23], concentration of trace metals on a hanging mercury drop [24, 25] and a pyrolytic graphite-coated tube [26], separation of trace elements by co-precipitation [27], and removal of chloride ions, e.g., by adding nitric acid [28, 29], sodium peroxide [30] or

*Present address: Department of Applied Chemistry, College of Engineering, University of Osaka Prefecture, Mozu-umemachi, Sakai 591 (Japan)

ammonium nitrate [31, 32]. However, these preconcentration and pretreatmen procedures are not desirable since they invariably lead to contamination, loss and change in the nature of species, in addition to being laborious and slow.

Segar and Gonzalez [1, 33] tried to overcome the matrix problem by using selective volatilization during the ashing step of the heating program of the graphite furnace (HGA-70) to determine trace metals in sea water. The non-specific absorption was decreased considerably. However, most of the elements investigated (Co, Cu, Mn, Ni and V) showed a markedly decreased sensitivity, probably because of co-volatilization losses of the trace elements with the major salts. Segar and Cantillo [5] reported reduced non-specific absorbance with the Perkin-Elmer HGA-2100 and showed that iron, manganese, copper and cadmium could be determined in their normal range of concentrations in sea water. Recently, Campbell and Ottaway [34] proposed a simple and rapid method for the direct determination of cadmium and zinc in sea water with an HGA-72 furnace without a charring step, in which a low atomization temperature (1492°C) is used in order to achieve separation in time of atomic and non-atomic absorption signals in an analogous manner to that of Lundgren et al. [35].

This paper describes a study of the possibilities of the direct determination, i.e., without preconcentration or separation, of traces of molybdenum in synthetic sea water by using graphite-furnace a.a.s. with careful control of the temperature program in order to volatilize and remove the salt matrix selectively and completely from the analyte during the stage prior to atomization. The aging of the pyrolytic graphite-coated tubes and time-resolved measurements of transient signals on a storage oscilloscope are also discussed.

EXPERIMENTAL

Apparatus

All experiments, except where noted otherwise, were done with a Perkin-Elmer atomic absorption spectrometer, model 603, equipped with a heated graphite atomizer (HGA-2100), an HGA ramp programmer and a deuterium arc background corrector. A Jarrell-Ash single-element molybdenum hollow-cathode lamp was used as a line source. All the graphite tubes were coated with a layer of pyrolytic graphite by in situ pyrolysis of methane, i.e. by heating the tube to 2100°C and maintaining an internal gas flow of 50 ml min^{-1} of a mixture of 10% methane and 90% argon for 10 min.

All temperatures below 1000°C were calibrated with a NiCr/Ni thermocouple. For higher temperatures, an automatic optical pyrometer, series 1100 (Ircon Inc., Niles, Ill.), was used; this was calibrated by the manufacturer and again in this laboratory by measurements with thermocouples and by the melting points of selected pure metals, to cover the entire range of temperatures. The temperature meter on the HGA-2100 power supply unit was calibrated by measuring the temperature inside the heated tube. The radiation from the inner wall of the tube was focused through the sample injection port

at the viewing lens of the optical pyrometer. The estimated accuracy of the measurement was ±50°C. The instrumental parameters are given in Table 1.

Time-resolved measurements of transient signals were made with the research apparatus described previously [36—39], equipped with a storage oscilloscope (Tektronix, model 549) combined with a Polaroid camera. All electron micrographs were taken with a JEOL model JSM-U3 scanning electron microscope.

Reagents

All reagents used were of ACS reagent-grade purity. A stock solution containing 1000 μg Mo ml^{-1} was prepared from molybdenum trioxide dissolved in 2 M ammonia and diluted to volume with ultrapure water. Ultrapure water of resistivity 18.3 megohm-cm was obtained direct from a Milli-Q Water System (Millipore Corporation). Synthetic sea water was made by dissolving the following five major constituents in ultrapure water at their sea-water concentrations, to give a salinity of approximately 35‰ as recommended by Kester et al. [40]: NaCl, $MgCl_2 \cdot 6H_2O$, Na_2SO_4, $CaCl_2 \cdot 2H_2O$ and KCl. Solutions of one or more constituents were also prepared. All test solutions were prepared with ultrapure water immediately before use.

Nitrogen gas of 99.95% purity (Roncar Oxygen Co.) was used to sheath the atomizer and to purge it internally; there was a little difference in molybdenum absorbance between nitrogen and argon.

Procedure

Experiments were performed to determine whether significant differences in the reproducibility of molybdenum absorbance and in the degree of signal

TABLE 1

Instrumental conditions for graphite-furnace a.a.s. of molybdenum in synthetic sea water without scale expansion.

	Sample injection volume (μl)				
	5	10	20	50	100
Drying stage	100°C, 20 s	100°C, 40 s	100°C, 60 s	110°C, 120 s (ramp: 80 s)	110°C, 120 s (ramp: 80 s)
Charring stage	Variable temperature				
	20 s	40 s	60 s	90 s (ramp: 40 s)	120 s (ramp: 85 s)
Atomization	2700°C, 8 s				
Heating-out stage	Maximum temperature (i.e., 2800°C), 5 s				
Wavelength	313.3 nm				
Lamp current	10 mA				
Slit width	1.0 mm (spectral bandpass, 0.7 nm)				
Nitrogen flow rate	1.0 l min^{-1} (total) with internal flow rate of 0.1 l min^{-1} and interrupt mode of internal gas flow				
Integration time	8 s				

suppression and enhancement would be found by measuring peak heights rather than areas. For all solutions studied, peak heights and integrated areas showed identical reproducibility and degree of interference, within experimental error. Consequently, absorbances were determined by measuring peak heights, unless otherwise stated. Peak heights were read on the digital meter of the spectrometer in the peak absorbance mode.

For each experiment, 5-, 10-, 20-, 50-, or 100-μl volumes of test solutions were introduced into the graphite furnace with Eppendorf pipettes fitted with disposable plastic tips. The sequential dry—char—atomize program of the HGA-2100 was followed, and the peak absorbance noted. The tube was fired at its maximum temperature, i.e., 2800°C, for 5 s after each sample to clear any residue from the tube surface. The results of five replicate analyses of each test solution were averaged. The internal gas interrupt mode at the atomizing stage was used at all times, so that the gas flow rate was not critical, the only requirement being that it must be sufficient to prevent oxidation of the graphite tube. Blanks were run regularly and their values were subtracted from the gross values to obtain the net values reported here.

RESULTS AND DISCUSSION

Effect of charring temperature on molybdenum absorbance

The influence of the "charring" temperature on the absorbance for molybdenum was investigated by using two aqueous solutions of molybdenum. Typical results obtained with the peak absorbance mode are shown in Fig. 1. Similar results (not shown) were obtained with the integrated absorbance mode. Such a high temperature of up to around 1900°C can be used for charring without any loss of molybdenum because its average appearance temperature, i.e., minimum atomization temperature, is 1967°C [41].

In the presence of graphite, molybdenum forms a thermally stable interstitial carbide [42, 43]. The absorbance drop around 1100°C, as shown in Fig. 1, was remarkably reproducible and much more pronounced in the absence of the sea-water salts. The absorbance drop means that molybdenum carbide might be most effectively produced around 1100°C, resulting in incomplete vaporization and atomization of molybdenum. An alternative explanation may be that molybdenum trioxide, produced during charring, has a sublimation point of 1155°C at ca. 0.1 MPa [44]. However, it is difficult to explain why the molybdenum absorbance increases slightly with an increase in charring temperature above 1100°C.

Effect of each constituent on molybdenum and non-specific absorbances

Figure 1 shows the molybdenum and non-specific absorbances at the 313.3-nm line from the hollow-cathode lamp caused by the presence of each constituent of synthetic sea water as a function of the charring temperature. For clarity, all absorbance scales in Fig. 1 are identical. The non-specific absorption was completely and selectively eliminated at higher temperatures

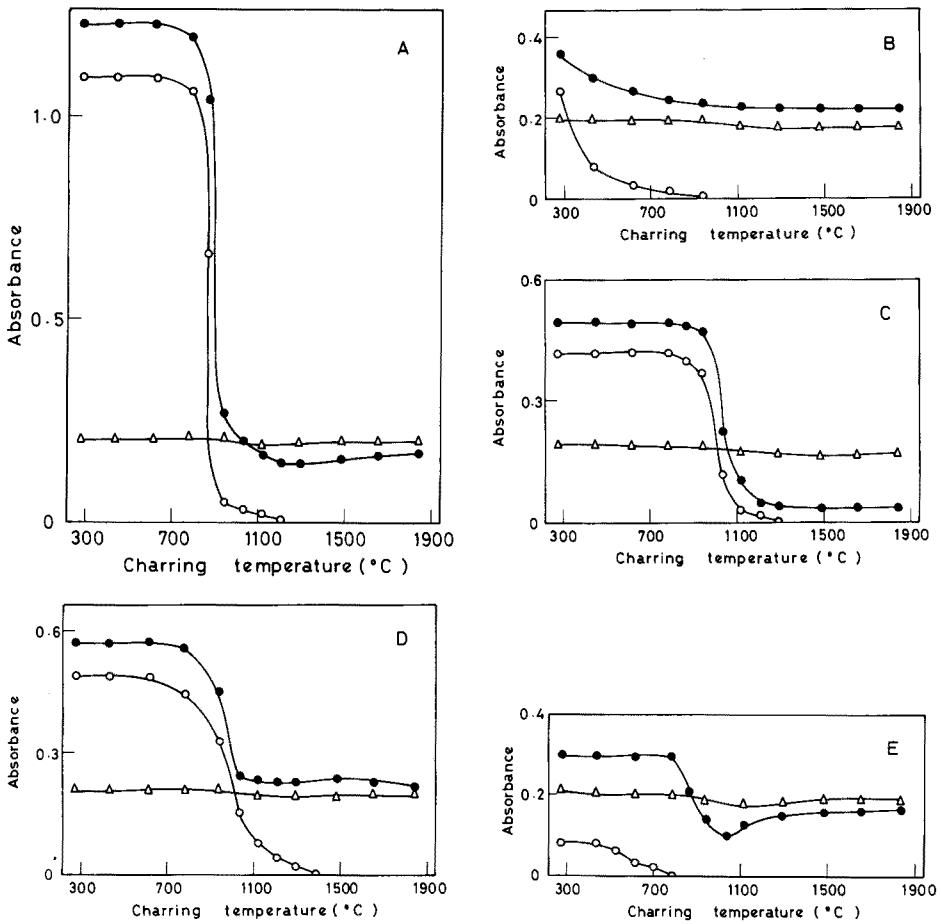

Fig. 1. Molybdenum and non-specific absorbances in the presence of five major constituents of sea water at their sea-water concentrations, as a function of charring temperature. (△) Molybdenum absorbance for 2.5×10^{-9} g Mo; (○) non-specific absorbance for each constituent; (●) absorbance for 2.5×10^{-9} g Mo with each constituent added. (A) NaCl with 20-μl samples; (B) $MgCl_2$ with 50-μl samples; (C) Na_2SO_4 with 20-μl samples; (D) $CaCl_2$ with 50-μl samples; (E) KCl with 10-μl samples.

during the charring cycle of the heating program. The temperatures over which the non-specific absorptions were completely removed at the charring stage were dependent not only on the individual constituents, but also on the sample injection volumes.

As can be seen from Fig. 1, the presence of the salt matrix caused depressive or enhancing interferences after the salt matrix was completely removed. The depressive interferences to which the presence of NaCl, Na_2SO_4 and KCl gave rise might be partially ascribed to co-volatilization losses of the analyte with the salts during the charring step, as previously reported [1, 33]. In the case of the enhancing interference in the presence of $MgCl_2$ and $CaCl_2$,

evaporation of trace or ultra trace $MgCl_2$ and $CaCl_2$ remaining after the charring state probably causes more effective introduction of molybdenum into the vapor phase.

Effect of combined constituents on molybdenum and non-specific absorbances

Experiments were carried out to determine whether the presence of $MgCl_2$ or $CaCl_2$ would be effective in eliminating the depressive interference from NaCl, Na_2SO_4 and KCl. The results obtained (Fig. 2) show that $MgCl_2$ is more effective at high charring temperatures than $CaCl_2$. It can also be seen that the presence of NaCl, Na_2SO_4, KCl, $MgCl_2$ and $CaCl_2$ (and most probably sea-water matrix) slightly enhanced the molybdenum absorbance compared with that for a simple aqueous solution of molybdenum. This behavior is very similar to that of $MgCl_2$ in eliminating depressive interferences in the determination of gallium [45], lead [46] and indium [47] with low-temperature flames. At the levels found in sea water, however, magnesium chloride chemically depresses the cadmium graphite-furnace atomic absorption signal [34]. These facts suggest that the matrix may affect not only the chemical form of the analyte deposited on the surface of graphite tube after drying and charring but also the rate and process of vaporization and dissociation of the analyte.

Molybdenum and non-specific absorbances from synthetic sea water

Figure 3 depicts the non-specific absorbance of synthetic sea water containing no added molybdenum with different sample volumes as a function of charring temperature. The temperatures over which the sea-water matrix can be completely volatilized during the charring cycle depend on the sample

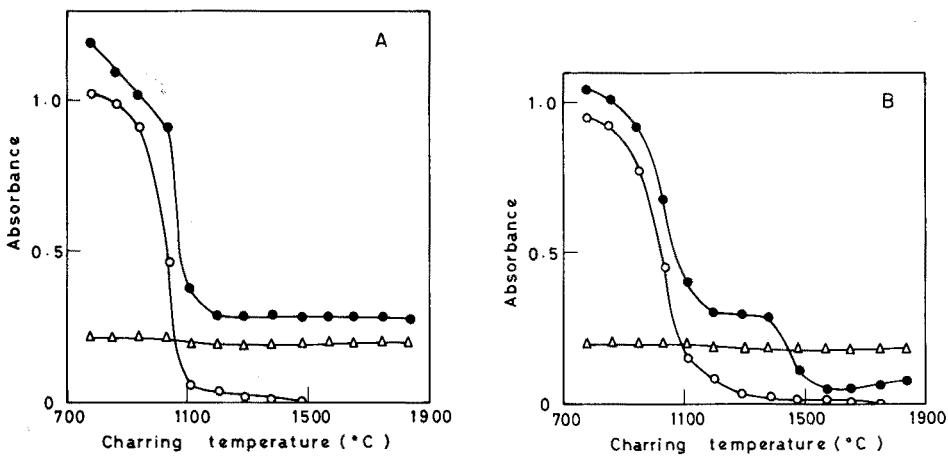

Fig. 2. Effects of $MgCl_2$ (A) and $CaCl_2$ (B) on the depressive interference from NaCl, Na_2SO_4 and KCl at their sea-water concentrations, as a function of charring temperature. (△) Molybdenum absorbance for 2.5×10^{-9} g Mo; (○) non-specific absorbance for NaCl, Na_2SO_4 and KCl, (●) absorbance for 2.5×10^{-9} g Mo and NaCl, Na_2SO_4 and KCl with $MgCl_2$ (A) or $CaCl_2$ (B) added: 20-μl sample.

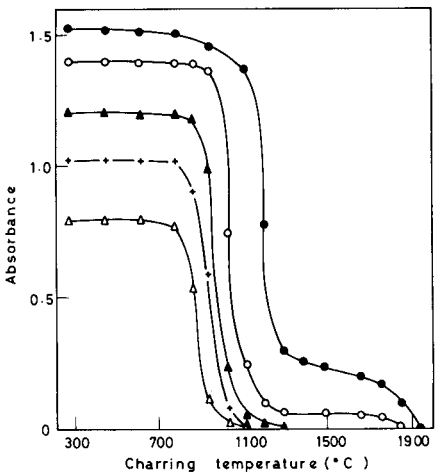

Fig. 3. Non-specific absorbance for synthetic sea water as a function of charring temperature. Sample injection volume: (△) 5 μl, (+) 10 μl, (▲) 20 μl, (○) 50 μl, (●) 100 μl.

injection volumes. As can be seen from Fig. 3, the sample volume which allowed complete and selective volatilization of the sea-water matrix was ⩽20 μl. The necessity for using such small volumes considerably limits the sensitivity and applicability of the present method.

Experiments were done to determine whether the selective volatilization technique without background correction would be effective for synthetic sea water. For comparison, the deuterium arc background corrector was used to ensure that no sea-water matrix remained after charring at high temperatures. The molybdenum absorbance curves as a function of charring temperature with sample volumes of 20, 50 and 100 μl are shown in Fig. 4. Similar results to those in Fig. 4(A) were obtained for sample volumes of 5 and 10 μl. At the highest temperature for charring (1850°C), a sample volume of 50 μl can also be applied, as shown in Fig. 4(B), but not at lower temperatures. The results in Fig. 4 are predictable from the experiments shown in Fig. 3. Thus, the matrix volatilization technique was successful for samples of ⩽50 μl, but not for samples of 100 μl. With use of the background corrector, however, a sample volume of 100 μl might be applicable in conjunction with the selective volatilization technique. The decreases of absorbance at a charring temperature of ca. 1950°C (Fig. 4(C)) are probably due to pre-atomization losses of molybdenum. The optimum charring temperature was found to be 1700—1850°C for samples less than 20 μl but 1850°C for a 50-μl injection.

Recommended procedure for analysis

The analysis for molybdenum of synthetic sea water containing five major sea salts in the concentration of 35‰ salinity is simple, rapid and free of salt interference when the following procedure is used. Inject a sample of ⩽50 μl

into the pyrolytic graphite-coated tube. Dry carefully without spitting under the conditions described in Table 1 and char to 1850°C, from the drying temperature. Atomize for 8 s at 2700°C, and measure the absorbance at 313.3 nm. Clean the tube by heating to maximum temperature (2800°C) for 5 s. For a 100-μl sample, background correction must be used.

Sensitivity, linear range, precision and accuracy

When the recommended method was used almost the same molybdenum absorbance was obtained with or without the deuterium arc background corrector. However, synthetic sea water gave slightly larger molybdenum absorbances than the solution of the molybdenum salt in ultrapure water, the sensitivities for 1% absorption being 5.0×10^{-11} g and 5.7×10^{-11} g, respectively. The calibration graph was linear up to an absorbance of 0.30, equivalent to 0.1—4.0 ng of molybdenum.

For examination of precision, five samples of synthetic sea water containing 2.5×10^{-9} g of molybdenum were analyzed by the recommended procedure. The precision depended on the sample injection volume but the average precision was better than 10%.

The accuracy of the determination of trace molybdenum in sea water could not be thoroughly evaluated because standard sea-water samples were not available.

Molybdenum absorbance as a function of tube age

Recently Sturgeon and Chakrabarti [48] described significant improvements in performance for molybdenum and vanadium (sensitivity, detection limit, precision and lifetime) by coating graphite-furnace tubes with pyrolytic graphite. Coated tubes were used throughout this work. Segar and Cantillo [5] reported linear decreases of absorbance over a tube lifetime when uncoated tubes were used. Experiments were undertaken to estimate the lifetime of the coated tubes; both peak and integration modes of measurement were used. The results obtained are shown in Fig. 5. Under the conditions described, the coated tubes showed no sign of aging up to ca. 150 firings, with continued high precision on replicate analyses. Molybdenum absorbance increased after ca. 150 firings, as the tube aged. Such increases were almost certainly caused by increasing atomizing temperatures at fixed temperature settings on the meter scale of the HGA-2100 control unit, resulting in faster rates of rise of temperature. At a fixed temperature setting of 2700°C for atomization, final atomization temperatures measured by the optical pyrometer were found to be 2650, 2690 and 2760°C for a used coated tube after ca. 100, 150 and 250 atomizations, respectively. In addition, loss in weight of the tubes was also measured by a chemical balance; the relative standard deviation in weighing ten new coated tubes was less than 0.5%. The losses in weight compared with a new coated tube were 2.1, 2.9 and 5.9% after ca. 100, 150 and 250 firings, respectively. Figure 6 shows electron micrographs of the interior surfaces of unused and used pyrolytic graphite-coated tubes, in which a radical change in the surface was observed after more than 150 firings.

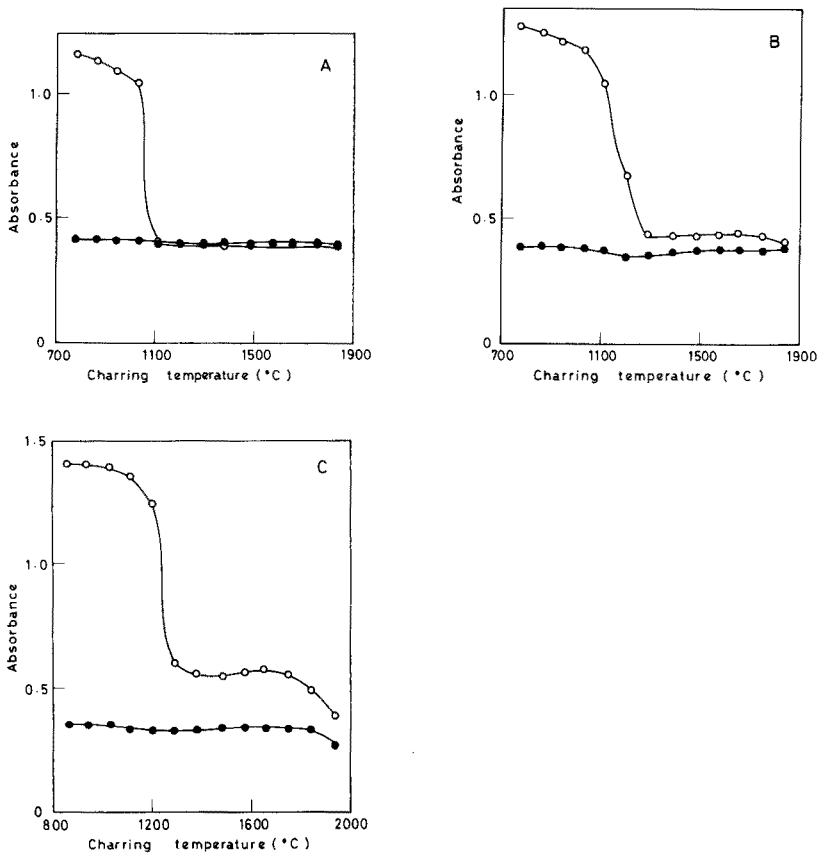

Fig. 4. Molybdenum and non-specific absorbances for synthetic sea water containing molybdenum (2.5×10^{-9} g) as a function of charring temperature with (•) and without (○) the use of the background corrector. Sample injection volumes: (A) 20 μl, (B) 50 μl, (C) 100 μl.

Time-resolved oscilloscopic measurements of transient signals

The transient signals were measured by means of the apparatus described previously [36, 37]. The graphite-furnace atomizer was a modified Perkin-Elmer HGA-2100 fitted with a larger cooling chamber to allow for more efficient temperature control during long or high-temperature atomization periods [38, 39]. Figure 7 shows the temperature—time curve at a final atomization temperature setting of 2700°C, corresponding to an initial atomizer heating rate of 1.23°C ms^{-1}, and also shows the absorbance—time curve for an ultrapure water solution of 2.5×10^{-9} g Mo. The ordinate of the temperature—time curve is the mV scale of the signal from the optical pyrometer, which directly corresponds to the temperature.

Figures 8 and 9 show time-resolved oscilloscopic traces of molybdenum and non-specific absorbances for synthetic sea-water and ultrapure water solutions of molybdenum at the Mo 313.3-nm line. As shown in Fig. 8, the non-specific

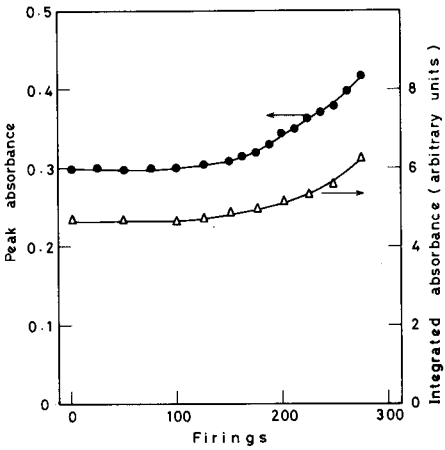

Fig. 5. Peak absorbance (•) and integrated absorbance (△) as a function of number of firings: 2.5×10^{-9} g molybdenum (10-μl samples); charring temperature, 1500°C.

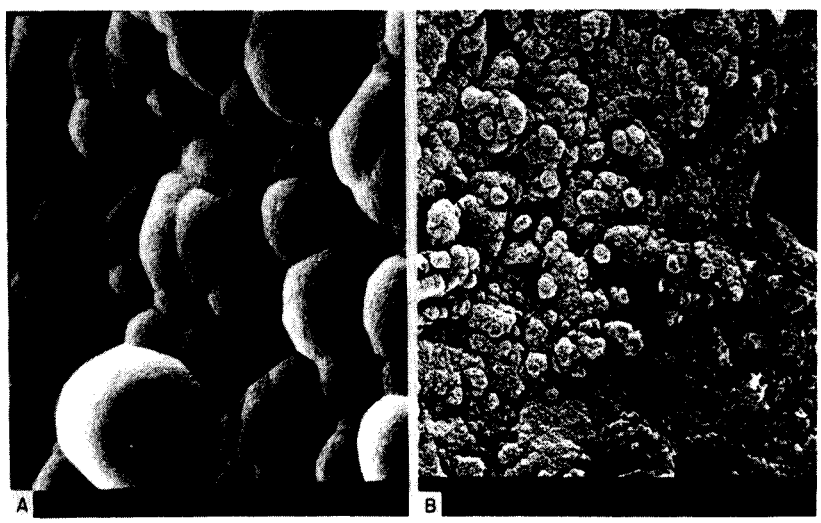

Fig. 6. Electron micrograph (500 ×) of the surface of (A) a new pyrolytic graphite-coated tube; (B) the same tube ca. 250 atomizations.

absorption signal of the sea-water matrix appeared much faster (i.e., at lower temperature) than the molybdenum absorption signal because selective vaporization of the matrix would occur at temperatures well below the boiling point of the analyte. Compared to the aqueous molybdenum solution (Fig. 8, curve B), the molybdenum peak from the synthetic sea water shifted to a lower temperature range (Fig. 8, curve A). This behavior might be explained partly by the "carrier effect" or "carrier distillation" as it is known in emission

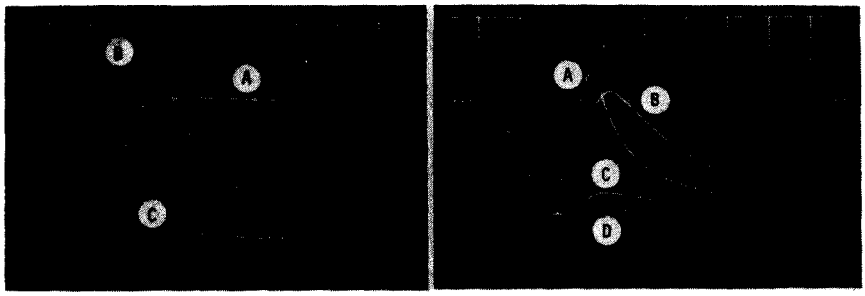

Fig. 7. Oscilloscopic traces of absorbance and temperature. Charring temperature, 400°C; the horizontal scale is the sweep speed (500 ms/scale unit) with a delay time of 200 ms. (A) Temperature—time curve: vertical scale, 2 mV/scale unit. (B) and (C) absorbance—time curves for 2.5×10^{-9} g Mo (5-μl sample) and a blank firing, respectively.

Fig. 8. Oscilloscopic traces of absorbance. Charring temperature, 400°C; sample volume, 5 μl; the horizontal scale is the sweep speed (500 ms/scale) unit with a delay time of 50 ms; the vertical scale is absorbance (0.2/scale unit). Absorbance—time curves (A) 2.5×10^{-9} g Mo in synthetic sea water; (B) 2.5×10^{-9} g Mo in ultrapure water; (C) synthetic sea water; (D) blank firing.

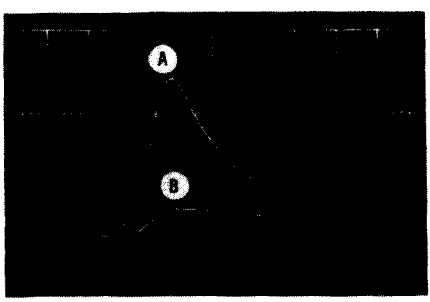

Fig. 9. Oscilloscopic traces of absorbance. Charring temperature, 1800°C. Absorbance—time curves: (A) 2.5×10^{-9} g Mo in synthetic sea water; (B) blank firing. Other conditions as in Fig. 8.

spectrometry [49]. Complete and selective vaporization (volatilization) of the salt matrix of sea water occurred predominantly during the charring cycle at 1800°C (Fig. 9). This ensures that the present method is successful in the direct determination of trace amounts of molybdenum in synthetic sea water under the conditions described above.

Conclusion

The selective volatilization technique described is highly suitable for the determination of traces of molybdenum in synthetic (and most probably real) sea-water samples. It has the advantages of freedom from contamination and loss during sample preparation, and is faster, and cheaper than procedures

involving separations. The sensitivity achieved should allow sea-water samples to be analyzed for molybdenum, because the concentration of molybdenum in sea water is usually 2.1—18.8 $\mu g\ l^{-1}$ [50]. The selected temperature of 1700—1850°C during the charring stage permits separation of the sea-water matrix from the analyte prior to atomization with the HGA-2100. Further experimental work on other trace elements, however, is required to substantiate the conclusions drawn in this study.

The authors express their thanks to Drs. R. E. Sturgeon and D. C. Grégoire for helpful discussion, to Dr. L. Ling for providing the electron micrographs, and to the National Research Council of Canada for financial support of this project. One of the authors (T. N.) is grateful to Carleton University for a research fellowship and to the University of Osaka Prefecture for the grant of a travel fellowship.

REFERENCES

1 D. A. Segar and J. G. Gonzalez, Anal. Chim. Acta, 58 (1972) 7.
2 B. R. Culver and T. Surles, Anal. Chem., 47 (1975) 920.
3 M. W. Prichard and R. D. Reeves, Anal. Chim. Acta, 82 (1976) 103.
4 F. J. Fernandez and D. C. Manning, At. Absorpt. Newsl., 10 (1971) 3.
5 D. A. Segar and A. Y. Cantillo, in T. R. P. Gibb, Jr. (Ed.), Analytical Methods in Oceanography, Advances in Chemistry Series, No. 147, American Chemical Society, Washington D. C., 1975, pp. 56—81.
6 R. J. Stolzberg, in T. R. P. Gibb, Jr. (Ed.), Analytical Methods in Oceanography. Advances in Chemistry Series, No. 147, American Chemical Society, Washington D. C., 1975, pp. 30—43.
7 T. H. Donnelly, J. Ferguson and A. J. Eccleston, Appl. Spectrosc., 29 (1975) 158.
8 T. Shigematsu, M. Matsui, O. Fujino and K. Kinoshita, Nippon Kagaku Kaishi, (1973) 212
9 T. Shigematsu, M. Matsui, O. Fujino, S. Mitsuno and T. Nagahiro, Nippon Kagaku Kaishi, (1975) 1328.
10 L. Danielsson, B. Magnusson and S. Westerlund, Anal. Chim. Acta, 98 (1978) 47.
11 K.-S. Sperling, At. Absorpt. Newsl., 15 (1976) 1.
12 A. Eaton, Mar. Chem., 4 (1976) 141.
13 J. M. Bewers, B. Sundby and P. A. Yeats, Geochim. Cosmochim. Acta, 40 (1976) 687.
14 K. Hiiro, T. Owa, M. Takaoka, T. Tanaka and A. Kawahara, Bunseki Kagaku, 25 (1976) 1
15 K. Kremling and H. Petersen, Anal. Chim. Acta, 70 (1974) 35.
16 P. G. Brewer, N. Frew, N. Cutshall, J. J. Wagner, R. A. Duce, P. R. Walsh, G. L. Hoffman J. W. R. Hutton, W. F. Fitzgerald, C. D. Hunt, D. C. Girvin, P. G. Clem, C. Patterson, D. Settle, B. Glover, B. J. Presley, J. Trefry, H. Windom and R. Smith, Mar. Chem., 2 (1974) 69.
17 J. M. Bewers, S. Hartling, R. Duce, P. Walsh, W. Fitzgerald, C. D. Hunt, H. Windom, R. Smith, C. S. Wong, P. Berrang, C. Patterson and D. Settle, Mar. Chem., 4 (1976) 389.
18 T. Shigematsu, M. Matsui and O. Fujino, Bunseki Kagaku, 22 (1973) 1162.
19 Y. Yamamoto, T. Kumamaru, T. Kamada, T. Tanaka and M. Kawabe, Nippon Kagaku Kaishi, (1975) 841.
20 P. E. Paus, Fresenius Z. Anal. Chem., 264 (1973) 118.
21 J. J. Albert, D. E. Leyden and T. A. Patterson, Mar. Chem., 4 (1976) 51.
22 A. Sato, T. Oikawa and N. Saitoh, Bunseki Kagaku, 24 (1975) 584.
23 R. A. A. Muzzarelli and R. Rocchetti, Anal. Chim. Acta, 64 (1973) 371; 69 (1974) 35; 70 (1974) 283.
24 W. Lund and B. V. Larsen, Anal. Chim. Acta, 72 (1974) 57.

25 F. O. Jensen, J. Dolezal and F. J. Langmyhr, Anal. Chim. Acta, 72 (1974) 245.
26 G. E. Batley and J. P. Matousek, Anal. Chem., 49 (1977) 2031.
27 E. A. Boyle and J. M. Edmond, Anal. Chim. Acta, 91 (1977) 189.
28 W. Frech and A. Cedergren, Anal. Chim. Acta, 88 (1977) 57.
29 E. J. Czobik and J. P. Matousek, Anal. Chem., 50 (1978) 2.
30 D. J. Churella and T. R. Copeland, Anal. Chem., 50 (1978) 309.
31 R. D. Ediger, G. E. Peterson and J. D. Kerber, At Absorpt. Newsl., 13 (1974) 61.
32 J. M. McArthur, Anal. Chim. Acta, 93 (1977) 77.
33 D. A. Segar and J. G. Gonzalez, At. Absorpt. Newsl., 10 (1971) 94.
34 W. C. Campbell and J. M. Ottaway, Analyst, 102 (1977) 495.
35 G. Lundgren, L. Lundmark and G. Johansson, Anal. Chem., 46 (1974) 1028.
36 R. E. Sturgeon, C. L. Chakrabarti, I. S. Maines and P. C. Bertels, Anal. Chem., 47 (1975) 1240.
37 R. E. Sturgeon, C. L. Chakrabarti and P. C. Bertels, Anal. Chem., 47 (1975) 1250.
38 R. E. Sturgeon and C. L. Chakrabarti, Anal. Chem., 49 (1977) 1100.
39 R. E. Sturgeon, C. L. Chakrabarti and P. C. Bertels, Spectrochim. Acta, Part B, 32 (1977) 257.
40 D. R. Kester, I. W. Duedall, D. N. Conner and R. M. Pytkowicz, Limnol. Oceanogr., 12 (1967) 176.
41 B. V. L'vov, Spectrochim. Acta, Part B, 33 (1978) 153.
42 A. K. Holliday, G. Hughes and S. M. Walker, in J. C. Bailer, Jr., H. J. Emeléus, R. Nyholm and A. F. Trontman-Dickenson, (Eds.), Carbon in Comprehensive Inorganic Chemistry, Vol. 1, Pergamon Press, Oxford, 1973, p. 1211.
43 J. H. Runnels, R. Merryfield and H. B. Fisher, Anal. Chem., 47 (1975) 1258.
44 R. C. Weast (Ed.), CRC Handbook of Chemistry and Physics, 56th edn., 1975—1976, CRC Press, Cleveland, 1975, p. B-115.
45 T. Nakahara and S. Musha, Anal. Chim. Acta, 75 (1975) 305.
46 T. Nakahara and S. Musha, Appl. Spectrosc., 29 (1975) 352.
47 T. Nakahara and S. Musha, Anal. Chim. Acta, 80 (1975) 47.
48 R. E. Sturgeon and C. L. Chakrabarti, Anal. Chem., 49 (1977) 90.
49 E. Schroll, Fresenius Z. Anal. Chem., 198 (1963) 40.
50 P. G. Brewer, in J. P. Riley and G. Skirrow, (Eds.), Chemical Oceanography, 2nd edn., Vol. 1, Academic Press, New York, 1975, pp. 415—496.

Analytica Chimica Acta, 104 (1979) 113—120

ELECTROTHERMAL ATOMIC ABSORPTION SPECTROMETRIC DETERMINATION OF CADMIUM, CHROMIUM AND COBALT IN URANIUM WITHOUT PRELIMINARY SEPARATION

B. M. PATEL, PARU M. BHATT, NEELAM GUPTA, M. M. PAWAR** and B. D. JOSHI*

Radiochemistry Division, Bhabha Atomic Research Centre, Trombay, Bombay 400085 (India)

(Received 28th April 1978)

SUMMARY

An atomic absorption spectrometric method with graphite tube atomization is described for the direct determination of cadmium (0.1—5 ppm), chromium (1—30 ppm) and cobalt (1—30 ppm) in uranium dissolved in nitric acid, with relative standard deviations of 5—10%. The presence of up to 7 mg of residual uranium in the carbon tube and 1000 ppm each of calcium, iron, silicon, tungsten and zinc in the sample did not cause any interference, but sample and standard solutions must contain the same concentrations of uranium.

Electrothermal atomizers have several advantages over conventional flame atomization systems. These include small sample size (0.5--100 μl), higher sensitivity and the capability for directly analysing a variety of liquid and solid samples. These features, coupled with the ease of installation of such an atomizer inside a glovebox for containment of radioactivity, make electrothermal atomic absorption spectrometry (a.a.s.) most attractive for the determination of trace metallic constituents in radioactive samples.

Flame a.a.s. is frequently used for the determination of trace metals in uranium after preliminary chemical separation from the matrix, and, for rapid analysis, similar determinations without prior chemical separation have been reported [1—9]. However, there has been only limited developmental work on the application of electrothermal a.a.s. for direct determination of trace metals in uranium. Buffereau and Robichet [10] have investigated the performance of a King furnace in a.a.s. Of the 27 metals studied in uranium, the detection limits were reported for 20 elements, while the detection of the other 7 elements was limited by the blank. Detailed studies of the influences of the uranium matrix and other elements on the analyte absorbance, and the range and precision of determinations were not reported. Bagliano et al. [11] have evaluated the use of a Perkin-Elmer graphite furnace (HGA-70) atomizer for direct determination of six metals in uranium and reported its suitability for Co, Cr, Fe and Mn. However, they reported that Mo and V cannot be determined by this technique.

**Present address: Asian Paints (India) Pvt. Ltd., Bhandup, Bombay 400078 (India).

The present paper describes the application of a.a.s. with the Varian-Techtron carbon "rod" atomizer (really a small graphite tube) for direct determinations of traces of cadmium, chromium and cobalt in uranium. These elements are directly atomized from a uranyl nitrate solution placed in the atomizer. The influences of uranium, its concentration, its residual build-up in the tube and the effect of other metals on the accuracy and precision of the determinations have been investigated.

EXPERIMENTAL

Apparatus

A carbon "rod" atomizer (Varian-Techtron Model CRA-63) was used in conjunction with a Varian-Techtron AA6 atomic absorption spectrometer. A 10-mV strip-chart recorder (Dynamaster Series 550, Bristol Co.) was used for recording the peak absorbance. The atomizer was enclosed in a PVC—stainless steel semi-rigid chamber with an aperture for loading the sample. This aperture was kept closed by a PVC sheet which could be raised when access to the atomizer was necessary. This chamber was connected to a glove box exhaust system. Containment of radioactivity was ensured through the use of Millipore filters and a good exhaust. No α-activity was detected during checks in the working area or in the air samples in the room.

Varian-Techtron hollow-cathode lamps for cadmium and hydrogen were operated at 3 mA and 25 mA, respectively. For chromium and cobalt, a Varian-Techtron Co-Cr-Cu-Fe-Mn-Ni lamp was operated at 10 mA. Spectral band widths of 0.5, 0.5 and 0.1 nm were used for cadmium, chromium and cobalt, respectively. An Excalibur 5 μl syringe with disposable Teflon tips was used for dispensing solutions.

Reagents

All the reagents used were of analytical grade. Nitric acid and water were distilled twice in a quartz distillation apparatus.

Specpure chemicals (Johnson Matthey, London) were used in the preparation of stock solutions of 2000 μg ml^{-1}, for each of the elements by dissolving appropriate weights of the metal or compound in 3 M nitric acid. Standard solutions were prepared by diluting stock solutions with water. The acid concentration in all the diluted solutions was maintained at 0.1 M with nitric acid.

A weighed amount of high-purity uranium was dissolved in concentrated nitric acid and the solution was evaporated to dryness. A stock solution of uranium (200 mg ml^{-1}) was prepared from this uranyl nitrate residue. From this stock solution two sets of cadmium standards in a 20 mg U ml^{-1} solution were prepared. One contained various concentrations of cadmium in the range 1—100 ng ml^{-1}; the other contained in addition to cadmium, 15 elements (Al, B, Ca, Co, Cr, Cu, Fe, Mg, Mo, Ni, Si, Sn, Ti, V and Zn) each in the concentration range 1—500 ng ml^{-1}. Similar sets of solutions containing chromium and cobalt in the range 0.01—0.6 μg ml^{-1} were also prepared.

Procedure for determination of Cd, Cr and Co in uranium metal or oxide

Uranium metal (200 mg) or U_3O_8 (235.9 mg) was dissolved in concentrated nitric acid and evaporated to dryness. The resulting uranyl nitrate was dissolved in 0.1 M nitric acid, and diluted to exactly 10 ml. The standard solutions, prepared as described above, contained exactly the same amount of uranium.

A 5 μl aliquot of sample or standard solution (see Table 1) was injected into the carbon tube atomizer, and the "dry" "ash" and "atomize" optimal settings given in Table 1 were followed, with 4.5 l min^{-1} argon or nitrogen used to provide an inert atmosphere around the atomizer. At least three atomic absorption measurements were made on each solution. The peak height was measured in each instance. In order to remove the memory effect for Co and Cr, blank atomization at the highest available temperature was necessary. A 10 μl injection of xylene solvent was used each time for pretreating the tube before injecting the sample solution.

RESULTS AND DISCUSSION

Impregnating the carbon tube with xylene prior to loading the sample was found to be advantageous, as reported earlier [12, 13]. The mean of ten measurements for 0.5 ppm and 1 ppm cadmium in uranium solution, after xylene pretreatment of the tube, showed an increase of 15% and 35%, respectively, and were more reproducible than the results obtained without xylene pretreatment, probably because of decreased sample loss arising from penetration in the tube. Xylene impregnation also increased tube life. A carbon tube which could be used only for 80—100 atomization cycles without pretreatment, could be used for nearly 200 atomization cycles with the xylene treatment.

TABLE 1

Optimum experimental conditions and analytical ranges for Cd, Cr and Co for direct atomization from uranium matrix

Element and wavelength (nm)	Carbon "rod" atomizer settings			Linear analytical range		Smallest amount determined (g)	Determination limit reported [10] (g)
	Dry (50 s)	Ash (45 s)	Atomize (3 s)	(μg ml^{-1})	(ppm)[a]		
Cd 228.8	5.5 135°C	8 900°C	7.5 2250°C	0.002—0.1	0.1—5	1×10^{-11}	2×10^{-10}
Cr 425.4	5 120°C	8 900°C	9 2680°C	0.02—0.6	1—30	1×10^{-10}	4×10^{-9}
Co 240.7	6 150°C	8 900°C	9 2680°C	0.02—0.6	1—30	1×10^{-10}	2×10^{-9}

[a]Concentration in uranium sample based on 0.1 mg of uranium in 5 μl of solution.

Effect of uranium matrix

The influence of the uranium in the solution on the atomization behaviour or the analytes was examined. Measurements on solutions containing 20 ng Cd ml^{-1} in 0.1 M nitric acid showed a mean peak absorbance of 1.30, whereas the same concentration of cadmium in a solution containing 20 mg U ml^{-1} showed a mean peak absorbance of only 0.295. This severe suppressive effect is probably due to a reduction in cadmium atomization efficiency. Similar studies with chromium and cobalt also indicated a suppressive interference, though to a lesser extent. It is essential therefore, to have standards matching the uranium content of the sample solutions, in order to analyse uranium samples directly. Non-specific absorbance from uranium was examined with the hydrogen lamp and was found to be insignificant.

Samples of air and wipes of surfaces around the atomizer did not show significant α-activity, suggesting that following the direct atomization of uranium solutions the major proportion of the uranium remained inside the carbon tube. X-ray diffraction studies of a residue from the tube showed it to be a uranium carbide. Recently, Hircq [14] has reported similar results for the residue obtained when uranium samples were atomized from a graphite filament.

Since the same carbon tube is used for many atomization cycles and uranium accumulates in the tube, the effect of uranium build-up in the tube on the absorption signals of cadmium was investigated. Aliquots (5 μl) of solution containing 10, 100 and 500 pg of cadmium and 100 μg of uranium were injected into the tube 70 times in succession and the absorption signals of cadmium were measured after each loading. With a build-up of uranium to 7 mg in the tube, there was no effect on the cadmium absorbance. Similar studies carried out with solutions containing 1 ng each of chromium and cobalt and 100 μg of uranium also showed no effect from up to 7 mg of uranium on the absorbance of these elements.

The influence of uranium concentration on absorption signals was investigated only for cadmium in order to examine the maximum amount of uranium that could be used in the sample solution and the highest relative sensitivity for cadmium determination that could be obtained, as cadmium needs to be determined at lower concentrations than chromium and cobalt. A series of sample solutions was prepared containing 100 pg of cadmium and various amounts (2—1000 μg) of uranium in 5 μl of solution . It was observed that the cadmium absorbance was not affected significantly (<10%) by uranium in the range 20—500 μg/5 μl. However, at lower concentrations the variation in absorption signals was much larger. It is, therefore, possible to obtain determination limits much lower than 0.1 ppm for cadmium by using larger uranium samples.

Effect of other elements

The cadmium absorbance measured on two sets of standard solutions, one having only cadmium and uranium and the other containing cadmium and

15 other elements (Al, B, Ca, Co, Cr, Cu, Fe, Mg, Mo, Ni, Si, Sn, Ti, V and Zn) at trace concentrations in uranium, did not show any significant difference. Further, the slopes of the calibration curves and the range of linearity were the same for the two sets of solutions. Similar studies with chromium and cobalt showed identical behaviour, thereby suggesting the absence of interference from other elements present at trace levels in uranium.

In the uranium used as fast nuclear reactor fuel, the maximum permissible concentrations of some impurities (Ca, Fe, Si, W, Zn, etc.) are much higher than for cadmium. It was, therefore, of interest to examine the effect of such high concentrations of these impurity elements on cadmium, cobalt and chromium absorbances. For the study with cadmium, a set of six uranium solutions was prepared, one of which contained 1 ppm cadmium alone and the other five solutions contained 1 ppm cadmium with 1000 ppm of one of the elements Ca, Fe, Si, W and Zn. The results for ten replicate absorbance measurements of cadmium in these solutions are shown in Fig. 1. The ranges of the values are shown by the horizontal lines and the circles represent the mean absorbance. The percentage changes in the mean absorbance caused by the presence of impurity element are also given. The maximum percentage variation is 8%, which indicates that these elements, even at 1000-fold greater concentrations than cadmium, do not interfere significantly in its determination. Similar studies with 10 ppm cobalt and 20 ppm chromium showed that the difference in the absorption signals was less than 8% in the presence of 1000 ppm of Ca, Fe, Si, W or Zn.

Analytical aspects

The details of optimum experimental conditions, analytical ranges and the

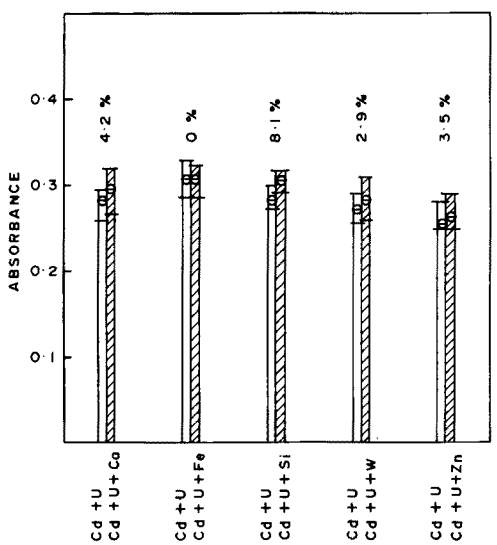

Fig. 1. Influence of 1000 ppm of Ca, Fe, Si, W and Zn on the absorbance of 1 ppm cadmium in uranium solutions.

smallest amounts of cadmium, chromium and cobalt determined directly in the uranium matrix are given in Table 1. These carbon tube temperatures quoted were obtained from the voltage–temperature correlation curves for the CRA-63 supplied by the manufacturers. The smallest amounts determined in this work are lower by factors of 5, 2.5, and 5 for cadmium, chromium, and cobalt, respectively, than those reported previously [10]. Further, comparison of the present results with those obtained by direct atomization of uranium solutions in flames [5] shows that the lowest concentrations determined for cadmium, chromium and cobalt in the present work are better than the reported values by factors of 20, 5, and 5, respectively.

The precision was determined for the three analytes at different concentrations in standard solutions. The results are shown in Table 2, and indicate that the relative standard deviations calculated from 15 peak absorbance measurements are 5—10%. This range is comparable to that previously reported for the carbon rod and furnace atomizers [13, 15].

Spiked sample solutions were prepared for the three analyte elements following dissolution of uranium metal. Results of the analysis of these samples are shown in Table 3, based on 5—10 replicate measurements, for each solution. The concentrations of the analytes determined in these samples are in very good agreement with the spike concentrations added to the uranium.

CONCLUSIONS

The a.a.s. technique with the carbon tube atomizer is shown to be suitable for the determination of traces of cadmium, chromium and cobalt by direct atomization of uranium samples. As no chemical separation is required, the

TABLE 2

Precision of absorbance measurements for cadmium, chromium and cobalt in uranium solutions

Analyte	Concentration ($\mu g\ ml^{-1}$)	Peak absorbance	Standard deviation	Relative standard deviation[a] (%)
Cd	0.002	0.058	0.004	7.5
	0.02	0.290	0.018	6.3
Cr	0.02	0.066	0.004	6.0
	0.10	0.146	0.011	7.5
	0.20	0.218	0.013	6.2
	0.40	0.386	0.022	5.7
Co	0.075	0.066	0.006	10.5
	0.10	0.084	0.005	6.3
	0.20	0.213	0.011	5.2

[a]Calculated from 15 replicate measurements.

TABLE 3

Results of direct determination of cadmium, chromium and cobalt in spiked uranium samples

Element	Concentration of spike			
	Added		Measured	
	(μg ml^{-1})	(ppm)[a]	(μg ml^{-1})	(ppm)[a]
Cd	0.004	0.2	0.0042	0.21
	0.005	0.25	0.0052	0.26
	0.020	1.0	0.019	0.95
	0.040	2.0	0.042	2.1
Cr	0.15	7.5	0.146	7.3
	0.30	15	0.32	16
	0.50	25	0.50	26
Co	0.10	5.0	0.102	5.1
	0.15	7.5	0.156	7.8
	0.25	12.5	0.240	12.0

[a]In uranium sample, giving solution 20 mg U ml^{-1}.

analysis is rapid and the risk of contaminating the sample is considerably reduced. Determinations of these analyte elements at the ng and sub-ng level are possible in the presence of a million-fold amount of uranium and large amounts of five common contaminating elements. However, it is necessary to have standards and sample solutions with approximately the same concentrations of uranium, because of the suppressive effect of uranium on the atomization of the metals under investigation.

The authors are grateful to Dr. M. V. Ramaniah, Head, Radiochemistry Division, for his keen interest and constant encouragement during the progress of this work.

REFERENCES

1 R. L. Graff and H. R. Mullin, Xth Conference on Analytical Chemistry in Nuclear Technology, Gatlinburg, Tenn., U.S.A., 1966.
2 R. Sassoulas and J. Serpinet, Spectrochim. Acta, Part B, 23 (1968) 227.
3 G. Baudin, J. Normand and J. Figalkowski, Spectrochim. Acta, Part B, 23 (1968) 587.
4 J. M. Scarborough, Anal. Chem., 41 (1969) 250.
5 M. Buffereau and J. Robichet, Rept. CEA-R- 3870 (1969).
6 R. D. Gardner, A. L. Henicksman and W. H. Ashley, USAEC Rept. LA-5232 (1973).
7 R. K. Dhumwad, V. T. Kulkarni and A. B. Patwardhan, Rept. BARC-767 (1974).
8 O. O. Guido and C. Amaya, Rept. CNEA-392 (1975).
9 C. R. Walker and O. A. Vita, Anal. Chim. Acta, 43 (1968) 27.
10 M. Buffereau and J. Robichet, Methodes Phys. Anal. (GAMS), 7 (1971) 138.
11 G. Bagliano, F. Benischek and I. Huber, At. Absorpt. Newsl., 14 (1975) 45.

12 J. P. Matousek, Am. Lab., June (1971) 45.
13 M. D. Amos, P. A. Bennett, K. G. Brodie, P. W. Y. Lung and J. P. Matousek, Anal. Chem., 43 (1971) 211.
14 B. Hircq, Spectrochim. Acta, Part B, 31 (1976) 153.
15 B. V. L'vov, Atomic Absorption Spectrochemical Analysis, translated by J. H. Dixon, A. Hilger, London, 1970.

Analytica Chimica Acta, 104 (1979) 121—127

SIMULTANEOUS DETERMINATION OF URANIUM AND THORIUM IN ORES BY INSTRUMENTAL EPITHERMAL NEUTRON ACTIVATION ANALYSIS

ERNEST S. GLADNEY*, JAMES W. OWENS and JOHN W. STARNER

University of California, Los Alamos Scientific Laboratory, P.O. Box 1663, Los Alamos, New Mexico 87545 (U.S.A.)

(Received 5th July 1978)

SUMMARY

Rapid scanning of numerous rock samples when prospecting for uranium and thorium ores can be facilitated by using the shorter-lived nuclides. The samples are activated during short epithermal neutron irradiations and the 20-min activities of ^{239}U and ^{233}Th are observed instrumentally with a small Ge(Li) detector. The detection limits for uranium and thorium are less than 1 ppm and 20 ppm, respectively.

With the current wide-ranging search for fissionable materials, analyses for uranium and thorium have become a commonplace demand. With the numbers of samples in the thousands, many accurate and precise techniques are falling into disuse because they require time-consuming chemical treatment of the sample (e.g., dissolution). Instrumental methods have come to the forefront because only minimal physical sample preparation is required (e.g., grinding).

Thermal and epithermal neutron activation analyses have become primary methods for analyzing large numbers of samples instrumentally. Uranium may be determined by delayed neutron analysis after a short (10—100 sec) thermal neutron bombardment [1, 2].

Neutrons emitted from neutron-rich fission products are counted with special neutron detectors made of boron or helium-3. This technique can only be employed for elements which fission in thermal, epithermal or fast neutron fluxes. Detection limits well below average crustal abundance of uranium can be easily achieved. Uranium may also be measured through fission-product counting after a thermal neutron irradiation (e.g., ^{131}I) [3] but this method lacks the sensitivity of delayed neutron assay. It may also be determined by counting ^{239}Np, a secondary activation product, after an epithermal neutron irradiation [4—8]. This nuclide is produced by the reaction $^{238}U(n,\gamma)\ ^{239}U(\beta^-)\ ^{239}Np$. Since ^{239}Np has a 2.35-d half-life, decay for several days after the irradiation is required to maximize the sensitivity. Optimum detection limits approach crustal abundance.

Protactinium-233, a secondary activation product produced during "long" thermal neutron irradiations (30 min or more), is commonly used to measure

thorium concentrations [9] via the reaction $^{232}Th(n,\gamma)\ ^{233}Th(\beta^-)\ ^{233}Pa$. The ^{233}Pa half-life is 27 days, so that a substantial decay time (two weeks or more) must be allowed after the irradiation to improve sensitivity through decay of shorter-lived activation products. The detection limits range down to about 1 ppm, well below average crustal abundance. The same reaction and counting scheme may also be used with epithermal neutrons , but the ultimate detection limit is not as good, because epithermal neutron fluxes are generally lower than thermal fluxes [7].

Thorium may also be measured by delayed neutron assay, but the procedure is more complicated than in the case of uranium. The uranium must first be determined in a thermal irradiation and then thorium plus uranium may be measured by using an epithermal irradiation. Thorium is then determined by difference [10, 11]. The presence of other fissionable isotopes (^{239}Pu) or anomalous isotopic uranium ratios, such as can be found in contaminated soils [8], can introduce large errors into this procedure.

This paper reports an evaluation of the possibilities of direct observation of the short-lived ^{239}U and ^{233}Th isotopes, simultaneously; these isotopes have half-lives of 23.5 min and 22.1 min, respectively. The isotopes are produced simultaneously during an epithermal neutron bombardment by the nuclear reactions $^{238}U(n,\gamma)\ ^{239}U$ and $^{232}Th\ (n,\gamma)\ ^{233}Th$.

The production rate is favoured by a factor of 20—50 over that of the most common activation products (Na, Mg, Al, P, Cl, K, V, Mn) in epithermal rather than thermal neutrons [7], so that these short-lived isotopes of uranium and thorium may be more easily observed. Another potential advantage is the rapid sample turn-round which can be achieved with short-lived activities. The determination of uranium by the short-lived approach has been reported [12—15].

EXPERIMENTAL

Samples (1g) of the standard reference ores were irradiated for 1—5 min each in the Los Alamos Omega West Reactor epithermal neutron facility. This irradiation port is equipped with a pneumatic transfer capability so that isotopes with half-lives of seconds may be studied. The end of the epithermal tube is surrounded by a 50:50 (v/v) mixture of powdered elemental boron and aluminum, hot pressed into a cylindrical sleeve (30 cm long, wall thickness 2.5 cm). This shield provides enough boron (ca. 2.3 g cm^{-2}) to give an estimated lower-energy filter cutoff of about 280 eV, and should provide essentially total absorption of thermal neutrons. Therefore, cadmium covers are not required in this facility. The epithermal flux is about 2×10^{12} n $cm^{-2}s^{-1}$ [1

The standard used was a solution of National Bureau of Standards Standard Reference Material 950a (U_3O_8) and high-purity ThO_2.

Samples were permitted to decay for 10 min after irradiation and were then counted for 5—10 min on a low-energy photon spectrometer; a 0.4-cm^3 Ge(Li) crystal with a resolution (FWHM) of 243 eV at 5.9 keV and 508 eV at 122

keV. The 74.66-keV line of ^{239}U and the 86.9-keV line of ^{233}Th were used [17]. The dead time was kept at less than 10% in all cases, by counting the samples at a distance of 30 cm from the detector. Spectra were accumulated in 1024-channel sections of a 4096-channel pulse-height analyzer and were stored on magnetic tape for off-line reduction.

RESULTS AND DISCUSSION

First, the uranium content of the 16 standard reference materials was examined by two other nuclear activation techniques. Most of the data on which the certifications of these materials are based are from non-nuclear techniques, and it seemed advisable to check the quality of the data. Uranium determinations by epithermal neutron activation based on the ^{239}Np daughter product [8], and by delayed neutron assay [2] are presented in Table 1. Two NBS standards (NBS SRM 950a and 1633) were employed in the delayed neutron measurements, while only NBS SRM 950a was used in the epithermal neutron activation. For ease of interpretation, the present results for uranium and thorium on the standard materials were normalized to the certified or informational concentrations for each material; a value of unity indicates agreement of the value determined here with the certified result, and the standard deviation amongst the normalized values is a measure of the precision of the method. As the means of the ratios of the present values to the certified values for uranium indicate, agreement with the certified values is excellent. The means are very close to 1.00 and the standard deviations amongst the three data sets are small.

Results for uranium determined by epithermal neutron irradiation and counting of the 74.66-keV γ-ray from ^{239}U decay are given in Table 2 along with the certified values. The mean ratio of the present values to the certified uranium contents is 1.00 ± 0.07, which demonstrates surprisingly good accuracy and precision for this rapid assay method. The detection limit (3 standard deviations above background) for this instrumental procedure is less than 1 ppm in silicate materials with the irradiation and counting scheme described above.

The detection limit for thorium is not nearly as low as that for uranium. The thorium measurements based on observation of the 86.9-keV line are shown in Table 3. For the ores with thorium concentrations greater than 40 ppm, this rapid epithermal neutron assay technique successfully reproduced the informational results. For the samples with thorium concentrations significantly greater than crustal abundance (SY-2, SY-3, DH-1, DL-1), the mean ratio of the epithermal data to the informational values is 0.97 ± 0.04, exhibiting satisfactory agreement and good precision. The detection limit ranges from 8 to 20 ppm. This limit is strongly influenced by the uranium content, because ^{239}U has a weak γ-ray at 86.72 keV [17], which is unresolved from the thorium line. The relative intensities of the 74.66- and 86.72-keV γ-rays are 100 : 0.12 [17] and the relative efficiency at these energies of the

TABLE 1

Uranium concentrations (ppm) in standard materials by several techniques with the ratio of the result obtained in the present work to the certified value

Sample	Certified value	Epithermal neutrons (NBS U_3O_8 Std.)	Ratio	Delayed neutrons (NBS U_3O_8 Std.)	Ratio	Delayed neutrons (NBS Fly ash Std.)	Ratio
CRM[a]							
SY-2	254[d]	254 ± 10	1.00	290 ± 30	1.14	300 ± 16	1.18
SY-3	678[d]	547 ± 10	0.81	670 ± 20	0.99	701 ± 55	1.03
MRG	none	<1	—	0.28 ± 0.02	—	0.27 ± 0.02	—
BL-1	220	213 ± 12	0.97	242 ± 9	1.10	222 ± 3	1.01
BL-2	4530	4200 ± 280	0.93	4870 ± 110	1.08	4340 ± 50	0.96
BL-3	10200	9600 ± 220	0.94	10820 ± 100	1.06	9640 ± 80	0.95
BL-4	1730	1700 ± 15	0.98	1800 ± 100	1.04	1700 ± 100	0.98
DH-1	1770	1650 ± 50	0.93	1815 ± 35	1.03	1700 ± 100	0.96
DL-1	41	43 ± 4	1.05	41 ± 2	1.00	41 ± 2	1.00
IAEA[b]							
S-2	2650	2920 ± 150	1.10	2599 ± 110	0.98	2510 ± 60	0.95
S-3	3540	3700 ± 160	1.04	3450 ± 20	0.97	3440 ± 25	0.97
S-4	3180	3300 ± 30	1.05	3130 ± 10	0.98	3100 ± 20	0.97
JEN[c]							
25	1190	1230 ± 100	1.03	1230 ± 100	1.03	1280 ± 100	1.08
33	4470	4440 ± 200	0.99	4700 ± 300	1.05	5100 ± 230	1.14
463	339	330 ± 12	0.97	326 ± 20	0.99	345 ± 30	1.02
467	119	137 ± 20	1.15	124 ± 10	1.04	124 ± 5	1.04
$\bar{x} \pm \sigma$			1.00 ± 0.08		1.03 ± 0.05		1.02 ± 0.07

[a]Canadian Certified Reference Materials Project, Radiometric Reference Material [18, 19]. [b]International Atomic Energy Agency — Reference Low Grade Ores. [c]Junta de Energia Nuclear, Madrid; prepared for IAEA. [d]Informational value only, not certified [18].

TABLE 2

Uranium concentrations in standard materials by epithermal activation and LEPS counting (ppm)

Sample	This work	Certified	Ratio	Sample	This work	Certified	Ratio
CRM				IAEA			
SY-2	291 ± 30	254[a]	1.15	S-2	2650 ± 20	2650	1.00
SY-2	617 ± 30	678[a]	0.91	S-3	3440 ± 170	3540	0.97
MRG	<1	—	—	S-4	3230 ± 60	3180	1.07
BL-1	226 ± 7	220	1.03				
BL-2	4510 ± 200	4530	1.00	JEN			
BL-3	10200	10200	1.00	25	1150 ± 80	1190	0.97
BL-4	1730 ± 40	1730	1.00	33	4190 ± 200	4470	0.94
DH-1	1800 ± 140	1770	1.02	463	302 ± 8	339	0.89
DL-1	41 ± 2	41	1.00	467	129 ± 11	119	1.08
					$\bar{x} \pm \sigma$		1.00 ± 0.07

[a]Informational value only, not certified.

TABLE 3

Thorium concentrations in standard materials (ppm)

Sample	This work via ^{233}Th	Informational value[a]	This work via ^{233}Pa	Sample	This work via ^{233}Th	Informational value[a]	This work via ^{233}Pa
CRM				IAEA			
SY-2	353 ± 30	350	340 ± 10	S-2	27 ± 19	—	15 ± 2
SY-3	964 ± 75	968	978 ± 50	S-3	<12	—	4.1 ± 1.1
MRG	<13	—	0.9 ± 0.2	S-4	<15	—	4.0 ± 0.4
BL-1	<21	15	11 ± 1				
BL-2	<20	16	12 ± 1	JEN			
BL-3	<20	15	19 ± 4	25	<8	—	7.7 ± 1.1
BL-4	<20	14	12 ± 2	33	<10	—	2.8 ± 0.4
DH-1	1010 ± 61	1040	1080 ± 120	463	<8	—	6.7 ± 2.3
DL-1	76 ± 19	83	86 ± 6	467	<8	—	7.3 ± 0.5

[a]Canadian Certified Reference Materials Project, Radiometric Reference Material [18, 19].

detector which was used was 12.5 : 11.1. The thorium data in Table 3 have been corrected for this uranium contribution. For a U/Th ratio of 20, a 50% correction to the thorium data is required.

Since the thorium data were not "certified", all samples were recounted on a large Ge(Li) detector after decay for 2—4 weeks to determine thorium through its ^{233}Pa daughter product. The intense γ-ray at 311.9 keV was used, although detection limits were affected by the 316.2-keV line from ^{239}Np ($t_{1/2}$ = 2.35d). Longer decay periods favor the measurement of ^{233}Pa, as interference from the 316-keV γ-ray is reduced.

When the low-energy region is used it is vital to be extremely careful in assessing potentially overlapping lines, both x-ray and γ-ray. Table 4 contains information about x-ray energies in this region. Data are not given when the energy is clearly above or below the region of interest. The K_α x-rays from lead and bismuth might interfere with the uranium measurement, while their K_β lines lie close to the ^{233}Th γ-ray. All lead shielding was removed from the immediate area of the detector to eliminate this source of interference, and the abundance of lead and bismuth is so low in the samples that they do not present a problem from self-fluorescence. Furthermore, the half-lives of neutron capture products of lead are short and those of bismuth are long, which further excludes these elements as contributors to the γ-peaks of interest. The x-rays from U, Th and their immediate decay products are all higher in energy than the gamma-rays used in this study.

Table 5 lists γ-emitters which have energies near those of the uranium and thorium lines. All of these may be eliminated as a source of concern through either low abundance, low production rate, long half-life or low branching ratio. Some difficulty with interference from ^{153}Sm has been encountered in the analysis of non-ore materials such as NBS Standard Reference Materials 1632 and 1633 (Coal and Fly Ash) for uranium.

TABLE 4

X-ray energies (keV) of potentially interferent nuclides [20]

Element	K_{α_2}	K_{α_1}	K_{β_1}	K_{β_2}
Ir	—	—	—	75.6
Pt	—	—	75.7	77.8
Au	—	—	77.9	80.1
Hg	—	—	80.2	82.5
Tl	—	—	82.5	84.9
Pb	—	74.97	84.8	87.3
Bi	74.8	77.1	87.2	89.2
Ra	85.4	88.5	—	—
Th	89.96	—	—	—
Pa	92.3	—	—	—
U	94.7	—	—	—
Np	97.1	—	—	—

TABLE 5

γ-ray energies of potentially interferent nuclides [20]

Nuclide	Energy (keV)	Branching ratio (%)
^{233}Pa	75.3	0.7
^{153}Sm	75.4	0.6
^{233}Pa	86.6	1.9
^{160}Tb	86.8	21
^{77}As	87.7	5

Attenuation and self-absorption are also problems frequently encountered when low-energy γ-rays are used for analyses. The data given here show that there was a good match between samples and standards, as little divergence from the certified values was seen. Since the method presented in this paper is largely intended to be a screening technique, small differences in γ-ray absorption arising from variations in the rock matrix should not be of importance. Promising samples could be reanalyzed by more precise nuclear methods.

We thank the staff of the Omega West Reactor for their assistance with the irradiations. This work was performed under the auspices of the U.S. Department of Energy.

REFERENCES

1 A. Amiel, Anal. Chem., 34 (1962) 1683.
2 W. K. Hensley and M. M. Minor, Presented at 20th Annual Conference of Analytical Chemistry in Energy and Environmental Technology, Gatlinburg, Tennessee, 13 Oct. 1976.
3 E. S. Gladney and H. L. Rook, Anal. Chem., 47 (1975) 1554.
4 H. A. Mahlman and G. W. Leddicotte, Anal. Chem., 27 (1955) 823.
5 H. Hamaguchi, G. W. Reed and A. Turkevich, Geochim. Cosmochim. Acta, 12 (1957) 337.
6 J. W. Morgan and J. F. Lovering, Anal. Chim. Acta, 28 (1963) 405.
7 E. Steinnes, in O. Brunfelt and E. Steinnes (Eds.), Activation Analysis in Geochemistry and Cosmochemistry, Universitets forlaget, Oslo, 1971, pp. 113—128.
8 E. S. Gladney, W. K. Hensley and M. M. Minor, Anal. Chem., 50 (1978) 652.
9 R. Dams, J. A. Robbins, K. A. Rahn and J. W. Winchester, Anal. Chem., 42 (1970) 861.
10 H. T. Millard, Jr., in F. J. Flanagen (Ed.), Descriptions and Analyses of Eight New USGS Rock Standards, USGS Professional Paper 840, 1976.
11 N. H. Gale, Proceedings of Radioactive Dating and Methods of Low Level Counting, IAEA, Vienna, 1967, pp. 431—452.
12 V. C. Turkowski, H. Stark and H. J. Born, Radiochim. Acta, 8 (1967) 27.
13 E. Steinnes and D. Brune, Talanta, 16 (1969) 1326.
14 E. Steinnes and J. J. Rowe, Anal. Chim. Acta, 87 (1976) 451.
15 E. S. Gladney, J. W. Owens and J. W. Starner, Anal. Chem., 48 (1976) 973.
16 A. Lyle, Omega West Reactor, Los Alamos Scientific Laboratory, private communication, 1978.
17 R. L. Heath, Gamma-Ray Spectrum Catalog, Aerojet Nuclear Company, ANCR-1000-2, 3rd. edn., Vol. 2, 1974, p. 92—239—1.
18 S. Abbey, SY-2, SY-3 and MRG-1: Report on the Collaborative Analysis of Three Canadian Rock Samples for use as Certified Reference Materials, Geological Survey of Canada, Ottawa, CANMET Report 76—36, Nov. 1976.
19 J. C. Ingles, R. Sutarno, W. S. Bowman and G. H. Faye, Radioactive Ores DH-1, DL-1, BL-1, BL-2, BL-3 and BL-4: Certified Reference Materials, Geological Survey of Canada, Ottawa, CANMET Report 77-Preliminary, 1977.
20 C. M. Lederer, J. M. Hollander and I. Perlman, Table of Isotopes, Wiley, New York, 6th edn., 1967.

Analytica Chimica Acta, 104 (1979) 129—138

REACTIONS (γ, xn) ET (γ, p) SUR Rh, Pd, Ag, Ir, Pt ET Au ENTRE 25 ET 50 MeV ET APPLICATION A L'ANALYSE DE RESIDUS RICHES EN METAUX PRECIEUX

PH. BREBAN, G. BLONDIAUX, M. VALLADON, A. GIOVAGNOLI et J. L. DEBRUN*

Centre National de la Recherche Scientifique, Service du Cyclotron Groupe "Application des Réactions Nucléaires à l'Analyse Chimique", 45045 Orleans Cedex (France)

M. DEVAUX et S. MICHEL

Comptoir Lyon-Alemand-Louyot, 13, rue de Montmorency, 75139 Paris (France)

(Reçu le 14 juin 1978)

RESUME

Les sensibilités et les interférences ont été étudiées entre 25 et 50 MeV pour les réactions (γ, xn) et (γ, p) sur Rh, Pd, Ag, Ir, Pt et Au. L'activation photonique à 35 MeV peut être utilisée pour le dosage précis de Au, Pt, Ir et Rh dans les "noirs" (résidus riches en métaux précieux), et pour le dosage de Ag et de Pd. Cette méthode exige beaucoup de temps du fait de l'attente de la décroissance de certains radioisotopes, mais elle exige très peu de main-d'oeuvre; elle présente l'avantage de ne nécessiter ni dissolution de l'échantillon ni séparations chimiques, ce qui évite les pertes.

SUMMARY

The (γ, xn) and (γ, p) reactions on Rh, Pd, Ag, Ir, Pt and Au between 25 and 50 MeV — Application to the analysis of residues rich in noble metals.

The sensitivities and interferences for the (γ, xn) and (γ, p) reactions for 25—50 MeV irradiation on Rh, Pd, Ag, Ir, Pt and Au are reported. Photon activation at 35 MeV can be used for the precise determination of Au, Pt, Ir and Rh in residues rich in precious metals (black concentrates), as well as for the estimation of Ag and Pd. The method is time-consuming because of the need to allow some radio-isotopes to decay, but little working time is involved. The procedure is non-destructive, so that losses are avoided.

Les "noirs" sont des résidus très riches en métaux précieux (Tableau 1). Par ailleurs, ces résidus sont très difficiles à solubiliser: il faut utiliser un mélange chlore—HCl sous très forte pression et à haute température, et même dans ces conditions, il faut plusieurs heures. Après solubilisation, il faut encore effectuer la séparation chimique des divers métaux précieux entre eux. Des analyses précises par des méthodes physiques (fluorescence-x, par exemple) qui ne nécessitent pas une mise en solution, ne sont pas possibles en raison de la complexité des échantillons et en raison de leur composition extrêmement variable. Il est donc évident que l'analyse des noirs est très délicate; il n'éxiste

TABLEAU 1

Composition des "noirs"

Element	Fe	Ni	Cu	Pb	Ba	Rh	Pd	Ag	Ir	Pt	Au
Teneur (%)	5	10	10	5	1	20—60	5—20	2—8	10—20	5—20	0,1—0,8

qu'une méthode d'analyse, d'ailleurs pratiquée par très peu de laboratoires, et toute méthode nouvelle est la bienvenue.

Nous nous sommes proposés de déterminer si la radioactivation pouvait être cette nouvelle méthode. La radioactivation neutronique a été écartée car il ne nous semblait pas possible d'obtenir une bonne précision, étant donné que certains métaux précieux ont de très fortes sections efficaces d'absorption des neutrons. Cette absorption conduit à une activation que n'est pas uniforme, ce dont il est très difficile de tenir compte avec précision, surtout dans le cas de matrices complexes et variables. La radioactivation au moyen de particules chargées ne peut pas non plus être retenue car le pouvoir d'arrêt des particules dans l'échantillon doit être connu d'avance, ce qui n'est pas le cas pour les noirs.

La méthode consistant à activer au moyen de photons de haute énergie nous a semblé la technique d'activation la mieux adaptée à l'analyse des noirs. En effet, il n'y a pas de problèmes de distorsion de flux et peu de problèmes d'étalonnage; en outre, Ag, Pd, Pt, Au, Ir et Rh semblaient pouvoir être analysés sans séparations chimiques, par simple spectrométrie-γ. Engelmann [1] avait d'ailleurs montré la possibilité de l'utilisation des photons de haute énergie dans l'industrie des métaux précieux. Le problème des interférences de raies-γ et des interférences nucléaires était à étudier; il restait également à étudier la méthodologie analytique.

PARTIE EXPERIMENTALE

Préparation des échantillons

Les échantillons se présentent sous la forme de pastilles de 1 mm d'épaisseur et 10 mm de diamètre. Celles-ci sont constituées de 20 mg de noir mélangés sous pression à 80 mg de cellulose. Ces faibles quantités permettent de négliger une éventuelle différence d'absorption des raies-γ émises lors du comptage, pour des noirs de compositions différentes.

Dispositifs d'irradiation et de transfert, et spectrométrie-γ

Nous avons utilisé l'accélérateur linéaire d'électrons AL60 du CEN de Saclay. La description complète du système d'irradiation, du système de refroidissement et du transfert d'échantillons est donnée par Engelmann [2]. Les conditions expérimentales que nous avons employées pour les dosages étaient: energie des électrons, 35 MeV; intensité du courant moyen, 66 μA.

Deux détecteurs ont été utilisés. Pour le dosage du palladium, notre choix s'est porté sur un détecteur Ge(Li) coaxial dont les caractéristiques sont:

resolution, 2,3 keV à 1332,5 keV (^{60}Co); efficacité (relative à un détecteur NaI(Tl) 75 mm × 75 mm), 19,9% pour la raie à 1332,5 keV (^{60}Co). Pour le dosage des autres éléments, nous avons utilisé un détecteur Ge(Li) coaxial (33 × 12,5 mm) de haute résolution [0,8—122 keV (^{57}Co) et 1,83—1332,5 keV (^{60}Co)], efficacité relative à un detecteur NaI(Tl): 1% pour la raíe à 1332,5 keV de ^{60}Co. Ces détecteurs sont reliés à un analyseur 4000-canaux interfacé à un ordinateur PDP 11/05. Le traitement des spectres-γ se fait automatiquement soit directement, soit après stockage sur disque RK05.

Etalonnage

Les étalons sont des feuilles minces de métaux purs, se présentant sous forme de disques de même diamètre que les échantillons. Pour l'irradiation, l'échantillon est placé en "sandwich" entre deux séries identiques d'étalons. Nous avons également effectué des expériences en utilisant comme référence des noirs dont la composition était préalablement déterminée en étalonnant à l'aide des feuilles minces.

RESULTATS ET DISCUSSION

Problèmes posés par les possibilités d'interférences

Les spectres-γ obtenus sont complexes. En effet, à 35 MeV, nous avons observé les réactions suivantes: (γ, γ'), (γ, n), $(\gamma, 2n)$, $(\gamma, 3n)$, (γ, p). Par contre, bien que leur seuil théorique soit atteint, les réactions (γ, np) n'ont jamais été décelées. Une étude préliminaire nous a confirmé l'impossibilité d'utiliser certaines raies-γ pour le dosage soit à cause de la faible activité spécifique des radioisotopes correspondants, soit à cause de l'existence d'interférences importantes. Ceci nous a amenés à sélectionner un certain nombre de raies-γ, qui ont ensuite été utilisées pour les dosages. Ces raies-γ ainsi que les isotopes correspondants sont présentés dans le Tableau 2. Il existe, pour ces radioisotopes, des réactions concurrentes ainsi que des interférences. Nous allons examiner successivement leurs effets sur le dosage de ces six éléments.

TABLEAU 2

Réactions, radioisotopes et raies utilisés pour les dosages

Elément	Réaction utilisée	Radio-isotope	Période	Raie-γ utilisée (keV)
Rh	^{103}Rh (γ,n) ^{102}Rh	^{102}Rh	206 j	475
	^{103}Rh (γ,n) ^{102m}Rh	^{102m}Rh	2,89 a	475
Pd	^{102}Pd (γ,n) ^{101}Pd	^{101}Pd	8,5 h	1289
Ag	^{107}Ag $(\gamma,2n)$ ^{105}Ag	^{105}Ag	40 j	280,3
Ir	^{191}Ir (γ,n) ^{190}Ir	^{190}Ir	11 j	186,7
Pt	^{196}Pt (γ,n) ^{195m}Pt	^{195m}Pt	4,1 j	98,86
	^{195}Pt (γ,γ') ^{195m}Pt	^{195m}Pt	4,1 j	98,86
Au	^{197}Au (γ,n) ^{196}Au	^{196}Au	6,183 j	355,72

Dosage de l'or. Le dosage s'effectue sur la raie-γ à 355,72 keV de ^{196}Au de période 6,183 j. Les diverses possibilités d'interférences sont rassemblées dans le Tableau 3. Un temps de décroissance de 8 jours permet d'éliminer toutes les interférences de radioisotopes de courtes périodes. Dans ces conditions, le nombre d'impulsions dû aux autres éléments est inférieur a 0,01% du nombre d'impulsions enregistré dans le pic à 355,72 keV.

Dosage de l'argent. Le dosage s'effectue sur la raie-γ à 280,3 keV de ^{105}Ag ($t_{\frac{1}{2}}$ = 40 j). Les diverses possibilités d'interférences sont rassemblées dans le Tableau 4. La seule interférence gênante est celle dûe au plomb: ^{204}Pb (γ, n) ^{203} Pb. La période de ^{203}Pb étant de 52,1 h, nous avons choisi un temps de décroissance minimum égal à 20 j. Dans ces conditions, l'erreur introduite par les interférences est inférieure à 0,2%, pour des teneurs habituelles en argent (2—8%).

Dosage de l'iridium. Le dosage d'effectue sur la raie-γ à 186,7 keV de ^{190}Ir ($t_{\frac{1}{2}}$ = 11 j). Les diverses possibilités d'interférences sont rassemblées dans le Tableau 5. Après un temps de décroissance de 20 j, il n'existe plus d'interférences décelables. La période de ^{190}Ir étant égale à 11 j, ce temps de décroissance diminue la sensibilité du dosage d'un facteur 4 seulement.

Dosage du platine. Le dosage s'effectue sur la raie-γ à 98,8 keV de ^{195m}Pt ($t_{\frac{1}{2}}$ = 4,1 j). Les interférences possibles sont rassemblées dans le Tableau 6. Le dosage du platine se fait 3 j après la fin de l'irradiation. Il ne subsiste plus alors qu'une seule interférence mesurable: celle de ^{195}Au ($t_{\frac{1}{2}}$ = 183 j). L'activité de ^{195m}Pt est obtenue par soustraction du nombre d'impulsions dû à l'isotope ^{195}Au.

Dosage du rhodium. Ce dosage est effectué sur la raie à 475 keV provenant des deux réactions: ^{103}Rh (γ, n) ^{102}Rh et ^{103}Rh(γ, n) ^{102m}Rh. Les deux radioisotopes formés ont comme période, respectivement, 206 j et 2,89 ans. Les interférences possibles sont rassemblées dans le Tableau 7.

TABLEAU 3

Interférences pour le dosage de Au

Isotope	Période	γ(keV)	Abondance[a]	Réaction
^{189}Pt	11 h	352,63	0,096	^{190}Pt (γ,n) ^{189}Pt
^{191}Pt	3 j	351,17	3,3	^{192}Pt (γ,n) ^{191}Pt
^{191}Pt	3 j	359,88	5,89	^{192}Pt (γ,n) ^{191}Pt
^{195m}Ir	3,8 h	356,38	1,9	^{196}Pt (γ,p) ^{195m}Ir
^{195m}Ir	3,8 h	359,35	4,8	^{196}Pt (γ,p) ^{195m}Ir
^{190}Ir[b]	11 j	361,2	10,83	^{191}Ir (γ,n) ^{190}Ir
^{188}Ir	41 h	350	0,25	^{191}Ir (γ,3n) ^{188}Ir
^{101}Pd	8,3 h	355,14	0,24	^{102}Pd (γ,n) ^{101}Pd
^{103}Pd	17 j	357,6	0,037	^{104}Pd (γ,n) ^{103}Pd
^{103}Pd	17 j	357,6	0,037	^{105}Pd (γ,2n) ^{103}Pd
^{133}Ba	10,7 a	355,86	67	^{134}Ba (γ,n) ^{133}Ba
^{57}Co	270 j	352,4	0,0028	^{58}Ni (γ,p) ^{57}Co

[a]Nombre de γ émis pour 100 désintégrations [3]. [b]Les raies à 355,72 et 361,2 keV sont complètement différenciées grâce au Ge(Li) de haute résolution.

TABLEAU 4

Interférences pour le dosage de Ag

Isotope	Période	γ(keV)	Abondance	Réaction
^{106m}Ag	8,5 j	282	0,47	^{107}Ag (γ,n) ^{106m}Ag
^{196m}Au	9,7 h	285,45	3,8	^{197}Au (γ,n) ^{196m}Au
^{190}Ir	11 j	282,9	0,25	^{191}Ir (γ,n) ^{190}Ir
^{189}Ir	13,3 j	275,7	0,6	^{191}Ir (γ,2n) ^{189}Ir
^{192}Ir	74,2 j	281,5	0,1	^{193}Ir (γ,n) ^{192}Ir
		283,4	0,35	
^{105}Rh	35,88 h	280,54	0,18	^{106}Pd (γ,p) ^{105}Rh
^{189}Pt	11 h	284,58	0,096	^{190}Pt (γ,n) ^{189}Pt
^{188}Pt	10,3 j	280,5	0,3	^{190}Pt (γ,2n) ^{188}Pt
		283	0,2	
^{189}Ir	13,3 j	275,7	0,6	^{190}Pt (γ,p) ^{189}Ir
^{195m}Ir	3,8 h	277	0,04	^{196}Pt (γ,p) ^{195m}Ir
		283	0,06	
^{197m}Pt	86 mn	278,9	2,3	^{198}Pt (γ,n) ^{197m}Pt
^{133m}Ba	38,9 h	275,9	17	^{134}Ba (γ,n) ^{133m}Ba
^{129}Cs	32,3 h	278	1,4	^{130}Ba (γ,p) ^{129}Cs
		282,6	0,26	
^{203}Pb	52,1 h	279,18	80,8	^{204}Pb (γ,n) ^{203}Pb

TABLEAU 5

Interférences pour le dosage de Ir

Isotope	Période	γ(keV)	Abondance	Réaction
^{190n}Ir	3,2 h	186,7	62,5	^{191}Ir (γ,n) ^{190n}Ir
^{189}Ir	13,3 j	185,9	0,24	^{191}Ir (γ,2n) ^{189}Ir
		188,4	0,1	
^{196m}Au	9,7 h	188,23	32,6	^{197}Au (γ,n) ^{196m}Au
^{101m}Rh	4,3 j	184	0,28	^{103}Rh (γ,2n) ^{101m}Rh
^{105}Ag	40 j	183,2	0,35	^{107}Ag (γ,2n) ^{105}Ag
^{101m}Rh	4,3 j	184	0,28	^{102}Pd (γ,p) ^{101m}Rh
^{189}Pt	11 h	186,7	1,4	^{190}Pt (γ,n) ^{189}Pt
^{188}Pt	10,3 j	187,6	22,5	^{190}Pt (γ,2n) ^{188}Pt
^{189}Ir	13,3 j	185,9	0,24	^{190}Pt (γ,p) ^{189}Ir
		188,4	0,1	
^{191}Pt	3 j	187,69	0,41	^{192}Pt (γ,n) ^{191}Pt
^{136}Cs	13,7 j	187,3	0,55	^{137}Ba (γ,p) ^{136}Cs

Nous avons décidé de compter le rhodium 20 jours après la fin de l'irradiation. L'erreur introduite, alors, par la présence des autres éléments est inférieure à 0,06% pour des teneurs en rhodium de l'ordre de 20% (les teneurs habituelles dans les noirs sont de 20 à 60%).

Les cinq éléments précédents (Au, Ag, Ir, Pt et Rh) sont comptés sur un détecteur Ge(Li) de haute résolution.

TABLEAU 6

Interférences pour le dosage de Pt

Isotope	Période	γ(keV)	Abondance	Réaction
^{195}Au	183 j	98,86	11,8	^{197}Au (γ,2n) ^{195}Au
^{190}Ir	11 j	97[a]	12,5	^{191}Ir (γ,n) ^{190}Ir
		100[a]	12,5	
^{189}Ir	13,3 j	95,3	0,2	^{191}Ir (γ,2n) ^{189}Ir
		97,8	0,1	
^{189}Pt	11 h	94,34	4,6	^{190}Pt (γ,n) ^{189}Pt
^{188}Pt	10,3 j	98,4	0,6	^{190}Pt (γ,2n) ^{188}Pt
^{189}Ir	13,3 j	95,3	0,2	^{190}Pt (γ,p) ^{189}Ir
		97,8	0,1	
^{191}Pt	3 j	96,52	3,22	^{192}Pt (γ,n) ^{191}Pt
^{195m}Ir	3,8 h	98,85	21	^{196}Pt (γ,p) ^{195m}Ir
^{195}Ir	2,5 h	98,85	9	^{196}Pt (γ,p) ^{195m}Ir

[a]Ces deux raies n'ont jamais été détectées.

TABLEAU 7

Interférences pour le dosage de Rh

Isotope	Période	γ(keV)	Abondance	Réaction
^{191}Pt	3 j	479,95	0,0557	^{192}Pt (γ,n) ^{191}Pt
^{195m}Ir	3,8 h	475,38	0,16	^{196}Pt (γ,p) ^{195m}Ir
^{190}Ir	11 j	478	1,5	^{191}Ir (γ,n) ^{190}Ir
^{188}Ir	41 h	478,1	16,3	^{191}Ir (γ,3n) ^{188}Ir
^{106m}Ag	8,5 j	473,8	1	^{107}Ag (γ,n) ^{106m}Ag

Dosage du palladium. Nos premiers essais de dosage du palladium ont été effectués sur la raie à 88 keV de ^{109}Pd ($t_{\frac{1}{2}}$ = 13,5 h). L'existence d'une interférence due à ^{120m}Sb nous a conduit à utiliser d'autres raies (307 et 1289 keV). L'énergie-γ de 307 keV correspond à la réaction ^{102}Pd (γ, n) ^{101}Pd $\xrightarrow{\beta^+}$ ^{101m}Rh. Le dosage s'effectue par déduction du nombre d'impulsions dû au rhodium: ^{103}Rh (γ, 2n) ^{101m}Rh. Etant donné les fortes teneurs en rhodium, un tel dosage est forcément imprécis: la valeur de l'estimation de l'écart type est de 7% (cf. Tableau 9). Nous recommandons donc d'effectuer le dosage sur la raie à 1289 keV de ^{101}Pd ($t_{\frac{1}{2}}$ = 8,5 h). Nous n'avons effectué qu'un seul dosage à l'aide de cette raie et n'avons donc pu étudier la répétabilité. L'exactitude semble bonne (environ 2% de déviation entre les teneurs mesurées par voie chimique et celles obtenues par ces dosages).

Dans le cas des dosages faits sur la raie à 1289 keV, les deux interférences théoriquement possibles sont ^{197}Au (γ, 3n) ^{194}Au ($t_{\frac{1}{2}}$ = 39,5 h) et ^{190}Pt (γ, n) ^{189}Pt ($t_{\frac{1}{2}}$ = 11 h). Dans les conditions de l'expérience, ces deux interférences n'influent nullement sur l'exactitude du dosage du palladium. Celui-ci est mis en comptage 5 h après la fin de l'irradiation, ceci à cause du temps mort introduit par l'activation du carbone contenu dans la cellulose (^{12}C (γ, n) ^{11}C, $t_{\frac{1}{2}}$ = 20,4 min)

Courbes d'activation

Nous avons irradié à des énergies de 26, 33, 39, 44 et 51 MeV des feuilles minces des différents éléments. Nous présentons dans la Fig. 1 les courbes correspondant aux différentes réactions: ^{103}Rh (γ, n) $^{102}Rh + ^{102m}Rh$; ^{102}Pd (γ, n) ^{101}Pd; ^{107}Ag (γ, 2n) ^{105}Ag; ^{191}Ir (γ, n) ^{190}Ir; ^{196}Pt (γ, n) ^{195m}Pt; ^{197}Au (γ, n) ^{196}Au. Après l'étude des radioisotopes obtenus, nous nous sommes limités, pour la suite des expériences, à une énergie de 35 MeV afin de minimiser les réactions concurrentes (γ, p) ou éventuellement (γ, np). En effet, pour le problème spécifique du dosage des noirs, il nous a semblé plus important de rechercher l'exactitude des résultats; la sensibilité ne jouant pas dans ce cas précis, un rôle important (teneurs élevées).

Influence de la méthode d'étalonnage et répétabilité des dosages

Nous avons testé deux méthodes. Nous avons dosé, à l'aide de feuilles minces servant d'étalon, deux séries de noirs (7517 et 2379) et nous nous sommes servis de ceux-ci pour analyser un noir inconnu (7516). Nous avons, par ailleurs, dosé ce noir inconnu en étalonnant avec des feuilles minces. Le Tableau 8 rassemble les résultats obtenus par les deux méthodes. Il semble donc que l'on puisse utiliser indifféremment les deux méthodes d'étalonnage sans pour cela affecter la précision des dosages, sauf peut-être pour le palladium.

Nous avons étudié la répétabilité pour le dosages de Rh, Ir, Pt, Au, Ag et Pd (Tableau 9).

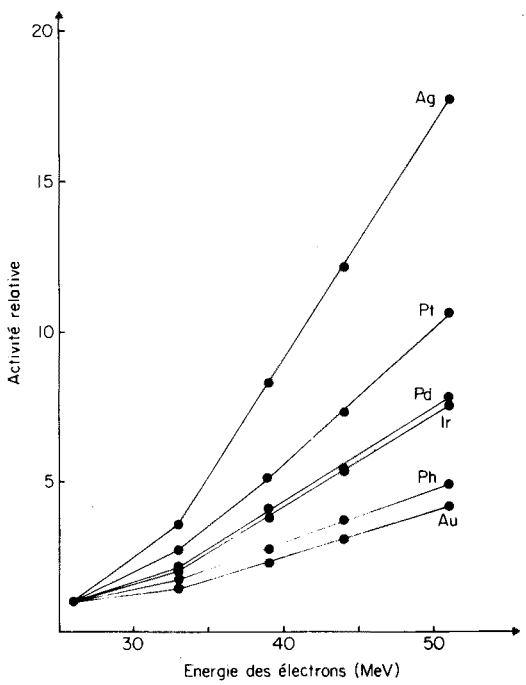

Fig. 1. Courbes d'activation.

TABLEAU 8

Analyse du noir 7516

Elément	Teneur (μg)		
	Etalon: feuilles minces	Etalon: Noir 7517	Etalon: Noir 2379
Rh	8950	8900	8855
Pd	188	180	183
Ag	742	730	735
Ir	320	320	335
Pt	910	915	910
Au	64	64	64

TABLEAU 9

Répétabilité des dosages de Rh, Pd, Ag, Ir, Pt et Au dans les noirs

Elément	Echantillon	Nombre de déterminations	Teneur (%)	s (%)
	7515	8	45,12	1,2
Rh	7516	8	44,81	1,5
	7517	10	31,16	2,1
	7515	4	1,06	7
Pd	7516	4	0,92	7,5
	7517	4	2,89	7
	7515	4	5	2
Ag	7516	8	3,8	6,5
	7517	6	1,62	6
	7515	8	1,75	2,4
Ir	7516	8	1,62	2,2
	7517	10	0,745	1
	7515	8	4,66	1,4
Pt	7516	8	4,63	1,8
	7517	10	14,69	2,1
	7515	8	0,315	2,2
Au	7516	8	0,312	2,2
	7517	10	2,08	2,6

Activités spécifiques et limites de détection à 35 MeV

Les activités spécifiques ont été calculées pour les six éléments. La formule utilisée est

$$A^* = A_0\,(1 - e^{-\lambda})/P \times I \times \text{Eff.} \times (1 - e^{-\lambda t_{irr}})\ (\gamma \text{ à } t_0/\text{min}_{irr}/\text{min}_c/\mu\text{A/mg})$$

avec A^*, activité spécifique; A_0, nombre d'impulsions par minute de comptage à t_0; t_{irr}, durée de l'irradiation (min); P, poids de l'élément (mg); I, intensité

moyenne du faisceau d'électrons (μA); Eff., efficacité du détecteur. Les résultats sont rassemblés dans le Tableau 10.

Dans le Tableau 11 sont indiquées les limites de détection théoriques correspondant aux étalons. Etant donné que, pour le calcul de ces limites de détection, nous n'avons pas tenu compte de la contribution des autres éléments (dont les teneurs varient avec les échantillons), les valeurs du Tableau 11 ne sont qu'indicatives. Les limites de détection ont été calculées pour un temps d'irradiation de 20 min et un temps de comptage de 50000 s.

Résultats des dosages

Les résultats sont présentés dans le Tableau 12. Si nous comparons les résultats obtenus par voie chimique et par activation nous constatons qu'ils sont en très bon accord sauf pour le dosage de l'or. Il semble que l'analyse chimique ne soit pas capable de doser correctement l'or dans les noirs aux concentrations inférieures à 1—2%; en effet l'or n'est déjà plus détecté à une teneur de 0,3%. En activation par contre, l'or est très bien détecté à faible concentration et les résultats obtenus peuvent être considérés comme valables.

Nous constatons que la reproductibilité est bonne pour le dosage de Rh, Ir, Pt et Au (1—2%) et qu'elle est très moyenne pour Ag et Pd (6—8%), en partie à cause de leur faible activité spécifique. Pour ces deux derniers éléments, la

TABLEAU 10

Activités spécifiques à 35 MeV

Elément	Raie-γ utilisée (keV)	Activité spécifique
Rh	475	3,3
Pd	1289	2
Ag	280,3	1
Ir	186,7	43
Pt	98,86	2,5
Au	355,72	380

TABLEAU 11

Limites de détection théoriques[a]

Elément	Période	Raie-γ utilisée (keV)	Temps de décroissance	Limite de détection	
				(μg)	(ppm)
Rh	206 j 2,89 a	475	20 j	1,5	75
Ir	11 j	186,7	20 j	0,2	10
Ag	40 j	280,3	20 j	5	250
Pd	8,5 h	1289	5 h	2,6	130
Pt	4,1 j	98,86	3 j	0,5	25
Au	6,183 j	355,72	8 j	0,02	1

[a]35 MeV, 66 μA; t_{irr} = 20 min; t_c = 14 h.

TABLEAU 12

Résultats des dosages

Elément	Echantillon	Teneur (%) mesurée par voie chimique	Teneur (%) mesurée par activation photonique à 35 MeV[a]
Rhodium	Noir 2379	33	33,2 ± 0,1
	Noir 7515	45,2	45,12 ± 0,5
	Noir 7516	44,2	44,81 ± 0,7
	Noir 7517	31	31,16 ± 0,6
Palladium	Noir 2379	14,9	13,45 ± 0,9
	Noir 7515	1	1,06 ± 0,07
	Noir 7516	0,9	0,92 ± 0,07
	Noir 7517	2,8	2,89 ± 0,2
Argent	Noir 2379	7,5	7,63 ± 0,7
	Noir 7515	4,9	4,91 ± 0,1
	Noir 7516	3,7	3,8 ± 0,2
	Noir 7517	1,6	1,62 ± 0,1
Iridium	Noir 2379	1,5	1,53 ± 0,04
	Noir 7515	1,7	1,75 ± 0,04
	Noir 7516	1,6	1,62 ± 0,04
	Noir 7517	0,7	0,745 ± 0,01
Platine	Noir 2379	4,7	4,71 ± 0,09
	Noir 7515	4,6	4,66 ± 0,06
	Noir 7516	4,6	4,63 ± 0,08
	Noir 7517	14,7	14,69 ± 0,3
Or	Noir 2379	0,3	0,6 ± 0,01
	Noir 7515	0	0,31 ± 0,01
	Noir 7516	0	0,31 ± 0,01
	Noir 7517	2	2,08 ± 0,05

[a]Les résultats sont donnés sous la forme $a \pm s$ avec (s) estimation de l'écart type pour le nombre de déterminations indiqué dans le Tableau 9.

valeur moyenne obtenue est tout à fait comparable à celle fournie par l'analyse chimique. Il ne nous est pas possible de discuter ici de la reproductibilité de l'analyse chimique, car il s'agit d'un point recouvert par le secret industriel.

Les méthodes valables pour l'analyse des noirs sont rares: l'activation photonique semble pouvoir prétendre à une place parmi ces méthodes et par conséquent pouvoir être utilisé comme référence ou pour les arbitrages.

BIBLIOGRAPHIE

1 Ch. Engelmann, Symposium sur les méthodes analytiques nucléaires dans la production et l'utilisation industrielle des métaux précieux; Bruxelles (16, 17 novembre 1971).
2 Ch. Engelmann, Thèse ORSAY n° 660 (24 juin 1970).
3 G. Erdtmann and W. Soyka, Die γ Linien der Radionuklide, Jül 1003—Ac, Julich, W. Germany, Sept. 1973.

Analytica Chimica Acta, 104 (1979) 139—144

SPECTROPHOTOMETRIC EVALUATION OF PHOSPHORUS PROFILES IN SILICON

PIETRO LANZA

Chemical Institute "G. Ciamician", University of Bologna, 40126 Bologna (Italy)

PIER LUIGI BULDINI*

C.N.R. — LAMEL Laboratory, Via de'Castagnoli 1, 40126 Bologna (Italy)

(Received 30th May 1978)

SUMMARY

A new method for the determination of phosphorus concentration profiles in semiconductor silicon slices makes use of spectrophotometry for concentration measurements and anodic oxidation for sectioning. Silicon layers in the 5—50-nm range can be removed reproducibly. The profile determination of phosphorus doping is possible for concentrations as low as 10^{19} atoms P cm^{-3}. Measurements of these profiles by the proposed procedure give excellent agreement with electrical evaluations. The method is simple and reliable, and expensive apparatus is not required. A medium-depth profile is normally completed in eight hours.

The determination of the distribution of impurity concentrations in semiconductor silicon as a function of depth is an interesting problem. The determination of the electrically active fraction and an understanding of the diffusion phenomena and semiconductor characteristics depend on a precise knowledge of the concentration profiles. This is attained by determining the dopant concentration in successive layers (5—50 nm) of the silicon sample. Anodic oxidation sectioning is a controlled way of reproducing the silicon layers perfectly. These can then be dissolved in dilute hydrofluoric acid and either the removed dopant or that remaining in the sample is measured by a suitable technique.

Phosphorus profiles in semiconductor silicon are usually determined by radioactivation [1, 2] or differential sheet resistivity measurements, by means of a four-point probe [3, 4] or the Hall effect [5, 6]. Resistivity measurements give only electro-active phosphorus, while electro-inactive precipitates or the presence of compensating impurities distort the meaning of the data. Radioactivation measurements are very sensitive and reliable, permitting determinations of 10^{17} atoms P cm^{-3}, but the required apparatus is very expensive and not widely accessible. The classical spectrophotometric determination of phosphoric acid was applied in the work described here.

EXPERIMENTAL

Apparatus

Measurements were made with a Bausch & Lomb Spectronic 21 UV-D Spectrophotometer. An Electronic Model C 633 direct current source, capable of delivering 300 mA at 500 V, was used to power the cell shown in Fig. 1. Slices of different diameters were easily oxidized by changing the upper plexiglass part. An In—Ga (1:3) alloy was used to ensure good electrical contact between silicon slice and brass support.

Pretreatment of the silicon slices

The samples are cleaned carefully as follows. Wash the slices in an ultrasonic distilled water bath for ca. 5 min. Rinse them in warm methanol in a quartz vessel, dry them in a nitrogen flow, and treat the dried slices with boiling trichloroethylene, then boiling acetone, and finally boiling methanol contained in quartz vessels (5 min each). Wash the samples for 15—30 min in running distilled water, and then dry them in a stream of nitrogen.

Anodic oxidation

Thin layers of material are removed from the surface by means of anodic oxidation. The silicon oxide is dissolved with dilute (0.1 M) hydrofluoric acid which does not react with the silicon substrate. Of the electrolytes proposed, 0.1 M boric acid and 0.1 M borax [7, 8] and ethylene glycol containing 0.05 M potassium nitrate and 10% of water [9, 10] seemed the most reliable. Reproducible and easily controlled oxidations may be obtained up to a silicon thickness of 50 nm with ethylene glycol. The electrolyte may be recycled for 20—30 oxidations.

Constant-current anodization is used; the voltage is monitored at the cell contacts. Figure 2 shows a typical cell voltage curve; the initial sharp drop is dependent on the electrolyte and slice resistivity and on the cell configuration.

For a given voltage, the amount of silicon removed is independent of: (a) the current density between 2 and 8 mA cm^{-2}; (b) the temperature between 10 and 40°C; and (c) the silicon type and resistivity.

The dependence of the silicon thickness on anodization voltage found by determining the silicon removed at known voltage values is linear up to 150 V, which gives a thickness of 36 nm of silicon.

Reliable use of the procedure requires suitable control of the uniformity of oxidation and the reproducibility of the layer thickness. The determination of silicon shows that the reproducibility of the anodic oxidation is better than ±5% for 5—30 nm layers, but for layers over 30 nm it is worse than ±5%. For layers exceeding 50 nm, it is not possible to control the thickness. The oxide growth is so rapid below 5 nm that it is difficult to obtain the prefixed layer without switching off automatically. To check the uniformity of oxidation and the removal of the surface layer, the physical profile of the treated surface

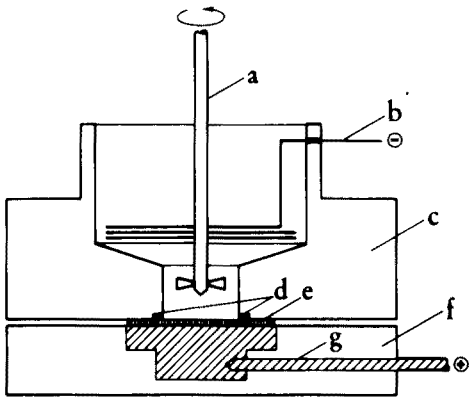

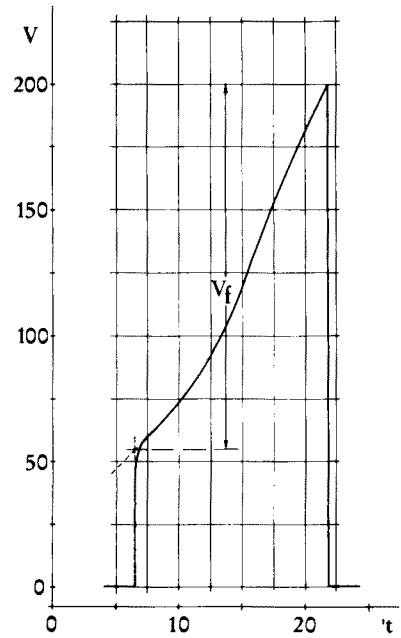

Fig. 1. Anodization cell (a) Stirrer; (b) Inox steel cathode wire; (c) Plexiglass; (d) silicone resin packing; (e) silicon slice; (f) PVC base; (g) brass support.

Fig. 2. Typical cell voltage curve (V_f is the net forming voltage).

was tested with a Talysurf 10 (Rank Precision Industries, Leicester, England). The result agreed well with the spectrophotometric silicon determinations.

The oxide growth from one oxidation to another was studied: even if the silicon slice was kept in contact with the ethylene glycol or air for several days, the surface oxidation depth did not exceed 1—2 nm Si and was thus similar to the standard deviation of a 25—30-nm layer.

Determination of silicon

Silicon was determined by a modification of the Sanders and Cramer method [11] which is not subject to phosphate interference.

Reagents. Reagent-grade chemicals were used and normal precautions for trace analysis were taken throughout. Solutions were stored in polyethylene bottles; polyethylene vessels and volumetric equipment were used exclusively to avoid any possible contamination from glass.

The reducing agent was prepared by dissolving 70 g of iron(II) ammonium sulphate in 1 l of 1.25% (v/v) sulphuric acid (10 mg Fe(II) ml^{-1}).

Procedure. At the end of the anodic oxidation of the slice, remove the electrolyte, wash the cell well with water, and dry completely. By pipette, add 1 ml of 0.1 M hydrofluoric acid to the slice surface and after 10 min (to allow

complete dissolution of the oxide layer), add to the cell 5 ml of 1.25% (v/v) sulphuric acid. Transfer the solution to a polyethylene volumetric flask and wash the cell 2—3 times with 5 ml of doubly distilled water, transferring the washings to the same flask. Add 5 ml of 1.6% (w/v) ammonium heptamolybdate tetrahydrate to give a solution of pH 1.5—1.6. Wait for 6 min to complete the molybdosilicic acid formation, add 5 ml of the reducing agent and 5 ml of 2.4% (w/v) sodium fluoride, dilute to 50 ml with doubly distilled water, and read the absorbance at 828 nm against water. Prepare a calibration curve by adding aliquots of standard solution (1 mg Si ml^{-1}) to 1 ml of 0.1 M hydrofluoric acid solution, proceeding as above. The curve is reproducible and linear to 0.8 μg Si ml^{-1} (0.54 absorbance units) and need not be checked frequently. The method permits determinations as low as 10 μg Si l^{-1}, with a standard deviation better than ±4%.

Determination of phosphorus

Phosphorus was determined by a modification of the Murphy and Riley method [12] based on the formation of molybdophosphoric acid and its reduction with ascorbic acid in the presence of potassium antimonyl tartrate, with measurement at 882 nm. Silicate does not interfere [12]. The fluoride interference is overcome by adding boric acid in excess.

Reagents. Prepare 0.1 M ascorbic acid daily by dissolving 1.32 g of ascorbic acid in 75 ml of doubly distilled water. Dissolve 0.274 g of potassium antimonyl tartrate in doubly distilled water and dilute to 100 ml (1 mg Sb ml^{-1}). Prepare the mixed reagent by mixing 125 ml of 2.5 M sulphuric acid, 37.5 ml of 4% (w/v) ammonium molybdate, 75 ml of 0.1 M ascorbic acid solution and 12.5 ml of potassium antimonyl tartrate solution. This reagent does not keep for more than 1 day. The mixed complexing reagent used contains two volumes of saturated boric acid solution per volume of the mixed reagent.

Procedure. After the anodic oxidation of the slice, remove the electrolyte, wash the cell well with water and dry completely. By pipette, add 1 ml of 0.1 M hydrofluoric acid to the slice surface and after 10 min (to allow complete dissolution of the oxide layer), add to the cell 1.5 ml of the complexing reagent. Transfer the solution to a test tube and continue with the successive oxidations. After 45 min, measure the absorbance of the solution at 882 nm against water. Prepare a calibration curve by adding potassium hydrogenphosphate standard solution (0.05—0.2 μg P) to 1 ml of 0.1 M hydrofluoric acid solution, proceeding as above. The curve is reproducible and linear up to 0.08 μg P ml^{-1} (0.56 absorbance units) and need not be checked frequently. The method permits determinations as low as 10 μg P l^{-1}, with a standard deviation better than ±5%. To check the profile procedure carefully, it is advisable to perform a silicon determination after every 10—15 phosphorus measurements.

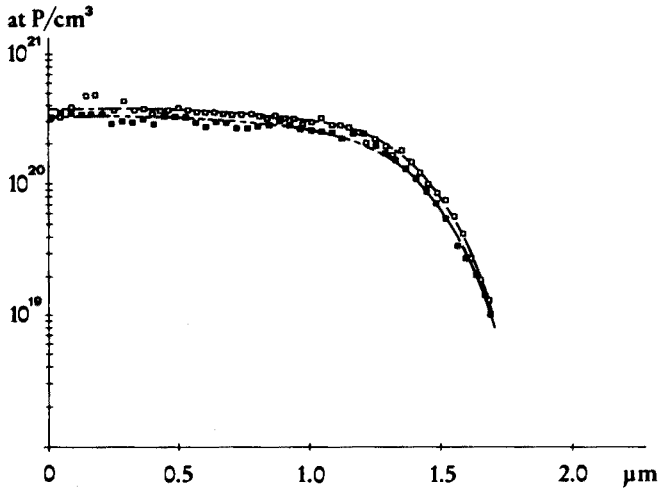

Fig. 3. Phosphorus profile in monocrystalline semiconductor silicon: (□) chemical measurements; (■) electrical measurements).

RESULTS AND DISCUSSION

The proposed method was used to analyze silicon slices (2.5 and 5 cm diameter). Slices were doped with between 10^{21} and 10^{19} atoms P cm^{-3} on their surfaces. Surfaces with diameters up to 40 mm were easily oxidized. In Fig. 3, a typical result is compared with electrical measurements.

The proposed method, used routinely to study the behaviour of heavily doped silicon slices, appears to be reliable and rapid. Under the conditions described, the method permits phosphorus determinations as low as 10^{19} atoms P cm^{-3}. This limit may be lowered by removing deeper layers. The time required for profile forming is practically independent of the phosphorus determinations and corresponds essentially to the time required for anodic oxidation and oxide dissolution. A medium depth profile (involving about 15 determinations) normally takes ca. 8 h.

The authors thank Prof. Dario Nobili for helpful suggestions and Dr. Sandro Solmi for differential sheet resistivity measurements.

REFERENCES

1 G. Restelli, F. Girardi, F. Mousty and A. Ostidich, Nucl. Instrum. Methods, 112 (1973) 581.
2 F. Burkhardt, A. Mertens and C. Wagner, Phys. Status Solidi, A 22 (1974) K45.
3 F. M. Smits, Bell Syst. Tech. J., 37 (1958) 711.
4 P. J. Severin, Philips Res. Rept., 26 (1971) 279.
5 L. V. Van den Pauw, Philips Res. Rept., 13 (1958) 1.
6 N. G. E. Johansson and J. W. Mayer, Solid-State Electron., 13 (1970) 317.
7 E. Tannenbaum, Solid-State Electron., 2 (1961) 123.

8 G. Dearnaley, J. H. Freeman, G. A. Gard and M. A. Wilkins, Can. J. Phys., 46 (1968) 587.
9 K. M. Busen and R. Linzey, Transaction AIME, 236 (1966) 306.
10 A. Manara, A. Ostidich, G. Pedroli and G. Restelli, Thin Solid Films, 8 (1971) 359.
11 W. F. Sanders and C. H. Cramer, Anal. Chem., 29 (1957) 1139.
12 J. Murphy and J. P. Riley, Anal. Chim. Acta, 27 (1962) 31.

Analytica Chimica Acta, 104 (1979) 145—151

SYNERGIC EFFECTS OF POLY(VINYLBENZYLTRIPHENYLPHOSPHONIUM CHLORIDE) ON THE SPECTROPHOTOMETRIC DETERMINATION OF LANTHANUM, ALUMINUM AND BERYLLIUM

T. MATSUSHITA*, M. KANEDA and T. SHONO

Department of Applied Chemistry, Faculty of Engineering, Osaka University, Yamada-kami, Suita, Osaka 565 (Japan)

(Received 8th May 1978)

SUMMARY

Poly(vinylbenzyltriphenylphosphonium chloride) reacts more strongly with acidic dyes than quaternary ammonium salts such as zephiramine. This polymer can be used to improve the spectrophotometric determinations of lanthanum, aluminum, and beryllium when it is added to the binary La—xylenol orange, Al—pyrocatechol violet and Be—chromazurol S systems. The molar absorptivities for these systems are similar to those obtained with quaternary ammonium salts, but there are advantages of greater stability and lower reagent consumption.

Quaternary ammonium salts such as zephiramine have been widely used in the spectrophotometric determination of various metal ions, to improve the sensitivity and selectivity available with conventional spectrophotometric reagents [1—6]. These salts form cationic micelles which associate with acidic dyes; addition to an aqueous solution of a suitable metal chelate frequently causes bathochromic and hypsochromic shifts, which may be explained in terms of ternary complex formation. However, this method involves several problems; for example, the absorption spectrum of the ternary complex changes with change in concentration of the quaternary ammonium salt, and the ternary complex may precipitate, unless a large molar excess of the quaternary ammonium salt is present.

Polysoaps such as alkylated poly(2-vinylpyridine) with n-dodecyl bromide have been reported [7] to form micelles more efficiently than the corresponding monosoaps, on the basis of their solubilizing ability for hydrocarbons. The present paper describes the synthesis and properties of the polyelectrolyte, poly(vinylbenzyltriphenylphosphonium chloride), and its application in the spectrophotometric determination of lanthanum, aluminum, and beryllium. This polyelectrolyte, which has the quaternary phosphonium salt structure in its side chain, forms polymeric micelles in aqueous solution, reacts more strongly than zephiramine or, with *p*-nitrophenol, and associates with sulfophthalein ligands such as xylenol orange, pyrocatechol violet and chromazurol S. Addition of this polyelectrolyte to aqueous solutions of binary metal complexes with these ligands results in considerable bathochromic shifts as

well as remarkable increases in absorbance. Except for the Al—pyrocatechol violet system, the molar absorptivities are slightly inferior to those obtained when quaternary ammonium salts are used, possibly because of steric hindrance effects. However, the proposed methods have some advantages in that the absorbances are stable, mixed working solutions are clear, and the 4P polymer can be used at lower concentrations.

EXPERIMENTAL

Reagents. Xylenol orange (XO), pyrocatechol violet (PV), chromazurol S (CAS), and zephiramine were obtained from Dozin Medical and Chemical Laboratory. The other reagents were of analytical grade. Metal solutions were prepared in the usual manner from appropriate salts.

Apparatus. A Hitachi Model EPS-3 recording spectrophotometer was used with matched 10-mm silica cells. A Yanagimoto Model pH-7 pH meter was used with a combined glass electrode.

General procedure. The buffer solution (25 ml) was transferred by pipet to a 50-ml volumetric flask, and aliquots of aqueous solutions of metal ion, dye, and cationic surfactant were added successively. The volume was made up with deionized water. After shaking the flask, the pH was checked and the absorbance was measured against a reagent blank. With the Al—PV ternary system, the maximum absorbance developed within 20 min. With the Be—CAS ternary system, the mixed solutions were warmed at 60°C for 20 min before adjustment of the volume.

Synthesis

Vinylbenzyltriphenylphosphonium chloride (abbreviated as 4P monomer) [8]. A mixture of *m*- and *p*-chloromethylstyrene (22.3 g, 0.15 mol; the *m*/*p* ratio was ca. 1.5) and triphenylphosphine (39.4 g, 0.15 mol) were dissolved in dimethylformamide (240 ml). The solution was stirred at 60°C for 6 h under nitrogen. After cooling, the solvent was evaporated under reduced pressure. The off-white solid was filtered off, washed with ether to remove starting materials, and dried in vacuo (yield 45.7 g). The crude product was recrystallized from a 5:1 ether—methanol mixture. The 4P monomer obtained as white needles is soluble in water, methanol, choroform, and dimethylformamide but insoluble in ether, benzene, and hexane.

I.r. (KBr), 1625 cm^{-1} (ν C=C); ^{1}H-n.m.r. ($CDCl_3$), δ 6.4 (methyne), 5.0—5.6 (methylene); m.p. > 300°C. Found, 78.0% C, 5.9% H; calculated for $C_{27}H_{24}PCl$, 78.2% C, 5.8% H.

Poly(vinylbenzyltriphenylphosphonium chloride) (abbreviated as 4P polymer). 4P monomer and azobis(isobutyronitrile) were dissolved in absolute methanol. The solution was degassed under vacuum and shaken in a water bath at 60°C for 4 h. The solution was poured into a large quantity of acetone, and the resulting precipitate (4P polymer) was collected on a sintered glass funnel and washed thoroughly with acetone. A methanolic

solution of the 4P polymer was then poured into a large quantity of ether. The white precipitate was filtered off, washed with ether, and dried in vacuo (yield, 62%). The i.r. spectrum of the polymer did not show the absorption band at 1625 cm^{-1} pertaining to the vinyl group of the monomer.

The intrinsic viscosity (η) was 0.37 at 25°C in aqueous 0.03 M KCl solution (measured with an Ostwald viscometer). Found 78.0% C, 5.6% H, 8.4% Cl; calculated for $C_{27}H_{24}PCl$, 78.2% C, 5.8% H, 8.5% Cl.

Both the 4P monomer and the 4P polymer are so hygroscopic that they must be kept in a desiccator after drying.

RESULTS AND DISCUSSION

The interaction between 4P polymer and acidic dye molecules

When quaternary ammonium salts such as zephiramine are added to aqueous solutions of *p*-nitrophenol, an acidic dye molecule containing an electron-withdrawing group and an electron-donating group, the absorption spectrum changes and a new absorption band appears at longer wavelengths [9]. This behaviour has been explained in terms of deprotonation of the acidic dye molecule promoted by dipole—dipole interaction between the dye and the quaternary ammonium salt on their micelle surface, because the wavelength of the new band is similar to that of the deprotonated dye species and there is a decrease in the pH of the solution [10].

Figure 1 shows the changes in the pH and the absorbance at 415 nm of an aqueous *p*-nitrophenol solution on addition of the 4P polymer. For comparison the changes on addition of zephiramine are included. With the 4P

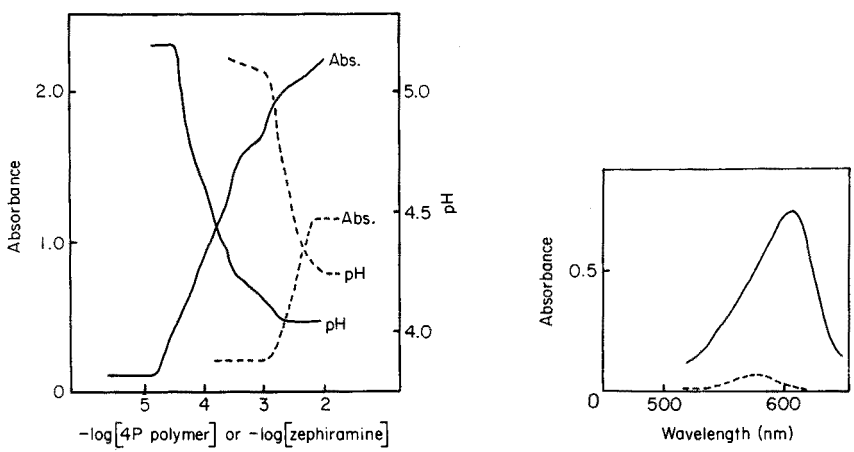

Fig. 1. Acid dissociation of *p*-nitrophenol (1.0×10^{-4} M) in the presence of 4P polymer (——) and zephiramine (- - -). Absorbances were measured at 415 nm for the 4P polymer and at 400 nm for zephiramine.

Fig. 2. Absorption spectra of the La—XO complex in the absence (- - -) and presence (——) of 4P polymer. Lanthanum, 1.00×10^{-5} M; XO, 4×10^{-5} M; 4P polymer, 6×10^{-4} unit M; pH 5.1.

polymer a new absorption band appeared at 415 nm, whereas with zephiramine a shoulder appeared at about 400nm. It can be seen that there are remarkable changes in the pH and absorbance at much lower concentrations of the 4P polymer (evaluated as monomer unit) compared with zephiramine. These results indicate that the 4P polymer interacts strongly with *p*-nitrophenol. The different reactivities of *p*-nitrophenol with the 4P polymer and zephiramine may arise from their micellar structures. Low-molecular-weight surfactants such as zephiramine form micelles when individual molecules aggregate in aqueous solution. In contrast, a polyelectrolyte has a loose helical structure in aqueous solution, which contracts in the presence of certain electrolytes to give a structure analogous to the zephiramine micelle [11]. Probably, therefore, the polymeric micelles interact more strongly with acidic dye molecules because of the concentrating effect of cations attached to the polymer chain. In fact, the apparent critical micelle concentration of the 4P polymer measured by using Rose Bengal Extra was found to be 1.6×10^{-5} M (as monomer unit), which is smaller than that of zephiramine (3.7×10^{-4} M) [1]. Moreover, the 4P monomer does not affect the absorption spectrum of *p*-nitrophenol in aqueous solution. These results prove the facile formation of polymeric micelles.

Application of the 4P polymer to spectrophotometric determinations

The above findings on the reaction of the 4P polymer prompted its application to spectrophotometric determinations with xylenol orange, pyrocatechol violet, and chromazurol S.

Lanthanum—xylenol orange

The addition of the 4P polymer causes the absorption band of the La—XO complex to shift from 580 to 610 nm with a marked increase in absorbance (Fig. 2). The absorbance is critically dependent on pH, with maximum absorbance occurring at pH 5.1 (Fig. 3); an acetic acid—sodium acetate buffer of ionic strength 0.1 was therefore used. Figure 4 shows the effect of the concentration of the cationic surfactants on the absorbance. Higher absorbances were observed with zephiramine than with the 4P polymer, but the absorbance was strongly influenced by the zephiramine concentration. Similar behaviour has been reported for most ternary complexes with quaternary ammonium salts, so that a large molar excess of the salt is needed to stabilize color development. In contrast, constant absorbance was obtained with the 4P polymer at low concentrations; only a 4-fold molar excess of XO over lanthanum was required.

The optimum conditions were thus established as: pH 5.1, a 4-fold molar excess of XO over lanthanum, and a 15-fold molar excess of 4P polymer (as monomer unit) over XO. Under these conditions, Beer's law was obeyed up to 1.39 ppm of lanthanum and the molar absorptivity was 74700 l mol^{-1} cm^{-1} at 608 nm. This value is slightly smaller than that observed [3] for zephiramine.

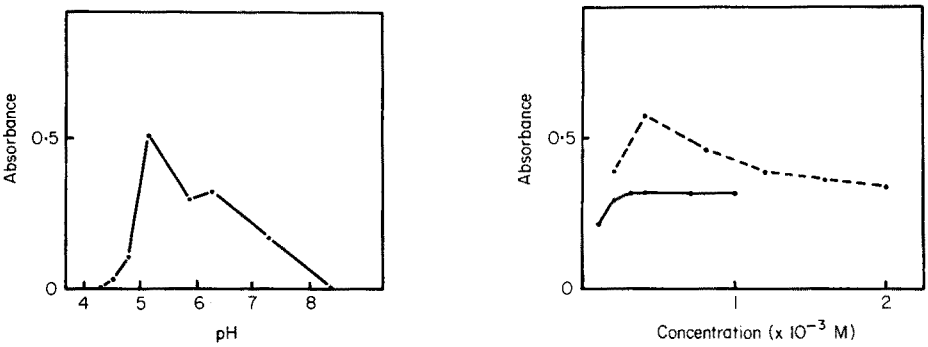

Fig. 3. Effect of pH on the absorbance of the La—XO complex in the presence of 4P polymer at 600 nm. Lanthanum, 5×10^{-6} M; XO, 2×10^{-5} M; 4P polymer, 2×10^{-4} unit M.

Fig. 4. Effect of concentration of cationic surfactants: (——) 4P polymer at 608 nm; (- - -) zephiramine at 614 nm. Lanthanum, 5×10^{-6} M; XO, 2×10^{-5} M; pH 5.1.

Aluminum—pyrocatechol violet

Tanaka and Yamayoshi [12] reported a colorimetric determination of aluminum with PV in acetate buffered solution, the molar absorptivity at 580 nm being 68300 l mol^{-1} cm^{-1} at pH 6.00. Later, Chester et al. [4] described a determination based on formation of the ternary complex with PV and cetyltrimethylammonium bromide (CTAB); the maximum color development occurred in the pH range 9.7—10.2, the effective molar absorptivity being 53000 l mol^{-1} cm^{-1} at 670 nm against a reagent blank. Hiiro [13] has shown that boron reacts with PV in weakly alkaline media to give a complex with maximum absorbance at 484 nm, and that the absorbance of PV itself at 600 nm decreases as the boron concentration increases. In alkaline media, PV is readily oxidized and the 4P polymer is liable to decompose to triphenylphosphine oxide. These considerations suggested that a pH of 6.25 (potassium dihydrogenphosphate—sodium borate) should be satisfactory for the present purpose.

The visible absorption spectrum of the PV solution at pH 6.25 (ionic strength 0.3) was not changed by addition of aluminum; possibly because of weak interaction of PV with the borate in the buffer. However, a new intense absorption band appeared at 670 nm (measured against a reagent blank) when the 4P polymer was added to a solution containing aluminum and PV, indicating the formation of a ternary complex. When CTAB was used, the absorbance of the ternary complex increased almost monotonously with pH in the pH range 6.2—9.0. When the 4P polymer was used, the absorbance at pH 6.25 was similar to that obtained with CTAB at pH 8.8. Since an acidic medium is desirable, as mentioned above, the 4P polymer

is more useful than CTAB. Optimal conditions were established as a 6-fold molar excess of PV and a 36-fold molar excess of 4P polymer over aluminium at pH 6.25.

Under such conditions, Beer's law was obeyed up to 0.43 ppm of aluminum and the molar absorptivity at 670 nm was 57900 l mol^{-1} cm^{-1}, which is slightly larger than that observed by Chester et al. but less than that observed by Tanaka and Yamayoshi.

Beryllium—chromazurol S

The addition of the 4P polymer to an aqueous solution of Be—CAS complex shifted the wavelength of maximum absorbance from 580 to 615 nm and increased the absorbance markedly. Maximum absorbance was found between pH 5.8 and 6.3, and an acetate buffer (ionic strength 0.1) was selected. Phosphate, citrate, and phthalate ions interfered with the color development. Maximum absorbance was observed with a 13-fold molar excess of CAS over beryllium, and a 6-fold molar excess of 4P polymer over CAS.

Calibration graphs prepared at pH 6.2 under the above conditions were linear up to 0.126 ppm of beryllium. The molar absorptivity at 615 nm was 64700 l mol^{-1} cm^{-1}, which is less than the value observed by Nishida [6] for zephiramine.

Effects of diverse ions in each system

The interferences are summarized in Table 1. Aluminum, iron, cerium, and mercury interfered seriously with determinations in the La—XO system. Iron and copper interfered in the Al—PV system, and aluminum and iron in the Be—CAS system, so that prior separations would be essential.

TABLE 1

Effect of diverse ions (in μg) on the determination of lanthanum, aluminum, and beryllium (The concentration of metal ion tested was equal to that of the analyte; the concentration of anion tested was a 25-fold molar amount.)

Added ion	La—XO	Al—PV	Be—CAS	Added ion	La—XO	Al—PV	Be—CAS
None	69.5	10.8	1.79	Cu(II)	66.1	23.2	2.01
Be(II)	72.4	10.8	—	Zn(II)	63.3	12.1	1.96
Mg(II)	69.1	10.8	2.17	Cd(II)	68.1	11.8	2.02
Al(III)	46.0	—	4.85	Sn(IV)	68.1	10.5	1.61
Ca(II)	69.0	9.8	2.04	Ce(III)	100.5	10.5	1.78
Cr(III)	70.0	11.1	1.99	Hg(II)	87.0	10.6	1.96
Mn(II)	69.8	11.1	1.96	Pb(II)	67.1	10.5	1.76
Fe(III)	37.0	15.4	3.84	SO_4^{2-}	67.8	10.8	1.88
Co(II)	78.9	10.8	2.08	PO_4^{3-}	69.5	—	1.75
Ni(II)	76.0	12.2	1.91	$B_4O_7^{2-}$	69.5	—	1.89

REFERENCES

1 K. Ueno, Bunseki Kagaku, 20 (1971) 736.
2 H. Nishida, Bunseki, (1977) 271.
3 M. Otomo and Y. Wakamatsu, Bunseki Kagaku, 17 (1968) 764.
4 J. E. Chester, R. M. Dagnall and T. S. West, Talanta, 17 (1970) 13.
5 H. Kohara, N. Ishibashi and K. Fukamachi, Bunseki Kagaku, 17 (1968) 1400.
6 H. Nishida, Bunseki Kagaku, 20 (1971) 1080.
7 U. P. Strauss and E. G. Jackson, J. Polym. Sci., 6 (1951) 649.
8 R. Asami and I. Watanabe, 33rd Annual Meeting of the Chemical Society of Japan, Abstract, Part II, 1975, p. 660.
9 H. Kohara, Bunseki Kagaku, 17 (1968) 1147.
10 H. Kohara, N. Ishibashi and T. Masuzaki, Bunseki Kagaku, 19 (1970) 467.
11 E. Jungermann, Cationic Surfactants, Dekker, New York, 1970, p. 179.
12 K. Tanaka and K. Yamayoshi, Bunseki Kagaku, 13 (1964) 540.
13 K. Hiiro, Bull. Chem. Soc. Jpn., 34 (1961) 1743; Nippon Kagaku Zasshi, 83 (1962) 81.

Analytica Chimica Acta, 104 (1979) 153—160

DETERMINATION OF POLY(VINYL ALCOHOL) VIA ITS COMPLEX WITH BORIC ACID AND IODINE

D. P. JOSHI, Y. L. LAN-CHUN-FUNG and J. G. PRITCHARD*

Department of Chemistry, North East London Polytechnic, Stratford, London E.15 (Great Britain)

(Received 28th April 1978)

SUMMARY

The maximum absorbance of the complex is proportional to initial polymer concentration over the range 0—100 mg dm^{-3} for PVA polymers with degrees of hydrolysis in the range 75—100 mole-%, in the presence of an excess of boric acid, iodine and potassium iodide. Within these limits 1-mg dm^{-3} solutions of several commercial and laboratory-prepared polymers have maximum absorbance 0.035 within ± ca. 3% in 1-cm cells. Sources of error in the determination of PVA are discussed, and the reduction in the absorbance at low iodine concentration is examined with respect to the mole-% hydrolysis. Absorbance measurements on two solutions with, respectively, high and low reagent concentrations allow the determination of both the concentration of polymer and its % hydrolysis. The equilibrium for complex formation by pure PVA at room temperature with low iodine concentration yields the values —150 kJ mol^{-1} and —498 J mol^{-1} K^{-1} for the enthalpy and entropy of reaction; for a large excess of iodine the reaction is complete. Variations in the wavelength of maximum absorbance of the complexes correlate approximately with their stability. Complex formation occurs through the alcohol groups of the partly hydrolysed poly(vinyl acetate) polymers and also the residual acetate groups of these polymers at the higher iodine concentrations

Poly(vinyl alcohol), PVA, forms a blue complex with triiodide in the presence of boric acid. For several years a method for the determination of PVA in paper coatings, based on spectrophotometric measurement of the complex at 690 nm as advocated by Finley [1] has been used in this laboratory [2]. However, λ_{max} for the complex often differs from 690 nm and depends on the source of the polymer. An error may be introduced into the determination if the polymer under test and the calibration standard give complexes with different λ_{max}. This paper explores the limits of error which arise from variation in λ_{max} and other features of the system when the method is applied to poly(vinyl acetate)-derived PVA polymers with the commercially interesting range of 0—25 mole-% of residual acetate groups.

EXPERIMENTAL

Materials

Gelvatol polymers were obtained from Monsanto Chemicals Ltd (London) and Alcotex polymers from Revertex Ltd (Harlow). The Gelvatol polymers were treated with periodate in aqueous solution to give polymers of lower molecular weight, which were recovered by precipitation with acetone; their molecular weights were calculated from the Flory—Leutner equation [3, 4]. Pure PVA (batch 99197) was obtained from ICN K & K Laboratories (Plainview, New York). Pure poly(vinyl acetate), also K & K batch 99197, was transesterified with ca. 0.04 M sodium methoxide in methanol to give partially hydrolysed polymers, and their degrees of hydrolysis were determined, as detailed elsewhere [5]. The conditions of preparation, where appropriate, and the properties of the polymers are listed in Tables 1 and 2.

Preparation and measurement of the complex

A reagent blank and five test solutions were prepared for each polymer, as follows. Into six 250-cm^3 volumetric flasks were placed 0, 10, 20, 30, 40 and 50 cm^3 of stock polymer solution containing 0.1000 g dm^{-3}, and, respectively, 125, 115, 105, 95, 85 and 75 cm^3 of distilled water were added. To each of these solutions was added in turn, with careful mixing to ensure homogeneity after each addition, 75 cm^3 of boric acid solution (40 g dm^{-3}), 15 cm^3 of iodine

TABLE 1

Properties of commercial polymers and the absorption coefficients of their complexes at 20°C with 0.194 M boric acid, 0.003 M iodine and 0.009 M potassium iodide

Polymer	Molecular weight[a]	Degree of hydrolysis (mole-%)	Test solution volume (cm^3)	Wavelength[b] for absorbance measurement (nm)	Absorbance × per mg dm^{-3} o polymer
K & K PVA pure	100000	99.9	50	676	3.57
Gelvatol 1-90	115000	99.5	250	678	3.56
Gelvatol 1-90	115000	99.5	50	678	3.48
Gelvatol 1-30	14000	99	250	654	3.46
Gelvatol 1-30	14000	99	50	654	3.36
Gelvatol 1-90	115000	99.5	250	690	3.46
Gelvatol 1-90	115000	99.5	50	690	3.37
Gelvatol 1-30	14000	99	250	690	3.13
Gelvatol 1-30	14000	99	50	690	2.95
G 1-90 cleaved	3300	99.5	250	678	3.36
G 1-30 cleaved	2800	99	250	654	3.41
Alcotex 99/10	23000	99	250	685	3.30
Alcotex 88/10	23000	88	250	658	3.15
Alcotex 78L	18000	78	250	641	3.00
Alcotex 75L	18000	75	250	652	2.91

[a]Approximate viscosity average. [b]λ_{max}, except when 690 nm.

TABLE 2

Conditions of transesterification of poly(vinyl acetate) with 0.04 M methoxide in methanol, % hydrolysis, and absorption coefficients at 20°C for complexes of the resultant PVA polymers[a] with 0.194 M boric acid, 0.003 M iodine and 0.009 M potassium iodide

Alcoholysis reaction temperature (°C)	Alcoholysis reaction time (min)	Degree of hydrolysis		λ_{max} (nm)	Absorbance × 10^2 per mg dm^{-3} of polymer
		(Weight-%)	(Mole-%)		
60	180	98.3	99.1	676	3.50
80	210	96.0	97.8	676	3.42
60	70	92.3	95.7	676	3.47
60	60	91.4	95.2	676	3.45
50	140	90.5	94.8	676	3.52
22	300	80.2	88.8	658	3.52
30	160	72.5	83.6	658	3.42
30	130	70.8	82.5	658	3.40
30	110	63.9	77.4	658	3.30
40	46	61.3	75.4	658	3.25

[a]Viscosity average molecular weight, 100000—135000.

solution (12.70 g dm^{-3}) containing potassium iodide (25 g dm^{-3}), and 35 cm^3 of distilled water to complete 250 cm^3. The six solutions thus contained 0—20 mg dm^{-3} of polymer in equal steps, 0.1940 M boric acid, 0.00300 M iodine and 0.009 M potassium iodide. The absorbances of the five green/blue test solutions in 1-cm cells at 20°C were scanned (Unicam SP700 spectrophotometer) with the reagent blank as reference. For some of the commercial polymers, this procedure was also repeated on one-fifth of the scale, the concentrations remaining the same. Prepared polymers were examined similarly on the 50-cm^3 scale at 20°C for the polymer concentration range 0—100 g dm^{-3} and for two sets of reagent concentrations. Complex formation by a 20 mg dm^{-3} solution of the K & K PVA was examined at several temperatures; the test solution and the reagent blank were allowed to stand for 90 min at each temperature before the measurement. Temperatures were held constant within ± 0.2°C. The wavelength scale of the spectrophotometer was calibrated with didymium glass, and photometric accuracy was checked with aqueous solutions of analytical-grade silver nitrate and potassium dichromate. Optically matched silica cells were cleansed of residual polymer between experiments by treatment with concentrated nitric acid followed by water and acetone rinses.

RESULTS AND DISCUSSION

Commercial polymers

Plots of the absorbance values vs. concentration yielded straight-line relationships for each polymer, in accord with Beer's law, which holds for the

range 0—80 mg dm^{-3} of PVA with the present method [2]. Correlation coefficients from regression analysis were not less than 0.999; the slopes (absorption coefficients) of the regression lines which pass strictly through the origin are given in Table 1 in absorbance units $\times 10^2$ per mg dm^{-3} of polymer. The coefficients for the 250-cm^3 test solutions were consistently ca. 3% higher than for the 50-cm^2 solutions, most probably because the more gradual mixing of the larger volumes in the former case gave more uniform boration and iodination of the polymers, and so the former results and associated procedure are preferred; the average deviation of experimental points about the least-squares lines (precision) was ca. 1% in both cases.

The first five results in Table 1 support the previous equation [2], $A = (0.0350 \pm 0.0007)\,C$, for the absorbance of the PVA—borate—iodine complex of other 99—100% hydrolysed PVA polymers measured under the same conditions with polymer concentration, C, in mg dm^{-3}. However, if the particular polymer gives a complex with λ_{max} appreciably less than 690 nm, it is better to measure absorbance at λ_{max} otherwise an error reducing A by e.g., ca. 10% with Gelvatol 1-30 can be introduced. Drastic reduction of molecular weight, to degrees of polymerization 76 and 63 for the cleaved Gelvatols 1-90 and 1-30, does not change λ_{max} nor reduce the amount of complex formed appreciably. Evidently, this degree of polymerization does not approach the lower limit for complex formation. The results for the Alcotex polymers are low even though measured under the optimum conditions. The extent to which these low results are due to residual acetate groups and/or other impurities is considered below.

Prepared polymers

The absorption coefficients listed in the final column of Table 2 for the prepared polymers refer to the concentrations of reagents used for the commercial polymer. All the values lie within the range 0.0350 ± 0.007 absorbance units per mg dm^{-3} of polymer and are independent of the degree of hydrolysis over the range 85—100 mole-%, but a small reduction to just below the lower limit may occur for the 75—85 mole-% range (ca. 60—75 weight-%). The regression line for the absorption coefficient (S) as a function of weight-% (w) is $S = 0.0300 + 0.0000511w$, which gives $S = 3.31$ at $w = 60\%$ and $S = 3.52$ at $w = 100\%$. The reduction in absorption coefficient over the 75—100 mole-% hydrolysis range for pure PVAc-A polymers, when 0.003 M iodine is used with 0—0.002 mol dm^{-3} of polymer segments is barely detectable; this fortuitous effect provides an analytical method which can be used with confidence to determine, by weight, a broad range of "PVA" products used in the paint, textile size, adhesives, paper coatings and emulsifier industries.

Comparison with the results for the Alcotex polymers strongly suggests that they contain impurities in addition to residual acetate groups. Moreover, these polymers are yellow in colour, and their aqueous solutions have absorption bands over the range 250—360 nm, with molar absorption coefficients in the range 0.2—0.4 dm^3 segment-mol^{-1} cm^{-1} for the 99/10 and 88/10 brands, and

2—4 dm^3 segment-mol^{-1} cm^{-1} for 78L and 75L. This suggests that the Alcotex polymers contain conjugated C=C and C=O double bonds as a result of dehydration and oxidation [6]. However, the reduction in absorption coefficient from this cause does not exceed ca. 10%.

When the iodine concentration was reduced to 0.0005 M, the amount of complex formed was still precisely proportional to the concentration of polymer for the whole range examined (0—0.002 segment-mol dm^{-3}), but in contrast to the foregoing situation the absorption coefficient (S_{low}) in absorbance units per mg dm^{-3} of polymer fell rapidly as the % of residual acetate groups increased (Table 3). When plotted against weight-% hydrolysis (w) the absorption coefficients give a regression line with correlation coefficient 0.995 and the value of the absorption coefficient decreases from 0.0266 (for w = 100%) at a rate which is slightly greater than the decrease in % hydrolysis, so that the coefficient reaches zero before the degree of hydrolysis reaches zero. The linearity of the relationship suggests a simple method for the determination of PVAc-A copolymers and their degree of hydrolysis by use of the high and low concentrations of reagent employed here and the appropriate equations for the absorption coefficients: S_{high} = 0.0342 and S_{low} = 0.0003024 w − 0.00363. Only a small error is introduced by taking an average value for S_{high} as a simplification. If the respective absorbances A_{high} and A_{low} are measured at λ_{max} for two test solutions containing the same unknown concentration C (mg dm^{-3}) of polymer, then $C = A_{high}/0.0342$ and $w = 113.1\ A_{low}/A_{high} + 12.0$.

The spectra of the test solutions of the prepared polymers with 0.0005 M iodine showed an approximately constant value of the absorbance of a shoulder at 480 nm (0.0049 abs. units per mg dm^{-3} of polymer ± 0.0002 standard

TABLE 3

Percent hydrolysis and colorimetric sensitivities at 20°C for complexes[a] of prepared PVA polymers[b] with 0.129 M boric acid, 0.0005 M iodine and 0.00017 M potassium iodide

Weight-% hydrolysis[c]	Absorbance × 10^2 per mg dm^{-3} of polymer	Absorbance × 10^2 per mg dm^{-3} of vinyl acetate units
99.9[d]	2.57	2.57
96.0	2.56	2.67
92.3	2.49	2.69
91.4	2.42	2.65
90.5	2.40	2.65
80.2	2.03	2.53
72.5	1.84	2.54
70.8	1.78	2.51
63.9	1.53	2.39
61.3	1.51	2.46

[a] λ_{max} over the range 685—694 nm. [b] Viscosity average molecular weight 100000—135000. [c] cf. Table 2. [d] Pure PVA (K & K Laboratories).

deviation). The use of such a constant absorbance (or one of known linear variation with % hydrolysis, of contrasting gradient to that observed for measurements of λ_{max} for the blue complex) would enable the concentration of polymer and its % hydrolysis to be determined by absorbance measurements at two wavelengths on one test solution. This matter must be investigated further before this is suggested as a general method because 480 nm is approximately the wavelength of maximum absorbance for the red PVAc—iodine complex, the absorbance of which appears to depend on the method of preparation of partly hydrolysed polymers with degrees of hydrolysis in the range of interest [7, 8].

Characteristics of the complex

Each iodine molecule requires not less than about 24 vinyl segments to form the helix of the complex [9—11], so there is at least a six-fold excess of iodine, even at a concentration of 0.0005 M, to account for the observed linearity of absorbance with initial polymer concentrations up to 0.002 segment-mol dm^{-3}.

The difference between the absorbance values for pure PVA at low and high iodine concentrations at 20°C indicates that the maximum amount of complex is not formed when the concentration of the iodine is 0.0005 M; at 0.003 M, however, the equilibrium of the complexation reaction is likely to be shifted entirely in favour of the complex. This view is confirmed by the behaviour of pure PVA with 0.0005 M iodine when the temperature is varied (Table 4). Lower temperatures favour [12] the formation of the complex and this is only sensibly complete at 0—5°C, giving the same value of absorbance as obtained with a very large excess of iodine.

If the borate, iodine and potassium iodide concentrations are in excess and thus effectively constant, an equilibrium constant may be formulated for the

TABLE 4

Colorimetric sensitivity at various temperatures for complexes of PVA[a] with 0.129 M boric acid, 0.0005 M iodine and 0.00017 M potassium iodide

Temperature (°C)	λ_{max} (nm)	Absorbance × 10^{-2} per mg dm^{-3} of polymer (A)	Equilibrium constant (K)[b]
5.0	694	3.55	
10.0	694	3.50	70.00
15.0	694	3.30	13.20
20.0	694	2.60	2.74
25.0	685	2.40	2.09
29.0	685	1.75	0.97
32.0	675	1.55	0.78
38.5	667	0.35	0.11

[a]Pure PVA (K & K Laboratories). [b]K = [complexed PVA]/[non-complexed PVA].

complexation: K = [Complexed PVA]/[Non-complexed PVA]. Hence, enthalpy (ΔH) and entropy (ΔS) changes may be calculated for formation of the complex in the constant medium.

$$\text{Log } K = \text{Log } \frac{A}{(A \text{ max} - A)} = \frac{-\Delta H}{2.303\,RT} + \frac{\Delta S}{2.303\,R}$$

The values in Table 4 give a linear relationship between log K and $1/T$, where T is the absolute temperature, with correlation coefficient 0.982 and slope 7838 K. Hence, for R = 8.306 J mol^{-1} K^{-1} the values of the thermodynamic constants are ΔH = −150,000 J mol^{-1} and, for 25°C, ΔS = −498 J mol^{-1} K^{-1}. The driving force ($-\Delta G$) for the forward reaction in the following equilibrium is therefore modest at room temperature.

Polymer random coil ⇌ Polymer helix complexed with borate and iodine

$$-\Delta G = -\Delta H + T\Delta S$$
(1.5) (150.0) (−148.5) (kJ mol^{-1})

The stability conferred on the complexed system by the loss of the heat of formation of new bonds is almost completely offset by the orientational requirement in the complex, which must have a highly ordered form compared with the random coil of the non-complexed polymer. It is also significant that the wavelength of λ_{max} decreases as the temperature increases. This no doubt reflects the formation of longer helixes, with relatively less stable ends, at the lower temperatures.

Two phases may be distinguished in the formation of the borate—iodine complex of partly hydrolysed PVAc. When the sensitivities measured at low iodine concentration are converted from absorbance units per mg of copolymer dm^{-3} to absorbance units per mg of vinyl alcohol segments dm^{-3}, through multiplication by the factor $100/w$, the resulting values are reasonably constant (Table 3) with a mean of 0.0256. This suggests strongly that only the vinyl alcohol segments in the copolymers are effective in complex formation at low iodine concentration. In this phase of the reaction, λ_{max} of the complexes tends to lie in the range 680—700 nm. The differences in the absorption coefficients listed in Tables 2 and 3 (abs. units per mg dm^{-3} of polymer) for the same degree of hydrolysis increase linearly with the amount (% w/w) of acetate present, and are clearly attributable to a second phase of reaction in which the λ_{max} of the complexes tends to lie in the range 660—680 nm.

In connection with the characteristics of formation of the red PVAc—iodine complex, recent evidence suggests that the hydroxyl groups in PVAc hydrolysed by base catalysis increasingly form block sequences [8, 13—15] when the degree of hydrolysis reaches 20 mole-% and leave short scattered blocks of acetate groups which cannot form the red complex when 80 mole-% hydrolysis is exceeded [5]. Concerning the blue complex under discussion here, it is suggested that the block sequences of hydroxyl groups react to partial completion with 0.0005 M iodine to form relatively stable helical complexes; with 0.003 M iodine, reaction with the OH block sequences is completed and

extends to include the acetate groups in less stable helices which have λ_{max}, accordingly, at a shorter wavelength. It is quite plausible that sequences of, say, 5—10 acetate groups would not preclude complex formation in the presenc of sufficient borate, which may serve to stabilise the helix turn-to-turn through the OH groups which make up the total number of vinyl units required for the helix to form ($\lesssim$ 24, as noted above).

The absorbance sensitivity observed for 0.003 M iodine is ca. 0.034 (44 + 0.42 M) per mM dm^{-3} of vinyl segments, where M is the mole-% of residual acetate groups. Thus, the mean sensitivity per vinyl segment increases over the range studied by approximately the same percentage as the mole-% of residual acetate groups. However, the results with 0.0005 M iodine suggest that the efficiency of complex formation with acetate groups included should not be higher than with alcohol groups alone. The observed trend with 0.003 M iodine must be an effect of the higher borate, iodine and iodide concentrations. Formation of the blue complex is assisted by crystallinity as shown (with low boric acid concentration) by stereoregular PVA [16], and the PVA—borate—I_2 system is partly gelled, especially at the higher borate and iodine concentrations [17, 18]. This gelling effect may counteract the increasing loss of crystallinity which occurs in the copolymers as the percentage of residual acetate groups increases.

The authors thank Ms. Manjit Kaur for contributing the u.v. spectra of the Alcotex polymers.

REFERENCES

1 J. H. Finley, Anal. Chem., 33 (1961) 1925.
2 J. G. Pritchard and D. A. Akintola, Talanta, 19 (1972) 877.
3 J. G. Pritchard and Y. L. Lan Chun Fung, Talanta, 23 (1976) 237.
4 P. J. Flory and F. S. Leutner, J. Polym. Sci., 3 (1948) 880; 5 (1950) 267.
5 D. P. Joshi and J. G. Pritchard, Polymer, 19 (1978) 427.
6 J. G. Pritchard, Poly(vinyl alcohol) — Basic Properties and Uses, Gordon and Breach, London, 1970, Chap. 2.
7 S. Hayashi, C. Nakano and T. Motoyama, Chem. High Polym., 20 (1963) 303.
8 K. Noro, Brit. Polym. J., 2 (1970) 128.
9 M. M. Zwick, J. Polym. Sci., Part A-1, 4 (1966) 1642.
10 T. Vasudevan, T. Balakrishnan, H. Kothandarman and M. Santappa, J. Polym. Sci., Polym. Chem. Ed., 14 (1976) 2319.
11 G. Uchman and L. Gawel, Acta Pol. Pharm., 32 (1975) 471.
12 C. D. West, J. Chem. Phys., 17 (1949) 219.
13 I. Sakurada, Gohsei Seni Kenkyu 1, (1972) 192.
14 R. K. Tubbs, J. Polym. Sci., Part A-1 4 (1966) 623.
15 S. Hayashi, T. Michihiro, I. Keneko and N. Hojo, Makromol. Chem., 176 (1975) 3221.
16 M. M. Zwick, J. Appl. Polym. Sci., 9 (1965) 2393.
17 S. N. Ushakov, Dokl. Akad. Nauk SSSR, 139 (1961) 160.
18 S. A. Glikman, S. N. Ushakov, E. P. Korchagina and E. N. Lavrienteva, Dokl. Akad. Nauk SSSR, 154 (1964) 372.

Analytica Chimica Acta, 104 (1979) 161—166

MECHANISM OF TIN(IV) EXTRACTION WITH *N*-BENZOYL-*N*-PHENYL-HYDROXYLAMINE FROM HYDROCHLORIC ACID SOLUTIONS

M. KOEVA

Department of Analytical Chemistry, Higher Institute of Chemical Technology, Sofia-56 (Bulgaria)

N. JORDANOV* and ST. MAREVA

Bulgarian Academy of Sciences, Institute of General and Inorganic Chemistry, 1113 Sofia (Bulgaria)

(Received 23rd May 1978)

SUMMARY

The mechanism of tin(IV) extraction with *N*-benzoyl-*N*-phenylhydroxylamine from hydrochloric acid media is discussed. The equilibrium $Sn(H_2O)_2Cl_4 + 2HBPHA \rightleftharpoons Sn(BPHA)_2Cl_2 + 2H^+ + 2Cl^- + 2H_2O$ is proposed on the basis of extraction data, elemental analysis and i.r. spectra. The value of the equilibrium constant is 6.80 ± 0.02 at 25°C and $I = 2$. The extracted species is considered to be a mixed neutral complex, $SnCl_2(BPHA)_2$.

The extraction of tin(IV) with *N*-benzoyl-*N*-phenylhydroxylamine (BPHA) from hydrochloric acid solutions has been studied by many authors [1—4]. At a constant concentration of BPHA, the percentage extraction of tin(IV) increases in the range 0.2—0.8 M HCl, then decreases quickly and becomes negligible above 2 M HCl. When the reagent is introduced into the aqueous phase along with ethanol, acetic acid or chloroacetic acid, extraction of tin(IV) is considerably enhanced [4], largely because of decreased BPHA extraction; the additives are effective in the order $C_2H_5OH < CH_3COOH < CH_2ClCOOH$. All the earlier work has indicated that the tin(IV)—BPHA complex is formed in the aqueous phase, and that the character of the extraction curves probably depends on the Sn(IV) species in hydrochloric acid solutions.

The present paper is concerned with elucidation of the extraction of Sn(IV) with BPHA. The problem is discussed on the basis of the electron configuration of Sn(IV) and the state of Sn(IV) in hydrochloric acid solutions. Extraction data as well as the elemental composition and i.r. spectra of the solid Sn(IV)—BPHA complexes are used to establish the mechanism.

EXPERIMENTAL

Reagents

A stock solution of tin(IV) (8.43×10^{-3} M $SnCl_4 \cdot 5H_2O$) was prepared in 6 M HCl and standardized gravimetrically [4]. BPHA (Merck analytical grade) was

used as a 1% (w/v) solution in 50% acetic acid (4.70×10^{-2} M), or a 0.1% solution in benzene or carbon tetrachloride (4.70×10^{-3} M). The solvents were distilled before use.

General procedures

Extraction procedure. The extraction was done as described previously [4]. Equal volumes of both phases (10 cm^3) were used in all experiments. Equilibrium was attained after stirring for 10 min at 25°C. Thermostated 50-cm^3 vessels were used. Tin(IV) in the aqueous phase and tin in the organic phase (after back-extraction with 8 M HCl) were determined spectrophotometrically [4].

Effect of the diluent. The extraction of tin(IV) with a solution of BPHA in chloroform, carbon tetrachloride and benzene was studied as a function of HCl concentration. The extraction curves are shown on Figure 1.

Effect of BPHA concentration. The distribution of tin(IV) (4.21×10^{-4} M) as a function of BPHA concentration was studied at constant ionic strength ($I = 2$) for three concentrations of HCl. BPHA was added to the aqueous phase as its acetic acid solution, the final concentration varying from 7.90×10^{-4} M to 4.79×10^{-3} M. Chloroform was used as organic phase.

Determination of chloride ions in the extracted complex. The number of chloride ions in the tin(IV)—BPHA complex was determined by means of extractions based on the fact that tin(IV) is not extracted with BPHA up to 5 M H_2SO_4 [5]. Chloride was added as NaCl solution, the ionic strength being maintained at 2 with Na_2SO_4 and sulfuric acid. Two concentrations of sulfuric acid — 0.5 M and 1 M — were studied. The ratio Sn:Cl in the aqueous phase was varied from 1:1 to 1:25, and 4.70×10^{-3} M BPHA in CCl_4 was used as organic phase.

Isolation of solid complexes. The tin(IV)—BPHA complex was isolated from the aqueous phase as follows: small amounts of tin(IV) were used to simulate extraction conditions and avoid the formation of polynuclear species, thus 4.21×10^{-4} M in 0.5 M HCl solution was precipitated with a 0.1% solution of BPHA in acetic acid. The precipitate was filtered on a sintered glass filter,

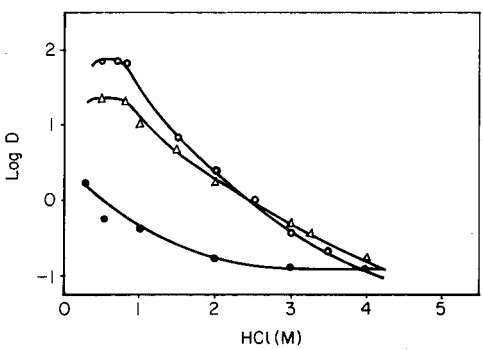

Fig. 1 Distribution of tin(IV) in the extraction with 4.7×10^{-3} M BPHA in different solvents: (○) carbon tetrachloride, (△) benzene, (●) chloroform.

washed quickly with small portions of 50% acetic acid to remove excess of reagent, dried at 105—110°C and recrystallized from ethanol.

To isolate the tin(IV)—BPHA complex from the organic phase, 10 cm^3 of a 0.1% solution of BPHA in CCl_4 was extracted stepwise with fresh 10-cm^3 portions of a 2.5×10^{-4} M Sn(IV) solution in 0.5 M HCl until the reagent was completely consumed (usually 10 extractions sufficed). Carbon tetrachloride was chosen because the distribution coefficient of Sn(IV) is higher than in chloroform. Then the organic phase was treated as described earlier [6]. The isolated complexes were analysed for tin, nitrogen and chlorine. The results are summarized in Table 1. I.r. spectra were measured (4000—250 cm^{-1}) in KBr on a Perkin-Elmer 457 spectrophotometer.

RESULTS AND DISCUSSION

In all the diluents studied, the tin(IV) extraction starts to decrease at the same HCl concentration, regardless of the K_d of the reagent or the nature of the diluent (Fig. 1). Investigations of the systems BPHA—HCl—$CHCl_3$, BPHA—HCl—C_6H_6 and BPHA—HCl—CCl_4 have shown that the reagent does not form dimers [7, 8], its K_d value remains constant up to 4—5 M HCl [8] and protonated species do not occur up to 6 M HCl [9]. The extraction curves cannot be explained by the instability of the complex at higher hydrogen ion concentrations as the distribution coefficient of tin(IV) decreases at HCl concentrations below 0.2 M. The extraction behaviour of tin(IV) is determined by changes in the state of tin(IV) in the aqueous phase with hydrochloric acid concentration. Up to 2 M HCl, the tetrachlorostannate(IV) species predominates, whereas at higher acidity $SnCl_5^-$ and $SnCl_6^{2-}$ are formed [10, 11]. Everest and Harrison [12] have established the presence of $SnCl_5^-$ and $SnCl_6^{2-}$ in less than 2 M HCl solutions. Comparison of these data with the extraction behaviour of tin(IV) indicate that quantitative extraction of tin(IV) with BPHA should be achieved in an acidity range where tin(IV) exists predominantly as the tetrachlorostannate species.

It is known that tin(IV) in anhydrous $SnCl_4$ is in sp^3 hybridization and the structure of $SnCl_4$ is perfectly tetrahedral. In the presence of water, hydrates with 2, 3, 4, 5 and 8 molecules of water may be formed [13]. Two molecules are linked coordinately, an electron pair from the water being transferred to

TABLE 1

Composition of the solid complexes

Composition	Sn (%)	Cl (%)	N (%)	Ratio	M.p. (°C)
Isolated from the aqueous phase	19.7	11.4	4.6		178—181
Isolated from the organic phase	19.4	11.45	4.7		178—180
Calculated	19.38	11.56	4.56	1:2:2	

the three 5*d*-orbitals of tin. An sp^3d^2 hybridization occurs and the tetrahedral structure becomes octahedral. The coordinately linked water molecules are in the *trans* position, the other molecules being hydrogen-bonded to chlorine atoms. Thus the ionic character of the Sn—Cl bond is increased [14], which is important for substitution with oxygen-containing ligands.

In hydrochloric acid solutions of $Sn(H_2O)_2Cl_4 \cdot nH_2O$, the increase in the HCl concentration increases the Cl^- activity, thus enhancing its complexing ability. Accordingly, water molecules are replaced and higher chloro complexes, $Sn(H_2O)Cl_5 \cdot nH_2O$ and $SnCl_6^{2-} \cdot nH_2O$ are formed. It is known that the six Sn—C bonds in $SnCl_6^{2-}$ are equivalent, and that the structure is octahedral. Thus the extraction behaviour of tin(IV) could be explained as follows: in slightly hydrochloric acid medium, tin(IV) is present as $Sn(H_2O)_2Cl_4 \cdot nH_2O$. In the presence of BPHA, one water molecule and one chlorine atom are replaced by one molecule of BPHA which acts as a bidentate ligand. The latter substitution is possible because of the imperfect octahedral structure of $Sn(H_2O)_2Cl_4 \cdot nH_2O$ and because the Sn—H_2O bond is weaker than the Sn—Cl bond. Owing to the *trans* effect of the BPHA molecule, one more molecule of BPHA may be introduced. At higher HCl concentrations, the predominant complex is $SnCl_6^{2-} \cdot nH_2O$, which is more stable and inert (perfect octahedral structure) so that the substitution of chlorine is hampered.

The number of BPHA species taking part in the extracted complex depends on the relationship $\log D / \log C_{HA_{tot}}$. In Fig. 2, the total concentrations of the reagent are plotted instead of the equilibrium concentrations, as these magnitudes are directly proportional [15]. The slopes of the curves for 0.5 M HCl, 1 M HCl and 1.5 M HCl are 2.04, 2.05 and 2.13 respectively. The results

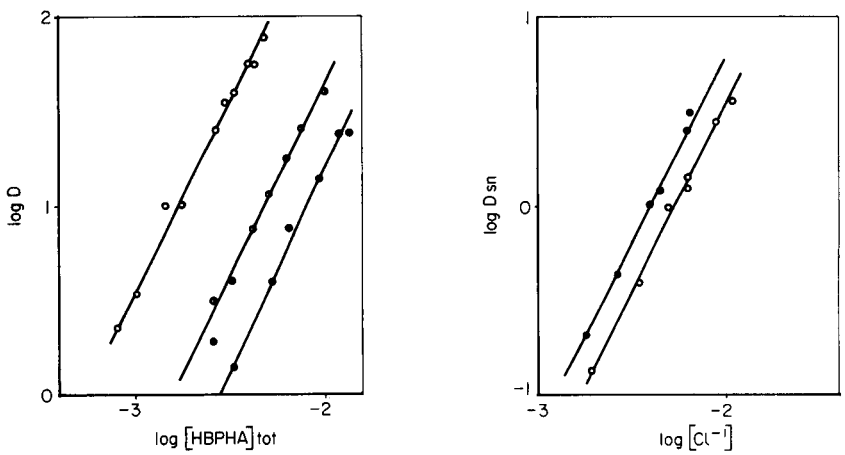

Fig. 2. Relationship between $\log D_{Sn}$ and $\log [HBPHA]_{tot}$ at: (○) 0.5 M HCl, (◒) 1.0 M HCl, (●) 1.5 M HCl. I = 2.0 (HCl + NaCl).

Fig. 3. Relationship between $\log D_{Sn}$ and $\log [Cl^-]$ at: (●) 0.5 M H_2SO_4, [○] 0.25 M H_2SO_4. [HBPHA] = 4.7×10^{-3} M; $I = 2(H_2SO_4 + Na_2SO_4)$.

indicate that the composition of the extracted complex is independent of the HCl concentration. The number of chlorine atoms in the extracted complex was determined from the dependence $\log D/\log [Cl]$ (Fig. 3). The slope of 2 obtained is in good agreement with earlier results [2]. The fact that the complex is effectively extracted from CCl_4 is evidence for the formation of a mixed neutral complex of the composition $SnCl_2(BPHA)_2$.

Investigation of the solid complexes

The structure of the tin(IV)—BPHA complex was studied by i.r. spectroscopy, the i.r. spectra of the complex and the free reagent being compared (Fig. 4) with regard to the C=O, N—OH and N—O stretching vibrations in the complexes.

The band of the free reagent at 1623 cm^{-1} is ascribed to —OH and —N—OH bonding because it disappears in the metal complex spectrum when hydrogen

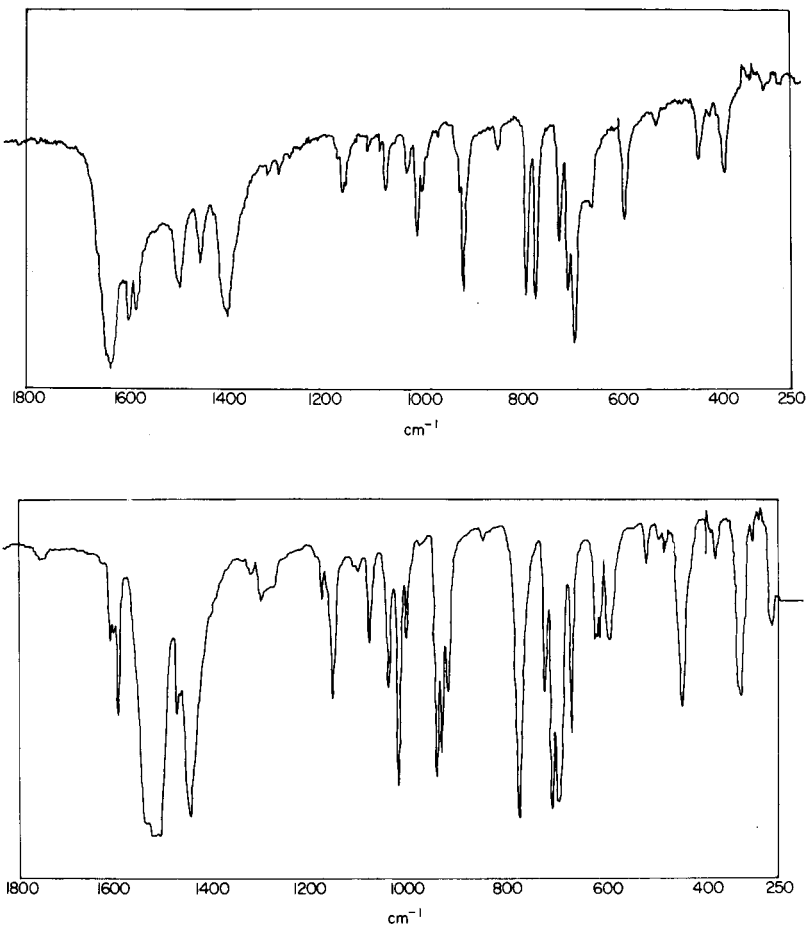

Fig. 4. I.r. spectra of (a) HBPHA and (b) the solid tin(IV)—BPHA complex isolated from hydrochloric acid medium.

atoms are replaced by metal atoms. The C=O stretching vibration in the compl is shifted to ca. 1510 cm^{-1} which corresponds to the formation of a coordinate CO— bond. N—O stretching of the free ligand is observed at 915 cm^{-1}; in the spectrum of the complex, this is shifted to two very close bands of medium intensity at 925 and 935 cm^{-1}. The shift to shorter wavelengths can be explaine by the proton replacement in the oxime group; the stronger the NO—M bond [16], the greater the shift. The band at 1015 cm^{-1} can also be assigned to the NO—M group; the N—O stretch bands of the complex are more intense than those of the free ligand. In the range 400—250 cm^{-1}, the new bands at 325 cm^{-1} (strong) and 375 cm^{-1} (weak) in the spectrum of the complex can be assigned to Sn—Cl, which is in good agreement with the data for the composition of the complex. The interpretation of the i.r. spectra of the complex confirms that the reagent is bidentate and that the extracted complex contains chloride.

In conclusion, the mechanism of the extraction process can be expressed by the equation

$$Sn(H_2O)_2Cl_4 + 2\ HBPHA \rightleftharpoons Sn(BPHA)_2Cl_2 + 2\ Cl^- + 2\ H^+ + 2\ H_2O$$

The extraction constant is

$$K_E = [SnCl_2(BPHA)_2]_0[Cl^-]^2[H^+]^2/[SnCl_4]\,[HBPHA]_0^2$$

As the complex is present in the organic phase, then $D_{Sn} = [Sn]_0/[Sn] = [SnCl_2(BPHA)_2]_0/[SnCl_4]$, and so $K_E = D_{Sn}\,[Cl]^2[H]^2/[HBPHA]_0^2$. At ionic strength 2 (0.5 M HCl + 1.5 M NaCl) and 25°C, the value obtained for the extraction constant was $K_{ex} = 6.80 \pm 0.02$ (with the restriction that no side-reactions involving complex formation occur in the aqueous phase).

The authors thank Mr. Konstantin Hashalov for the i.r. spectra.

REFERENCES

1 D. E. Ryan and G. D. Lutwick, Can. J. Chem., 31 (1953) 9.
2 S. J. Lyle and A. D. Shendrikar, Anal. Chim. Acta, 36 (1966) 286.
3 O. A. Vita, W. A. Levier and E. Litteral, Anal. Chim. Acta, 42 (1968) 87.
4 N. Jordanov, St. Mareva and M. Koeva, Anal. Chim. Acta, 59 (1972) 75.
5 E. E. Rakovsky and O. P. Petrukhin, Zh. Anal. Khim., 18 (1963) 538.
6 R. F. Fouche, H. I. le Roux and J. Phillips, J. Inorg. Nucl. Chem., 32 (1970) 1949.
7 D. Dyrssen, Acta Chem. Scand., 10 (1956) 353.
8 E. B. Smolina, I. V. Sokolova and I. P. Alimarin, Vestn. Mosk. Univ., 5 (1970) 629.
9 F. I. Lobanov, A. Kasak, B. N. Tarasovitch and I. M. Gibalo, Vses. Konf. Khimii Kompl. Soed., 1974.
10 B. Z. Iofa, P. Mitrofanov and M. V. Plotnikova, Radiokhimija, 6 (1964) 419.
11 M. Ishibashi, I. Yamamoto and Y. Inoue, Bull. Inst. Chem. Res., 37 (1959) 38.
12 D. A. Everest and J. H. Harrison, J. Chem. Soc., (1957) 1439.
13 R. S. Brune and W. Zeil, Z. Phys. Chem. N.F., 32 (1962) 384.
14 R. Negita, T. Okuda and M. Mishima, Bull Chem. Soc. Jpn., 42 (1969) 2509.
15 J. Hala, J. Inorg. Nucl. Chem., 29 (1967) 187.
16 A. T. Pilipenko, E. A. Schpak and L. L. Schevchenko, Zh. Neorg. Khim., 12 (1967) 463.

Analytica Chimica Acta, 104 (1979) 167—171

Short Communication

AN ION COUNTING—MULTICHANNEL ANALYSER SYSTEM FOR NEGATIVE-ION QUADRUPOLE MASS SPECTROMETRY

TOSHIHIRO FUJII

Division of Chemistry and Physics, National Institute for Environmental Studies, Yatabe, Tsukuba, Ibaraki 300-21 (Japan)

(Received 2nd May 1978)

Detection is an important problem in negative-ion quadrupole mass spectrometry. The negative-ion signals obtained from an electron multiplier have been processed with a commercially available negative-ion electrometer [1], but the electron multiplier and subsequent detection system must float at a high voltage; most mass spectrometers do not have this capacity. In addition the electrometer methodology does not meet sensitivity requirements sufficiently, particularly for negative-ion work in electron impact ionization mass spectrometry (m.s.).

The ion-counting technique enables very small ion currents [2, 3] to be measured, and a digital output of the ion-counting device is easily acquired with a multichannel analyser, which gives an accumulating facility similar to photoplate recording of sector-type m.s. Combination of the ion-counting device with the multichannel analyser [4, 5] therefore facilitates the processing of relatively low ion signals in negative-ion m.s.

The present communication reports the development of the ion counting—multichannel analyser system to meet sensitivity requirements in quadrupole m.s.; the combination is applied to negative-ion work at low signal levels and measurement of the negative-ion mass spectrum of acetonitrile given by conventional electron impact ionization quadrupole m.s. with the new method.

Experimental

Negative-ion counting techniques. Figure 1 shows a block diagram of the proposed system. The ion detector was a continuous dynode electron multiplier (Type H751, Galileo Electro-Optics Corp., Sturbridge, Mass.). The first dynode was maintained at 1000 V. The pulse output of the multiplier was capacitively coupled to the ion-counting device (Princeton Applied Research, Princeton, NJ). The 0.001-μF condenser coupling of the output permitted the multiplier anode to be operated at the maximum potential (5 kV) required for negative-ion detection.

The ion-counting device consisted of a preamplifier and an amplifier/discriminator [6] which discriminated against signals from background noise, e.g. photons, x-rays, or neutral molecules arriving at the detector.

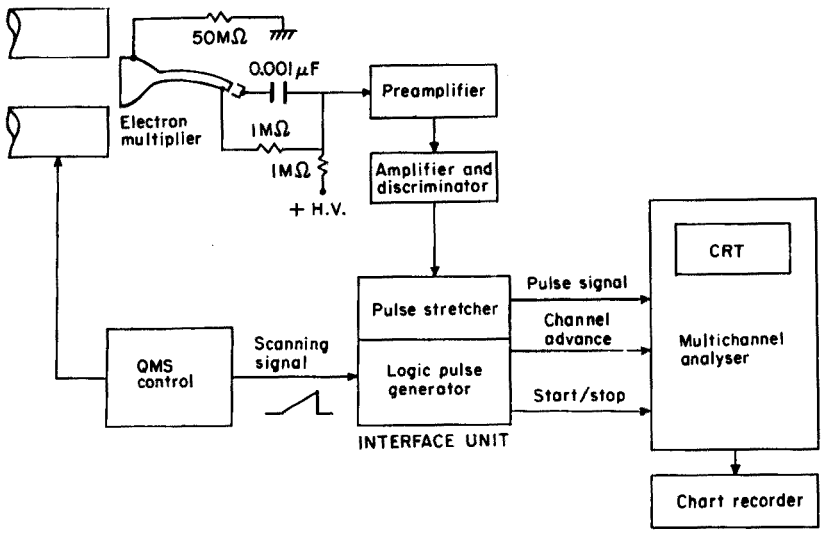

Fig. 1. Block diagram for ion-counting device—multichannel analyser combination and ion detector for negative-ion quadrupole m.s.

The system was designed for use with a 4100-C multichannel analyser (Canberra, Meriden, Conn.) without modification. To acquire the output of the ion-counting device at the analyser, an interface unit was manufactured in this laboratory. It consisted of a pulse stretcher to adjust the pulse signal of the ion-counting device to the acceptable input of the analyser and a logic pulse generator (triggering electronics). The quadrupole m.s. scan signal (ramp voltage, 0—10 V) was converted to supply logic pulses to the analyser for channel advance and start/stop of channel advance.

The analyser was operated in the multiscaling mode; the intensity is recorded in the channel memory as a function of m/e. Data in the channel memory were displayed in analog form on the oscilloscope (c.r.t.) of the analyser. Vertical displacement was proportional to ion count level and horizontal displacement was proportional to mass number. An alphanumeric indication of parameters, such as integrated counts over the channel memory and channel number, could be provided on the c.r.t. When the analyser was operated in the recurrent multiscaling mode, the periodic signals of the m.s. peaks were stored and accumulated in the memory of the analyser.

Figure 2 shows the timing diagram of the triggering logic pulses. The channel advance was automatically started by the pulse obtained from the starting signal of the periodical scan of the m.s. The stopping pulse was given by the returning signal of the scan. Both pulses were repeated throughout the duration of measurement. The pulse for channel advance was generated whenever a change of ca. 10 mV occurred in the ramp voltage of the m.s. scan signal.

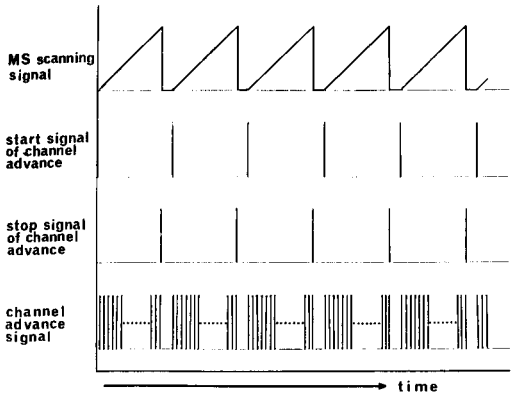

Fig. 2. Timing of the logic pulses for the analyser in the recurrent multiscaling mode.

Mass spectrometer. Negative-ion mass spectra were obtained with a Finnigan 3300F quadrupole m.s., operated in the electron impact ionization mode at an ion chamber potential of −2.5 V and a focusing lens potential of 22 V. The electron trap electrode was connected electrically to the ion chamber. The ion source power supply was modified to provide the optimum electrode voltage for negative-ion operations.

Operations. Measurement was performed as follows. The repetitive scanning of the m.s. started in the preset interval when the sample was introduced through the batch inlet. The resulting negative-ion currents, processed by the ion-counting device, were stored and accumulated with the analyser in the recurrent multiscaling mode until peaks of sufficient intensity were obtained. The accumulated mass spectral data were read out on a chart recorder.

Results and discussion

Figure 3 shows the negative-ion mass spectrum of acetonitrile in the single scanning mode; the intensity of the peaks is indicated by ion count numbers. The scan time was 5 s and the scanning mass range was from 1 to 50 amu. Acetonitrile (reagent grade, Wako Chemicals, Osaka, Japan) was introduced from a conventional batch inlet system with a needle valve as a molecular leak to the m.s. ion source. Sample pressure was 5×10^{-6} Torr. An electron energy of 8 eV gave the most abundant peak at m/e 40 (CH_2CN^-). The emission current was 12 μA.

The negative-ion mass spectrum of acetonitrile obtained in the 100 times recurrent multiscaling mode is shown in Fig. 4. The repetitive scan interval was 5 s. Other conditions were as in the single scanning mode.

Two additional peaks, CNH^- and C_2H^-, appeared in the accumulated mass spectrum compared with the mass spectrum in the single scanning mode. The accumulating property of the analyser enabled these negative fragment ions to be observed at very low signal levels.

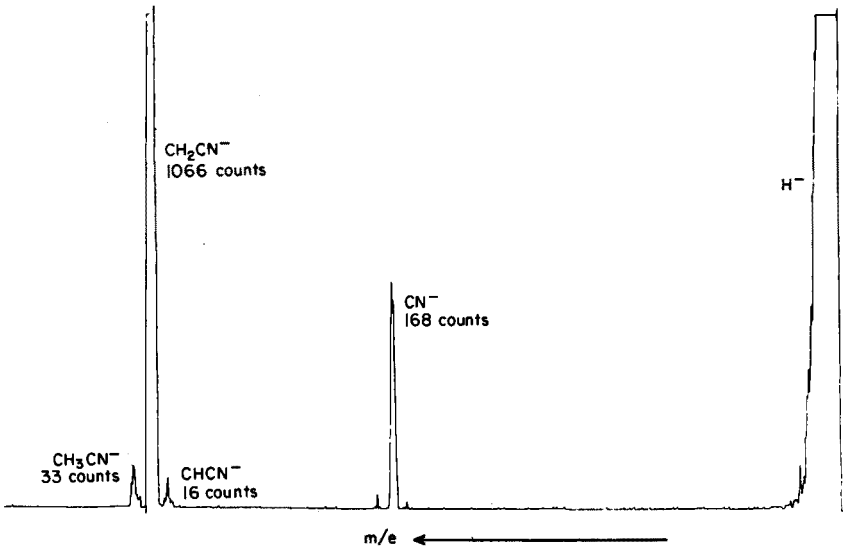

Fig. 3. Negative-ion mass spectrum of CH_3CN given by quadrupole m.s. in the single scanning mode.

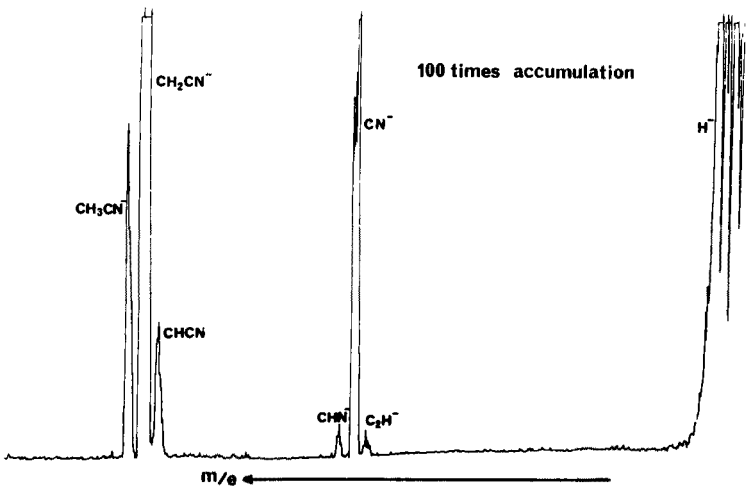

Fig. 4. Negative-ion mass spectrum of CH_3CN obtained in the 100 times recurrent multi-scaling mode, showing fragment ion peaks of CNH^- and C_2H^-.

This report may stimulate further applications of this method, e.g. negative-ion mass spectra corresponding to unknown peaks in gas chromatographic traces can be obtained after modification of the triggering electronics.

REFERENCES

1 A. L. C. Smit, M. A. J. Rossetto and F. H. Field, Anal. Chem., 48 (1976) 2042.
2 G. Goby and L.-D. Nguyer, Int. J. Mass Spectrom. Ion Phys., 20 (1976) 305.
3 E. Yellin, L. I. Yin and I. Adler, Rev. Sci. Instrum., 41 (1970) 18.
4 H. Miyake and M. Michijima, Mass Spectrom. (Jpn.), 19 (1971) 110.
5 J. Freudenthal and L. G. Gramberg, Anal. Chem., 49 (1977) 2205.
6 T. Fujii, Anal. Chim. Acta, 92 (1977) 117.

Analytica Chimica Acta, 104 (1979) 173—176

Short Communication

THE DETERMINATION OF TRACE AMOUNTS OF ARSENIC IN WASTEWATERS BY NON-DISPERSIVE ATOMIC FLUORESCENCE SPECTROMETRY AFTER HYDRIDE GENERATION

TAKETOSHI NAKAHARA*, SYOJI KOBAYASHI and SÔICHIRÔ MUSHA

Department of Applied Chemistry, College of Engineering, University of Osaka Prefecture, Mozu-umemachi, Sakai 591 (Japan)

(Received 24th February 1978)

A recent paper reported [1] that the smallest amount of arsenic determinable by a.f.s. is limited principally by the high reagent blank (ca. 20 ng of arsenic) to around 30 ng of arsenic in the zinc—tin(II) chloride—potassium iodide reduction method. Some authors have reported lower reagent blanks for arsenic in the sodium borohydride reduction method by a.a.s. [2] and a.f.s. [3]. This communication describes the non-dispersive a.f.s. of arsenic by the $NaBH_4$ method and a comparison with the $Zn—SnCl_2—KI$ method. The method is applied to the determination of trace amounts of arsenic in wastewater samples.

Experimental

Reagents and apparatus. The reagents and apparatus were essentially as described [1, 4] unless otherwise specified. The optimum acidities for 20-ml samples are 0.1 and 2.0 M hydrochloric acid in the $NaBH_4$ and $Zn—SnCl_2—KI$ methods, respectively.

Procedure. Arsine generated by reduction for 60 and 80 s in the $NaBH_4$ method (0.05 g $NaBH_4$) and $Zn—SnCl_2—KI$ method (one zinc tablet containing 0.6 g Zn [4], 1.0 ml of 10% $SnCl_2$ and 1.0 ml of 20% KI), respectively, is introduced into the premixed argon (entrained air)—hydrogen flame (hydrogen, 4.0 l min^{-1}; argon carrier gas, 4.0 l min^{-1}; argon auxiliary gas, 2.0 l min^{-1}) and is atomized in the flame. Fluorescence, excited with an arsenic electrodeless discharge lamp, is detected at right angles to the axis of the optical path with a "solar blind" photomultiplier (R-166, Hamamatsu TV Co.) and recorded simultaneously on a pen recorder and a digital integrator for peak height and peak area measurements, respectively. Other optimum conditions were as reported previously [1, 4].

Results and discussion

Analytical working curve, sensitivity and precision. Analytical working curves for arsenic by non-dispersive a.f.s., under the optimized conditions,

are shown in Fig. 1; the smallest amount of arsenic determinable by the borohydride method is ca. one order of magnitude lower than by the Zn—$SnCl_2$—KI method. The detection limits [5], are 2 and 0.5 ng of arsenic in the borohydride and Zn—$SnCl_2$—KI methods, respectively. Thus in the borohydride method the lowest determinable amount of arsenic is not restricted by the reagent blank (ca. 1 ng of arsenic).

The precision of the determination of arsenic by non-dispersive a.f.s. is shown in Table 1.

Effect of acids. In the Zn—$SnCl_2$—KI method, the presence of perchloric, phosphoric and sulfuric acids in the range up to 2.0 M causes no interference, whereas more than 0.001 M nitric acid interferes with the fluorescence measurements [1]. The effects of nitric, perchloric, phosphoric and sulfuric

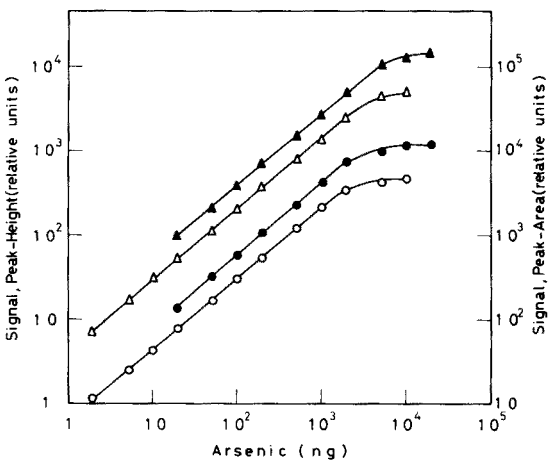

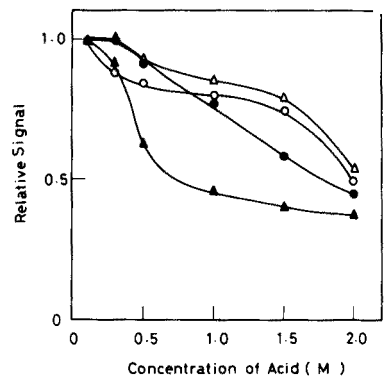

Fig. 1. Analytical working curves for arsenic by non-dispersive a.f.s. (▲) Zn—$SnCl_2$—KI method, peak-area measurement; (△) $NaBH_4$ method, peak-area measurement; (●) Zn—$SnCl_2$–method, peak-height measurement; (○) $NaBH_4$ method, peak-height measurement.

Fig. 2. Effect of acids on a.f.s. of arsenic in the $NaBH_4$ method. (△) Nitric acid; (○) sulfuric acid; (●) perchloric acid; (▲) phosphoric acid.

TABLE 1

Precision of the non-dispersive a.f.s. of arsenic

Arsenic (ng)	$NaBH_4$ method (%)[a]		Zn—$SnCl_2$—KI method (%)[a]	
	Peak height	Peak area	Peak height	Peak area
1000	3.3	2.7	7.3	5.2
100	3.4	3.2	10.9	8.9
10	5.6	4.6	—[b]	—[b]

[a]Relative standard deviation calculated from ten measurements.
[b]Not measurable because of reagent blank.

acids on the fluorescence signal from 400 ng of arsenic in the $NaBH_4$ method are shown in Fig. 2; the relative atomic fluorescence signal is the ratio of the peak-height signal for arsenic in the presence of the acid to that for arsenic alone. The interference of nitric and sulfuric acids is similar to that observed in the a.a.s. of arsenic [6].

Effects of diverse elements. For a.a.s. of arsenic combined with a hydride generation technique, the effects of diverse elements have been reported [2, 6, 7]. The effects of 1000-fold amounts of diverse elements (compounds as used [1] previously) on the fluorescence signal of 500 ng of arsenic are shown in Table 2 (relative atomic fluorescence signal as stated for Fig. 2). Table 2 also compares the results of the interference study for the Zn—$SnCl_2$—KI method described previously [1] with those for the $NaBH_4$ method. The results are close to those reported for a.a.s. [6, 7]. Most of the interferences from diverse elements are probably related to the reduction process for arsenic to arsine. The remarkable enhancement of arsenic fluorescence by bismuth in the borohydride method has been discussed [4, 8]. In the Zn—$SnCl_2$—KI method, production of bismuth hydride appears to be insignificant [1]. There is little or no significant difference in the effect of diverse elements on peak-height and peak-area measurements (Table 2).

TABLE 2

Effect of diverse elements on the a.f.s. of arsenic

Element	Compound added	Relative atomic fluorescence signal		
		$NaBH_4$ method		Zn—$SnCl_2$—KI method Peak height (Ref. 1)
		Peak height	Peak area	
Au	$HAuCl_4$	0.01	0.01	1.01
Co	$CoCl_2$	0.28	0.28	0.89
Fe	$FeCl_3$	0.49	0.56	0.88
Ni	$NiCl_2$	0.06	0.05	0.88
Pd	$PdCl_2$	0.00	0.01	0.05
Pt	H_2PtCl_6	0.00	0.01	0.07
Bi	$Bi(NO_3)_3$	5.89	6.95	0.84
Sb	$SbCl_3$	0.40	0.57	0.51
Se	SeO_2	0.51	0.44	0.76
Sn	$SnCl_2$	0.30	0.35	—
Te	metal in HCl	0.19	0.20	0.41

No interference[a] in the $NaBH_4$ method: Ag[b], Al[c], B[c], Ba[d], Be[c], Ca[c], Cd[c], Ce[b], Cr[d], Cs[b], Cu[b], Ga[b], Hg[d], In[b], K[b], La[c], Li[d], Mg[b], Mn[b], Na[b], Pb[b], Rb[b], Si[b], Sr[b], Tl[c], V[b], W[b], Y[b] and Zn[b].

[a]Relative atomic fluorescence signal of 0.9—1.1.
[b]No interference in the Zn—$SnCl_2$—KI method [1].
[c]Relative atomic fluorescence signal of 0.8—0.9 except for boron which gives a relative atomic fluorescence signal of 1.15 in the Zn—$SnCl_2$—KI method [1].
[d]Relative atomic fluorescence signal of 0.3—0.8 in the Zn—$SnCl_2$—KI method [1].

TABLE 3

Determination of arsenic in wastewaters by a.f.s. and a.a.s. (Results are given in ppb.)

Sample	A.f.s.[a]		A.a.s.[b]
	Peak height	Peak area	
1	11.2 ± 1.0	10.8 ± 0.6	10.9
2	8.8 ± 0.4	8.7 ± 0.4	8.5
3	1.09 ± 0.12	1.18 ± 0.09	—[c]
4	0.32 ± 0.05	0.33 ± 0.02	—[c]
5	0.29 ± 0.04	0.32 ± 0.04	—[c]
6	0.27 ± 0.03	0.28 ± 0.02	—[c]
7	0.25 ± 0.03	0.25 ± 0.02	—[c]

[a]Average of five determinations. [b]Average of three determinations. [c]Not determinable.

Application to the determination of arsenic in wastewaters. A sample taken at the inlet of the Wastewater Treatment Facility, University of Osaka Prefecture, was immediately acidified to give a hydrochloric acid concentration of 0.1 M. The arsenic was determined (analytical working curve linearities of ca. three orders of magnitude) by the borohydride method. The results obtained for peak-height and peak-area measurements are shown in Table 3. Atomic absorption measurements at 193.7 nm in a premixed argon (entrained air)—hydrogen flame produced with a "multi-flame" burner [9—11] gave results in good agreement with those obtained by non-dispersive a.f.s.

REFERENCES

1 T. Nakahara, T. Tanaka and S. Musha, Bull. Chem. Soc. Jpn., 51 (1978) 2046.
2 Y. Yamamoto and T. Kumamaru, Fresenius Z. Anal. Chem., 281 (1976) 353.
3 K. C. Thompson, Analyst, 100 (1975) 307.
4 T. Nakahara, S. Kobayashi and S. Musha, Anal. Chim. Acta, 101 (1978) 375.
5 IUPAC, Nomenclature, Symbols, Units and their Usage in Spectrochemical Analysis, Part II, Section 4.1, Revision 1975 [Pure Appl. Chem., 45 (1976) 99].
6 F. D. Pierce and H. R. Brown, Anal. Chem., 49 (1977) 1417.
7 A. E. Smith, Analyst, 100 (1975) 300.
8 R. M. Dagnall, K. C. Thompson and T. S. West, Talanta, 14 (1967) 1467.
9 T. Nakahara, H. Date, M. Munemori and S. Musha, Bull. Chem. Soc. Jpn., 46 (1973) 637.
10 T. Nakahara and S. Musha, Anal. Chim. Acta, 75 (1975) 305.
11 T. Nakahara and S. Musha, Anal. Chim. Acta, 80 (1975) 47.

Analytica Chimica Acta, 104 (1979) 177—180

Short Communication

DETERMINATION OF ARSENIC IN URINE BY ATOMIC ABSORPTION SPECTROMETRY WITH ELECTROTHERMAL ATOMIZATION

F. PETER*, G. GROWCOCK and G. STRUNC
Laboratory Services Branch, Ontario Ministry of Health, Box 9000, Toronto, M5WIR5 (Canada)

(Received 7th April 1978)

A widely used, sensitive and convenient method for the determination of arsenic in urine is flameless a.a.s. Manual methods [1—3] are rather tedious when large numbers of samples are to be assayed. An automated system for the determination of arsenic in water [4, 5] has been applied to the determination of arsenic in atmospheric particulate matter [6] and in soil and vegetation [7] after digestion of the samples. The optimal conditions of the automated assay have been determined and the method used to evaluate the range of arsenic in urine samples from the general population and from a group of industrial workers.

Experimental

Reagents. A mixture of nitric acid and perchloric acid (1 + 1) was used to digest the urine samples. The digested specimens were treated with sodium borohydride to convert arsenic(V) to arsine. Sodium borohydride solutions were prepared by dissolving 5, 10, 20, 30 and 40 g of $NaBH_4$ (96%, BDH) in 0.05 M sodium hydroxide solution and adjusting to 1 l.

To release hydrogen from alkaline $NaBH_4$ solution, dilute sulphuric acid was used; 0.125, 0.25, 0.5, 0.75 and 1.25 M solutions were tested.

For the calibration curve, 50—200 ppb arsenic solutions, prepared from 1000-ppm atomic absorption arsenic standard (Fisher Scientific) by serial dilution with distilled water, were used.

Apparatus. The on-stream generation of arsine was carried out with a Technicon proportioning pump III and the manifold shown in Fig. 1. Arsine, separated in a gas—liquid separator, was swept with purified nitrogen into the heated optical cell To eliminate water vapour, the arsine was passed through concentrated sulphuric acid in a gas washing bottle. The effect of the flow rate of nitrogen was studied over the range of 100—600 ml min^{-1}.

The atomic absorption of arsenic was measured with a Varian-Techtron AA Model 1250 spectrometer with automatic background corrector (Model BC-6). The absorption peaks were recorded with a Varian-Techtron recorder, set at 10-mV full scale sensitivity. The spectrometer was operated in the concentration mode with 20-fold scale expansion.

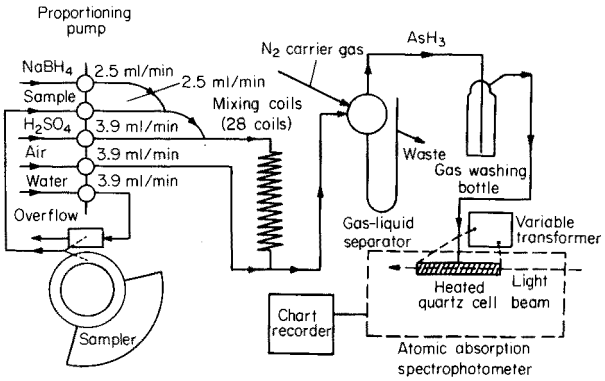

Fig. 1. Manifold for arsenic determination.

The optical cell (10 mm i.d., 160 mm long), wound with insulated chromel "A" wire, B & S gauge 22 (Fisher Sci.) to which 84 V was applied, was thermally insulated with two layers of asbestos string.

Procedure. Urine (2 ml) was pipetted into test tubes (18 × 150 mm) held in an aluminium heating block. The digesting acid (2 ml) was added and the heating block was kept on a hot plate (200 ± 20°C) until ca. 0.5 ml of fluid remained (4—6 h). This fluid was transferred to a graduated conical tube and the volume was made up to 4 ml with distilled water. The tubes were covered with Parafilm, vortex-mixed for 15 s and placed in a water bath (50°C) for 1 h. During this time any precipitate dissolved completely. The clear solutions were transferred to 10-ml Technicon sample cups. The samples were mixed in the manifold with sodium borohydride, and then with sulphuric acid. The generated arsine was separated from the liquid in a gas—liquid separator, dried as described, and swept by a stream of nitrogen into the heated quartz tube positioned in the light path of the arsenic lamp for measurement at 193.7 nm.

Results and discussion

Determination of optimal conditions. To determine the optimal conditions with the automated system, the following parameters were investigated with a solution of arsenic (100 ppb).

The peak height reached a maximum when the borohydride concentration was increased from 5 to 20 g l^{-1}, hence a 20 g l^{-1} concentration was chosen. The effects of using 0.125—1.25 M sulphuric acid solutions were studied. There was no significant increase in peak height at concentrations over 0.75 M which was therefore selected.

The effect of the flow rate of nitrogen was tested for 100—600 ml min^{-1}. The lower the flow rate, the higher the peak, but with decreasing flow rate, the carryover increases as there is insufficient nitrogen to purge the optical cell between consecutive samples. The optimal flow rate of 300 ml min^{-1} was chosen since at this flow rate the carry over was eliminated and a satisfactory sensitivity was still obtained. Peaks of arsenic up to 2 mg l^{-1} can be recorded with this flow rate.

With 20 g l^{-1} sodium borohydride solution, 0.75 M sulphuric acid, and 300 ml min^{-1} of nitrogen, the peak height increased as the sampling time was increased from 5 to 40 s but over 40 s no further increase was observed. Although 40 s would have ensured the greatest sensitivity, 20 s was chosen as the optimum because the peak became too broad at greater sampling times and the proportionality between concentration and peak height was lost.

The effect of washing time was investigated at 20, 40, 60, 80 and 100 s for the conditions recommended above. The 100-ppb standard was sampled three times, consecutively, to find how reproducible were the peaks and how the washing time influenced the peak height. At short washing times there is some carryover which leads to a gradual increase in peak height in consecutive recordings; moreover, the peaks did not return to the baseline and a false positive result would be obtained for a sample with low arsenic concentration following a sample with a high arsenic concentration. Although the carryover was eliminated at a washing time of 80 s, a cam that gave a sampling time of 20 s and a washing time of 100 s, with which 30 samples can be handled per hour, was used.

Determination of the range of arsenic in urine. To determine the normal level of arsenic in urine, specimens from 200 hospital patients apparently free from any symptoms of arsenic poisoning were used. Specimens from 50 workers in a lead battery plant were used to find if industrial workers, not directly exposed to an arsenic environment, showed any elevation in their arsenic level. For these 250 samples, the optimal assay conditions (2% $NaBH_4$, 0.75 M H_2SO_4, 300 ml min^{-1} nitrogen, 20-s sampling time, 100-s washing time) were used.

To see whether digestion of the urine samples influenced the results, peak heights for the five standard arsenic solutions were determined with and without digestion. The results showed that digestion does not influence the recovery of arsenic. An arsenic-free urine sample (arsenic concentration less than 1 ppb) was spiked with arsenic to give 20, 40, 60, 80 and 100 ppb arsenic concentrations. After digestion, the spiked samples were brought to volume; the arsenic recoveries varied between 96% and 110% with no apparent trend as a function of the concentration. This indicated that the other constituents of urine do not influence the recovery of added arsenic after digestion.

The calibration curve was constructed from peak heights of 28, 47, 60 and 70 scale divisions for 50, 100, 150 and 200 ppb of arsenic, respectively. Reproducibility of the peaks was checked at low (50 ppb) and high (200 ppb) concentrations. The relative standard deviation was 2.80% at low concentration and 1.67% at high concentration, both based on 20 replicate assays. The peak height is influenced by the nitrogen flow rate, the temperature of the heated absorption cell, and the volumes of the sample and of the reagents; as these parameters are not entirely reproducible from day to day, the calibration curve must be recorded each time the system is used.

The results indicated that the normal population, not directly exposed to an arsenic environment, has an arsenic level in urine of less than 10 ppb. Only

4 urine specimens, all from lead battery plant workers, had arsenic levels between 10 and 30 ppb. The toxic level of arsenic is considered to be ca. 100 ppb.

The authors express their appreciation to Mr. P. N. Vijan for helpful suggestions in setting up this method.

REFERENCES

1 R. C. Chu, G. P. Barron and P. A. W. Baumgarner, Anal. Chem., 44 (1972) 1476.
2 T. Maruta and G. Sudoh, Anal. Chim. Acta, 77 (1975) 37.
3 R. D. Wauchope, At. Absorpt. Newsl., 15 (1976) 6467.
4 P. D. Goulden and P. Brooksbank, Anal. Chem., 46 (1974) 1431.
5 F. D. Pierce, T. C. Lamoreaux, H. R. Brown and R. S. Fraser, Appl. Spectrosc., 30 (1976) 38
6 P. N. Vijan and G. R. Wood, At. Absorpt. Newsl., 13 (1974) 33.
7 P. N. Vijan, A. C. Rayner, D. Sturgis and G. R. Wood, Anal. Chim. Acta, 82 (1976) 329.

Analytica Chimica Acta, 104 (1979) 181—183

Short Communication

SPECTROPHOTOMETRIC DETERMINATION OF THE pH SCALE IN ETHANE-1,2-DIOL

M. BREANT*, N. ARNAUD and S. DESMETTRE

Equipe de Recherche associée au C.N.R.S. n° 474, Laboratoire de Chimie Analytique III, Université Claude Bernard - Lyon I, F-69621 Villeurbanne Cedex (France)

(Received 1st May 1978)

Acid—base equilibria in ethane-1,2-diol have been investigated by means of potentiometric determinations with a hydrogen [1, 2] or glass [3] electrode and by a "potentiometric—spectrophotometric" method [3]. Following on previous work in *N*-methylpyrrolidone [4], dimethylacetamide [4] and formic acid [5], the present communication deals with the establishment of a pH scale in ethane-1,2-diol by spectrophotometric determinations. The general principles of this method have been reported previously for the other solvents.

Experimental

Chemicals and apparatus. Ethane-1,2-diol (Carlo Erba RP) was used without further purification. Acids, bases and indicators (Merck, Fluka, Carlo-Erba or R.A.L.) were as received.

Absorbances were measured with a Beckman 24 Spectrophotometer; potentiometric acid—base titrations were performed with a MINISIS Tacussel-Solea millivoltmeter. The flow cell assembly used was similar to that described by Bréant and Buisson [6]; the solution was circulated with a minipump (Jobin and Yvon).

Procedure. Acids were titrated with tetramethylguanidine, imidazole, or sodium hydroxide, and bases with *p*-toluene sulfonic acid or salicylic acid, according to their strength. The titrations were followed by simultaneous absorbance and potentiometric measurements; a glass electrode filled with ethane-1,2-diol was used with an Ag/AgCl reference electrode (KCl_{sat} in ethane-1,2-diol). The potentiometric curves were used only for locating the end-point of the titrations so as to avoid calibration of the solutions; pK_A values were determined exclusively from spectrophotometric data.

Results

The sequence of the determinations is summarized in Fig. 1, where the values of the acidity constants, pK_a, of the considered product are shown; K_i is the self-ionization product of the solvent.

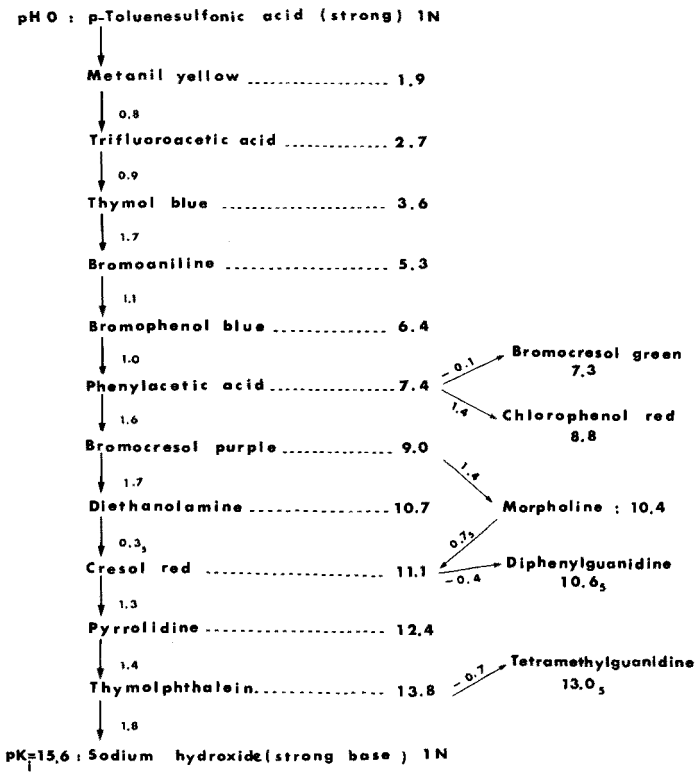

Fig. 1. Spectrophotometric determination of pK_a values. Arrows indicate the order of the determinations. Large numbers show the pK_a value of the product considered. Small numbers show the differences between the pK_a values of the indicators and acids or bases.

TABLE 1

Comparison between spectrophotometric (S) and potentiometric (P) determinations of some acidity constants in ethane-1,2-diol

Solute	$S \pm 0.2$ at 25°C	P[a]
Trifluoracetic acid	2.7	$2.6_5 \pm 0.2$[b]
Thymol blue	3.6	3.39 ± 0.01 (3)
Bromoaniline	5.3	5.4 ± 0.2[b]
Bromophenol blue	6.4	6.49 ± 0.07 (3)
Bromocresol green	7.3	7.38 ± 0.02 (3)
Phenylacetic acid	7.4	8.06 ± 0.03 (1)
Bromocresol purple	9.0	9.00 ± 0.03 (3)
Morpholine	10.4	10.14 ± 0.03 (1)
Diphenylguanidine	10.6_5	10.9 ± 0.2[b]
Diethanolamine	10.7	$10.5_3 \pm 0.03$ (1)
Cresol red	11.1	11.07 ± 0.02 (3)
Tetramethylguanidine	13.0_5	12.9 ± 0.2[b]
pK_i	15.6	15.2 ± 0.3 (2)
		15.60 ± 0.02 (1)
		15.4 ± 0.2 (7)

[a] [1] at 30°C; [2, 3, 7] at 25°C. [b] At 25°C; unpublished results from this laboratory.

A comparison of the present spectrophotometric determinations with the results previously obtained by potentiometry shows a close fit between the different values of the constants pK_a or pK_i (Table 1). The successful use of the indicators for acid—base titrations in glycol has been reported [8].

REFERENCES

1 K. K. Kundu and M. N. Das, J. Chem. Eng. Data, 9 (1964) 82.
2 M. Bréant and J. Georges, J. Electroanal. Chem., 68 (1976) 165.
3 P. Zikolov and O. Budevsky, Talanta, 20 (1973) 487.
4 M. Bréant, A. Auroux and M. Lavergne, Anal. Chim. Acta, 83 (1976) 49.
5 M. Bréant, C. Beguin and C. Coulombeau, Anal. Chim. Acta, 87 (1976) 201.
6 M. Bréant and C. Buisson, Anal. Chim. Acta, 56 (1971) 197.
7 G. Velinov, P. Zikolov, P. Chakarova and O. Budevskii, Talanta, 21 (1974) 163.
8 M. Bréant, A. Aurox and M. Lavergne, Analusis, 6 (1978).

Analytica Chimica Acta, 104 (1979) 185—189

Short Communication

FLOW MULTI-INJECTION ANALYSIS — A SYSTEM FOR THE ANALYSIS OF HIGHLY CONCENTRATED SAMPLES WITHOUT PRIOR DILUTION

JENS MINDEGAARD

The Central Laboratory, Roskilde County Hospital, DK-4000 Roskilde (Denmark)

(Received 16th May 1978)

Since the introduction of flow injection analysis (f.i.a.) [1], the general principle has evolved very quickly [2]. In f.i.a. a liquid sample is injected into a carrier stream of reagent without air segmentation; the precisely timed reactions can provide good accuracy and precision. This simple cheap analyzer utilizes slow pumping rates which result in low reagent costs. This technique, however, could not be recommended for analyses of highly concentrated samples because the large dispersion required in such systems would give significant carryover resulting in low sampling rates.

This communication describes a medium-dispersion design for the analysis of highly concentrated samples without prior dilution. In this design, which may be called flow multi-injection analysis, the sample is injected in parallel with reagent(s) into the carrier stream. For precise synchronization of the injections, a multi-injector is utilized. For the analysis of concentrated samples, the fall (or rise) of the sample injection peak is synchronized with the peak maximum of the reagent(s), thus producing a dilution proportional to the distance between the sample and reagent(s) peaks. This method of dilution is independent of the other characteristics of the f.i a. system.

The proposed method was tested by injection of dichromate solutions and for the determination of human albumin by the bromocresol green method.

Experimental

Instrumentation. Carrier streams were pumped with an Isomatec Mini S840 peristaltic pump into the manifold (Fig. 1), into which sample and reagent were introduced by an injector (Fig. 2). The mixture passed through a flow-cell (see below) placed in a Gilford Stasar III spectrophotometer and thence to waste. The spectrometer signal was continously recorded with a Servogor S recorder

Polyethylene tubes (0.50 mm i.d.) were used throughout the manifold.

Injector. The circular sandwich-type injection unit (Fig. 2A) was made from two perspex cylindrical stators (each 10-mm high, 50-mm diameter) separated by a cylinder (15-mm high, 30-mm diameter). A 4-mm hole was drilled

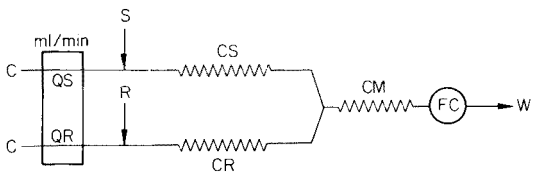

Fig. 1. The double injection system consisting of a pump which feeds carrier streams, C, at pumping rates QS and QR into the coils CS and CR (0.50-mm i.d.) which merge in the reaction coil, CM, leading to the flow cell, FC, and then to waste, W. S and R mark the points of injection of the sample and reagent with the same injector.

through the centres of the three cylinders (Fig. 2B). Parallel to this, two holes were drilled near the edge of the stators. The central hole held the pivot, and the two other holes held pins which prevented the stators from turning with the rotor and also served as stop pins. The pivots were fixed to a flat metal base mounted on a support. The top of the central pivot was provided with a spring and nut to keep the stator/rotor contact surfaces together at an adjustable but constant pressure. Pairs of axially drilled bores (0.8 mm) 8 mm from the centre, had conical outlets for mounting the tubes, and were furnished with bypasses between the two stators.

The volume of the bore through the rotor, which can be varied with bore height and diameter, was the volume of the injection chamber. In the present experiments, the diameters were 0.8 and 1.1 mm which produced injection volumes of 8 and 15 μl

Sample and reagent were introduced (cf Fig. 2C and D) into the injection chambers by aspirating through a 0.4-mm i.d. tube. Because this diameter was smaller than that of the rest of the system, this loading tube served as a filter — which was easy to clean or change if necessary. The dead space of the loading system can be reduced to less than 50 μl; by aspirating air and a few μl of the next sample and air, the injector can be cleaned in a few seconds, so that the carryover will be less than 1%.

Flow cell. A 1.0-mm wide hole was drilled centrally in the 13 × 8-mm side of a perspex block (13 × 14 × 8 mm). Near the ends of this bore, 0.8-mm holes were drilled as shown in Fig. 3; these holes had conical outlets to fit the polyethylene tubes (i.d. 0.50 mm). This 11-μl cuvette (pathlength 14 mm) was sealed by glueing 0.1 × 4 × 4 mm glass windows with araldite over the ends of the 1.0-mm bore. The window on the detector side was covered with black tape which had an aperture of 0.9-mm diameter. Two screws through the 13 × 14 mm face fixed the cuvette block to a 1 × 10 mm steel body which formed a three-point, adjustable support.

Reagents. The carrier solution used throughout was a 0.1% solution of Brij 35 (Merck) in distilled water. Potassium dichromate (Merck p.a.) solutions in 5×10^{-3} M sulfuric acid were used to test the system. The bromocresol green reagent used was that described by Webster [3]. A 10% human serum albumin standard (AV KABI) was diluted with distilled water to give solutions containing 10, 20, 30, 40, 50, 60 and 70 g l^{-1}.

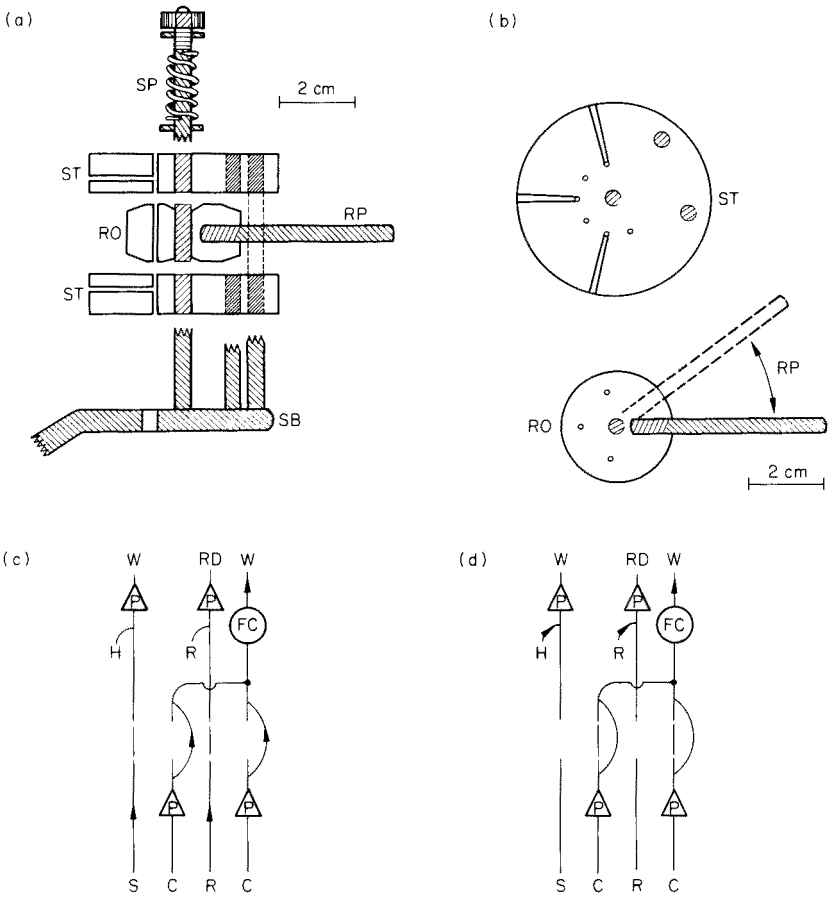

Fig. 2. Double injection system. (A) Side view of injector: the steel body, SB, furnished with three pivot pins, forms the base against which the spring on the central pivot, SP, presses the stators, ST, and the rotor RO, at a constant but adjustable pressure; the bore in the rotor forms the injection chamber whereas the bores in the stators are connected to a bypass. To turn from the loading to the injection position, the pin, RP, is moved between the two pivot pins which also prevent the stators from turning round the central pivot. (B) Top view of injector: the stator, ST, fixed by three pivots, is shown with three pairs of bores and their radial bypasses; the rotor, RO, can be turned between the loading and injection positions by the pin, RP. (C) Loading position: sample, S, is aspirated into an injection chamber by pump, P, and from there to waste, W; reagent, R, is introduced in the same manner, but its excess, diluted by one injection volume per injection, can be accumulated for re-use at RD (or go to waste); in this injector position, carrier solution, C (the same solution is used here for sample and reagent), is pumped via bypasses to the detector, FC, and then to waste, W. (D) Injection position: the sample and reagent chambers are turned into the carrier stream so that the carrier, C, flows through the chambers and pushes selected volumes of sample and reagent into their respective coils; the sample tube aspirates water, H (or sample waste) in a parallel high-resistance coil. The reagent tube aspirates reagent, R (or RD or water) in a parallel high-resistance coil leading to a reagent deposit (RD) which can be re-used.

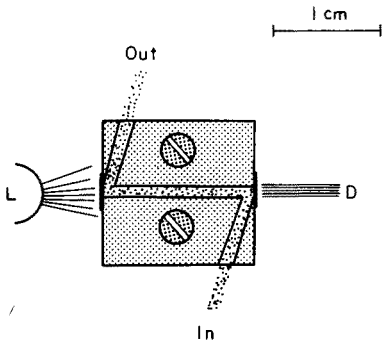

Fig. 3. Flow cell. The transmitted signal from light source L is detected by D; the cell is fixed to the support by the two screws shown.

Results and discussion

The injector (Fig. 2) was found to be very reliable and easy to inspect and clean. It was convenient to place several pairs of bores through the injector for multi-injection purposes. The flow cell is of simple construction. The optical pathlength and type of windows (quartz, glass or optical filters) can be chosen as required. There were no air-bubble problems.

The dichromate tests with measurements at 370 nm showed that it is possible to overlap peak profiles by simultaneous injection of two solutions (Fig. 4), the precision of the resulting peak measurements being better than 1%. With maximal overlap the sampling rate will be the same as in conventional f.i.a.

Serum albumin was determined by the bromocresol green method (Fig. 5) by calculation from the height of the second peak formed on measurement

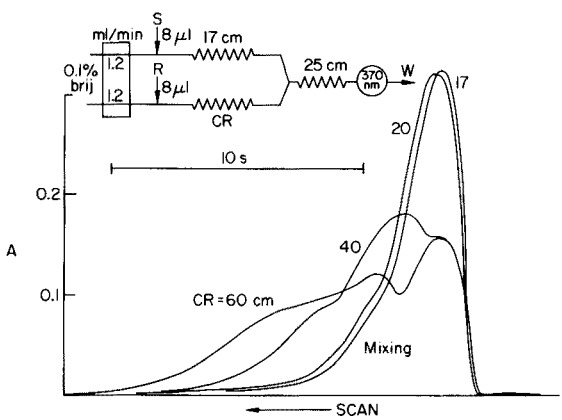

Fig. 4. Mixing patterns formed by systems with various coil lengths. At points S and R were simultaneously injected 8 µl of 2.0×10^{-3} M dichromate solution. By changing the length of CR from 17 to 60 cm, different peak forms can be obtained.

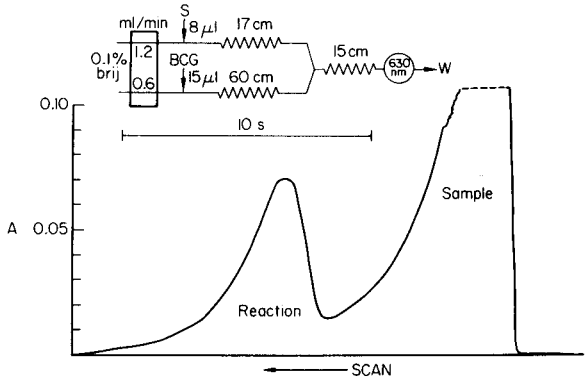

Fig. 5. Albumin determination. Two Brij 35 solution carrier streams were used, and 8 µl of albumin standard (S) and 15 µl of bromocresol green reagent (BCG) were injected simultaneously. After mixing in the coils, and merging of the streams, the reaction started. In this experiment, the reagent was delayed by using slower pumping rate and longer coil than in the sample line. The absorbance at the reagent peak position originates mainly from reaction, because BCG itself does not absorb in this system, and the sample absorbance was negligible at the reagent position.

at 630 nm. The standard curve (A = 0.0029 × concentration (g l^{-1}) − 0.004) was linear up to 60 g l^{-1} with a correlation coefficient of 0.999). The precision at the 20-g l^{-1} level was 2%. The sampling rate of 300 samples per hour at the 50-g l^{-1} level, was almost as high as in most f.i.a. systems. Reagent consumption was 15 µl per determination in the recycling mode; this is 0.4% of the reagent consumption in a typical manual method (3).

In analyses where the flow detector signals are already at optimal levels, the multi-injection system is not necessary. However, even then, the low reagent consumption and the detergent carrier stream may have significant advantages. For most purposes a system with medium dispersion is recommended, in which the peak maxima are synchronized and a maximal signal is produced.

Very dilute samples can also be analyzed in this way, as has recently been shown for phosphate determinations [4].

The author thanks J. Růžička, E. H. Hansen and F. J. Krug for advice and co-operation; and J. Poulsen and J. Hansen for construction of the injector.

REFERENCES

1 J. Růžička and E. H. Hansen, Anal. Chim. Acta, 78 (1975) 145.
2 J. Růžička and E. H. Hansen, Anal. Chim. Acta, 99 (1978) 37.
3 D. Webster, Clin. Chem., 23 (1977) 663.
4 H. Bergamin F°, E. A. G. Zagatto, F. J. Krug and B. F. Reis, Anal. Chim. Acta, 101 (1978) 17.

Analytica Chimica Acta, 104 (1979) 191—194

Short Communication

SPECTROPHOTOMETRIC DETERMINATION OF COBALT(II) WITH 2,2'-DIPYRIDYL-2-PYRIMIDYLHYDRAZONE

R. B. SINGH, P. JAIN, B. S. GARG and R. P. SINGH*

Department of Chemistry, Delhi University, Delhi-110007 (India)

(Received 25th April 1978)

In recent years many nitrogen-containing heterocyclic hydrazones derived from 2-hydrazinopyridine [1—6] and 2-hydrazinoquinoline [7—10] have been prepared and tested as possible analytical reagents. Lions and co-workers [11, 12] first reported the analytical properties of these compounds. However, hydrazones derived from 2-hydrazinopyrimidine have not been investigated in detail for analytical purposes.

In this communication, the synthesis of 2,2'-dipyridyl-2-pyrimidylhydrazone (DPPH, I) and its application in the determination of micro amounts of cobalt are described.

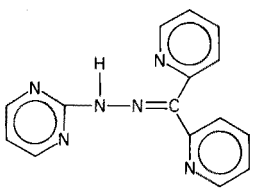

(1)

In aqueous solution, DPPH reacts with cobalt(II) to form a yellow complex (λ_{max} = 460 nm). This yellow complex on addition of strong acid shows a hypsochromic shift from 460 nm to 440 nm and is stable even in the presence of 6.5 M perchloric acid. Since all other transition metal complexes formed by DPPH are decomposed in strongly acidic media, this property can be utilized to create a selective method for the determination of cobalt(II).

Experimental

Apparatus. A Unicam SP600 spectrophotometer and a Metrohm E350 pH meter were used.

Synthesis of 2,2'-dipyridyl-2-pyrimidylhydrazone. 2-Chloropyrimidine was prepared by the method of Kogon et al. [13] and converted to 2-hydrazinopyrimidine by the method of Shrikawa et al. [14]. An ethanolic solution of equimolar quantities of 2-hydrazinopyrimidine and di-(2-pyridyl)ketone (Fluka) was refluxed for 6 h. The residue obtained after the removal of ethanol, by using a rotary evaporator, was crystallized with benzene to give pale yellow crystals (m.p. 160°C). Purity was checked by t.l.c. on silica gel. Elemental analysis confirmed the synthesis (calc. 65.2% C, 4.3% H; found 65.5% C, 4.9% H).

Reagent solutions. DPPH solutions were prepared in ethanol (95%) and stored in amber glass bottles. Such solutions are stable for several weeks. A stock solution of Co(II) was prepared by dissolving pure cobalt metal in perchloric acid and the resulting solution was standardized by titration with EDTA. Dilute solutions of perchloric acid and sodium hydroxides were used for pH adjustments.

All other solutions of cations and anions were prepared by dissolving analytical-grade chemicals in doubly distilled water.

Recommended procedure. To an aliquot containing 4.7—16.5 μg of Co(II), add 1 ml of an ethanolic 10^{-2} M solution of DPPH. Adjust the acidity of the solution to 3 M by adding perchloric acid of suitable concentration. Dilute the solution to 10 ml in a volumetric flask and measure the absorbance of the complex at 440 nm against a water reference.

Results and discussion

Spectral behaviour of the complex. A pH study of the complexation of DPPH with cobalt(II) showed that the yellow complex (λ_{max} = 460 nm) gives a constant absorbance in the pH range 2.5—11.5. The wavelength of maximum absorption shifts from 460 nm to 440 nm when perchloric acid is added. This new complex is stable even when 6.5 M perchloric acid is present.

Effect of DPPH concentration and stability of the complex. Complete complexation is obtained with a 3-fold (molar) excess of ligand, independently of acidity. The reagent itself does not absorb at the wavelength of maximum absorption in either case, hence the excess of the reagent is not critical and a blank is not necessary. Both the complexes remain stable for more than 15 h.

Characteristics of the complexes. The Co(II)—DPPH complex is formed in the pH range 2.5—11.5. Complex formation is instantaneous. However, if DPPH is added to highly acidic solutions, the complex in not formed because of the strong protonation of the ligand. At pH 2.5—11.5 Beer's law is obeyed up to 2.1 ppm of cobalt(II). The optimum concentration range, evaluated by the Ringbom method, is 0.47—1.99 ppm. The Sandell sensitivity is 0.0020 μg Co cm^{-2} and the molar absorptivity is 2.95×10^4 l mol^{-1} cm^{-1} at 460 nm.

In 2.5—6.5 M perchloric acid Beer's law is again obeyed up to 2.1 ppm of cobalt(II). The optimum concentration range, evaluated by the Ringbom method, is 0.47—1.65 ppm. The Sandell sensitivity is 0.0018 μg Co cm^{-2} and the molar absorptivity is 3.15×10^4 l mol^{-1} cm^{-1} at 440 nm.

A study of the composition of the complexes, as determined by Job's method of continuous variations, showed that the metal-to-ligand ratio is 1:2 in both cases.

Effect of diverse ions. Synthetic solutions containing known amounts of cobalt(II) and varying amounts of diverse ions were prepared, and the recommended procedure was followed for determination of cobalt(II). An error of ±2% in the absorbance reading was considered tolerable. In the determination of 0.59 ppm of cobalt, the anions tolerated (in ppm given in parentheses) are as follows: bromide, sulphite, sulphate, nitrite, chloride, acetate, citrate,

tartrate (2000 ppm each); fluoride, thiocyanate, thiourea, nitrate (1000 ppm each); phosphate (600 ppm); thiosulphate (500 ppm); iodide (100 ppm); oxalate (50 ppm) and borate (50 ppm). The metal ions tolerated are: Ca(II), Sr(II), Ba(II), Mg(II), Pb(II) (800 ppm each); Al(III), Sn(II), Mo(VI) (400 ppm each); Be(II), Zn(II), Pt(IV), Cd(II), Hg(II), Sb(III), W(VI) (150 ppm each); Ru(III), Rh(III), Ir(III), Os(VIII), Ti(IV), Mn(II), Ag(I), Fe(II) (50 ppm each); Cu(II), Ni(II), Pd(II) and V(V) (30 ppm each), when the amount of perchloric acid is increased from 3 M to 5 M.

EDTA, persulphate and cyanide interfere seriously.

Determination of cobalt in alloys. Cobalt can be determined in alloys with DPPH in highly acidic conditions (Table 1).

Comparison with other reagents. The present method with DPPH as the reagent for cobalt(II) compares favourably with other methods known for the purpose. The determination can be carried out over a wide pH range, i.e. pH 2.5—11.5, or in 2.5—6.5 M perchloric acid medium even in the presence of large amounts of foreign ions. Complex formation is instantaneous and the complexes formed are stable for many hours. Large amounts of ligand do not interfere, which is an advantage over the nitrosonaphthol reagents. The sensitivities of the different methods for the determination of cobalt are compared in Table 2.

TABLE 1

Determination of cobalt (in %) in alloys
(The average of n determinations is reported with the relative standard deviation.)

Alloy	Co reported	Co found	n	R.s.d. (%)
"K" Monel wire	0.51	0.50	6	4.6
Nilo-K wire	17.4	17.7	6	1.3

TABLE 2

Sensitivities of methods for the spectrophotometric determination of cobalt(II)

Method	Sensitivity (μg Co cm^{-2})	Reference
Nitroso-R salt	0.0019 (420 nm) 0.0042 (520 nm)	15
o-Nitrosoresorcinol	0.0025 (430 nm)	15
Thiocyanate	0.055 (625 nm) 0.009 (310 nm)	15
Dithioxamide	0.0046 (400 nm)	16
2,2'-Dipyridylketoxime	0.0029 (388 nm)	17
2,3-Quinoxalinedithiol	0.0016 (505 nm)	18
Phenanthrenequinone monoxime	0.0033 (420 nm)	19
DPPH (pH 2.5 — 11.5) (2.5 — 6.5 M $HClO_4$)	0.0020 (460 nm) 0.0018 (440 nm)	Present method

Advantages of pyrimidylhydrazones over the pyridyl and quinolyl analogues. Pyrimidylhydrazones on complex formation absorb at shorter wavelengths than their pyridyl and quinolyl analogues. This is the most striking difference observed between the two types. The initial pH values required for chelation with different metal ions are more widely separated than in the case of the pyridyl and quinolyl analogues. DPPH is capable of providing very good selectivity by careful pH control in analytical applications.

REFERENCES

1 M. L. Heit and D. E. Ryan, Anal. Chim. Acta, 32 (1965) 448.
2 J. E. Going and R. T. Pflaum, Anal. Chem., 42 (1970) 1098.
3 R. T. Pflaum and E. S. Tucker, Anal. Chem., 43 (1971) 458.
4 V. Zatka, J. Abrahm, J. Holzbecher and D. E. Ryan, Anal. Chim. Acta, 54 (1971) 65.
5 H. Alexaki-Tzivanidou, Anal. Chim. Acta, 75 (1975) 231.
6 A. A. Schilt, J. F. Wu and F. H. Case, Talanta, 22 (1975) 915.
7 M. L. Heit and D. E. Ryan, Anal. Chim. Acta, 34 (1966) 407.
8 S. P. Singhal and D. E. Ryan, Anal. Chim. Acta, 37 (1967) 91.
9 B. K. Afghan and D. E. Ryan, Anal. Chim. Acta, 41 (1968) 167.
10 R. W. Frei, G. H. Jamro and O. Navratil, Anal. Chim. Acta, 55 (1971) 125.
11 F. Lions and K. Martin, J. Am. Chem. Soc., 80 (1958) 3858.
12 J. F. Geldard and F. Lions, J. Am. Chem. Soc., 84 (1962) 2262; Inorg. Chem., 2 (1963) 27
13 I. C. Kogon, R. Minin and C. G. Overberger, Org. Synth., 35 (1955) 34.
14 K. Shrikawa, S. Ban and M. Yoneda, J. Pharm. Soc. Jpn., 73 (1953) 598.
15 E. B. Sandell, Colorimetric Determination of Traces of Metals, Interscience, New York, 3rd edn., 1965, p. 414.
16 W. D. Jacobs and J. H. Yoe, Anal. Chim. Acta, 20 (1959) 332.
17 W. J. Holland and J. Bozic, Talanta, 15 (1968) 843.
18 R. W. Burke and J. H. Yoe, Anal. Chem., 34 (1962) 1378.
19 K. C. Trikha, M. Katyal and R. P. Singh, Talanta, 14 (1967) 977.

Now available in English

H. ENGELHARDT

High Performance Liquid Chromatography

Translated from the German by G. GUTNIKOV

1978. Approx. 70 figures, 9 tables. Approx. 300 pages
(Chemical Laboratory Practice)
Cloth DM 64,–; US $ 35.20
ISBN 3-540-09005-3
Prices are subject to change without notice

Contents:
Chromatographic Processes.– Fundamentals of Chromatography.– Equipment for HPLC.– Detectors.– Stationary Phases.– Adsorption Chromatography.– Partition Chromatography.– Ion-Exchange Chromatography.– Exclusion Chromatography. Gel Permeation Chromatography.– Selection of the Separation System.– Special Technique.– Purification of Solvents.– Subject Index.

This simple and non-mathematical introduction to high-performance-liquid chromatography (HPLC) emphasizes the practical aspects of achieving a successful separation. This method usually permits analyses to be carried out more rapidly than by gas chromatography and is, moreover, eminently suited for the separation of heatlabile, high-boiling, or nonvolatile substances, without lengthy or tedious derivatization. In principle, all substances that are stable in solution are amenable to separation by HPLC.

HPLC equiment is described in terms of the individual components, their expected performance capabilities and suitability for certain applications.
The areas of applications of the various separation techniques (adsorption, partition, ion-exchange, exclusion) are pointed out in order to facilitate selection of the most appropriate technique by the worker for his particular problem. Considerable discussion is devoted to the parameters that are important in optimizing or improving a given separation.
The application of HPLC to actual problems in organic chemistry, pharmacological research, medicine, biochemistry and petrochemistry are illustrated by numerous relevant examples. This book is a translation of the wellknown and very successful German edition.

**Springer-Verlag
Berlin
Heidelberg
New York**

(continued from outside of cover)

Short Communications

Printed in The Netherlands

VOL. 104 No. 1 ANALYTICA CHIMICA ACTA JANUARY 1, 1979

CONTENTS

(continued on inside page of cover)